The Carboniferous of the Netherlands and surrounding areas; a basin analysis

Hendrik Kombrink

GEOLOGICA ULTRAIECTINA

Mededelingen van de
Faculteit Geowetenschappen
departement Aardwetenschappen
Universiteit Utrecht

No. 294

Members of the dissertation committee:

Prof. Dr. P.L. de Boer
Faculty of Geosciences,
Utrecht University, the Netherlands

Dr. J.D. Collinson
John Collinson Consulting,
Staffordshire, United Kingdom

Prof. Dr. A. Schäfer
Steinmann Institute – Geology,
University of Bonn, Germany

Prof. Dr. D.A. Spears
Department of Analytical Sciences,
University of Sheffield, United Kingdom

Prof. Dr. P.A. Ziegler
Institute of Geology and Paleontology,
University of Basel, Switzerland

The research for this thesis was carried out at
TNO – Geological Survey of the Netherlands and
Utrecht University, Faculty of Geosciences.

www.tno.nl
www.geo.uu.nl

ISBN/EAN: 978-90-5744-160-8

Graphic design: GeoMedia (7320), Faculty of Geosciences, Utrecht University

Cover illustration: "Kaart van Noordwest-Europa in den Boven Carboontijd." Figure 1 from Van Waterschoot van der Gracht (1918), Eindverslag der Rijksopsporing van Delfstoffen 1903-1916. Martinus Nijhoff ('s-Gravenhage), 644 pp.

The Carboniferous of the Netherlands and surrounding areas; a basin analysis

(met een samenvatting in het Nederlands)

PROEFSCHRIFT

ter verkrijging van de graad van doctor aan de Universiteit Utrecht
op gezag van de rector magnificus, prof. dr. J.C. Stoof,
ingevolge het besluit van het college voor promoties
in het openbaar te verdedigen
op vrijdag 19 december 2008 des middags te 14.30 uur

door

Hendrik Kombrink

geboren op 19 december 1979
te Terneuzen, Nederland

Promotoren:
Prof. dr. Th.E. Wong
Prof. dr. C.J. van der Zwan

Contents

– Schön ist eigentlich alles, was man mit Liebe betrachtet –

Christian Morgenstern, Stufen

CHAPTER 1

Introduction

1.1 General introduction

Carboniferous sediments of the Netherlands and surrounding areas accumulated in an east-west striking basin in a period of 60 million years (359 – 299 Myr). This basin is known as the Northwest European Carboniferous Basin (NWECB). The present-day contour of the NWECB (white dashed line in figure 1.1) is not a genetic basin but the remnant of a much larger shelf complex (Fig. 1.1) of which the distal parts have been shortened, partly eroded and incorporated in the Rheno-hercynian fold and thrust belt (Fig. 2.2).

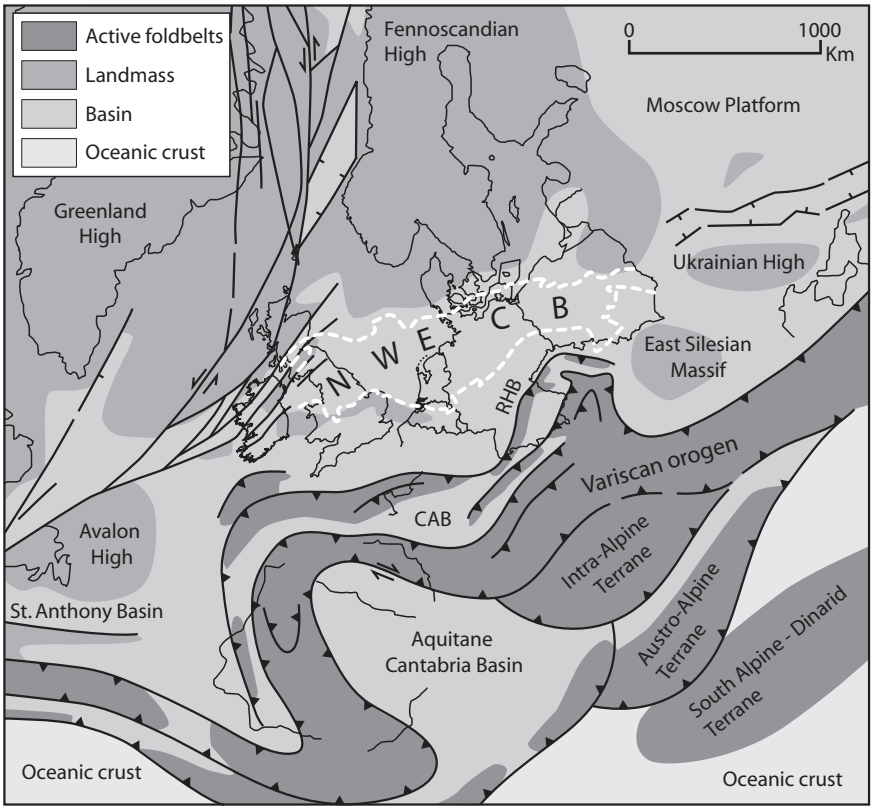

Figure 1.1 Palaeotectonic map of Northwest Europe during the Early Carboniferous. The dashed white line indicates the present-day contours of the Northwest European Carboniferous Basin. RHB: Rhenohercynian Basin, CAB: Central Armorican Basin. Redrawn after Ziegler (1989).

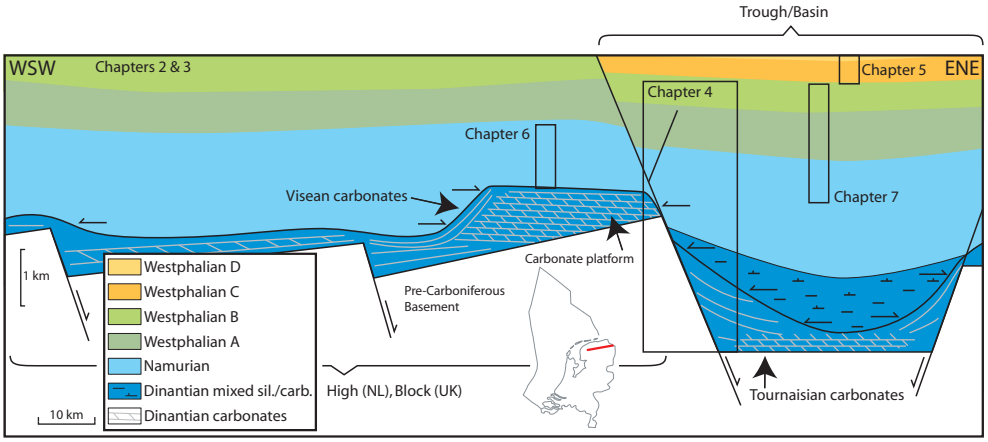

Figure 1.2 Schematic cross-section of the Carboniferous in the Netherlands. The stratigraphic distribution of the chapters in this thesis is indicated.

In general, the Early Carboniferous is characterised by carbonate deposition on shelves and isolated platforms while in intervening basins calciturbidites and mudstones were deposited (Ziegler, 1990; Geluk et al., 2007; Figs 1.2 & 3.1). The Namurian is characterised by increasing siliciclastic influx from the rising Variscan Mountains in the south and the Fennoscandian Shield in the north (Ricken et al., 2000; Collinson, 2005). In this way, Namurian sediments progressively in filled and blanketed the submarine relief that had existed during the Early Carboniferous (Fig. 1.2). Due to an ongoing regressive trend, Namurian basinal shales and turbidites were gradually replaced by delta-plain conditions at the end of the Namurian. This marks the onset of the Westphalian. Most of the economically interesting coal seams formed during the Westphalian A and B in a lower delta plain environment (Drozdzewski, 2005; Van Buggenum & den Hartog Jager, 2007). An increase in sand content and a shift towards dryer conditions, leading to a decrease in the number of coal seams, took place during the Westphalian C and D and Stephanian (Besly et al., 1993).

The Carboniferous of the Netherlands and surrounding areas is of great economic importance since coal seams have been and still are being mined, while their deeply buried equivalents are the most important hydrocarbon source rocks in the area (Van Buggenum & den Hartog Jager, 2007). However, in spite of the economic significance, a number of factors cause the Carboniferous to be still poorly known in major parts of the NWECB. Since the Upper Carboniferous is mostly assumed to be the lower limit of the economic fairway (Cameron & Ziegler, 1997), the majority of the wells only drilled the topmost part. As soon as the base of the Rotliegend – the most important reservoir unit in the NWECB – was penetrated, drilling stopped. Only in the northeastern part of the Netherlands (Coevorden area) and on the Cleaverbank High (Fig. 1.3), where Carboniferous reservoir rocks have been found, a number of wells drilled a considerable Carboniferous section. Burial depth is the second limiting factor. Following deposition of the Carboniferous sedimentary sequence, net tectonic subsidence caused these sediments to be deeply buried in most parts of the Netherlands (Fig. 1.3). The top of the Carboniferous shows the greatest depth (up to 6 km) in Jurassic basins like the Central Graben (Fig. 1.3). The Ruhr Valley Graben can easily be recognised by the high density of wells on the flanking horst blocks. The thickness of the Carboniferous section is the third limiting factor. A schematic cross-section through the Netherlands (Fig. 1.4) shows that the Carboniferous sequence often exceeds the thickness of all overlying strata. The

(compacted) maximum thickness is approximately 5.5 km (Van Buggenum & den Hartog Jager, 2007). This explains the scarcity of wells penetrating the base of the Carboniferous: apart from some wells located at the margins of the basin, the only well in the Netherlands is Winterswijk-1 (Fig. 2.6).

1.2 History of research on the Carboniferous in the Netherlands

From 1850 to 1860 Staring led the first geological mapping campaign of the Netherlands (Felder, 1981). Simultaneously, coal exploration activities started in Limburg (Jongmans, 1944). Systematic research on Carboniferous rocks took place since the foundation of the "State Service for the Exploration of Mineral Resources" (Dienst der Rijksopsporing van Delfstoffen in Nederland) in

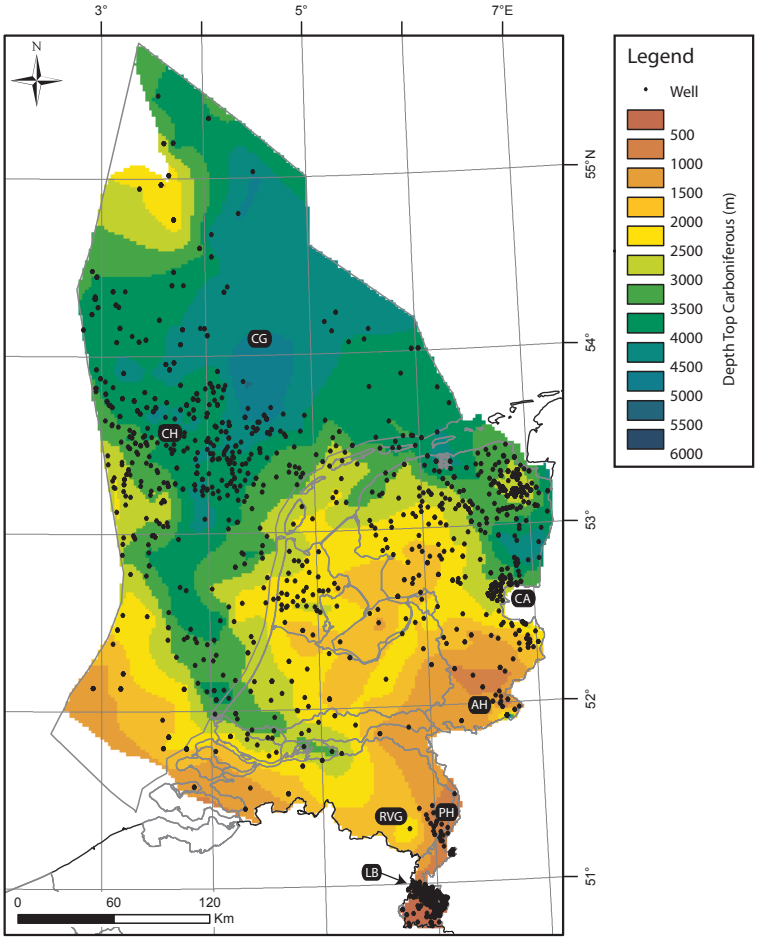

Figure 1.3 Depth of the Top Carboniferous in the Netherlands. The wells used to make this map are shown as black dots. AH: Achterhoek, CA: Coevorden area, CG: Central Graben, CH: Cleaverbank High, LB: Limburg, PH: Peelhorst and RVG: Ruhr Valley Graben.

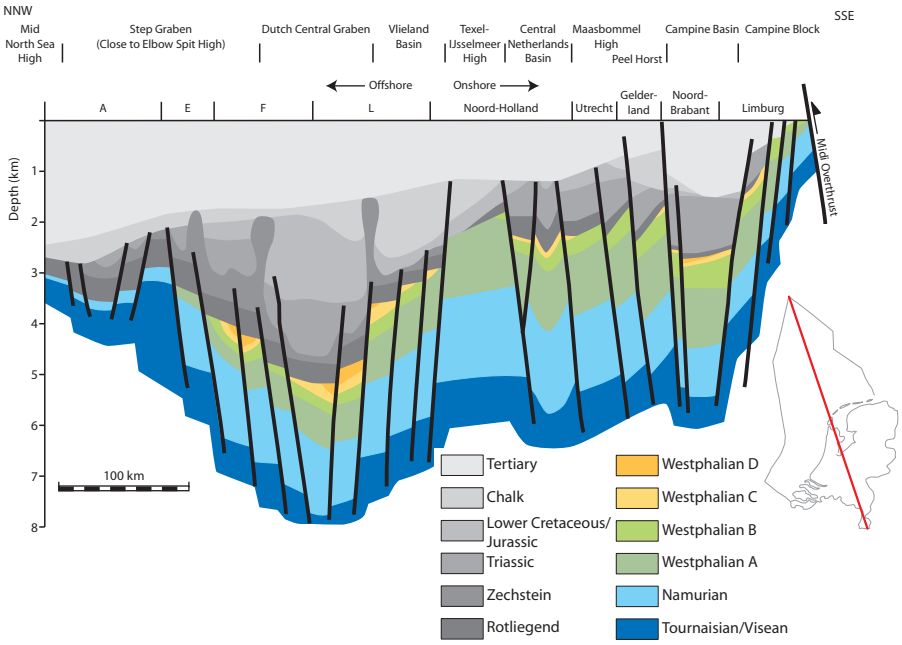

Figure 1.4 Schematic cross-section through the Netherlands showing the thickness distribution of Carboniferous strata (slightly modified after Van Buggenum & den Hartog Jager (2007)).

1903 (Van Waterschoot van der Gracht, 1918). The task of this department was to search for coal resources outside the classical mining area in southern Limburg. The first well (number 5A) outside this area that reached the Carboniferous was drilled near Helenaveen on the Peelhorst (1906). In the Achterhoek area the first well showing the presence of Carboniferous rocks was Plantengaarde (1908; Visser, 1987). In his classic work, published in 1918, Van Waterschoot van der Gracht for the first time presented a detailed study on (Carboniferous) geology in the Netherlands. In the same year, the Geological Survey of the Netherlands was established. The office in Heerlen, where Jongmans assembled an impressive collection of palaeontological and stratigraphical data, set an example for other mining areas (Beijer & Fermont, 1987). Jongmans was a driving force behind the organisation of the first International Carboniferous Congress in 1927 in Heerlen. Three more congresses (1935, 51 and 57) were held, resulting in the establishment of a supra-national stratigraphic scheme for the Carboniferous. Up to 1950, numerous scientific papers on the Carboniferous geology of Limburg, the Peel and the Achterhoek were published (Fig. 1.5). Some decades later, Bless et al. (1976) Kimpe et al. (1978) and Bless et al. (1980) summarised and updated the knowledge on Carboniferous geology in Limburg. Extensive reports on the Peel (Peelcommissie, 1963) and the Achterhoek (RGD, 1986) discuss the coal-potential of these areas.

The discovery of the Groningen Gasfield in 1959 marks the onset of a new energy-policy in the Netherlands; the last mine was closed in 1974. The recognition of Carboniferous coals acting as an important gas source (Patijn, 1963b) and the finding of Carboniferous gas reservoirs (Coevorden Field) caused the interest for Carboniferous geology to shift towards the expanding oil and gas industry (Thiadens, 1963). A simple query in a literature database (keywords Carboniferous and Netherlands in the abstract) clearly shows this transition (Fig. 1.5). Since petroleum companies

are not eager to publish their results (Van Buggenum & den Hartog Jager, 2007), the number of scientific publications decreased significantly. In this period, many consultancy and in-house reports were written, but none of them has been published. In the last years there is a slight increase in publications on the Carboniferous of the Netherlands, partly related to the Carboniferous and Permian Stratigraphy congress which was held in Utrecht in 2003. Moreover, the release of petroleum-industry data stimulates publication nowadays. Van Buggenum & den Hartog Jager (2007) presented the most recent overview of Carboniferous geology of the Netherlands in which much information from petroleum companies is used. To stimulate further exploration activities, the Southern Permian Basin Area Atlas (SPBA Atlas) is currently under construction in which a detailed (petroleum) geological overview of the region will be presented. In close collaboration with geologists from the UK, Denmark, Belgium, the Netherlands, Germany and Poland, knowledge on the Carboniferous of the SPBA will be summarised and illustrated by – amongst others – well correlation panels and palaeogeographic maps (see chapter 2).

1.3 Aims and summary of this thesis

The factors limiting the knowledge on Carboniferous geology, described in paragraph 1.1, and the overview of the research carried out so far, make clear that the Carboniferous of the Netherlands is scientifically underexplored. Therefore, a PhD project was initiated of which this thesis is the result. The release of new exploration data, the need to further stimulate exploration activities and the possible extension of the lower exploration limit formed an appropriate background to carry out such a study. The main aim of this thesis is to better understand the Carboniferous basin evolution in the Netherlands and surrounding areas. In the section below a short outline is given of the various topics addressed in this thesis.

The Netherlands were part of the Southern Permian Basin. This area is mature in terms of hydrocarbon exploration (Atkinson et al., 2001; Moscariello, 2005). To stimulate further exploration, the Southern Permian Basin Area Atlas (SPBA Atlas) is currently in preparation (see 1.2). **Chapter 2** in this thesis is a shortened version of the Atlas' chapter on the Carboniferous.

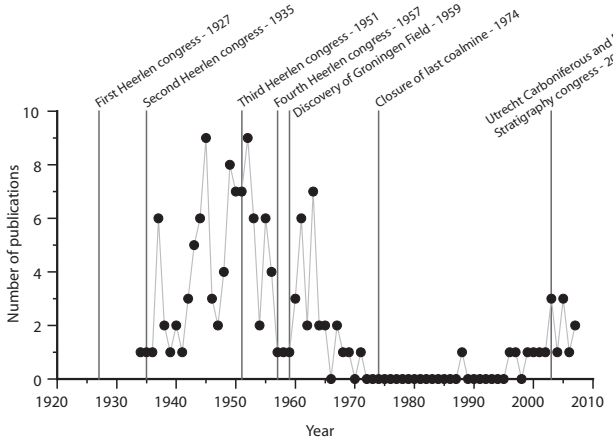

Figure 1.5 Publications dealing with the Carboniferous of the Netherlands from 1933 onwards. The search has been performed in Georef. Note that in the period 1905 – 1933 even more papers have been published.

Here, the aim is to present an overview of the Carboniferous geological setting in the Southern Permian Basin Area. As such, this chapter forms a comprehensive introduction and background to the following chapters.

An interesting research question is whether Carboniferous carbonate platforms such as found along the margins of the NWECB, also occur in the basin centre (northern part of the Netherlands and German onshore and southern offshore areas). Numerous authors presented palaeogeographical reconstructions of this area (Bless et al., 1976; Ziegler, 1990; Bridges et al., 1995; Gerling et al., 1999; Collinson, 2005; Geluk et al., 2007; Korn, 2008; Van Hulten & Poty, 2008), but the interpretations suffered a serious lack of hard data. Surprisingly, high-quality seismic data allowed the recognition of carbonate platforms in the northern part of the Netherlands. Two large and one small platforms were interpreted. The large ones occur below the Groningen Gasfield (Groningen High) and on the Friesland Platform. In between these platforms, the Lauwerszee Trough most likely was an Early Carboniferous basin with a thicker Lower Carboniferous sedimentary succession compared to the adjacent carbonate platforms. This configuration is also found in northern England where the grabens in between the carbonate platforms contain a very thick Lower Carboniferous section (Gawthorpe et al., 1989; Fraser & Gawthorpe, 1990; Gutteridge, 1991). The carbonate platforms formed on stable horst blocks. Based on these data, it is suggested that the central part of the NWECB is characterised by a complex of horst blocks (and associated carbonate platforms) during the Early Carboniferous. The aims of **chapter 3** are: (1) to demonstrate the presence of Early Carboniferous carbonate platforms in the central part of the NWECB, (2) to put these results in a geological framework and (3) to discuss the implications for the structural setting.

In literature, a number of subsidence mechanisms have been proposed for the accumulation of the very thick Carboniferous section. The most important ones are: (1) flexural subsidence along the southern margin of the NWECB (Gayer et al., 1993; Warr, 1993; McCann, 1999; Burgess & Gayer, 2000; Drozdzewski, 2005; Kornpihl, 2005) and (2) thermal subsidence following an Early Carboniferous rifting event (Leeder & McMahon, 1988; Coward, 1990; Fraser & Gawthorpe, 1990; Maynard et al., 1997). The contribution of these mechanisms to the total subsidence is poorly understood (Coward, 1993; Quirk, 1993; Süss, 1996; Maynard et al., 1997; Ricken et al., 2000; Drozdzewski, 2005). The aims of **chapter 4** are: (1) to quantify the geometry of the Variscan foreland basin and the associated subsidence in the Netherlands; (2) to quantify the amount of (thermal) subsidence that might be explained by an Early Carboniferous rifting event and (3) to propose a number of alternative subsidence models. These are: (1) one that assumes an additional Namurian rifting event, (2) a model incorporating dynamic topography and (3) compressional intra-plate stress. In close collaboration with the Free University in Amsterdam, a modelling experiment was set up to constrain the dimensions (width and depth) of the foreland basin. It is clearly demonstrated that flexural subsidence only played an important role along the southern margin of the NWECB. Therefore, another mechanism must have been active simultaneously. Conform the suggestions of many other authors, a model of thermal subsidence is adopted, following an Early Carboniferous rifting event. Even the incorporation of this mechanism did not result in a satisfactory fit to the tectonic subsidence curves derived from well data. To effectively explain the tectonic subsidence curves in the central part of the NWECB, an additional Namurian extensional phase is proposed. The interaction of these mechanisms is the next point discussed in chapter 4. When drawing a north-south cross-section through the NWECB, the large-scale asymmetry in tectonic subsidence is evident. The wavelength observed in this cross-section exceeds the one caused by flexural subsidence. In analogy to foreland basin systems in other areas (Coakley

& Gurnis, 1995; Pang & Nummedal, 1995; Burgess & Moresi, 1999; Pysklywec & Mitrovica, 2000; Liu & Nummedal, 2004), it is proposed that mantle convection due to subducting plates to the south might have caused a subsidence component which has an asymmetric form and is manifest at very high wavelengths (dynamic topography). Considering this assumption, the gradual thickness changes might be well explained. Regarding the proximal position of the Variscan thrust front, compressional intra-plate stress might be another candidate to account for additional subsidence in the study area.

The results described in **chapter 5** are dealing with the inversion sequence in the NWECB. During the Late Westphalian, the NWECB became fragmented as a consequence of large-scale folding and faulting (Leeder & McMahon, 1988; Fraser & Gawthorpe, 1990; Coward, 1993; Corfield et al., 1996; Süss, 2001; Schroot & de Haan, 2003). Most Carboniferous gas reservoirs in the Netherlands' on- and offshore areas occur in fluvial sandstones deposited during this inversion phase. In the northeastern part of the Netherlands, these sandstones belong to the Tubbergen Formation. British Carboniferous gasfields, which can be found in a similar setting, are well described in the literature (Ritchie & Pratsides, 1993; Ritchie et al., 1998; Aitken et al., 1999; Conway & Valvatne, 2003; Hayward et al., 2003; O'Mara et al., 2003) but no data on Dutch fields have been published to date. The aim of chapter 5 is to present the alluvial architecture of the Coevorden Gasfield in the northeastern part of the Netherlands. Twelve wells have been used to reconstruct the orientation and spatial distribution of individual channel sandstone bodies.

Deposition of Namurian shales in Northern England is thought to have occurred under varying salinities, ranging between marine and lacustrine conditions (Ramsbottom et al., 1979; Holdsworth & Collinson, 1988; Martinsen et al., 1995). This is based on the observation of a cyclic occurrence of fossil phases (Ramsbottom et al., 1962) and geochemical investigations (Amin, 1979; Spears & Amin, 1981; Leeder et al., 1990). Goniatite-bearing intervals are interpreted to record fully marine conditions while intervals characterised by fish remains (Fish phase) are thought to reflect lacustrine conditions. The validity of this model was questioned because these inferences are based on: (1) the absence of certain fossils rather than the presence of freshwater species and (2) the geochemistry might be well explained in terms of varying organic matter contents and grain size variations. The aim of this study, described in **chapter 6**, is to better investigate these proposed salinity changes in the western part of the NWECB. Three sections from three cores were sampled where palaeontological control is excellent. Major and trace elemental data were obtained as well as total organic matter (TOC) concentrations. Although the Fish phase samples are characterised by a slightly lower trace element enrichment compared to the goniatite-bearing intervals, they still show marked enrichment in trace elements commonly enriched in marine black shales. Since most of the trace elements show a positive correlation with TOC, it is proposed that TOC has a direct or indirect control on the variation in trace element enrichment. Therefore, a salinity change is not necessary to explain the differences in geochemical behaviour. It is concluded that the proposed salinity changes are not supported by the geochemical characteristics of the sediments. Basin waters probably remained marine throughout deposition of the Namurian shales.

Marine bands are thin trangressive mudstone horizons (up to several meters) deposited under marine or brackish conditions. These marine bands are important stratigraphic markers in the Westphalian since they occur in between thick packages of monotonous fluvial-lacustrine sediments and may be recognised over large distances (Ramsbottom et al., 1979; Leeder & McMahon, 1988; Leeder et al., 1990; Dusar et al., 2000). Much research has been carried out on the fossil content of these shales (Rabitz, 1966; Ramsbottom, 1969; Paproth et al., 1983b; Dusar et al., 2000). In order to distinguish marine bands without fossil control, attempts have been made to recognise them

using the gamma-ray readings (Archard & Trice, 1990; Hollywood & Whorlow, 1993; Davies & McLean, 1996). This is based on the observation that some marine bands show enhanced Uranium (U) concentrations, mainly in the goniatite-bearing intervals (Fisher & Wignall, 2001).

In general, Westphalian marine bands can be sudivided in Goniatite and *Lingula* marine bands. Goniatites indicate relatively distal and deep marine environments while *Lingula*s indicate deposition in a nearshore or even brackish environment. All marine bands found in a number of Dutch wells with completely cored Carboniferous successions show marine bands dominated by *Lingula*-associations. Moreover, based on gamma-ray measurements there are no indications that marked U-enrichment occurs. The aim of **chapter 7** is to investigate why these *Lingula* marine bands do not show marked enrichments in U and other trace elements. They are compared with some lacustrine beds (because these show broadly the same sedimentary development) and a Goniatite marine band. The results show that the *Lingula* marine bands show systematically lower TOC contents than the Goniatite marine band. A higher siliciclastic sedimentation rate during transgression is inferred to explain the lower TOC contents. Low TOC concentrations and high sedimentation rates most likely prevented an effective scavenging of trace elements. Therefore, it is proposed that detection of marine bands with a gamma-ray device is only promising when they are found in goniatite facies. Along the margins of the basin, where marine bands occur in shallow-marine *Lingula* facies, this method will probably fail.

1.4 Stratigraphy and timescales

In Central and Western Europe, the Carboniferous has traditionally been subdivided into two units, "Lower Carboniferous" and "Upper Carboniferous", separated at the base of the Namurian. The Namurian is defined by the first occurrence of the goniatite species "*Cravenoceras*" (= *Emstites*) *leion* which is equivalent to the Brigantian/Pendleian boundary (Fig. 1.6). In 1960, the subsystems "Dinantian" and "Silesian" were formally established, synonymous to "Lower" and "Upper Carboniferous" in this definition. However, in 1996, the IUGS-Executive-Committee ratified the definition of the Mid-Carboniferous boundary between the Mississippian and the Pennsylvanian in the GSSP (Global Stratotype Section and Point) Arrow Canyon (Nevada, USA) by the first occurrence of the conodont *Declinognathodus noduliferus*. This boundary is approximately equivalent to the boundary between the *Eumorphoceras* and *Homoceras* ammonoid (goniatite) zones in central Europe (Lane et al., 1999). These ammonoid zones equate to the Arnsbergian and Chokierian substages. Because of the lack of diagnostic fossils, the international Mid-Carboniferous boundary is difficult to identify in central Europe. Therefore, in accordance with the rules of stratigraphic nomenclature (Herbig, 2005; Dusar, 2006), the traditional units Visean, Namurian, and Westphalian are still valid as regional units. In this thesis, the regional Central and West European stratigraphic nomenclature on series, stage and substage level will be used (e.g. Dinantian, Namurian and Westphalian C). The correlation of the regional and global Carboniferous timescales is shown in figure 1.6 and is also given in all stratigraphic tables in this thesis.

Dinantian stratigraphy was mainly determined using corals and brachiopods, but later also by foraminifera, conodonts and microflora (Paproth et al., 1983a; Stoppel & Amler, 2006). In the Namurian, most stage boundaries are defined by new goniatite faunas, found in marine bands. The Westphalian stage boundaries occur at the bases of the most widespread marine bands (Ramsbottom et al., 1979). The use of macrofossils was well possible in the mining areas but

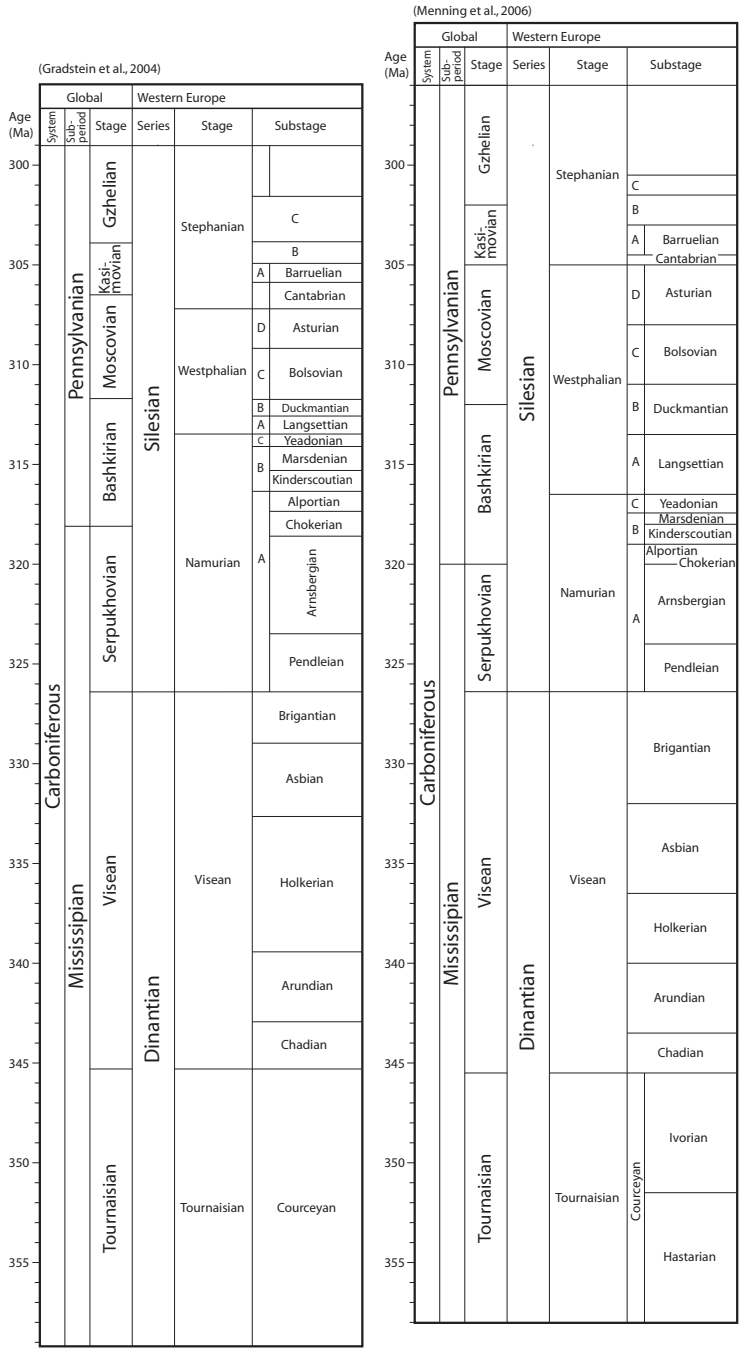

Figure 1.6 Timescales showing sub-periods and stage boundaries for the Carboniferous Period after Gradstein et al. (2004) and Menning et al. (2006).

turned out to be difficult to apply to exploration wells where only cuttings and sometimes a limited amount of cored section are available. Therefore, the application of palynology became (and still is) the standard tool to date the Carboniferous rocks drilled by petroleum companies (Van Wijhe & Bless, 1974; McLean et al., 2004). It is based on the pioneer work of Neves et al. (1973), Clayton et al. (1977) and Owens et al. (1977) and is recently refined by McLean et al. (2004). Unfortunately, the palynostratigraphical resolution is, in general, less than the marine bands resolution, which inhibits detailed correlation (Bruce & Stemmerik, 2003). In barren sequences (Westphalian C – Stephanian), chemostratigraphy has been applied (Pearce et al., 1999; Pearce et al., 2005) to gain more stratigraphical control. Due to the relative lack of reliable biostratigraphic information in large areas in the NWECB (especially in the central, deep part), correlations are based on lithostratigraphy. For instance, the Tournaisian/Visean subdivision of the UK offshore is only based on lithostratigraphy as this is thought most appropriate considering the clear lithological differences on which the formations are based (Fig. 2.3) and the poor biostratigraphic constraints. Also, the current subdivision of the Carboniferous of the Netherlands is entirely lithostratigraphic except for the mining areas in the south.

There are several timescales which can be used for the Carboniferous. The most important ones are from Gradstein et al. (2004) and Menning et al. (2006; Fig. 1.6). The main difference between these timescales is the age of the stage boundaries. Since the Gradstein (2004) timescale will be used in the Southern Permian Basin Atlas project, it was decided to use this timescale for the other chapters too. However, in chapter 4, the timescale of Menning (2006) has been used for the following reason: the Gradstein (2004) timescale assumes the combined duration of the Westphalian A and B to be 1.8 Myr. Menning et al. (2006) assume a length of 5.5 Myr, which resulted in a much better match between observed and modelled tectonic subsidence curves. When a duration of 1.8 Myr is used, an abnormal high and abrupt change in tectonic subsidence (at the Namurian-Westphalian transition) is needed to accommodate the thick section of Westphalian A and B sediments.

CHAPTER 2

Tectonics and sedimentation in the Northwest European Carboniferous Basin

This chapter is based on: Henk Kombrink, Bernard M. Besly, John D. Collinson, Daan G. den Hartog Jager, Michiel Dusar, Günter Drozdzewski, Peer Hoth, Henk J.M. Pagnier, Lars Stemmerik, Maria I. Waksmundzka and Volker Wrede (in prep.): The Carboniferous. In: Petroleum Geological Atlas of the Southern Permian Basin Area (Doornenbal, J.C. & Stevenson, A., eds). European Association of Geoscientists and Engineers, Houten.

2.1 Introduction

From a petroleum geological point of view, the Carboniferous of northwestern Europe is of primary importance. Carboniferous coals have been intensely mined in this area during the second half of the 19th century and the first half of the 20th century. The (Lower) Carboniferous Limestone series, Millstone Grit and Coal Measures had already been defined by Whitehurst in 1778 (Paproth et al., 1983b; Harland et al., 1990). Although mining activities decreased dramatically in the 20th century, the economic value remain as the coals that used to be mined (Fig. 2.1) turned out to be the most important source of gas. In addition, Visean/Namurian basinal shales proved to be a source for oil in parts of the Northwest European Carboniferous Basin (NWECB).

Carboniferous rocks have been extensively studied in the mining areas and in places where they are exposed at the surface. These areas are mainly found along the current margins of the NWECB (Fig. 2.1). In the UK, Carboniferous successions can be traced from outcrops in the northeast of England, the Pennine area and the English Midlands. The folded Namur-Dinant Basin, south of the London-Brabant Massif (LBM) in Belgium offers many classical Palaeozoic type sections (Tournai, Visé, Dinant and Namur) and the famous Meuse profile between the cities of Namur and Givet. In the far south of the Netherlands, Namurian outcrops occur in the Geul Valley. Carboniferous rocks can be seen at outcrop in Germany along the southern margin of the NWECB in the Eifel, Rhenish and Harz Mountains, the Aachen and Ruhr Coalfields and the Ibbenbüren/Osnabrück and Flechtingen Hills. In Poland, Carboniferous rocks are exposed in the Lower Silesian Coal Basin and the Holy Cross Mountains.

The discovery of gas in the 1960's stimulated exploration throughout the entire NWECB. Areas with a relatively high well density are the Silverpit area and Cleaverbank High in the offshore UK and Netherlands respectively (Fig. 2.11). Carboniferous rocks along the northern margin of the LBM in the UK, Belgium and the Netherlands have often been drilled. In the northeastern part of the onshore Netherlands and adjacent area in Germany the Westphalian sedimentary succession is relatively well known. The area just north of the Ruhr mining district (Fig. 2.1) has been drilled extensively for coal exploration. Further to the northeast, the island of Rügen in northeastern Germany is another important source of information on Carboniferous rocks. In Poland, the Upper Silesia and Lublin Basins are the areas best known. There is limited information

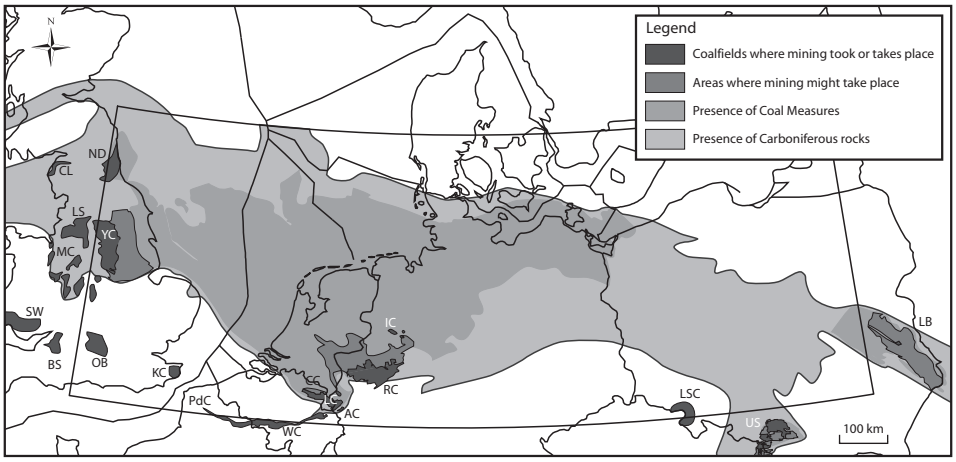

Figure 2.1 Map displaying the present-day distribution of Carboniferous rocks and Coal Measures in the NWECB. The coal mining areas are mainly located along the margins. Areas where coal mining may be possible in the future due to shallow occurrence of coal seams are also given. AC: Aachen-Erkelenz Coalfield, BS: Bristol-Somerset Coalfield, CC: Campine Coalfield, CL: Cumberland Coalfield, IC: Ibbenbüren Coalfield, KC: Kent Coalfield, LC: Limburg Coalfield, LB: Lublin Coalfield, LS: Lancashire Coalfield, LSC: Lower Silesia Coalfield, MC: Midland Coalfields, ND: Northumberland-Durham Coalfield, OB: Oxfordshire-Berkshire Coalfield, PdC: Pas de Calais Coalfield, RC: Ruhr Coalfield, SW: South Wales Coalfield, US: Upper Silesia Coalfield, WC: Wallonian Coalfield, YC: Yorkshire Coalfield.

from the German offshore and northern onshore area, the Polish Trough and the western part of the offshore Netherlands and adjacent area in the UK.

As well as many regional and local studies, compilations of Carboniferous geology throughout the entire NWECB have been published before: Paproth (1989), Ziegler (1990), Bénard & Bouché (1991), Maynard et al. (1997) and Gerling et al. (1999). There has been no systematic review of Carboniferous stratigraphy for the onshore UK area for some time (George et al., 1976; Ramsbottom et al., 1978) but one is currently in preparation. Offshore, a stratigraphic scheme was proposed by Cameron (1993) but this has been subject to considerable revision by Collinson (2005) and Besly (2005). The Carboniferous in the Danish Central Graben was reviewed by Bruce & Stemmerik (2003) whereas little attention has been paid to the onshore succession since the original stratigraphic work of Michelsen (1971) and Bertelsen (1972). Since Paproth et al. (1983a, 1983b), Delmer et al. (2001) and Poty et al. (2001) redefined the Belgian lithostratigraphy. Overviews on the Namur-Dinant Basin and the Campine Basin were published by Poty (1997) and Hance et al. (2001) and by Langenaeker (2000) respectively. Van Buggenum & den Hartog Jager (2007) recently presented an update of Carboniferous geology in the Netherlands. The Carboniferous stratigraphy and palaeontology of Germany has been summarized in two extensive volumes by Wrede (2005) and Amler & Stoppel (2006). An overview of Carboniferous rocks in Poland is presented in the volume entitled "The Carboniferous system in Poland" (Zdanowski & Żakowa, 1995). The latest stratigraphic schemes are presented in the „Stratigraphic table of Poland" (Wagner, 2007), whilst numerous regional studies have been published (Szulczewski et al., 1996; Żelaźniewicz et al., 2003; Buła et al., 2004; Konon, 2006; Matyja, 2006; Krzywiec, 2007; Narkiewicz, 2007; Matyja, 2008).

As shown here, a lot of new literature appeared since the last integrating study of Carboniferous geology in the NWECB. This chapter presents an up to date overview illustrated by new maps and figures. The basin development will be described using a tectonostratigraphic correlation panel (Fig. 2.3), a new Permian subcrop map (Fig. 2.4), well correlation panels (Figs 2.6, 2.7, 2.9, 2.10, 2.12, 2.13, 2.15 & 2.16) and palaeogeographical maps (Figs 2.5, 2.8, 2.11 & 2.14). Geographical names can be found in one of the palaeogeographical maps and figures 2.1 and 2.2.

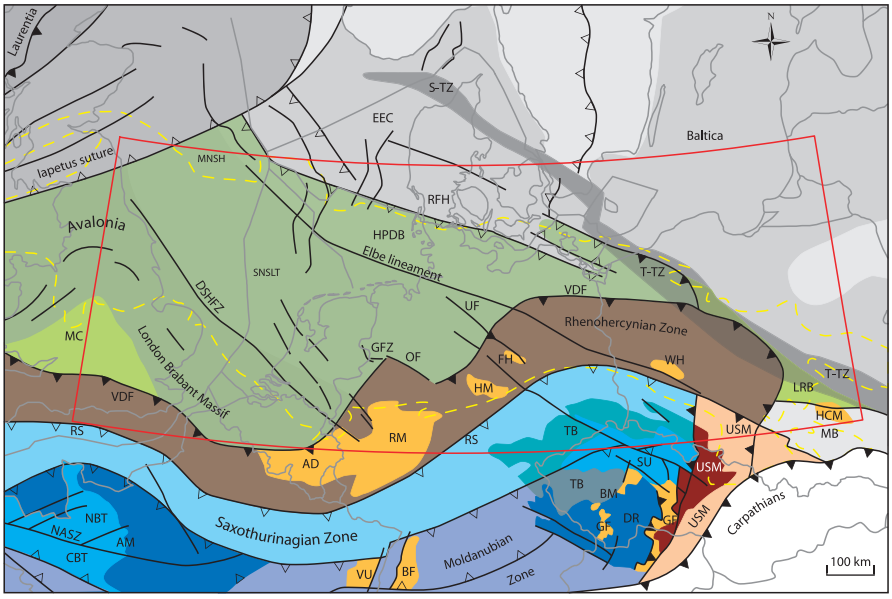

Figure 2.2 Structural elements of the NWECB. The grey areas represent Laurentia and Baltica. The greenish central part of the map indicates the Avalonian microcontinent. The Rhenohercynian Zone represents the external fold and thrust belt of the Variscan orogen that was thrusted onto the southern margin of Avalonia. Orange: areas of outcropping Carboniferous rocks. The bluish zones form micro-continents accreted during the Variscan orogenic cycle. The yellow dashed line indicates the extent of Carboniferous rocks in the SPB area. Oceanic sutures, open ticks; orogenic frontal zones, filled ticks.
Key: Post-Palaeozoic platforms: MNSH: Mid North Sea High, RFH: Ringkøbing-Fyn High. Postulated Palaeozoic terranes and possible terrane/sub-terrane boundaries: CBT: Central Brittany Terrane, DSHFZ: Dowsing-South Hewett Fault Zone and continuation in Roer Valley Graben (SE), GFZ: Gronau Fault Zone, OF: Osning Fault Zone, RS: Rhenohercynian Suture Zone, SNSLT: Southern North Sea Lüneburg Terrane, LRB: Łysogóry-Radom Block, MB: Malopolska Block, UF: Uelzen Fault. Proterozoic-Palaeozoic tectonic elements: AD: Ardennes, AM: Armorican Massif, BF: Black Forest, BM: Bohemian Massif, DR: Drosendorf Unit, EEC: East European Craton, GF: Gföhl Unit, HCM: Holy Cross Mountains, HM: Harz Mountains, MC: Midland Craton, NBT: North-Brittany Terrane, RM: Rhenish Mountains, S-TZ: Sorgenfrei-Tornquist Zone, SU: Sudetes Mountains, TB: Tepla-Barrandian Basin, T-TZ: Teisseyre-Tornquist Zone, USM: Upper Silesian Massif, VDF: Variscan Deformation Front, VU: Vosges Unit, WH: Wolsztyn High. Map is mainly based on Pharaoh (1999) with modifications using Drozdzewski et al. (2005), Narkiewicz (2007) and Ziegler (1990).

2.1.1 Plate-tectonic setting

The crust on which the NWECB developed mainly consists of (Eastern) Avalonia (Pharaoh, 1999, Verniers et al., 2002; Fig. 2.2). This Gondwana-derived micro-continent consolidated with Baltica during the Late Ordovician, thereby closing the Tornquist Ocean (Cocks & Fortey, 1982; Tait et al., 1997; Cocks & Torsvik, 2005). The Iapetus Ocean, separating Baltica/Avalonia from Laurentia was closed during the Silurian; these continents formed the Old Red Continent or Laurussia. The establishment of the Old Red Continent belongs to the Caledonian orogenic cycle (Cambrian – Early Devonian). The Precambrian basement of Avalonia west of the Dowsing-South Hewett fault zone (DSHFZ, Fig. 2.2) is characterised by mildly metamorphosed arc-magmatic rocks (Pharaoh, 1999). This area is part of the Anglo-Brabant Fold Belt, of which the London Brabant Massif (LBM) is the eastern limb (Fig. 2.2). The Cambro-Silurian shales of the LBM were deformed into low-grade metamorphosed slates during the Late Silurian – Early Devonian (De Vos, 1997). This deformation is related to the oblique accretion of eastern Avalonia with Baltica and Laurentia (Sintubin, 1999). The LBM is probably underpinned by a granitic body, emplaced at the end of the Ordovician, which may have caused this massif to be a stable block through time (De Vos, 1997). From the area east of the DSHFZ (Lüneburg terrane, Verniers et al., 2002) no information on the pre-Devonian basement is available (Pharaoh, 1999).

During the Variscan orogenic cycle (Early Devonian – Permian) Gondwana and Gondwana-derived micro-continents collided with Laurussia. By Middle and Late Devonian times, Gondwana converged in a dextral oblique, clockwise rotational mode, with initial contact in the area of Iberia and northwest Gondwana during the Famennian (Ziegler, 1990). Other Gondwana-derived terranes, such as the terranes in the Saxothuringian and Moldanubian zones (Fig. 2.2), started to collide earlier in the Devonian. An important event for the NWECB is the opening of the Rhenohercynian Rift Basin during late Early Devonian along the southern margin of the Old Red Continent (more or less the southern margin of the Rhenohercynian Zone, Fig. 2.2; Ziegler, 1990; Oncken et al., 1999; Burgess & Gayer, 2000; Narkiewicz, 2007). In this basin, which is also known as the Lizzard-Giessen-Harz back-arc basin, a thick pile of Devonian and Lower Carboniferous sediments was deposited, sourced from the Mid German Crystalline High in the south and the Old Red Continent in the north. The basin, which must have remained relatively narrow as it cannot be recognised by palaeomagnetics (Tait et al., 1997), started to close during the Middle Devonian by SE directed subduction (Acadian orogenic pulse, Franke, 2000). Renewed back-arc extension took place during the Late Devonian but gave way to compression again at the Devonian-Carboniferous transition (Bretonian orogenic pulse). Via another phase of extension during the Tournaisian-Early Visean, final closure took place during the late Early Visean (Ziegler, 1989; Ziegler, 1990; Franke, 2000; Ziegler et al., 2004). There is only limited evidence for Devonian extensional reactivation in the North German-Polish Caledonides (Banka et al., 2002; Krawczyk et al., 2002), the area associated with the southwest to south-dipping Teisseyre-Tornquist suture (Fig. 2.2) along which East-Avalonia was welded to the East-European Craton.

The Early Carboniferous was characterised by northward subduction of the Palaeo-Tethys Mid Ocean Ridge (the ocean separating Gondwana from the (micro)continents in the north) and southward subduction of the Rhenohercynian Basin beneath these Mid-European terranes, which led to the formation of the Variscan mountains (Franke, 2000; Stampfli & Borel, 2002). Around the Visean/Namurian boundary, the Rhenohercynian accretionary wedge collided with the passive margin in the north (Oncken et al., 1999; Narkiewicz, 2007), while accretion followed during the Namurian. In the northwestern part of the NWECB (the British Isles), the Early Carboniferous is characterised by extension, related to the development of the Arctic-North Atlantic rift system.

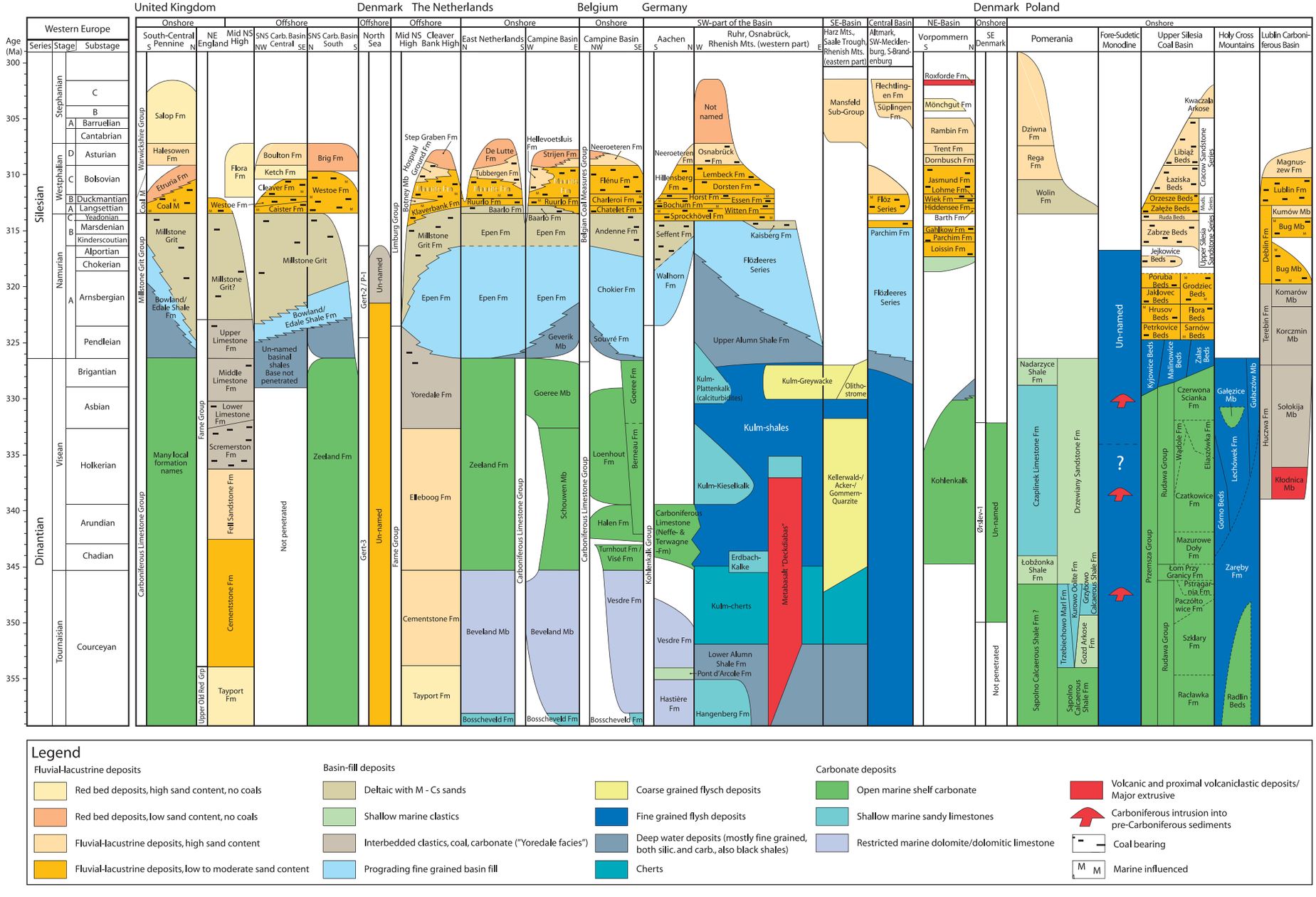

Figure 2.3 Carboniferous lithostratigraphy for the SPB area, based on Michelsen (1971), Bertelsen (1972), Cameron (1993), Delmer et al. (2001), Poty et al. (2001), Menning & German-Stratigraphic-Commission (2002), Besly (2005), Collinson (2005), Van Buggenum & Den Hartog Jager (2007) and Wagner (2007).

By end-Westphalian times, the NWECB was characterised by large-scale folding and inversion (Drozdzewski & Wrede, 1994). Stephanian-Early Permian reorientation of the convergence between Gondwana and Laurasia induced extensive wrench deformation of the Variscan orogen and its northern foreland. These wrench deformations were accompanied by an extensive intrusive and extrusive magmatism (Timmerman, 2004) and caused profound disruption of the European Carboniferous foreland basin and deep truncation of its sedimentary fill.

2.2 Dinantian

2.2.1 Subsidence mechanisms

Along the southern margin of the NWECB, a flexural foreland basin started to develop during the Dinantian (Fig. 2.5), but the greatest part of the NWECB experienced a tensional regime during this time.

Late Devonian – Early Brigantian N-S extension in northern England (north of the LBM) initiated a series of linked, strongly asymmetric, half-grabens acting along a series of NW-SE and NE-SW trending faults which are themselves related to Caledonian structural weakness (Fraser & Gawthorpe, 1990; Coward, 1993; Hollywood & Whorlow, 1993). Some of these fault blocks are under-pinned by Devonian granites which behaved in a buoyant fashion and led to areas of markedly reduced subsidence. Onshore examples are the Askrigg and Alston blocks of northern England (Fig. 2.5). Similar granite-cored highs are suggested in the offshore area by gravity data (Donato et al., 1983; Donato & Megson, 1990). A comparable fault-block setting is interpreted north of the LBM in Belgium, although the intervening basins do not show a clear deep water facies (Muchez et al., 1991). Based on results described in chapter 3, a model of Dinantian extension, resulting in a horst and graben complex, is also proposed for the Netherlands. This was already suggested by Bless et al. (1983). The Polish part of the NWECB also developed in a tensional setting (Ziegler, 1990; Narkiewicz, 2007). A system of NW-SE longitudinal fault zones predominated in the Lublin Basin, related to Variscan reactivation of the Teisseyre-Tornquist Zone (Krzywiec, 2007).

Along the southern margin of the NWECB (from the UK to Poland) a series of (underfilled) foreland basins (Kulm) developed during the Visean as a consequence of loading of the subducting plate (Fig. 2.5). This changed the northern shelf margin of the Rhenohercynian Basin into an active margin (Ziegler, 1990; Burgess & Gayer, 2000; Ricken et al., 2000; Narkiewicz, 2007). Sediments deposited in these flexural basins have been studied in the Rhenish Massif in western Germany where Ricken et al. (2000) showed deposition in asymmetrical wedges.

2.2.2 Basin fill

During the Early Carboniferous, transgression of the Old Red Continent continued. This caused a change from predominantly red-bed facies during the Devonian in the central and northern part of the NWECB to carbonate and deltaic depositional environments during the Early Carboniferous. Along the southern margin of the NWECB – south of the LBM and in the western part of the Rhenish Mountains – carbonate deposition continued across the Devono-Carboniferous boundary (Hance et al., 2001; Gursky, 2006). These carbonates are referred to as Kohlenkalk. In northeast Germany, the Devonian-Carboniferous boundary is a regional unconformity (McCann, 1999). The Holy Cross Mountains is the only area in Poland where sedimentation continued at the Devono-Carboniferous transition whilst in the other areas non-deposition or condensation

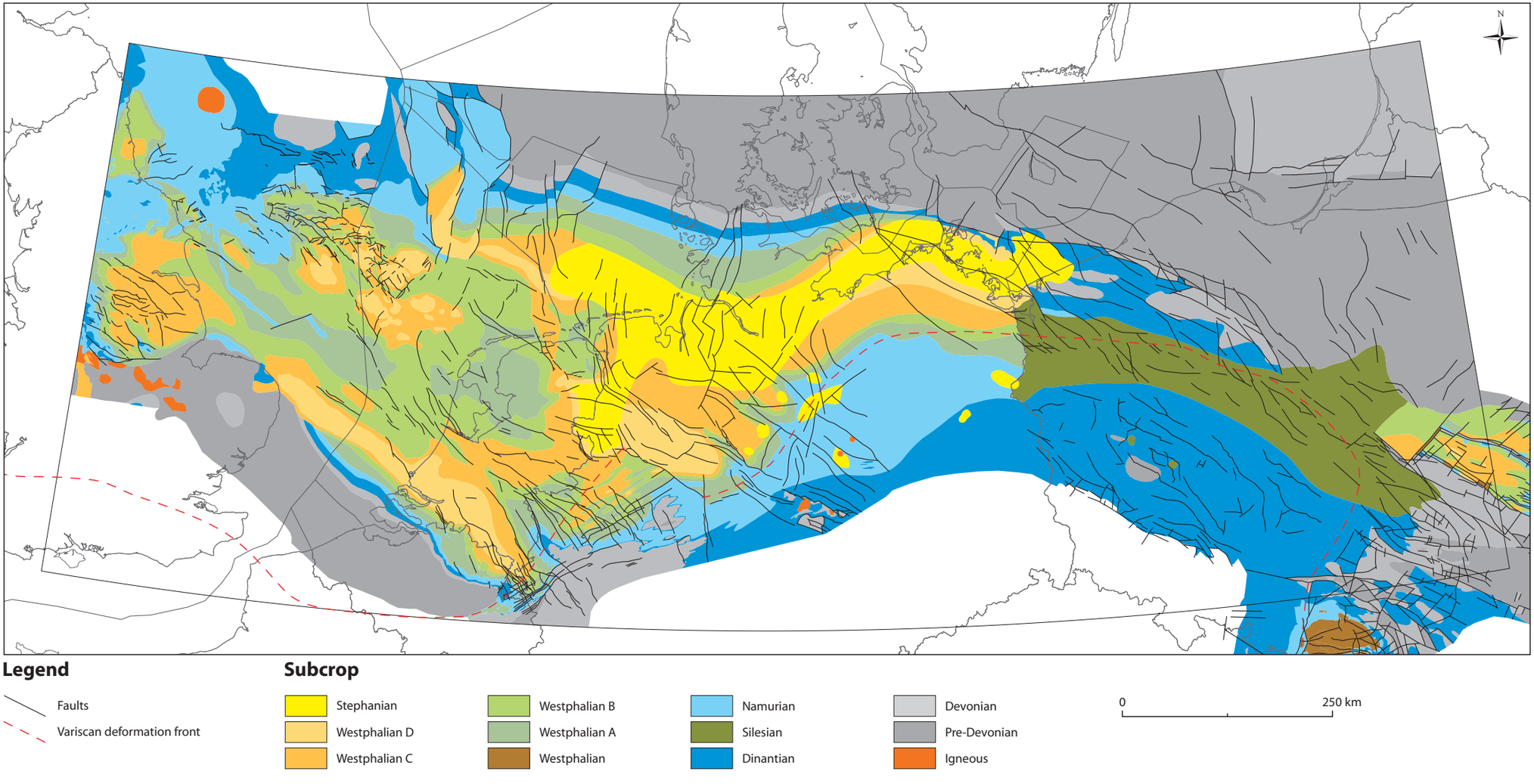

Figure 2.4 Base Permian subcrop map of the SPB area.

occurred (Fig. 2.3). In the northern and eastern parts of the Lublin Basin, the Carboniferous may rest upon older Palaeozoic, Vendian and Riphean formations, or even on the crystalline basement (Cebulak, 1988).

While the Lower Carboniferous succession in the southern NWECB is characterised by carbonate deposition, in northern England and adjacent southern North Sea a major fluvio-deltaic system developed (Figs 2.3, 2.5 & 2.6; Collinson, 2005). The sediment source appears, from palaeocurrent and heavy mineral evidence, to have lain to the north or northeast and is thought to have been a high-relief mountainous area probably within the Scandinavian or Greenland Caledonides. From the Scremerston Fm onward, marine influence increased, which led eventually to deposition of the Yoredale cyclothems (Limestone Fms, Figs 2.3 & 2.6). The three Yoredale Fms are characterised by a cyclic pattern of deposition with laterally extensive

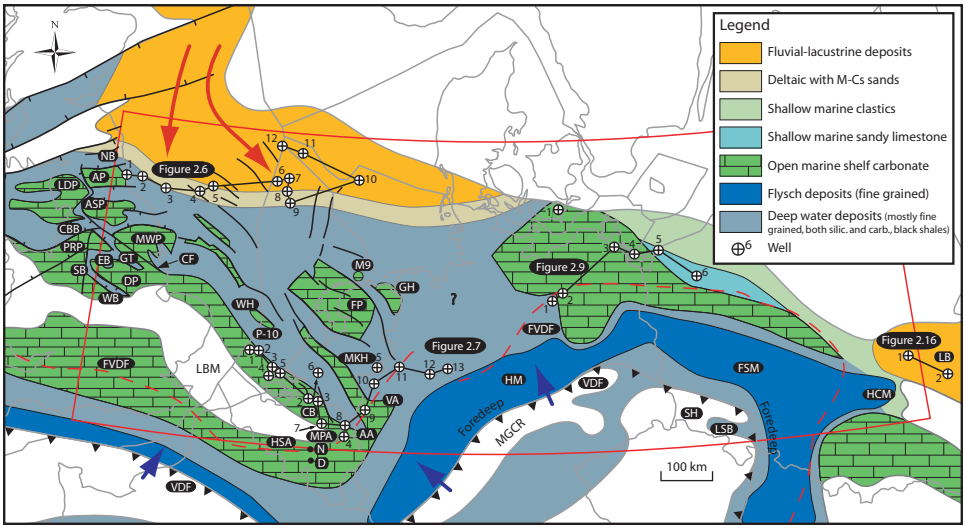

Figure 2.5 Dinantian palaeogeography. Note that the western part of the NWECB is presented in more detail in figure 3.1. AA: Aachen area, AP: Alston Platform, ASP: Askrigg Platform, CB: Campine Basin, CBB: Craven/Bowland Basin, CF: Craven Fault, DP: Derbyshire Platform, D: Dinant, EB: Edale Basin, FP: Friesland Platform, FVDF: Final Variscan Deformation Front, FSM: Fore-Sudetic Monocline, GH: Groningen High, GT: Gainsborough Trough, HSA: Hainaut Sedimentation Area, HM: Harz Mountains, LDP: Lake District Platform, LBM: London Brabant Massif, LSB: Lower Silesian Coal Basin, LB: Lublin Basin, M9: M9 Platform, MKH: Maasbommel-Krefeld High, MPA: Maastricht – Puth area, MWP: Market Weighton Platform, MGCR: Mid German Crystalline Rise, N: Namur, NB: Northumberland Basin, PRP: Pennine/Rossendale Platforms, SB: Staffordshire Basin, SH: Sudetic High, VDF: Variscan Deformation Front, VA: Velbert Anticline, WH: Winterton High and WB: Widmerpool Basin.
Wells in figure 2.6: Harton-1 (1), 41/1-1 (2), 41/10-1 (3), 42/10-2 (4), 43/2-1 (5), A16-1 (6), A14-1 (7), E2-1 (8), E6-1 (9), C/15-1 (10), A/9-1 (11) and 39/7-1 (12). Wells in figure 2.7: O18-1 (1), P16-1 (2), S2-2 (3), S5-1 (4), BHG-1 (5), Beerse-Merksplas (6, located between Heibaart and Turnhout wells), Halen-Citrique (7), Geverik-1 (8), Schwalmtal-1001 (9), Isselburg-3 (10), Münsterland-1 (11), Versmold-1 (12) and Bielefeld (13). Wells in figure 2.9: Eldena 1/74 (1), Parchim 1/68 (2), Loissin 1/70 (3), Pudagla 1/86 (4), Strzezewo 1 (5) and Czaplinek IG 1 (6). Wells in figure 2.16: Stezyca-1 (1) and Lublin IG-1 (2). Other wells: Ørslev-1 (1), Heibaart-wells (2), Turnhout (3), 's Gravenvoeren (4) and Winterswijk-1 (5).

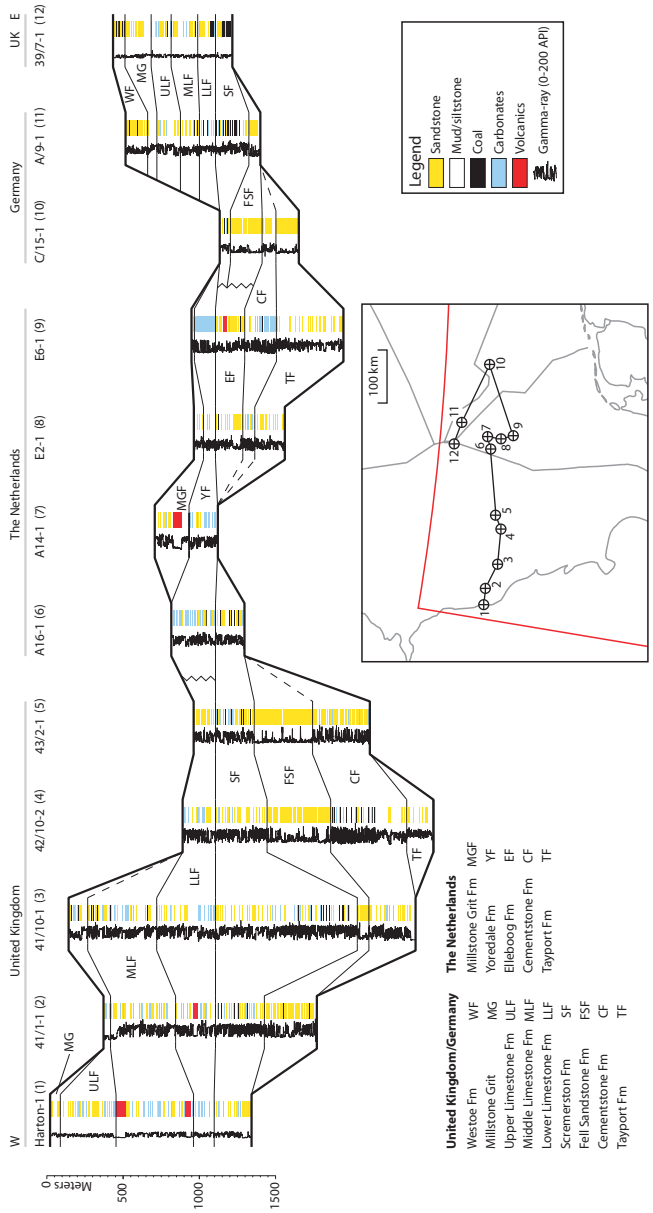

Figure 2.6 Well correlation panel Dinantian Southern North Sea. The Carboniferous section of the German wells used for this correlation panel has been subdivided according to the UK stratigraphic classification scheme. The basal sandy interval of the Elleboog Fm in well E2-1 may be a lateral equivalent of the Fell Sandstone Fm as found further west in UK waters. Although the Scremerston Fm is not formally known in the Netherlands Carboniferous nomenclature, the basal interval in well A16-1 is interpreted as the Scremerstone Fm because of the close correspondence with UK wells. For location of this panel, also see figure 2.5.

limestones overlain by upwards-coarsening units. In some cases, these cycles are several tens of metres thick with sandstones at the top which may be of mouth-bar, shoreface or channel origin (e.g. well 41/10-1, Fig. 2.6). The onset of this pronounced cyclicity during the Late Asbian may indicate glacio-eustatic control which dominates much of the later Carboniferous. Wells along the southern margin of the Mid North Sea High, from the UK coast to the German sector, have penetrated comparable sequences of fluvio-deltaic Dinantian rocks (Figs 2.5 & 2.6). Further to the east (Denmark), the Dinantian succession in well Ørslev-1 (Figs 2.3 & 2.5) indicates an alternation of open marine carbonate ramp and siliciclastic-dominated shelf environments. The log and core data indicate seven such shifts during the Early Visean.

South of this fluvio-deltaic belt in the northwestern part of the NWECB, Lower Carboniferous sediments consists of a limestone and mudstone succession in the onshore UK area either because the area was distal from coarse-grained clastic supply, such as along the southern margin of the Askrigg Platform, or because platforms were isolated from all clastic supply such as on the Derbyshire Platform (Fig. 2.5). The carbonate platforms developed on the footwall areas (e.g. Derbyshire block) whilst relatively deep-water settings occurred in the neighbouring hanging wall areas (e.g. Craven and Widmerpool Basins). These platform carbonates have steep margins towards the adjacent deep-water basins with carbonate-rich mudstones and are fringed by limestone turbidites. The platform margins have fringing and pinnacle reefs and, in some cases, extensive fore-reef breccias.

Tournaisian sedimentation across the area from western Germany (Aachen area and Lower Rhine embayment) along the southern margin of the LBM to Ireland took place on a carbonate ramp, characterised by the development of Waulsortian buildups. These buildups produced an irregular submarine topography. By Middle and Late Visean times, sedimentation was governed by an aggrading carbonate shelf, which caused the blanketing of the pre-existing topography. During the Middle Visean, open marine conditions were restricted to the north while evaporites developed in the south (Saint Ghislain borehole, Rouchy et al., 1984). This inversion of the normal sedimentation pattern was probably related to an early phase of Variscan shortening.

Visean deposits in the Campine Basin are typically shallow-marine limestones of Kohlenkalk type, comprising microbial/cryptalgal buildups and breccias. The succession varies in thickness in response to the general half-graben structure of the basin, but also locally as a result of block faulting. The maximum drilled thickness for the Visean is approximately 760 m (Halen borehole in the eastern Campine Basin, Fig. 2.7) versus 314 m (Heibaart dome) in the western Campine Basin (Fig. 2.5). In the southeastern Netherlands and adjoining area in Belgium, proximal carbonate turbidites are derived from the productive shallow platform on the margins of the LBM. These were deposited on the steep ramp of the relatively deep Maastricht – Puth Basin which filled up during the Visean (well Geverik-1, Figs 2.5 & 2.7).

Until recently, it was not clear whether the carbonate platforms such as found in Belgium and the UK also exist further eastwards in the Southern North Sea, the Netherlands and northwestern Germany. Despite the lack of wells penetrating the Dinantian sequence in this area, (most likely) Visean carbonate platforms have been recently interpreted on seismics (Fig. 2.5 and chapter 3). These results show that carbonate platforms were not only confined to the margins of the NWECB. In Chapter 3 an extensive description of the carbonate platforms in the NWECB is given.

The flexural foreland basin along the southern margin of the NWECB area is shown in figure 2.5 in dark blue. In combination with the sediment-starved basin further northwards in western Germany, this area is called the Kulm Basin. The Velbert Anticline (Fig. 2.5), where slope

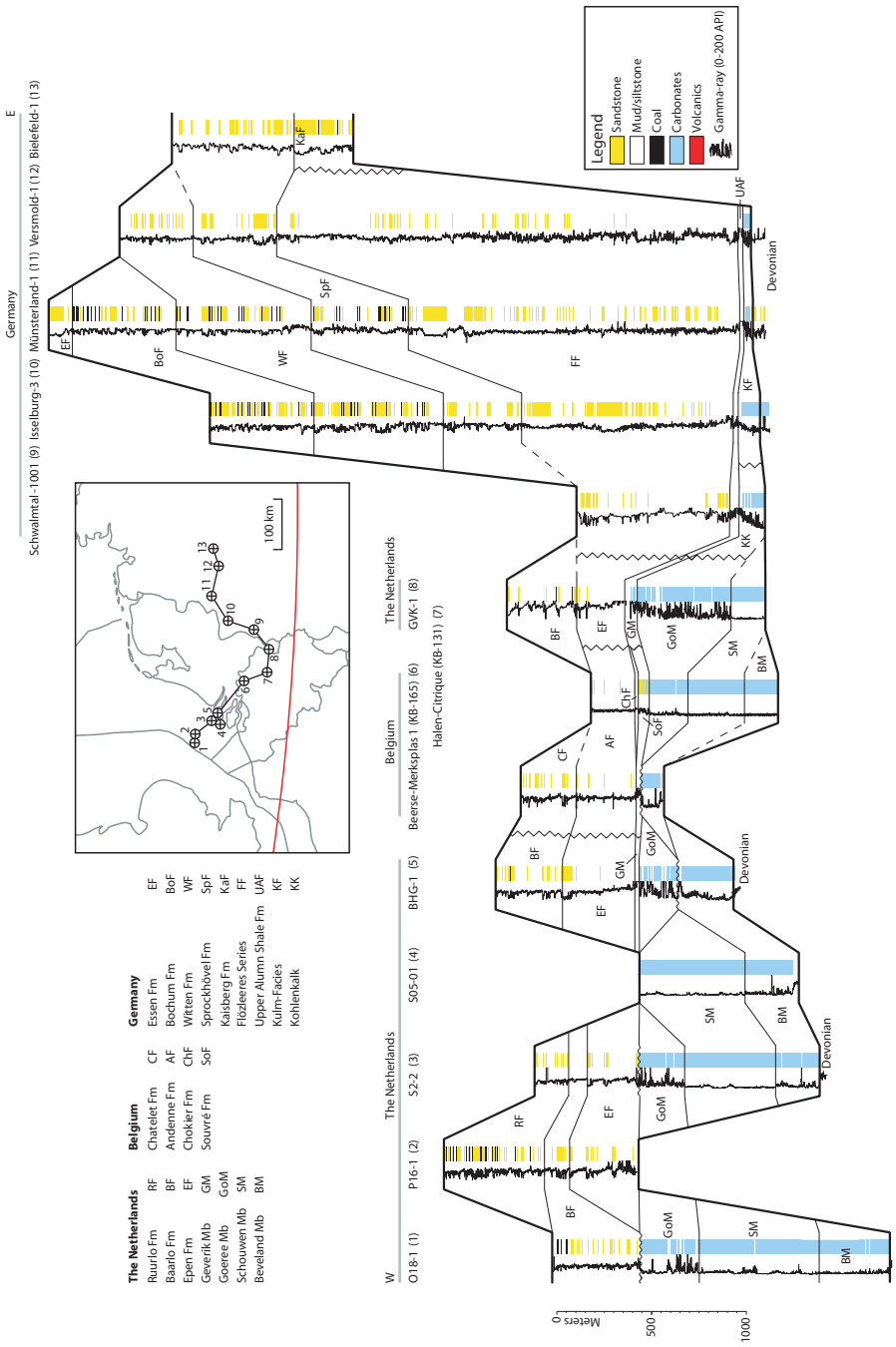

Figure 2.7 Well correlation panel displaying Dinantian – Namurian rocks along the London Brabant Massif up to the Ruhr Basin in the east. The very sandy Andenne Formation in the Halen-Citrique well is probably faulted and therefore the thickness is overestimated in this section. For location of this panel, also see figures 2.5 and 2.8.

sediments have been found, marks the transition between the LBM and the Kulm Basin in the west (Amler & Herbig, 2006). The Kulm Basin was filled with clastics derived from the Mid German Crystalline Rise (MGCR), which started to deliver sediments from the Early Frasnian (Franke, 1989). A maximum palaeowater depth of less than 200 m is assumed for the Kulm Basin. It was differentiated into intrabasinal shallow-water platforms (Gursky, 2006), which also provided sedimentary detritus, and deep swells (Amler & Herbig, 2006). Sediments comprise shales, alum shales, siliceous sediments, cephalopod limestones, carbonate and siliciclastic turbidites (Fig. 2.3), with a strongly variable thickness of up to 1000 m. Due to the asymmetry of the foredeep (Ricken et al., 2000), sediment thickness decreases northwards. The effect of this can be seen in figure 2.7, where the Lower Carboniferous is very thin in those wells that are located north of the foredeep (Schwalmtal – Versmold wells). Therefore, sediment-starved conditions must have prevailed during the Early Carboniferous in this part of the NWECB and it is likely to be the case for much larger areas in the central part of the basin. Sediment from the south was captured in the foredeep while the northern-derived sediment only reached the northern part of the NWECB. The Dinantian section in the Harz Mountains is similar to the one in the west. It shows a Kulm facies with more or less equivalent lithostratigraphic units ("Liegende Alaunschiefer", "Kulm Kieselschiefer", "Kulm Tonschiefer", "Kulm Grauwacken", Fig. 2.3; Buchholz et al., 2006).

In NE Germany, carbonate deposition started during the Visean (Figs 2.3 & 2.5; McCann, 1999). Shallow-marine siliciclastic sedimentation prevailed across the major part of Poland; carbonate platforms were limited to elevated intra-shelf highs and coastal basement blocks (Przemsza Group, Upper Silesia Coal Basin, Figs 2.3 & 2.5; Paszkowski & Szulczewski, 1995; Belka et al., 1996; Narkiewicz, 2007). The northeastern boundary of the basins approximately paralleled the Teisseyre-Tornquist Zone (Fig. 2.2). In the proximal parts of the Lower Silesian Coal Basin, deposition of flysch-type clastics (1500m), derived from the rising Sudetic High to the west, had already commenced during the Late Devonian and became progressively more important during the Dinantian (Ziegler, 1990). This Kulm flysch also occurred in the Fore-Sudetic Monocline, with sediments also derived from the Sudetic High (Unrug & Dembowski, 1971). In eastern Poland (Lublin Basin), the deposition of clastics alternating with carbonates and „Yoredale facies" limestones took place during the Visean (Huczwa Fm, lower part of the Terebin Fm, Figs 2.3, 2.5 & 2.16; Skompski, 1996).

2.3 Namurian

2.3.1 Subsidence mechanisms

Following the Early Carboniferous rifting event in the western part of the NWECB (north of the LBM), subsidence during the Namurian was largely controlled by a broad and regional thermal component (Fraser & Gawthorpe, 1990). However, subsidence rates may actually have continued to be high even with much reduced extensional movement. The relict Visean bathymetry and the compaction of the dominantly fine-grained basin fill ensured that Namurian sedimentation was influenced by fault bounded blocks and basins (Davies et al., 1999). In the central part of the NWECB, Kombrink et al. (2008) showed that an additional Namurian stretching event is needed to accommodate the very thick Namurian/Westphalian succession (chapter 4). Subsidence along the southern margin of the NWECB continued to be controlled by thrust-loading (Warr, 1993; McCann, 1999; Drozdzewski, 2005; Kornpihl, 2005; Narkiewicz, 2007). The Polish part of the NWECB underwent a strong restructuring during Namurian times (Narkiewicz, 2007). Since

uplift took place in Pomerania, this area acted as a source of clastic material for the sedimentary basins of central and southern Poland. The Holy Cross region also became a land area (Fig. 2.8). The Lublin Basin experienced an extensional regime up to the Namurian A, followed by strike-slip movements along the Teisseyre-Tornquist Zone during the remainder of the Namurian.

2.3.2 Transition carbonate platform and basinal shales

The transition from carbonate to siliciclastic sedimentation took place from east to west around the Visean-Namurian boundary (Fig. 2.3). Initially, sedimentation rates remained low, resulting in black shale deposition in major parts of the NWECB. In the Czech Foreland Basin, carbonate platforms were drowned already in the Early Visean (Kornpihl, 2005). Somewhat further to the northwest, siliciclastic deposition in the Upper Silesia Coal Basin started at the Holkerian-Asbian boundary (Fig. 2.3; Szulczewski et al., 1996) and in the NE German Variscan Foreland Basin during Asbian times (Kornpihl, 2005). Westwards, in the Ruhr Basin, the transition from carbonate platform facies to the "Hangende Alaunschiefer" (Fig. 2.3) occurs in the Brigantian (Amler & Herbig, 2006). Visean carbonate platforms in the UK and Belgium were drowned and covered with black shales during the Namurian A (Bowland Shale Fm in well 41/24-2 in Fig. 2.10 or Geverik Mb. in well GVK-1 in Fig. 2.7). It is important to note that the Bowland Shale Fm

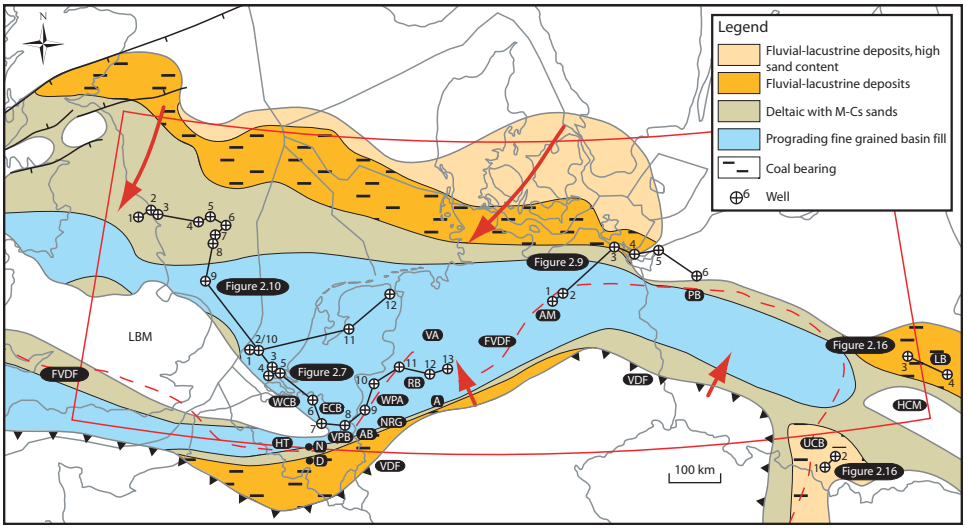

Figure 2.8 Namurian palaeogeography. AB: Aachen Basin, AM: Altmark, A: Arnsberg, D: Dinant, ECB: Eastern Campine Basin, FVDF: Final Variscan Deformation Front, HT: Hainaut Trough, HCM: Holy Cross Mountains, LB: Lublin Basin, N: Namur, NRG: Niederrhein Graben, PB: Pomeranian Basin, RB: Ruhr Basin, UCB: Upper Silesia Coal Basin, VDF: Variscan Deformation Front, VPB: Visé-Puth Basin, WCB: Western Campine Basin and WPA: Wuppertal/Kettwig area.
Wells in figure 2.7: O18-1 (1), P16-1 (2), S2-2 (3), S5-1 (4), BHG-1 (5), Beerse-Merksplas (6), Halen-Citrique (7), Geverik-1 (8), Schwalmtal-1001 (9), Isselburg-3 (10), Münsterland-1 (11), Versmold-1 (12) and Bielefeld (13). Wells in figure 2.9: Eldena 1/74 (1), Parchim 1/68 (2), Loissin 1/70 (3), Pudagla 1/86 (4), Strzezewo 1 (5) and Czaplinek IG 1 (6). Wells in figure 2.10: Kirby-Misperton-1 (1), Cloughton-1 (2), 41/24-2 (3), 43/21-2 (4), 43/17b-2 (5), 43/25-1 (6), 43/28-1 (7), 48/3-3 (8), 48/23-3 (9), P16-1 (10), NAG-1 (11) and TJM-2 (12). Wells in figure 2.16: Goczalkowice IG-1 (1), Chelmek IG-1 (2), Stezyca-1 (3) and Lublin IG-1 (4).

not only represents black shales but also the normal grey (marine) shales belonging to the overall basin fill succession (Fig. 2.3).

In Belgium and the Netherlands, Namurian black shales onlapping the LBM cover a karst surface, indicating the existence of a hiatus (Bouckaert, 1967; Dreesen et al., 1987; Poty, 1997). In some cases, the Namurian is even absent and Westphalian rocks directly overlie Visean carbonates (O18-1 in Fig. 2.7). The more rapidly subsiding areas (Hainaut Trough south of LBM, Souvré Fm in the eastern Campine Basin and Visé-Puth Basin around Maastricht northeast of the LBM, Fig. 2.8), are characterised by siliciclastics alternating with carbonates in the Brigantian that give way to black shales of Arnsbergian age (GVK-1 in Fig. 2.7; Langenaeker, 2000). In the Southern North Sea area, the earliest age of the Bowland shales is Brigantian, suggesting that that area too had been basinal in Late Visean times (Fig. 2.3).

2.3.3 Basin fill

The Namurian basin fill succession in the north and west of the NWECB can be subdivided in four units (Collinson, 2005). The first part consists of a basinal shale unit, whose base may be of earliest Namurian or even Visean age (see above). It is overlain by a second unit consisting of turbiditic sandstones of variable thickness (e.g. well 41/24-2 in Fig. 2.10). These, in turn, are overlain by coarsening-upward siltstones (see Bowland Shale Fm in well 43/17b-2 and Epen Fm in wells TJM-2 and NAG-1, Fig. 2.10), whose thickness relates to the basin depth, and finally by a unit comprising channel sandstones. Some of these may be multistorey and tens of metres thick (Top Bowland/Epen/Flözleeres Series and base of overlying formations, Figs 2.7 & 2.10; e.g. BHG-1 in Fig. 2.7). Palaeosols and coals, deposited in near-emergent conditions, first occur above these channel sandbodies. The basin fill succession represents the progradation of a turbidite-fronted delta system where turbidity currents by-passed the silt-dominated slope via feeder channels. The rapidly deposited slope deposits may be affected by soft-sediment deformation in the form of slumps and growth faults. Above the basin fill succession, the remainder of the Namurian can be characterised as "cyclic": Millstone Grit in the UK and time-equivalent formations elsewhere in the NWECB (Fig. 2.3). The cyclothems are upwards coarsening in character and overlie marine bands (thin mudstone beds). The individual cyclothems are typically a few tens of metres thick. The upper sandstones are deposited as mouth-bar and channel sandstones. Some thicker (20-30m), multi-storey coarse-grained examples are thought to be incised palaeovalleys fills formed during periods of rapidly falling base level. They are thought to result from successive progradations from the north of a major delta system, comparable in scale and style to the present-day Lena Delta of eastern Siberia.

Onshore UK at outcrop, the Namurian shows a progressive north to south in-fill of deep sub-basins with the most northerly Craven/Bowland Basin being filled in the Pendleian, the more southerly Edale Basin being filled in the Kinderscoutian and the most southerly Staffordshire Basin during the mid-Marsdenian (Fig. 2.5). The Northumberland Basin never experienced deep-water conditions in the Namurian as a consequence of its proximal setting. Offshore UK and offshore Netherlands (northern part), a similar situation seems to apply. In the Namurian of the northern Netherlands onshore area a distal setting is likely, regarding the very thick shale sequence (>2000m) with only minor thin sandstone beds (Van Buggenum & Den Hartog Jager, 2007; wells TJM-2, NAG-1, Fig. 2.10). The boundary between the areas with a northern source (Fennoscandia and Old Red continent) and a southern source (Variscan Mountains) is still unclear (Frank et al., 1992). The sediments deposited in the Campine Basin (Fig. 2.8) came from the southeast. Here, coal seams and seat earths as early as the Late Kinderscoutian (Namurian B) have been found,

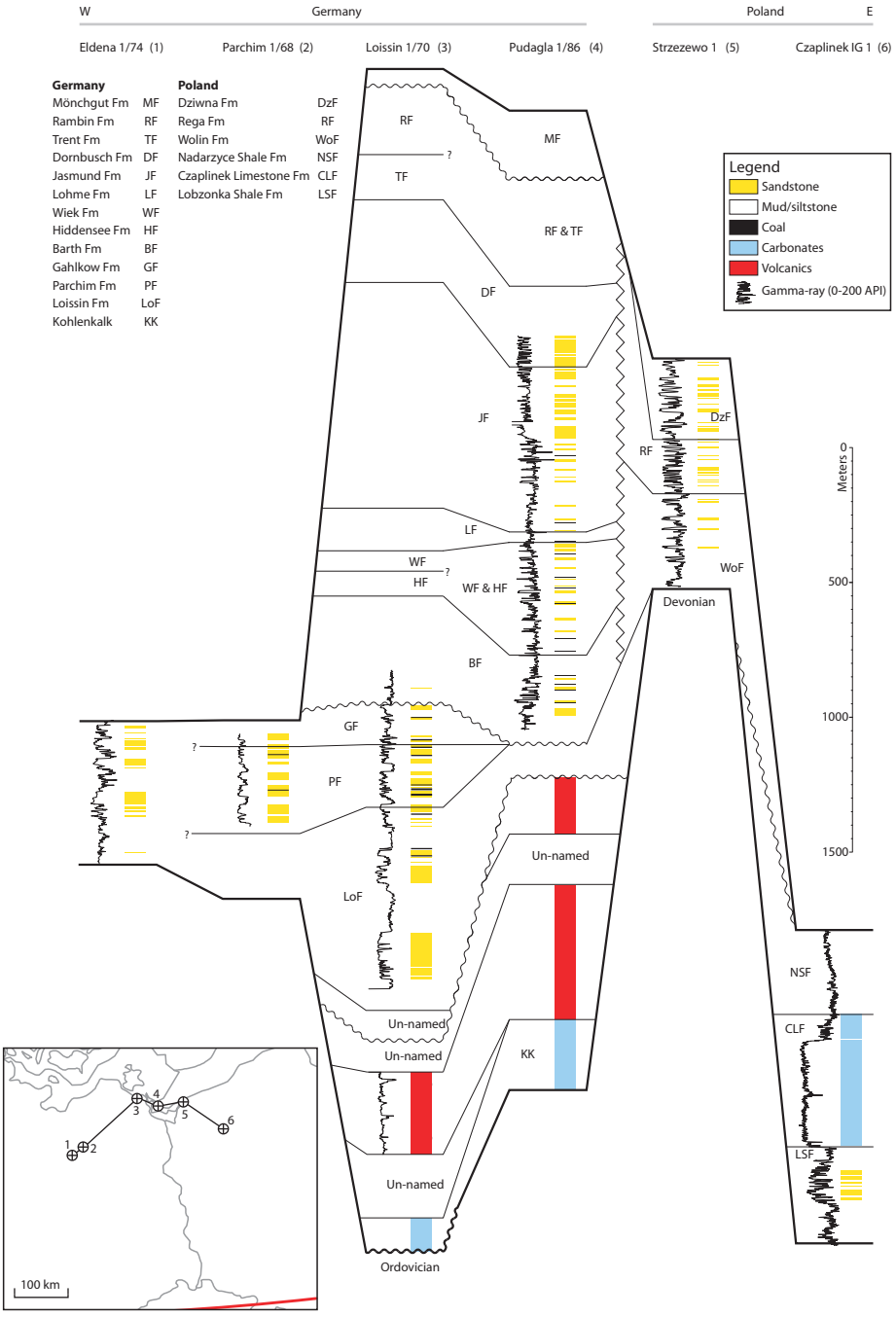

Figure 2.9 Well correlation panel in the Altmark – Rügen – Pomerania area. Unconformities in Loissin 1/70 from Kornpihl (2004). For location of this panel also see figure 2.8.

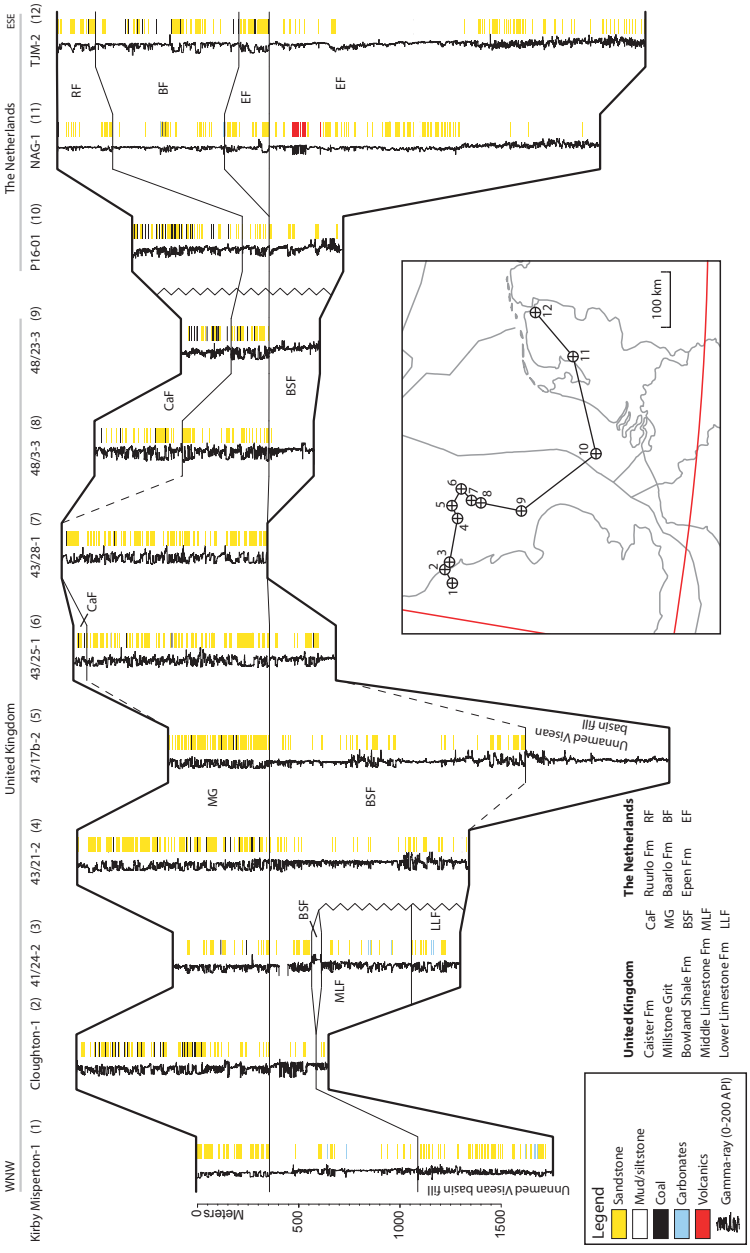

Figure 2.10 Well correlation panel showing mainly Namurian rocks in the Southern North Sea and onshore Netherlands. For location of this panel also see figure 2.8.

whilst in the western Campine Basin no coals or seat earths are known from the Namurian (Fig. 2.3; Langenaeker, 2000). These strata progressively overlap the LBM (Bouckaert, 1967). In the southernmost coal basins (Dinant Synclinorium and eastern part of the Namur-Vesdre Syncline, closer to the current location of the Variscan deformation front, Fig. 2.8), coal deposition already occurred during the Arnsbergian.

In the greatest part of the Ruhr Basin, the Lower Namurian A represents a continuation of sediment-starved conditions that prevailed during the Early Carboniferous (Drozdzewski, 2005). The Lower Namurian A is poorly developed (20-200m) or even absent in parts of the Ruhr Basin (Fig. 2.8), except in the area around Arnsberg, where it has a thickness of around 800 m. In the meantime, flysch deposition (Fig. 2.3) continued further south. Sedimentation rate increased during Late Namurian A and B when approximately 1350 m of flysch was deposited in the Ruhr Basin (Flözleeres Series, Figs 2.3 & 2.7; Wrede, 2000). The Niederrhein Graben (Fig. 2.8) possibly functioned as a main discharge zone from the Variscan foredeep to the north (Drozdzewski, 2005). In the Aachen Basin the first coal seam occurs in the Namurian A, similar to the adjoining Belgian deposits south of the LBM. In the Ruhr Basin paralic sedimentation started in Namurian B, similar to the Campine Basin north of the LBM in Belgium (Kaisberg Fm, Fig. 2.7). In northeastern Germany, paralic depositional environments prevailed during the Namurian (evidence of coal seams), grading to a deeper marine environment in the south (McCann, 1999; Fig. 2.7). In this area (Altmark) a gradual shallowing took place from deep marine during Namurian A to paralic deposition in the Westphalian (Hoth et al., 2005). For example, in well Parchim 1/68, paralic Namurian B rocks have been found (Fig. 2.9, Loissin Fm).

In the Lublin Basin, cyclic coal deposition continued varying from shallow shelf, deltaic and fluvio-lacustrine environments with low to moderate sand content (Waksmundzka, 2007b; Fig. 2.16). These rocks form the upper part of the Terebin Fm and the Bug Member (Fig. 2.3). In the Upper Silesia Coal Basin paralic sedimentation started in the Namurian A (Kotas, 1995; Figs 2.3, 2.8 & 2.16).

2.4 Westphalian

2.4.1 Subsidence mechanisms

In the western part of the NWECB, north of the LBM, passive thermal cooling that already started during the Namurian (see above) continued into the Westphalian (Fraser & Gawthorpe, 1990). Along the southern margin of the NWECB, the axis of the flexural foreland basin migrated northwards (McCann, 1999; Drozdzewski, 2005; Fig. 2.11) in response to foreland-ward propagation of the Varsican nappe stack. Besides regional thermal subsidence, Drozdzewski et al. (2008) suggest that sedimentation in the NWECB may be controlled by NW-SE striking faults (e.g. Elbe Lineament, Uelzen and Osning Faults, Fig. 2.2) and a less important N-S to SSW-NNE fault-trend. These faults are probably inherited from the Caledonian basement.

During mid-Westphalian C times, a compressional tectonic regime was established in the western parts of the NWECB (Fraser & Gawthorpe, 1990; Ziegler, 1990), reflecting the build-up of collision-related intraplate compressional stresses (Ziegler et al., 1995; Ziegler et al., 2002; Ziegler & Dèzes, 2006). This Variscan inversion event resulted in the development of a series of broad anticlines in the hanging walls of basin-bounding faults (Fraser & Gawthorpe, 1990). For instance, in both the UK onshore and Silverpit areas the influx of sand during the mid Westphalian C marks the onset of tectonic deformation *within* the Pennine/UK Southern North Sea Basins.

In the Ruhr and Campine Basins, Variscan folding only commenced in or after Stephanian time at about 300 Ma (Drozdzewski et al., 2008). This is comparable to the external parts of the Variscan fold belt in Poland in which compressional deformation commenced only during the Late Westphalian D and Early Stephanian (Narkiewicz, 2007).

2.4.2 Basin fill

The Westphalian sedimentary sequence in the NWECB reflects continued aggradation at or near emergent conditions. The Early Westphalian is characterised by deltaic to fluvio-lacustrine deposits with numerous coal layers, giving way to well drained fluvial sediments (eventually red beds) in the Late Westphalian.

2.4.2.1 Westphalian A

During the Westphalian A, deltaic and sometimes cyclic depositional sedimentation continued in the southernmost parts of the UK North Sea, the Netherlands, the Campine, NE Germany and western Poland (e.g. wells 44/19-3 and K1-2 in Fig. 2.12 and wells Goldhoorn-1 and Münsterland-1 in Fig. 2.13). In the Ruhr Basin, the Westphalian A shows a fluvio-lacustrine facies in the south but give rapidly way to deltaic sedimentation in the north (Fig. 2.11 and well-logs in Fig. 2.13). Compared to the Namurian succession, there are fewer marine bands and increasingly important coal seams mark a transition to deposition under fluvio-lacustrine conditions (Fig.

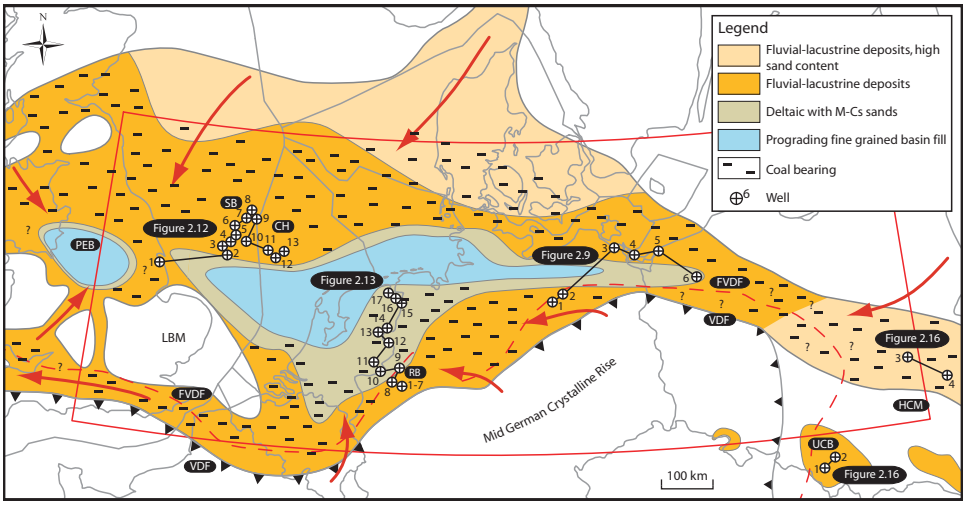

Figure 2.11 Westphalian A palaeogeography. CH: Cleaverbank High, FVDF: Final Variscan Deformation Front, LB: Lublin Basin, LBM: London Brabant Massif, PEB: Pennine Basin, RB: Ruhr Basin, SB: Silverpit Basin (SB), UCB: Upper Silesian Coal Basin and VDF: Variscan Deformation Front.
Wells in figure 2.9: Eldena 1/74 (1), Parchim 1/68 (2), Loissin 1/70 (3), Pudagla 1/86 (4), Strzezewo 1 (5) and Czaplinek IG 1 (6). Wells in figure 2.12: Tetney Lock-1 (1), 48/10b-4 (2), 48/5-1 (3), 44/26c-6 (4), 44/26-SA04 (5), 44/21-3 (6), 44/18-2z (7), 44/13-1 (8), 44/19-3 (9), 44/23-4 (10), K1-2 (11), K5-2 (12) and K2-2 (13).
Wells in figure 2.13: Alte-Fahrt-1 (1), Vogelsang-5 (2), Schorfheide-2 (3), Holtkamp-5 (4), Vogelsheide-3 (5), Altenkamp-3 (6), Specking-1 (7), Münsterland-1 (8), Winterswijk-1 (9), Ruurlo-1 (10), Hengevelde-1 (11), Tubbergen-8 (12), Hardenberg-2 (13), Dalen-7 (14), Nieuweschans-1 (15), Goldhoorn-1 (16) and Tjuchem-2 (17). Wells in figure 2.16: Goczalkowice IG-1 (1), Chelmek IG-1 (2), Stezyca-1 (3) and Lublin IG-1 (4).

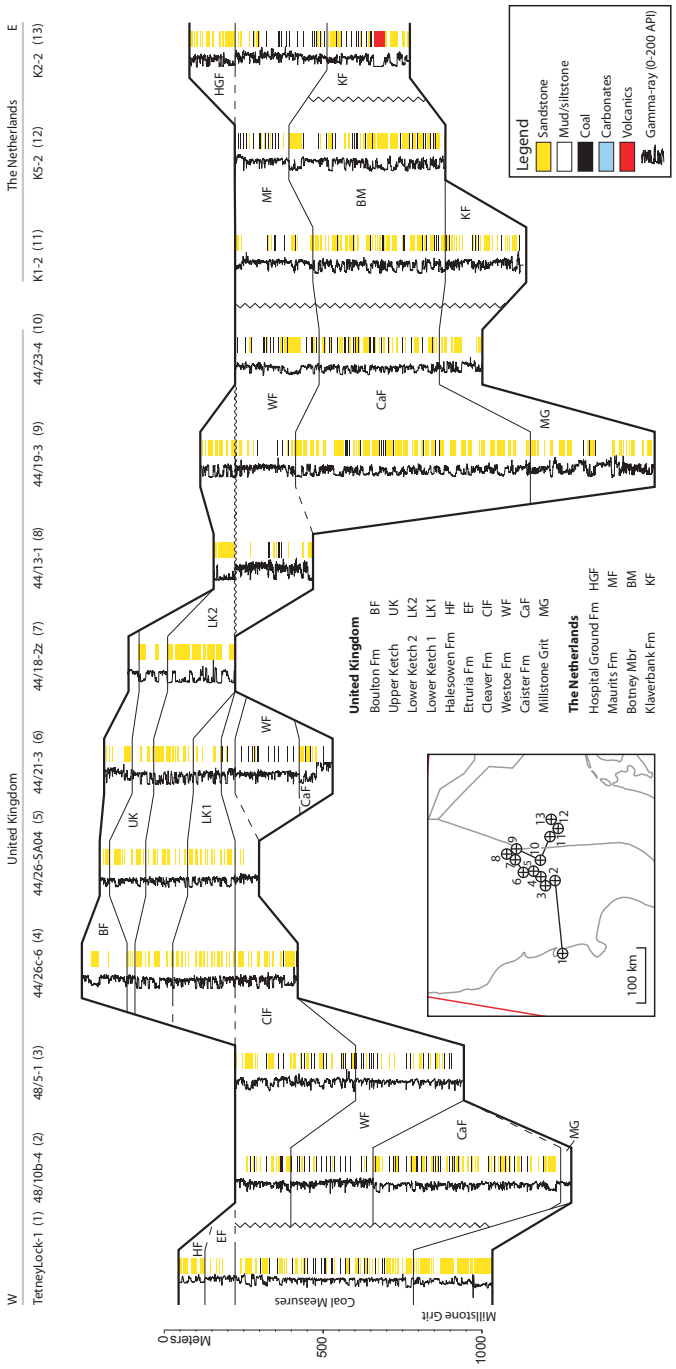

Figure 2.12 Well correlation panel showing mainly Westphalian rocks in the Southern North Sea. For location of this panel also see figure 2.11.

2.11). In southern and western Poland, transpressional uplift of the Malopolska and Holy Cross massifs resulted in the isolation of the Upper Silesian Coal Basin of the Variscan foreland basin (Ziegler, 1990; Narkiewicz, 2007). Coal deposition continued in a fluvio-lacustrine environment (Bojkowski & Dembowski, 1988) characterised by a low to moderate sand content (Mudstone Series, Figs 2.3 & 2.16), but marine bands do not occur any more. In the Lublin Basin the number of sandstones is higher than in the Upper Silesia Coal Basin (Fig. 2.16).

2.4.2.2 Westphalian B

The Westphalian B is characterised by the highest number of coal seams, deposited in a lower delta plain environment (Waksmundzka, 1998; Drozdzewski, 2005; Hoth et al., 2005; Van Buggenum & den Hartog Jager, 2007). Although a shift from lower to upper delta plain conditions (high sand content) already took place during the Westphalian B along the margins of the basin (e.g. the Campine Basin; Paproth et al., 1996), the sand-content on average is at a minimum during the Westphalian B. In the Southern North Sea area, the sand-poor, dominantly fine-grained Westoe Fm in UK waters (Figs 2.3 & 2.12) equates to a part of the onshore UK Westphalian succession in which the sandstone provenance is from the southwest (Morton et al., 2004). The coal-rich Westoe Fm reflects a distal position in this dispersal system. In the UK onshore and Silverpit/Cleaverbank areas there is a marked increase in sandstone content in the coal-bearing succession during mid Westphalian B (Botney Member in the Netherlands, Cleaver Fm in UK, Figs 2.3 & 2.12). This sediment is partly derived from the Ringkøbing-Fyn High, which became the dominant sediment source. During the Lower Westphalian B, the lowest sand percentages (10-15%) occur in the Ruhr Basin (Essen and Horst Fm, Fig. 2.13). The Variscan Mountains acted as the source of these sands from where they were transported basin-parallel to the Ruhr Basin (Drozdzewski, 2005). In the Netherlands, palaeoflow directions indicate transport from the northeast and southeast (Van Buggenum & den Hartog Jager, 2007). A maximum number of coal seams are also found in eastern Germany during Westphalian B times. Sandstone percentages are somewhat higher in Altmark than in Vorpommern (Hoth et al., 2005). As in the Westphalian A, the Westphalian B in the Lublin and Upper Silesia Coal Basins in Poland is also characterised by fluvio-lacustrine conditions (Fig. 2.3).

2.4.2.3 Westphalian C

From Westphalian C times onwards an increasing amount of fluvial red beds occur, related to changes in patterns of fluvial input. This is caused by the onset of intrabasinal Variscan deformation and by a gradual drying of the climate (Besly et al., 1993). The red-bed formations are characterised by reddened, bioturbated lacustrine mudrocks, lacustrine deltas, palaeosol-dominated overbank successions and alluvial channel systems. The succession contains variable amounts of sandstone, depending on the proximity to fluvial input and the nature of the fluvial catchment areas. The trend towards more red-bed deposits is first apparent in the western part of the NWECB in the Westphalian C: by Westphalian D times red-beds were developed over the entire area.

In the northern part of the UK, northerly-derived reddened sediments of the Ketch and Flora Fms were deposited in this stage. From latest Westphalian B onwards, a significant red-bed development (Etruria Fm) is also found in the southern part of the Pennine Basin, prograding to the north through time (Fig. 2.3). Between the northerly-derived Ketch system and the southerly-derived Etruria system there is an area, in Yorkshire, in which Westphalian C red beds are absent (Fig. 2.14). It would appear that this area was not reached by red-bed drainage conditions; it marks an area of persistent subsidence and coal-swamp formation (Pennine depocentre). It

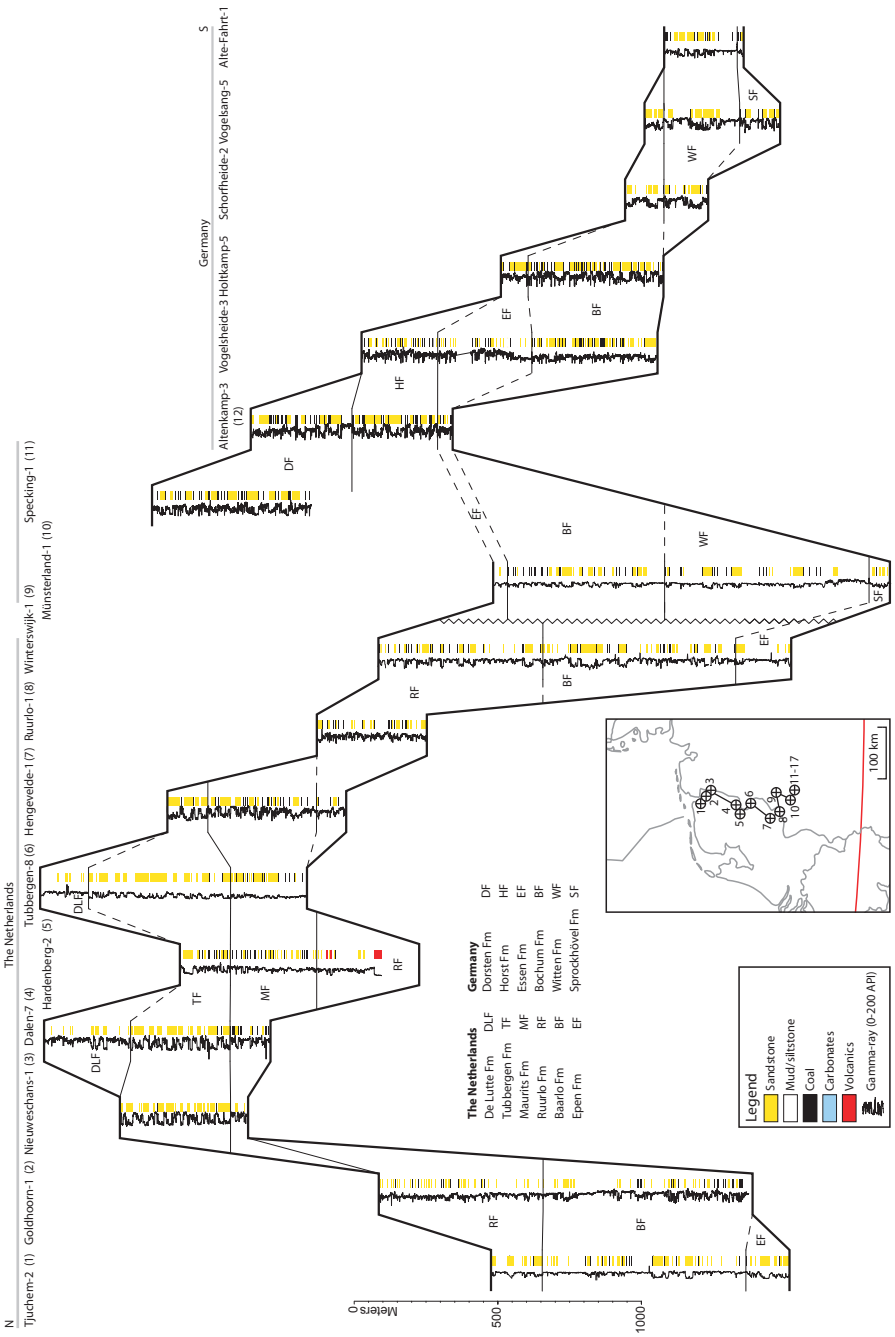

Figure 2.13 Well correlation panel showing Westphalian rocks in a line running from the Ruhr Basin to the northern Netherlands. For location of this panel also see figure 2.11.

is possible that fluvial systems derived from the Variscan front and the Ringkøbing-Fyn area drained westwards through this subsidence centre in northern England (Fig. 2.14), although their subsequent fate is not known. The southerly derived sediments, the first in the UK part of the NWECB, were sourced from the uplifted LBM. This in turn reflects the onset of significant deformation in southern England (Besly, 1988). In contrast, subsidence and coalification trends suggest no significant uplift of the LBM took place further to the east in Belgium.

Simultaneously, in the Netherlands onshore area, relatively thick fluvial sandstones (up to 40 m) were deposited during Westphalian C (Tubbergen/Hellevoetsluis Fms, Figs 2.3 & 2.13). A similar increase in southerly-derived sands is found in the Westphalian C in the Campine Basin and the Ruhr Basin (Lembeck and Dorsten Fms, Fig. 2.3). No significant red-bed development took place, but the coal content is lower than in the Westphalian B. In contrast to the Westphalian C rocks in the Ruhr area and the Netherlands, the Westphalian C in NE Germany is however rather low in sand content (<25 %; Hoth et al., 2005). Here, the Westphalian C can be seen as a transitional facies from poorly drained sediments with coal seams to well drained conditions. Slightly further to the east, in Pomerania, the transition from deltaic to fluvial conditions took place during the Westphalian C only (Figs 2.3 & 2.9). In the isolated Upper Silesia Coal Basin sandstone percentages increase during the Westphalian C.

2.4.2.4 Westphalian D

Due to better drainage conditions, red beds expanded from the Variscan fold and thrust belt into the southern parts of the Pennine and UK Southern North Sea where they form the Boulton and Brig Fms (Fig. 2.3). Some of these red-bed deposits have low sand contents and must be seen as distal flood plain deposits, with only a minor amount of intercalated sheetfloods. These are found in the eastern part of the Netherlands (De Lutte Fm, Fig. 2.15; Pagnier & van Tongeren, 1996). In other areas, fluvial activity was much more vigorous, resulting in high sand contents. In the Osnabrück area (Fig. 2.15), the Westphalian D is characterised by sand percentages of up to 80%, deposited in major river systems. Here, some thin coal seams are found. This also applies to the Campine Basin, where the Neeroeteren sandstones form a facies-equivalent of the Tubbergen Fm of the Netherlands (Westphalian C). Further east, in the Rügen area, Westphalian D rocks were deposited under well-drained conditions in a braided fluvial system (Hoth et al., 2005). The sand percentages are relatively high. It is uncertain whether sedimentation during the Westphalian D continued in central Poland (Pomerania) and whether a connection existed between the Rügen area and the Lublin Basin.

2.5 Stephanian

2.5.1 Subsidence mechanisms

The regional stress pattern in the NWECB changed dramatically at the Westphalian-Stephanian boundary. The latest Westphalian termination of orogenic activity in the Variscan fold belt was followed by the establishment of a system of dextral and sinistral wrench faults (Ziegler, 1990; Ziegler & Dèzes, 2006). This resulted in the development of a system of transtensional and pull apart basins. The most important example of such a basin in the NWECB is the Ems/North Sea/Stralsund Basin (Fig. 2.4; Krull, 2005). This Stephanian basin probably owes its existence to the presence of the underlying Teisseyre-Tornquist Zone (the Caledonian suture zone between Avalonia and the Eastern European Craton). Activation of the Teisseyre-Tornquist Zone wrench

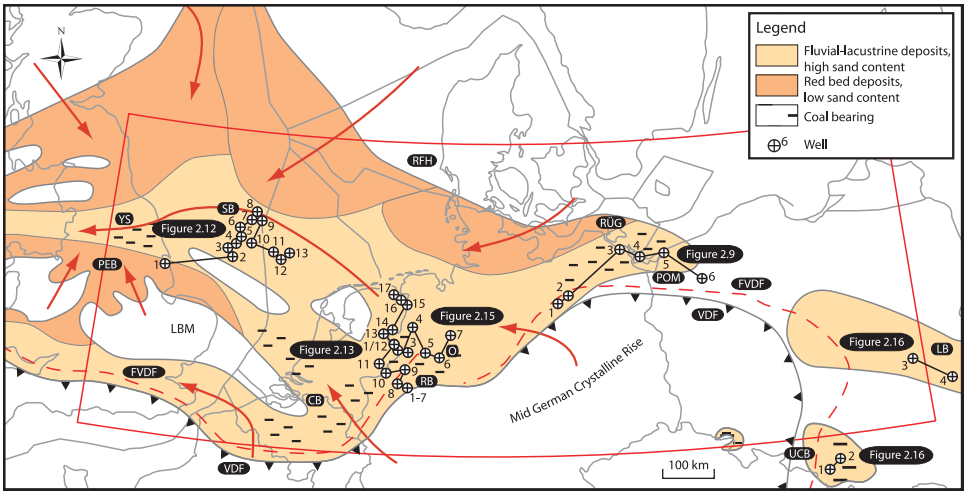

Figure 2.14 Westphalian C/Westphalian D palaeogeography. CB: Campine Basin, FVDF: Final Variscan Deformation Front, LBM: London Brabant Massif, LB: Lublin Basin, O: Osnabrück area, PEB: Pennine Basin, POM: Pomerania, RFH: Rinkøbing-Fyn High, RÜG: Rügen, RB: Ruhr Basin, SB: Silverpit Basin, UCB: Upper Silesian Coal Basin, VDF: Variscan Deformation Front and YS: Yorkshire.
Wells in figure 2.9: Eldena 1/74 (1), Parchim 1/68 (2), Loissin 1/70 (3), Pudagla 1/86 (4), Strzezewo 1 (5) and Czaplinek IG 1 (6). Wells in figure 2.12: Tetney Lock-1 (1), 48/10b-4 (2), 48/5-1 (3), 44/26c-6 (4), 44/26-SA04 (5), 44/21-3 (6), 44/18-2z (7), 44/13-1 (8), 44/19-3 (9), 44/23-4 (10), K1-2 (11), K5-2 (12) and K2-2 (13). Wells in figure 2.13: Alte-Fahrt-1 (1), Vogelsang-5 (2), Schorfheide-2 (3), Holtkamp-5 (4), Vogelsheide-3 (5), Altenkamp-3 (6), Specking-1 (7), Münsterland-1 (8), Winterswijk-1 (9), Ruurlo-1 (10), Hengevelde-1 (11), Tubbergen-8 (12), Hardenberg-2 (13), Dalen-7 (14), Nieuweschans-1 (15), Goldhorn-1 (16) and Tjuchem-2 (17). Wells in figure 2.15: Tubbergen-8 (1), De Lutte-6 (2), Norddeutschland-8 (3), Apeldorn-Z2 (4), Bockraden-6 (5), Osnabrück-Holte-Z1 (6) and Rehden-21 (7). Wells in figure 2.16: Goczalkowice IG-1 (1), Chelmek IG-1 (2), Stezyca-1 (3) and Lublin IG-1 (4).

zone is documented by the latest Westphalian-early Stephanian onset of magmatic activity in the Oslo Graben (Sundvoll et al., 1992). Basins such as the Ems Basin (N-S striking belt of Stephanian deposits in northwest Germany, Fig. 2.4) should be seen as products of a secondary shear system linking the major systems, such as the Teisseyre-Tornquist Zone (Ziegler et al., 2006). It is likely that Stephanian rocks had a much wider distribution, but Early Permian uplift (Saalian unconformity) caused intense erosion (see the isolated remnants of Stephanian rocks in eastern Germany; Ziegler, 1990; Krull, 2005). For instance, thermal modelling in the Ruhr area showed that a thick sequence of Stephanian rocks might have been present (Littke et al., 2000). In most areas, Stephanian rocks are found unconformably overlying Westphalian or Namurian strata. Only in the axial parts of the Ems/North Sea/Stralsund Basin, Stephanian deposits rest conformable on Westphalian rocks (Ziegler, 1990). It has to be realised that the areal extent of Stephanian deposits as shown in figure 2.4 represents the sedimentary rocks. On top of these, extensive Stephanian/Early Permian volcanic complexes occur in some areas, which may exceed the areal distribution of the sedimentary rocks.

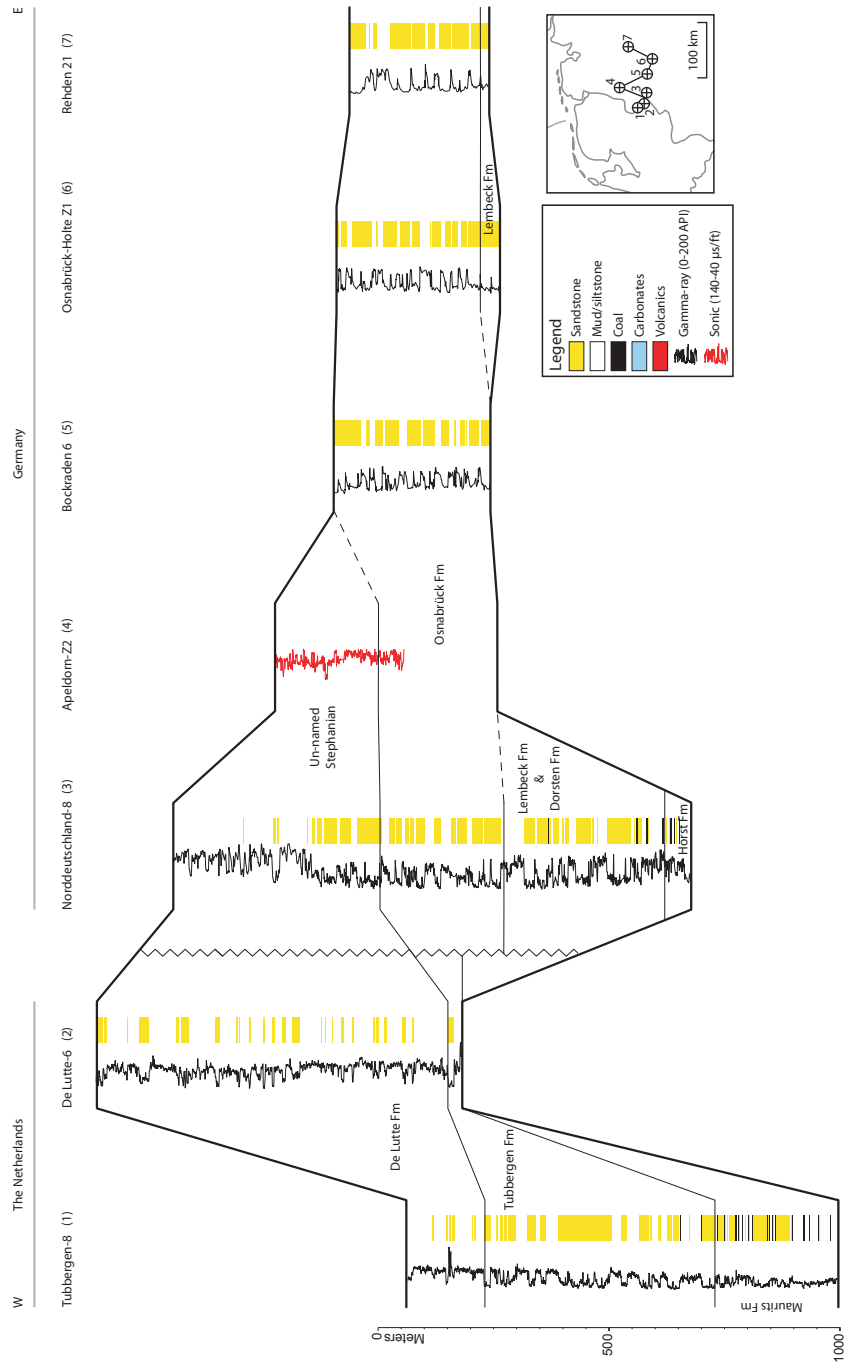

Figure 2.15 Well correlation panel showing Westphalian and Stephanian rocks the Ems area. For location of this panel also see figure 2.14.

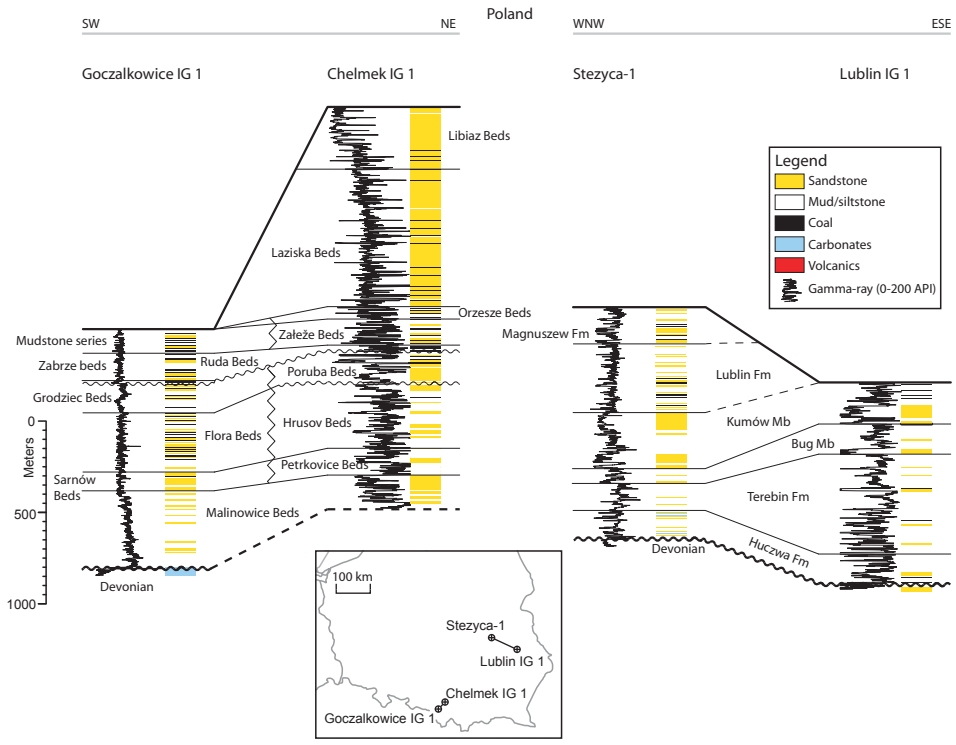

Figure 2.16 Well correlation panel showing Carboniferous rocks in the Upper Silesia Coal Basin and the Lublin Basin in Poland. The transition between the Malinowice Beds and the underlying Devonian cannot be seen in figure 2.3; this is only a local feature. For location of this panel also see figures 2.5, 2.8, 2.11 and 2.14.

2.5.2 Basin Fill

The Stephanian succession reflects deposition under slightly more arid conditions compared to Westphalian D sediments. Therefore, dating the Stephanian barren sequence is often problematic (Hartkopf-Fröder, 2005). The most distal facies in the Ems/North Sea/Stralsund Basins is found in the North Sea area. Here, wells penetrating Stephanian deposits show a slightly lower sand content than in the Ems Basin (Selter, 1990). Krull (2005) mentions grey (poorly drained) claystones and even some coal layers. In the Ems Basin, sand content (max 45%) increases relative to the Westphalian D, which is interpreted as narrowing of the basin (Selter, 1990; Fig. 2.15). These sands were deposited in alluvial fan systems, draining to the north. Moderately developed vertisols and calcretes are common in these deposits. The Netherlands, next to the Variscan Mountains in the south, were a significant sediment source during the Stephanian. In northeast Germany (Rügen), sand contents are slightly higher; the younger Stephanian deposits, unconformably overlying older Stephanian rocks, contain 55-70% of sand (Hoth et al., 2005). Most of the red beds have been deposited in alluvial fan systems. Marine influence could not be proven. Fluvio-lacustrine deposition with high sand content persisted through the Stephanian over only a small part of Pomerania (Dziwna Fm) and the Upper Silesia Coal Basin (Kwaczała Arkose). In the remaining areas, erosion took place. The youngest Stephanian deposits in NE Germany consist of andesitic volcanics. These mark the onset of the Permo-Carboniferous magmatic cycle which led to the emplacement of granitic bodies of Greifswald, Roxförde and Flechtingen around 300 Ma.

CHAPTER 3

Seismic interpretation of Early Carboniferous (Dinantian) carbonate platforms in the Netherlands; implications for the palaeogeographical and structural development of the Northwest European Carboniferous Basin

This chapter is based on: Henk Kombrink, Henk van Lochem and Kees J. van der Zwan, Seismic interpretation of Early Carboniferous (Dinantian) carbonate platforms in the Netherlands; implications for the palaeogeographical and structural development of the Northwest European Carboniferous Basin. Submitted to Journal of the Geological Society.

Abstract

An important element of the Dinantian in the Northwest European Carboniferous Basin (NWECB) is a series of carbonate platforms and intervening shale-dominated troughs. These structures have been mainly found along the margins of the NWECB; e.g. northern England, along the London Brabant Massif, in western Germany and in Poland. To date, a lack of (well)data prevented the construction of a palaeogeographical and structural framework of the Dinantian in the centre of the NWECB (the northern part of the onshore Netherlands and adjacent areas). However, recent investigation of high quality seismic 3D surveys revealed a series of buildups in this area. Based on a comparison with platform dimensions in the NWECB and time-equivalent structures outside the NWECB, it is concluded that these buildups represent Dinantian carbonate platforms. Three platforms have been interpreted. The largest platforms (> 20 km in length) occur on the Friesland Platform and the Groningen High. In between these platforms, the Lauwerszee Trough probably represents a Dinantian basin. A third and relatively small platform could be interpreted in the M09 offshore block. Based on these findings and the publication of some recent data on the Dinantian of the NWECB, the following depositional and structural model for this area is proposed. During the Tournaisian, ramp-type carbonate sedimentation took place in the basinal areas. Due to ongoing subsidence (probably induced by rifting, such as observed in the UK) carbonate deposition gradually onlapped onto the topographically higher areas. During the Late Visean, a change from ramp-type to rimmed shelf deposition took place, by analogy with observation from the UK and Belgium. The mapped buildups probably represent these rimmed shelf carbonate platforms.

3.1 Introduction

In 1918, Van Waterschoot van der Gracht could only speculate on the existence of Carboniferous rocks in the northern part of the Netherlands as the most northerly wells were located in the Achterhoek area (Fig. 3.1). Following the Groningen Field discovery in 1959 and other gasfields in the Southern North Sea, it became clear that Upper Carboniferous rocks are omnipresent. However, it took some more years for geologists to realise that the (Upper) Carboniferous Coal Measures were the most important source for gas (Patijn, 1963b).

Due to deep burial, the palaeogeographical and structural setting of Dinantian rocks in the centre of the NWECB have remained speculative until today. Widely varying palaeogeographical

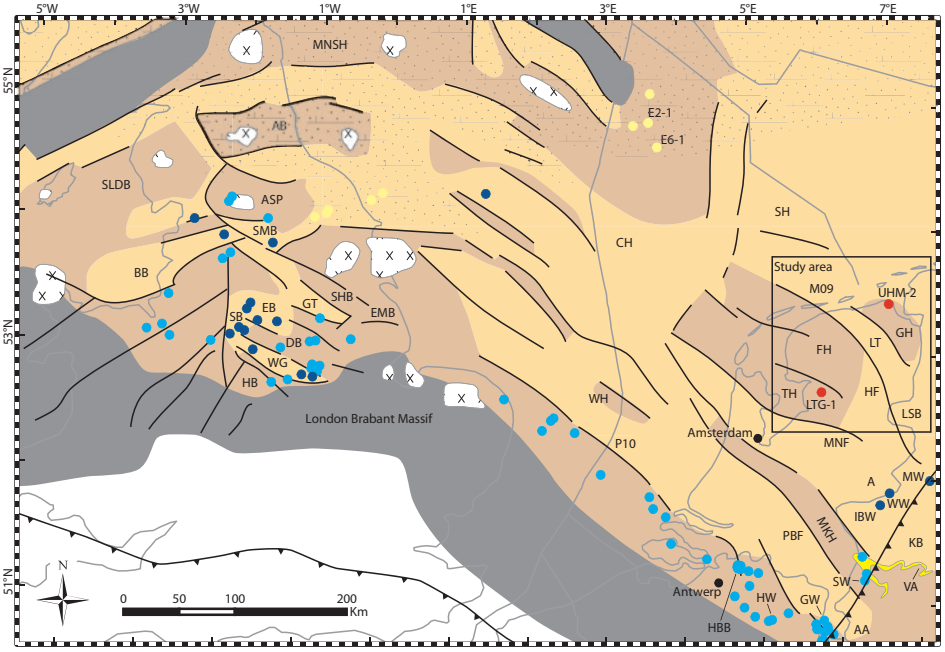

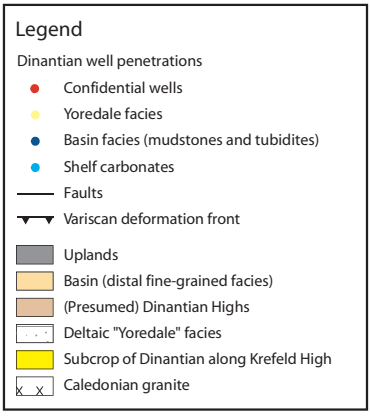

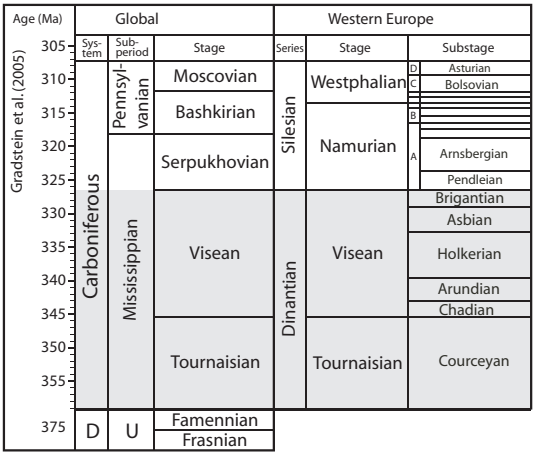

interpretations have been postulated (Bless et al., 1976; Ziegler, 1990; Bridges et al., 1995; Gerling et al., 1999; Collinson, 2005; Geluk et al., 2007; Korn, 2008; Van Hulten & Poty, 2008). Along the (southern) margins of the NWECB, the Dinantian is characterised by the development of carbonate shelves and intervening basins; e.g. in northern England, around the London Brabant Massif (LBM) and in western Germany (Fig. 3.1, see below for an extensive description). In Poland and northeastern Germany (Rügen), carbonate platforms also occurred during the Dinantian (McCann, 1999; Kornpihl, 2005; Narkiewicz, 2007; Matyja, 2008). Together, these belong to the extensive series of carbonate platforms that fringed the Old Red continent during the Dinantian (Korn, 2008). The northwestern part of the NWECB, however, was characterised by a major siliciclastic belt (Yoredale facies), which might have prevented the development of carbonate platforms in this area (Figs 2.5 & 3.1).

Figure 3.1 shows that all wells penetrating Dinantian rocks in the NWECB are located along its margins. The wells Uithuizermeeden-2 (UHM-2) and Luttelgeest-1 (LTG-1) in the Netherlands form an exception. Those wells targetted the Dinantian (Van Hulten & Poty, 2008) but are still confidential. Since well data are lacking, seismic surveys are the only source of information to study the Dinantian of the central part of the NWECB. The overburden may strongly complicate interpretation as reflections are often hard to distinguish from multiples generated by Zechstein carbonates. Noise from reflective Westphalian coal packages can locally hinder detailed mapping. Therefore, seismic interpretation of the top of Dinantian carbonates and other deep markers is rarely performed in the Netherlands (Geluk et al., 2007; Van Hulten & Poty, 2008). The relatively shallow burial of Carboniferous rocks in northern England allowed seismic interpretation to be carried out there (Lawrence et al., 1987; Fraser & Gawthorpe, 1990; Fraser et al., 1990; Evans & Kirby, 1999; Chadwick & Evans, 2005). In the western Campine Basin (Belgium) the top of the Heibaart carbonate buildup (Fig. 3.1) has been mapped on seismic (Dreesen et al., 1987). The margin of the platform surrounding the LBM has also been mapped locally but no published results are available to date (B. Laenen, pers. comm.). Surprisingly, recent investigation of public-domain 3D surveys (migrated post stack, quality controlled, 25 m in/crossline separation) in the

← *Figure 3.1* Palaeogeography of the Northwest European Carboniferous Basin during the Dinantian. The area south of the London Brabant Massif (LBM) is not incorporated in the map. The Dinantian Highs onshore UK and around the LBM are characterised by carbonate platforms; in the Southern North Sea and the Netherlands, the location and Dinantian facies of these highs is poorly constrained. Note that Dinantian Highs are also present in the northwestern part of the NWECB where siliciclastic sedimentation took place. In the timescale the studied time-interval is marked in grey. The Devonian (D) is not to scale (U: Upper Devonian). Achterhoek area (A); Aachen area (AA); Alston Block (AB); Askrigg Block (ASP); Bowland Basin (BB); Cleaverbank High (CH); Derbyshire Block (DB); East Midlands Block (EMB); Edale Basin (EB); Friesland High (FH); Gainsborough Trough (GT); Geverik-1 well (GW); Groningen High (GH); Halen well (HW); Hantum Fault (HF); Hathern Block (HB); Heibaart buildup (HBB); Isselburg-1 well (IBW); Kulm Basin (KB); Lower Saxony Basin (LSB); M09 offshore block (M09); Maasbommel-Krefeld High (MKH); Mid Netherlands Fault (MNF); Mid North Sea High (MNSH); Münsterland-1 well (MW); Lauwerszee Trough (LT); P10 offshore block (P10); Peel Boundary Fault (PBF); Schillgrund High (SH); Schwalmthal-1001 well (SW); Southern Lake District Block (SLDB); South Humberside Block (SHB); Staffordshire Basin (SB); Stainmore Basin (SMB); Texel-IJsselmeer High (TH); Velbert Anticline (VA); Widmerpool Gulf (WG); Winterswijk-1 (WW); Winterton High (WH). Redrawn after Fraser & Gawthorpe (1990), Ziegler (1990), Corfield et al. (1996), Pagnier et al. (2002), Gradstein et al. (2004) and Amler & Herbig (2006).

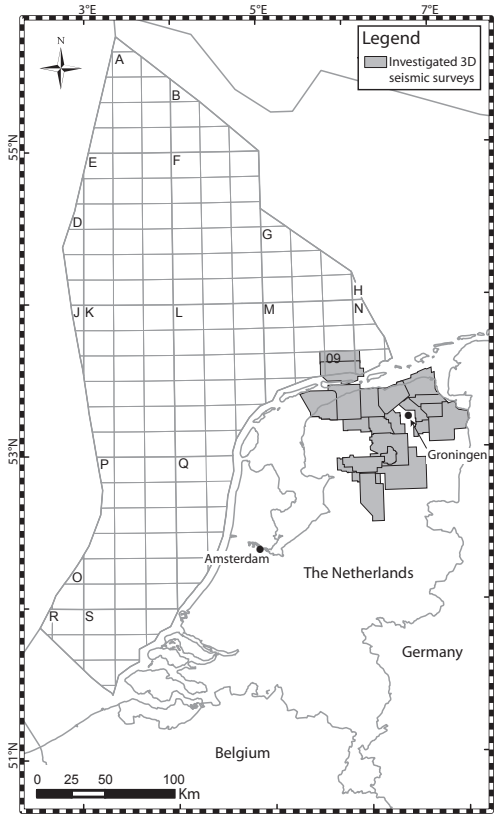

Figure 3.2 Map displaying the surveys used for this study.

northern part of the onshore Netherlands (Fig. 3.2) clearly revealed some reflectors which can probably be interpreted as the top of carbonate platforms.

Due to the lack of well data to calibrate the age and sedimentological characteristics of the interpreted structures, the following questions have to be answered first: (1) are these structures carbonate platforms and (2) what age can be assigned to them? In plan view (Fig. 3.9A), the mapped reflectors show a structure of well developed buildups. Especially the untilted Groningen buildup in the east shows a flat top and well developed slopes and margins (Fig. 3.3). The slopes are characterised by onlapping strata in most cases (Figs 3.6 & 3.7). Although two buildups could not be entirely mapped, the length probably varies from 20 to 60 km. The vertical offset between the top and base of the slopes varies between 2 and 3 km. Unfortunately, the seismic data available does not permit the interpretation of a clear internal hierarchy. Comparison of these structures with carbonate platforms described in northern England (Gawthorpe et al., 1989; Gutteridge, 1989; Fraser & Gawthorpe, 1990) shows that the dimensions (length, vertical offset between top and base of slopes) are well comparable. Moreover, when figure 3.3 is compared with figure 10 of Weber et al. (2003; a view of the Tengiz carbonate platform in Kazachstan) the similarities are evident. Based on these observations, the structures shown in figures 3.2 and 3.9A are proposed to be carbonate platforms. There is no direct evidence for the age of these platforms. A minimum age is relatively easy to infer. The well Tjuchem-2 drilled a thick succession of Namurian mudstones

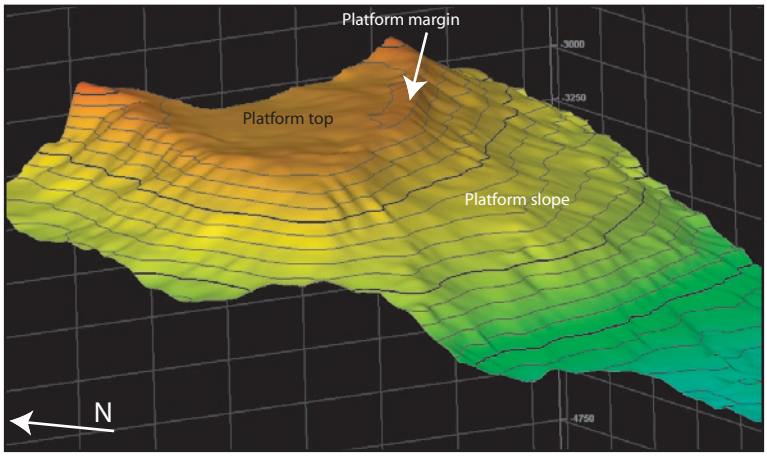

Figure 3.3 Perspective view of the top of the Groningen carbonate platform from the west.

(Fig. 3.4). Since the Namurian shales directly onlap onto the carbonates, a Visean age is well possible unless a large hiatus is assumed. The late Middle to early Late Devonian may also be taken as a candidate for platform development in the NWECB (Ziegler, 1990; Geluk et al., 2007). Little is known on Devonian palaeogeography in the Netherlands. Carbonates have been found around the Mid North Sea High in the UK (Kyle Group; Cameron, 1993), along the London Brabant Massif, on the Krefeld High and in the wells Münsterland-1 (Fig. 3.1) and Q-1 (Ziegler, 1990; Geluk et al., 2007). Latest Devonian marine or continental sediments are expected to overly these carbonates (Banjaard Group, Geluk et al., 2007). This model hampers the assignment of a Devonian age to the interpreted platforms since the Namurian shales directly onlap onto the carbonates. Based on these observations, a Dinantian (Visean) age is proposed for the platforms mapped in this study. The transition of ramp-dominated shelfs (Tournaisian) to rimmed shelf-dominated geometries during the Visean in the adjacent countries (Gawthorpe et al., 1989; Aretz & Chevalier, 2007) supports this view.

For the first time, 3D seismic interpretation displays the contours of 3 Dinantian carbonate platforms: (1) in the M09 offshore block, (2) below the Groningen Gasfield, and (3) in the province of Friesland (Fig. 3.1). Integration of these findings with recently published data on Dinantian geology of the Netherlands (Total E&P UK, 2007; Kombrink et al., 2008; Van Hulten & Poty, 2008) sheds more light on the Dinantian geological setting of the central part of the NWECB. So far, no important hydrocarbon accumulations have been proven in the Dinantian series of the UK and the NWECB (Fraser & Gawthorpe, 1990; Geluk et al., 2007). This chapter may contribute to future exploration activity in this still unknown play system.

3.2 Geological setting

This section describes the setting of Dinantian carbonate platforms and basins in the areas surrounding the Netherlands where a lot of research has been carried out. It will be used as a template to the interpretation of our seismic data. Figure 3.5 shows the terminology used. To prevent confusion by the use of the terms platform and high, the *structural* highs and platforms

(e.g. the Friesland Platform) are both denoted as *highs* while the term platform is used to indicate *carbonate platforms*.

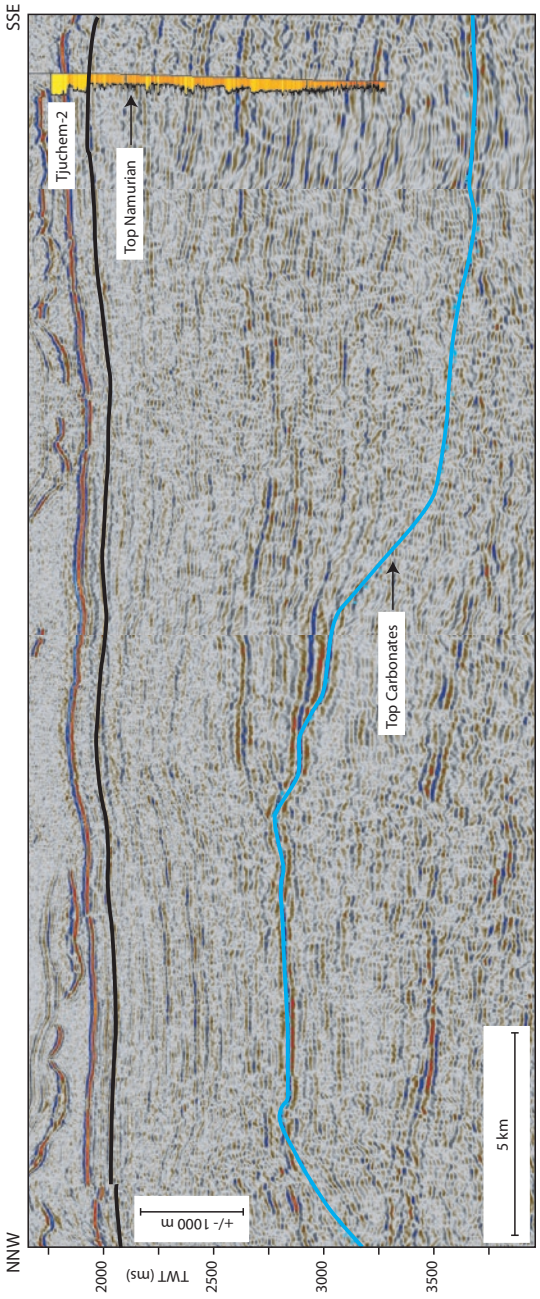

3.2.1 Block-and-basin model

Northern England is a classical area in which many of the concepts related to Dinantian basin development were formed (Evans & Kirby, 1999). The 'block and basin' hypothesis (Phillips, 1836; Rayner, 1953; Kent, 1966; Johnson, 1967) served as a model for onshore exploration in the Dinantian of Britain for more than 30 years (Falcon & Kent, 1960). The rationale behind the block-and-basin model is the recognition of areas of rapid subsidence with expanded Dinantian sequences and areas of much slower subsidence (blocks) characterised by a thin sequence of predominantly shallow-water carbonates. However, Grayson & Oldham (1987) questioned the validity of this model because important thickness and facies differences turned out to be not restricted to the basin-block boundaries only. They proposed a tilted fault block model such as presented in figure 3.5.

Rifting is thought to be responsible for the development of the blocks and basins or tilted fault blocks during the Dinantian (Fraser & Gawthorpe, 1990; Hollywood & Whorlow, 1993). The explanations for this rifting event are diverse: Leeder (1992) assumed that Devonian and Dinantian back-arc extension in the Rheno-Hercynian Basin played a dominant role. Coward (1993) proposed a model of escape tectonics whereby Avalonia/Baltica were expulsed eastwards causing NW-SE directed extension. Since Dinantian rifting in the UK coincides with sinistral translation along the Arctic-North Atlantic mega-shear, Ziegler (1990) proposed a genetic link between these events.

By analogy with northern England, Middle Devonian to Dinantian block faulting has been documented from both the northern flank of the London Brabant Massif (Muchez & Langenaeker, 1993; Poty et al., 2001) and the Mid North Sea High (Maynard & Dunay, 1999). The Southern North Sea basins are thought to have a similar structural framework as northern England, with a number of granite-cored blocks (Donato et al., 1983; Donato & Megson, 1990) flanked by half-grabens (Corfield et al., 1996). Block faulting is also suggested for the Netherlands (Cameron & Ziegler, 1997; Gerling et al., 1999; Hoffmann et al., 2005). Pagnier et al. (2002) postulated an extension of the "block and basin" model (Besly, 1998) towards the Netherlands (Fig. 3.1). De Jager (2007) presented a deep seismic line from the Friesland High to the ENE (Lower Saxony Basin, his figure 6) in which he interprets a number of tilted fault blocks which could form proof of this assumption.

3.2.2 Carbonate platforms UK

The establishment of carbonate platforms on structural highs in the UK only took place during late Dinantian times after a period of progressive flooding (Gawthorpe et al., 1989). Rimmed shelf platforms (with a distinct platform slope) are mainly limited to the Late Visean. For instance, the Derbyshire High was fully transgressed during Arundian and Holkerian times to

← *Figure 3.4* Seismic composite section crossing the Groningen carbonate platform (blue line) and the well Tjuchem-2 which almost drilled the entire Namurian sequence. Since the age of the Namurian rocks drilled near the well's final depth is Pendleian, it is likely that the sedimentary sequence in between the well and the interpreted top carbonates partly consists of Visean basinal sediments. The steepness of the slopes on both sides of the platform cannot be well compared in this section because it crosses the platform at different angles. The black line indicates the top Carboniferous/base Rotliegend. The drilled Namurian sequence has a thickness of slightly more than 2.5 km. Yellow colours in the well-log (gamma-ray) indicate sand-rich intervals while orange colours represent finer-grained sediments. The topmost (yellow) part of the well-log above the clear reflector represents Zechstein evaporites. For location of the cross-section, see figure 3.9.

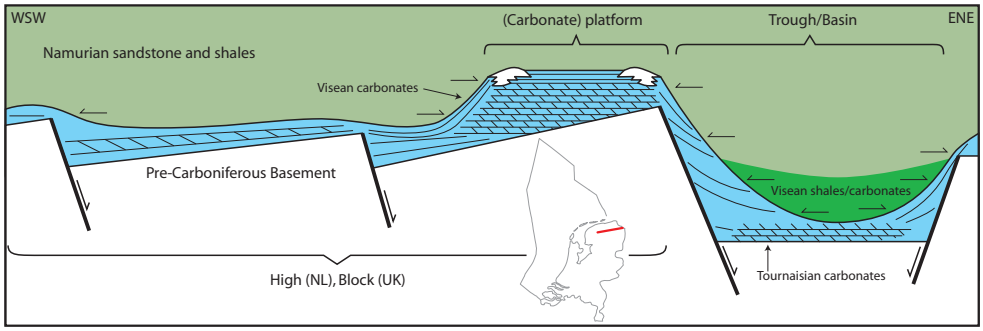

Figure 3.5 Schematic cross-section showing the interpretation of the Dinantian structural and stratigraphical setting in the study area. The interpreted reflector follows the top of the Dinantian carbonate sequence (light blue). Some of the terminology used in this chapter is also shown.

form a continuous platform. The Askrigg High shows progressive onlap until complete flooding during Late Arundian while the Southern Lake District High was fully transgressed during early Arundian (Gawthorpe et al., 1989). The Derbyshire carbonate platform developed into a rimmed shelf surrounded by a high-angle margin during the Asbian (Gutteridge, 1991). A rimmed shelf occurred along the southern margin of the Askrigg Block during Late Arundian to early Asbian times. The marginal facies of these carbonate shelves typically consist of so-called *Cracoean* reefs, with a thickness of up to 200 m (Mundy, 1994).

During tectonic activity the size of carbonate ramps or shelves generally decreased due to inundation of the hanging walls and emergence of the footwalls. Intervals of tectonic quiescence are characterised by downward progradation of rimmed shelves over hanging wall slopes (Gawthorpe et al., 1989). Overall, the Dinantian carbonate sequence varies from 500 to 1000 m in thickness on the structurally elevated areas (Fraser & Gawthorpe, 1990). Carbonate buildups are reported on several of these platforms (Bridges et al., 1995; Gutteridge, 1995).

Carbonate deposition in the basinal areas started much earlier (Gawthorpe et al., 1989). In the Bowland Basin, Late Tournaisian and Chadian wackestones and packstones indicate deposition on a ramp, giving way to calciturbidites sourced from the northerly Askrigg High while mudstones predominate in the southern part of the basin. The oldest shallow subtidal carbonates in the Staffordshire Basin have an Early Tournaisian age, and are covered by calciturbidites from Late Tournaisian to Asbian age (Gawthorpe et al., 1989). In contrast, the Stainmore Basin shows continuous sedimentation of shelf carbonates during the entire Dinantian. Sedimentation in the Edale Basin was dominated by resedimented shallow-water carbonates with the occasional deposition of periplatform carbonates (Gutteridge, 1991). The Bowland Basin has been proposed to contain more than 4000 m of Dinantian rocks (Gawthorpe et al., 1989) while in most basins between 2000 and 3000 m of Dinantian is inferred (Fraser & Gawthorpe, 1990).

The most important reason for carbonate production to stop in northern England has been increased siliciclastic input during the Brigantian and earliest Namurian. Since the main sediment source was located in the north, the northerly located platforms such as the Southern Lake District High experienced mixed carbonate-siliciclastic sedimentation during the Early Brigantian (Gawthorpe et al., 1989). In the south, where the siliciclastic sediment supply remained very limited until far into the Namurian (see Chapter 6), carbonate production must have ceased for another reason (changing circulation or temperature).

3.2.3 Carbonate platforms Belgium

In the Campine Basin, north of the LBM, the Tournaisian is largely unknown, but it is proven to be absent in the Heibaart area (Langenaeker, 2000). During the Visean, northward progradation of a shallow-marine facies belt lead to the establishment of a carbonate shelf (M. Aretz, pers. comm.). Syn-sedimentary faulting played an important role, resulting in variations in thickness of the Visean section in the Campine Basin. The maximum drilled thickness is approximately 760 m (Halen borehole in the eastern Campine) versus 314 m (Heibaart Dome) in the western Campine Basin. Just east of the LBM, Poty (1991) distinguished a number of fault blocks characterised by lateral facies and thickness changes. Microbial reefs developed on the elevated areas (Aretz & Chevalier, 2007). In a NNW-SSE striking horst just east of Antwerp, a series of reef-like buildups developed, which can be several hundreds of metres in width and up to about 150 m in height (Aretz & Chevalier, 2007). In the Heibaart and Poederlee boreholes, which drilled one of these buildups (Fig. 3.1, Heibaart), thick packages of Visean microbial boundstones and peloidal packstones-wackestones are found (Muchez et al., 1987). The microbial reefs in the Visé area and the Heibaart and Poederlee boreholes are very similar to reefal structures recognised in northern England (Mundy, 1994), and point to the synchronous development of a barrier of large microbial reefs along the platform edge north of the LBM (Aretz & Chevalier, 2007).

3.2.4 Carbonate platforms in western Germany

The eastern edge of the LBM influenced facies patterns as far as western Germany. The most easterly extension of carbonate sedimentation is found at the Velbert Anticline (Fig. 3.1). Carbonates were also found in wells on the Krefeld High (Amler & Herbig, 2006; Fig. 3.1). To the north and east, siliciclastic deposition took place in the Kulm basin. Here, the Dinantian consists of a thin succession of black shales in the wells Münsterland-1 and Isselburg-1 (Fig. 3.1) and Versmold-1 (not shown; Drozdzewski, 2005). However, based on a study on calciturbidites in the eastern part of the Rhenish Mountains, Korn (2008) proposed the existence of isolated carbonate platforms in the Kulm Basin. This confirmed the results of Eder et al. (1983) who found southward-directed sediment transport based on sole marks in these calciturbidites. During the latest Visean, subsidence of the carbonate platforms in this area increased which led to deposition of turbidites, recorded in the wells Schwalmtal-1001 and also in Geverik-1 in the southern part of the Netherlands (Mathes-Schmidt, 2000).

3.2.5 Carbonate platforms in the Netherlands and the Southern North Sea

To date, the existence of extensive carbonate platforms in the Southern North Sea (SNS) and the Netherlands remains unclear (Geluk et al., 2007). However, small carbonate buildups on the Texel IJsselmeer High (Kombrink et al., 2008; chapter 4), the P10 offshore block (Van Hulten & Poty, 2008) and the Winterton High (Total E&P UK, 2007) have been reported recently (Fig. 3.1). In palaeogeographic reconstructions, the Netherlands and the SNS areas are interpreted to be part of one extensive carbonate platform (Ziegler, 1990; Maynard et al., 1997) or a siliciclastic basin (Bridges et al., 1995) with some isolated mud-mounds (Gursky, 2006). Based on released seismic data, Maynard & Dunay (1999) assumed that the carbonate facies extends northwards possibly as far as the Cleaver Bank High and Schill Grund High. A mixed siliciclastic-carbonate sedimentary sequence has been drilled in the wells E2-1 and E6-1, north of Cleaverbank High (Fig. 3.1). Bless et al. (1976) already speculated on the existence of shoals between the Kulm Basin in the south and the northern margin of the NWECB, where some wells penetrated shallow-marine

carbonates (Rügen area and Orslev-1 well, Michelsen, 1971). These examples show that there is no general agreement on Dinantian palaeogeography in the Netherlands.

Recently, Geluk et al. (2007) and Van Hulten & Poty (2008) presented some further suggestions on the distribution of Dinantian carbonate platforms in the Netherlands, although no detailed mapping has been carried out. Van Hulten & Poty (2008) interpreted the existence of carbonate platforms based on the Carboniferous subcrop pattern against the base Permian (their figure 6). They proposed Dinantian Highs (hence carbonate platforms) to be present where Westphalian A or B subcrop. The basins are thought to be located where younger Westphalian C and D or Stephanian strata are found. In this way, several highs can be distinguished (Fig. 3.1): (1) The Winterton High; (2) The Maasbommel-Krefeld High; (3) The Texel-IJsselmeer High; (4) The Friesland High (will be described as High in this chapter to prevent confusion with carbonate terminology) and (5) The Groningen High. According to this approach, the Cleaverbank and Schillgrund Highs are not highs, because here younger Carboniferous subcrops. Geluk et al. (2007) show the same highs, but also interpret the Cleaverbank and Schillgrund areas as Dinantian highs (their figure 9). In both papers, it is concluded that fault-bounded basins occur between the highs. Active faults are thought to have included the Peel-boundary, Hantum and Mid-Netherlands fault zones (Fig. 3.1). Furthermore, Geluk et al. (2007) mention that scarce seismic data suggest that the Dinantian is very thin on the highs, e.g. the Texel IJsselmeer High, possibly as a result of condensed sedimentation. Public domain seismic lines running across the Texel IJsselmeer High would show a high-amplitude reflector below the Upper Carboniferous sediments, very similar in character to the reflector at the top of Dinantian carbonates along the LBM (Geluk et al., 2007).

3.2.6 Role of Dinantian highs during Late Westphalian inversion in the UK

As a consequence of the ongoing Variscan Orogeny, the NWECB experienced a compressional phase at the end of the Westphalian leading to inversion of former (Dinantian) basins. This event has been well described in the UK (Fraser & Gawthorpe, 1990; Corfield et al., 1996). The degree of inversion is highly dependent on the direction of the basin bounding faults. Since compression was NW-SE to NNW-SSE, the basins characterised by NE-SW axes were strongly inverted, such as the Bowland Basin (Corfield et al., 1996). NW-SE trending faults probably moved in a strike-slip mode with small vertical fault displacement (Fraser & Gawthorpe, 1990). As a consequence, the inverted Dinantian basins in the UK show the oldest subcropping Carboniferous rocks. For the Netherlands, Van Hulten & Poty (2008) argue otherwise: they suggest that the Dinantian topography instead of the Variscan deformation phase is the primary cause of the subcrop pattern. They assume excessive shale compaction in the basins relative to the highs, creating accommodation space for younger Westphalian strata. In this way, they neglect the inversion event and the consequences this could have had on the subcrop pattern. This will be further addressed in section 3.4.

3.2.7 Time-equivalent carbonate platforms outside the NWECB

Time-equivalent carbonate platforms have, amongst others, been studied in the Caspian region (Lisovsky et al., 1992; Cook et al., 2002; Weber et al., 2003; Francis et al., 2004), northern Spain (Kenter et al., 2002; Della Porta et al., 2004) and the Norwegian Barents Sea (Stemmerik et al., 1999; Elvebakk et al., 2002).

The Tengiz Field just northeast of the Caspian Sea in Kazachstan is a well known example of a Dinantian carbonate platform. The platform developed on an isolated basement high in a time of tectonic quiescence, after Middle-late Devonian back-arc rifting (Weber et al., 2003). It shows

the transition from an initial broad platform during the Late Devonian to an isolated carbonate platform during the Dinantian as a consequence of accentuated vertical growth and punctuated backsteps (Francis et al., 2004). The Carboniferous carbonate succession at Tengiz is approximately 1200 m thick. Lithofacies stack into shallowing-upward packages. More than 50 cycles are present, ranging in thickness from 2 to 15 m. The top of the Bashkirian platform was approximately 1500 meters above the basin floor (Weber et al., 2003). The well developed rim around the perimeter of the Tengiz Platform is probably related to: (1) platform-margin aggradation and (2) higher compaction of intra-platform strata compared to marine-cemented Serpukovian upper-slope boundstones (Weber et al., 2003).

A very thick sequence of carbonates can be found in the Bolshoi Karatau Mountains in southern Kazachstan. From the latest Frasnian to lower Bashkirian the Bolshoi Karatau platform (4000-4500 m thick) developed in an open ocean-passive margin setting (Cook et al., 2002). The platform evolved from a reef-rimmed platform in the Famennian via a ramp during Tournaisian to a shoal-rimmed platform margin during Visean and Serpukovian. Finally, a reef-rimmed platform developed during the early Bashkirian (Cook et al., 2002). This well exposed sequence of platform carbonates in Kazachstan forms an analogue for the giant platforms found in the North Caspian Basin (e.g. the Tengiz Field, Cook et al., 2002).

In northern Spain, Kenter et al. (2002) and Della Porta et al. (2004) studied the outcrops of intact and seismic-scale Serpukhovian-Moscovian carbonate platforms, which also served as an analogue of subsurface reservoirs in the Caspian area. The nucleation of a low-angle ramp represents the initial phase of platform growth which is followed by aggradation and the formation of a steep margin (Kenter et al., 2002). The relief across the slope of the carbonate platforms, which attain a thickness of 1.5 – 2 km, locally is up to 850 m.

Carbonate buildups are often found on top of carbonate platforms (Stemmerik, 2003; Aretz & Chevalier, 2007; Colpaert et al., 2007). In a seismic interpretation study of carbonate buildups in the Norwegian Barents Sea, Elvebakk et al. (2002) found a direct correlation between underlying pre- and syn-sedimentary faults and buildup location. The buildups are typically located along the down-dip margins of the underlying footwall blocks (Elvebakk et al., 2002). Their thickness varies between 350 and 1200 m and they can be very long-lived regarding growth-time intervals of approximately 35 Ma (Elvebakk et al., 2002). Similar structures are reported by Colpaert et al. (2007) on the Eastern Finnmark platform in the Barents Sea.

3.3 Results

3.3.1 Carbonate platforms

The carbonate platforms mapped in the centre of the NWECB are shown in figure 3.9A. Except for the platform in the M09 offshore block, the others formed on structural highs; the Groningen, Friesland and the Texel-IJsselmeer Highs. For the calculation of the depth of the reflectors, a mean velocity of 4200 m/s for the Carboniferous has been used, based on velocity data from the well Tjuchem-2.

Below the northernmost part of the Slochteren Gasfield, the untilted Groningen carbonate platform was the easiest one to interpret. Along the perimeter of the platform, which occurs at a depth of approximately 4950 m, a well developed rim is observed (Fig. 3.3). A comparable but more pronounced feature is reported for the Tengiz platform (Weber et al., 2003). The southern platform slope mostly consists of a clear reflector with onlap of Namurian and possibly older

rocks (Fig. 3.6). Since the northern slope is characterised by a set of slope-parallel reflectors, it is less distinct than the southern one (Fig. 3.6). The slopes of the Groningen Platform can be traced further to the WSW and S, where they show a relatively horizontal course up to the boundary of the Lauwerszee Trough (5 in Fig. 3.7). The vertical distance from the platform top up to this

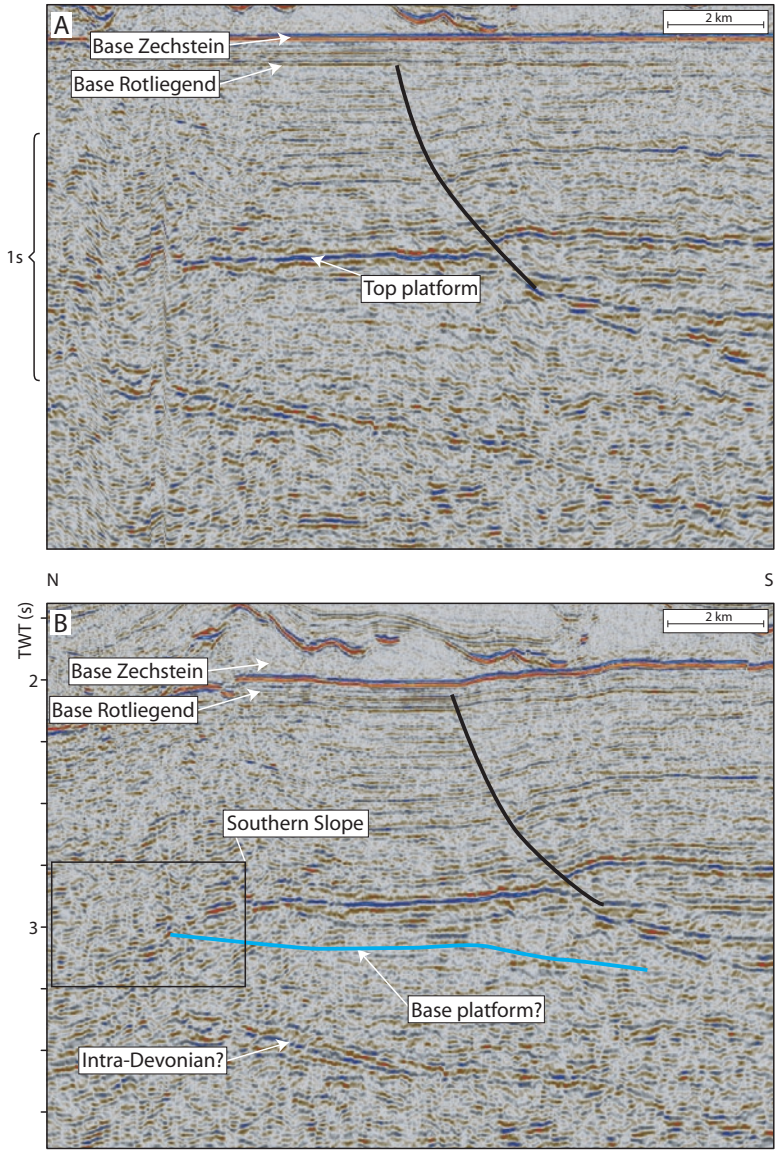

Figure 3.6 North-south seismic sections crossing the Groningen Platform. (A) Flattened on base Zechstein and (B) unflattened. Especially the southern slope of the platform can be well distinguished through the onlapping (Namurian and possibly Visean) strata. In 3.6A, a gentle anticline is seen in the south. This anticline is interpreted to be an inversion anticline. In 3.6B, a southward dipping reflector is observed which is tentatively attributed to an intra-Devonian marker.

level is approximately 1800 m. Another steep slope subsequently grades into the axial parts of the Lauwerszee Trough (Fig. 3.7). Although the carbonate platform could not be mapped entirely, it probably has a WNW – ESE orientation.

In contrast to the untilted Groningen Platform, the Friesland Platform has been tilted to the northeast. Moreover, the structure has been faulted in the north and along its southwestern boundary (Figs 3.7 & 3.9A). The northeastern margin of the platform immediately borders the Lauwerszee Trough, resulting in a long slope. The difference between the platform top and the base of the Trough is about 1500 ms TWT (3150 m). The southern part of the Friesland Platform will be described using seismic section A in figure 3.7. At the point marked with 1 in figure 3.7, a slope seems to be present. However, the reflectors in the overburden do not support this interpretation since they do not onlap the slope (as can be seen at the Groningen Platform, Fig. 3.6). Instead, they lie approximately parallel to the top of the platform. 10 km further southwards, a small slope is interpreted with clear onlapping strata (2 in Fig. 3.7). Due to a lack of data, the western margin of the platform could not be mapped. In the northwest, a steep slope could again be interpreted (Fig. 3.7).

The third and smallest platform is located in the M09 offshore block (Fig. 3.9A). Unfortunately, the available seismic data do not allow to correlate this platform with the Friesland Platform. The top occurs at approximately 6000 m depth. Similar to the Friesland Platform, it is tilted to the northeast, and at least one NW-SE striking normal fault cuts the platform (Figs 3.8 & 3.9A). An interesting feature of this platform is the concave inlets at the northeastern margin (Fig. 3.9A), which can also be seen at the northeastern margin of the Friesland Platform.

As mentioned above, the reflectors that have been used to interpret the outlines of the Friesland and Groningen Platforms could be traced into the Lauwerszee Trough. Both interpretations (one from the Groningen and the other from the Friesland Platform) could be easily linked, supporting the view that they reflect the same seismic event. The difference in elevation between the top of the platforms and the base of the Lauwerszee Trough is approximately 3700 m at maximum. Comparable offsets have been found in the UK where the difference in elevation between the top of Chadian carbonates in the Widmerpool Gulf and the East Midlands Platform is appr. 2.5 km, while the base of the Carboniferous shows an offset of 3 km between the Hathern shelf and the Widmerpool Through (Fraser & Gawthorpe, 1990).

3.3.2 Internal structure of the platforms

Due to the absence of well data, the interpretation of the internal architecture of the platforms is severely hampered. Evans & Kirby (1999) concluded that the seismic facies of the platforms they interpreted in the UK show a predominantly transparent facies. However, the Groningen Platform, which has the highest potential to reveal information on the internal architecture, does not clearly show a transparent facies. Especially in the central part of the platform an alternation of horizontal and parallel reflectors is observed (Fig. 3.6), while the platform margin shows less contrast. A tentative base of the platform has been interpreted on the basis of a subtle change in seismic facies (Fig. 3.6). It is slightly inclined relative to the top of the platform. The maximum thickness of the carbonate succession is estimated to be around 800 m. This is in the same order of magnitude as the thicknesses found in the UK (Fraser & Gawthorpe, 1990).

3.3.3 Structure of the Namurian and Westphalian overburden

Overall, the Carboniferous rocks in the study area are characterised by a sub-horizontal layering. However, in the southern part of the study area a well developed WNW-ESE trending syncline

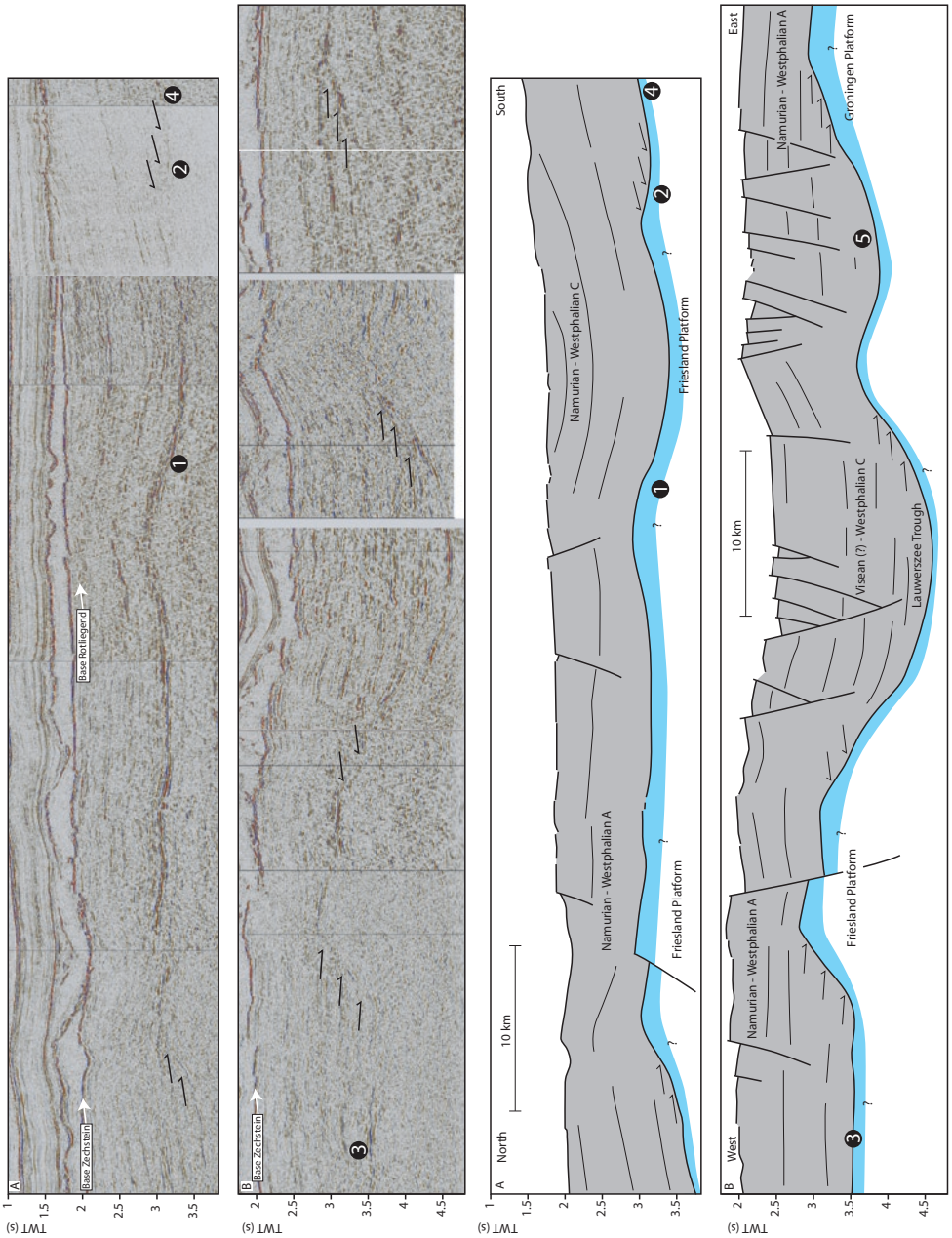

Figure 3.7 Composite seismic sections displaying the interpreted platforms. The blue layer represents the top of Dinantian carbonates. For location of these cross-sections, see figure 3.9A. The grey area represents the Carboniferous succession in between the base Rotliegend and the interpreted reflector of which the approximate age-ranges (not the boundaries) are given.

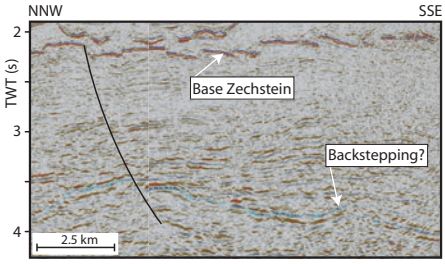

Figure 3.8 NNW-SSE seismic section trough the M09 platform showing (presumed) backstepping. For location of this cross-section, see figure 3.9. The dotted blue line indicates the top of the platform carbonates.

is apparent (between points 1 and 2 in Fig. 3.7). A gentle anticline can be observed just south of the southern margin of the Groningen Platform (Fig. 3.6). These structures will be further discussed below. Comparison of a map displaying the depth of the Base Zechstein (Fig. 3.9C) with the location of the interpreted platforms leads to the observation that the platforms are found on stable blocks where the Base Zechstein is not as deeply buried and faulted compared to the adjacent areas. Moreover, in line with the predictions by Van Hulten & Poty (2008) the outlines of the platforms mainly correspond to areas of Westphalian A and B subcrop (Fig. 3.9B). The subcrop pattern in the Lauwerszee Trough seems to be a more complicated. Here, Westphalian C rocks do occur, as predicted by Van Hulten & Poty (2008). However, these rocks are mainly found in the western part (also at the Friesland Platform), while the Westphalian B also subcrops in some areas.

3.4 Discussion

3.4.1 Dinantian carbonate platforms

For the first time, data are presented that support the existence of Dinantian platform carbonates in the central part of the Northwest European Carboniferous Basin (Fig. 3.1). This allows for a better understanding of the structural setting. Equivalents of these platforms occur in northern England (e.g. Derbyshire Block) and along the margin of the London Brabant Massif where well-data prove the age of these carbonates to be mainly Visean.

In northern England the most important Dinantian carbonate platforms are found on intrabasinal structural highs (Gawthorpe et al., 1989). The Friesland and Groningen Platforms also developed on structural highs, in agreement with propositions by Pagnier et al. (2002), Geluk et al. (2007) and Van Hulten & Poty (2008). Underneath the Groningen Platform, a SW-dipping reflector (Fig. 3.6) may represent a tilted fault block, comparable to the structures described by De Jager (2007) in the Lower Saxony Basin. Unfortunately, the seismic data did not allow the identification of a similar type of reflector underneath the Friesland Platform. However, a tilted fault block model for our study area is proposed, in line with earlier suggestions by Cameron & Ziegler (1997), Gerling et al. (1999), Hoffmann et al. (2005), De Jager (2007) and Geluk et al. (2007). The M09 platform is situated just north of the Friesland High in an area interpreted as the Lauwerszee Trough. This platform might be related to a small fault block in the Hantum Fault zone, which might have been active during the Dinantian (Geluk et al., 2007). The Holme High (not shown in figure 3.1 because it is too small), described by Gutteridge (1991) and Chadwick &

Evans (2005) possibly is an analogue for the M09 platform. This small platform was found in the Edale Basin, in between the extensive Derbyshire and Askrigg carbonate platforms (Gutteridge, 1991). This illustrates the possibility that relatively small platforms are found in areas thought to be characterised by basinal facies only.

The platforms mapped in this study only occupy the northeastern parts of the (Friesland and Groningen) structural highs. Apparently, these were the only areas favourable for the establishment or continuation of carbonate platform development. In northern England, (ramp-type) carbonate deposition in the basinal areas started during the Tournaisian and gradually onlapped the (structurally) elevated areas (Gutteridge, 1989). Once carbonate platforms had established at these structural highs, deposition of calciturbidites and basinal shales characterised the majority of the adjacent basins. An analogue for this situation is the Bowland Basin where the transition from carbonates to basinal shales took place during the Chadian while carbonates continue to be deposited on top of adjacent highs (Gawthorpe et al., 1989). A similar model is proposed for our study area, in which a process of a gradual retreat of carbonate deposition is envisaged together with a change from a ramp-type to rimmed shelf type during the Visean (Fig. 3.5). In other words, it is suggested that the reflector (which is thought to record the transition from basinal sediments above to a carbonate-dominated sequence below) represents a diachronous event: the transition from carbonates to basinal sediments first took place in the basins (e.g. Lauwerszee Trough, Tournaisian) while only during the Namurian the tops of the (Visean) platforms were covered with basinal sediments. An example of the retreat of carbonate deposition is observed at the M09 platform. Here, the stepwise character of the interpreted top platform reflector suggests backstepping (Fig. 3.8), also visible in figure 3.9A. Another indication for the presence of Dinantian rocks on top of the reflector in basinal areas is shown in figure 3.4. In this figure, the well Tjuchem-2 is plotted into the seismics. The basal section in Tjuchem-2 has been dated Pendleian. This suggests that the base Namurian is not far below the well's final depth. The interpreted reflector occurs at a significantly deeper level, which strongly suggests that the succession in between the base of the well and the reflector has a Visean age.

A few aspects of these platforms need extra attention. These are: (1) the difference in seismic facies between the northern and southern slope of the Groningen Platform (Fig. 3.6), (2) the rim around the perimeter of the Groningen Platform (Fig. 3.3) and (3) the concave structures at the northeastern margins of the M09 and Friesland Platforms (Fig. 3.9A). The northern slope of the Groningen Platform consists of a number of slope-parallel reflectors, in contrast to the southern slope, where one clear reflector marks the transition between carbonates and onlapping strata (Fig. 3.6B, inset). An explanation for this phenomenon might be periodical instability leading to (partial) failure of the margin. Since this slope is located on the northern margin of the Groningen High, movements along the faults bordering the Groningen High might have triggered the failure of the platform slope. This process has been described in the Bowland Basin where resedimentation of major units of carbonate conglomerate was suggested to have been caused by tectonic activity (Gawthorpe et al., 1989).

By analogy with the Tengiz platform, the rim around the Groningen Platform might be related to: (1) platform-margin aggradational growth or (2) differential compaction of the platform strata to less-compacted marine-cemented boundstone facies (Weber et al., 2003). Both explanations allow the presence of reefs comparable to those described in northern England and in Belgium (Mundy, 1994; Aretz & Chevalier, 2007).

The concave structures at the northeastern margin of the Friesland and M09 platforms (Fig. 3.9A) are not seen at the Groningen Platform. Possibly these features relate to an early phase of

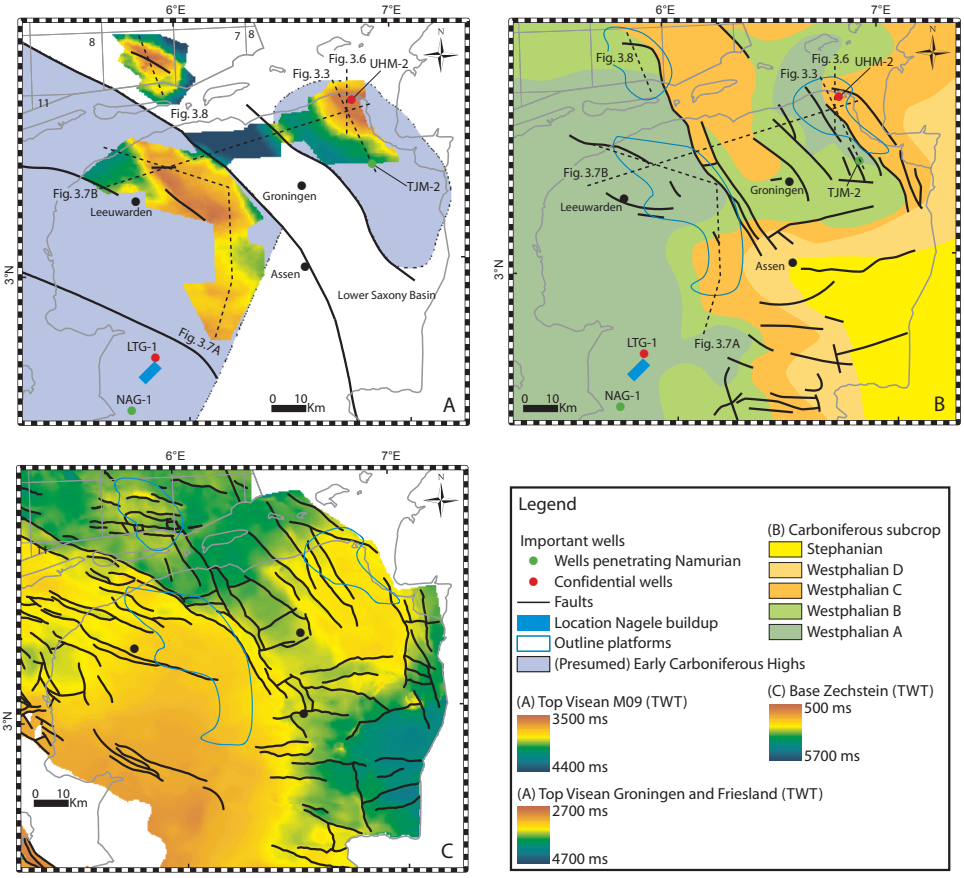

Figure 3.9 (A) Top Carbonate reflector (TWT) and continuation on the adjacent highs and in the Lauwerszee Trough; (B) Carboniferous subcrop pattern; (C) Base Zechstein (TWT) together with faults. Note that the contours of the platforms are plotted on this map.

(minor) tilting to the northeast whereby erosion products from the platform top are shed towards the northeast. This process might have caused the development of erosional valleys at this side of the platforms. Since the Groningen Platform was not tilted (Fig. 3.7), these structures are absent there.

Next to the platforms reported here, a recent Total-publication (Total E&P UK, 2007) presents a seismic section across the Winterton High in the UK blocks 53/5-c and 54/6 where a similar platform was interpreted (Fig. 3.1). It seems likely that this platform is present in the Dutch extension of the Winterton High as well, but the 3D seismic volume covering this area is still confidential. A small carbonate buildup (Nagele) has been recently identified on a 2D seismic line located on the Texel IJsselmeer High (Fig. 3.9), reported in Kombrink et al. (2008). Van Hulten & Poty (2008) propose the existence of another carbonate buildup in the P10 block (Fig. 3.1). The Nagele buildup is assumed to have developed on top of the carbonate platform covering the Texel-IJsselmeer High. In this respect, it may be comparable to structures found in the Barents Sea (Elvebakk et al., 2002; Colpaert et al., 2007) where large buildups have been identified

on carbonate platforms (Colpaert et al., 2007). Moreover, according to Pickard (1996) Visean buildups, particularly in northwestern Europe were often restricted to relatively shallow water over tectonically controlled topographic highs.

Altogether, these results suggest that an extension of the tilted fault block model can be applied to the Dutch onshore area. The structural highs have been sites where Dinantian platforms preferentially developed, but it cannot be ruled out that smaller carbonate platforms exist on smaller scale structural highs located in the graben areas, as illustrated by the M09 platform.

3.4.2 Dinantian basins

The seismic interpretation carried out here implies that the Silesian and probably also the Dinantian is thicker in the Lauwerszee Trough than on the bounding platforms (Fig. 3.7). In addition, De Jager (2007) shows a deep seismic line running from the Friesland High towards the ENE (Lower Saxony Basin, his figure 6) where he interprets a number of Devonian (?) tilted fault blocks. Along this line, the (Devonian?) reflector shallows towards the Friesland High, suggesting that the Carboniferous succession is thicker in the Lower Saxony Basin (Jurassic) than on the platforms. In addition, Bless et al. (1980) mentioned the strong similarity between the sedimentation patterns in the Carboniferous Campine Basin and the Jurassic West Netherlands Basin/Roer Valley Graben. These observations support the view that the Dinantian basins are characterised by a thicker siliciclastic sedimentary sequence and possibly form the precursors of Jurassic basins.

3.4.3 Inversion

At the end of the Westphalian, the NWECB was inverted (Ziegler, 1990; Ziegler et al., 1995; Ziegler et al., 2002; Ziegler & Dèzes, 2006; Narkiewicz, 2007). Studies in the UK showed that the degree of inversion of Dinantian basins depended on the strike of the basin-bounding faults (Fraser & Gawthorpe, 1990; Corfield et al., 1996). NE-SW trending basins like the Bowland Basin were severely inverted since the direction of maximum shortening was NW-SE to NNW-SSE. In contrast, NW-SE trending basins, parallel to the shortening direction, only show mild inversion. In the study area, inversion is indicated by: (1) the syncline between locations 1 and 2 in figure 3.7, and (2) a gentle anticline just south of the Groningen Platform (Fig. 3.6). This anticline is probably related to the carbonate platform which acted as a stable block causing the development of a fold just south of it. The anticline seems to be bordered by a fault that propagates through the entire Carboniferous sequence. This (normal) fault might have been formed during the Namurian and Westphalian in the area of two different compaction regimes (caused by the thickness differences). During the inversion phase it was slightly reactivated in a reverse trend along with the development of the inversion anticline. This is confirmed by the subcrop map (derived from Van Buggenum & den Hartog Jager, 2007), which indicates a fault-bounded transition between Westphalian A and C at that location (Fig. 3.9B).

There is one striking difference between the Netherlands and northern England subcrop patterns: in the former, Late Westphalian rocks are almost entirely limited to the Dinantian basins (Lower Saxony Basin and Lauwerszee Trough, Fig. 3.9B). In the East-Midlands (a carbonate platform area during the Dinantian) Westphalian C rocks subcrop over large areas (Fraser & Gawthorpe, 1990). The Winterton High, which has also been a carbonate platform, shows a subcrop of Westphalian C as well. Although the subcrop map for the study area (Fig. 3.9B) shows that Westphalian C strata do occur on top of the platform areas, it is not as much as in northern England. Apparently, Late Westphalian inversion did not cause significant uplift of the Dinantian

basins, resulting in a continuation of Late Westphalian sedimentation in these areas. It remains to be investigated why this relationship seems to be quite straightforward in the Netherlands onshore while in the UK it is more complicated. There, the areas showing subcrop of Late Westphalian rocks do certainly not correspond to the location of Dinantian basins (Fraser & Gawthorpe, 1990). The proposition of Van Hulten & Poty (2008) that subcrop of Lower Westphalian would indicate the presence of Dinantian highs seems to work out coincidentally in the Netherlands, as: (1) they do not address the inversion problem and (2) the situation in the UK is much more complicated.

3.5 Conclusions

The large structures in the deep subsurface of the Netherlands (the central part of the Northwest European Carboniferous Basin (NWECB)) have a great likelihood of being carbonate platforms. Seismic data from the northern part of the Netherlands onshore particularly allowed the detailed mapping of a (most likely) Top Visean reflector.

Based on the data presented in this study and by comparison with extensively studied, time-equivalent carbonate platforms in northern England and outside the NWECB, a tilted fault block setting for the northern part of the Netherlands during the Dinantian is suggested. Initially, carbonate deposition occurred in the basinal areas. Due to continuing subsidence, carbonates onlapped and transgressed the structural highs. Deposition in a ramp-type environment during the Tournaisian was replaced by rimmed shelfs during the Visean, which has been well described in other parts of the NWECB. Three Visean rimmed shelf carbonate platforms have been mapped. The Groningen and Friesland platforms developed on the Groningen and Friesland Highs respectively. The M09 carbonate platform, the smallest, is located in the Lauwerszee Trough. This platform is probably confined to a small fault block, related to the Hantum Fault Zone. Comparable types of platforms have been reported from the UK.

A comparison of the Carboniferous subcrop pattern – partly controlled by the Late Carboniferous inversion phase – between northern England and the Netherlands reveals a striking difference: in the latter, Late Westphalian rocks seem to be mainly limited to Dinantian basins while in the former these rocks extensively occur in Dinantian platform areas. This observation requires more investigation in the Netherlands.

CHAPTER 4

Late Carboniferous foreland basin formation and Early Carboniferous stretching in Northwestern Europe – Inferences from quantitative subsidence analyses in the Netherlands

This chapter is based on: Henk Kombrink, Karen A. Leever, Jan-Diederik van Wees, Frank van Bergen, Petra David & Theo E. Wong (2008): Late Carboniferous foreland basin formation and Early Carboniferous stretching in Northwestern Europe – Inferences from quantitative subsidence analyses in the Netherlands. Basin Research 20, 377-395.

Abstract

The large thickness of Upper Carboniferous strata found in the Netherlands suggests that the area was subject to long-term subsidence. However, the mechanisms responsible for subsidence are not quantified and poorly known. In the area north of the London Brabant Massif, onshore UK, subsidence during the Namurian – Westphalian B has been explained by Dinantian rifting followed by thermal subsidence. In contrast, south and east of the Netherlands, along the southern margin of the Northwest European Carboniferous Basin, flexural subsidence due to Variscan orogenic loading caused the development of a foreland basin. It has been proposed that foreland flexure was responsible for Late Carboniferous subsidence also in the Netherlands. In the first part of this chapter a series of modelling results is presented in which the geometry and location of the Variscan foreland basin was calculated on the basis of kinematic reconstructions of the Variscan thrust system. Although a lot of uncertainties exist, it is concluded that most subsidence calculated from well data in the Netherlands can not be explained by flexural subsidence alone. Therefore, it is investigated whether a Dinantian rifting event could adequately explain the observed subsidence by inverse modelling. The results described in chapter 3 indeed suggests that a Dinantian rifting event took place in the Netherlands. This study shows that if only a Dinantian rifting event is assumed, such as described for the UK, a very high palaeowater depth at the end of the Dinantian is required to accommodate the Namurian – Westphalian B sedimentary sequence. To better explain the observed subsidence curves, (1) an additional stretching event during the Namurian, (2) a model incorporating an extra dynamic component, or (3) compressional intra-plate stress are proposed.

4.1 Introduction

The Northwest European Carboniferous Basin (NWECB) is a large sedimentary basin extending from Ireland in the west to Poland in the east (Fig. 4.1A), which developed north of the Variscan Rheno-Hercynian belt. In a N-S direction, the width of the basin across western Germany and the Netherlands is up to 600 km. The maximum preserved sediment thickness of the Carboniferous succession is up to 6 km. In this chapter, the term Central NWECB (CNWECB) will be used to indicate the English/Welsh, Dutch and West-German parts of this basin.

Two subsidence mechanisms have been proposed for different parts of the basin. North of the London Brabant Massif (LBM), in the northern part of the UK, subsidence has been explained by thermal relaxation following a Dinantian rifting event (Leeder & McMahon, 1988; Coward, 1990; Fraser & Gawthorpe, 1990; Maynard et al., 1997). In the Danish offshore, a Palaeozoic rifting event possibly during the Carboniferous was identified on seismic data (Scheck et al., 2002). In contrast, subsidence along the southern margin of the NWECB has been attributed to thrust-loading by the advancing Variscan orogenic wedge, causing the development of a flexural foreland basin (Ziegler, 1990; Gayer et al., 1993; Warr, 1993; McCann, 1999; Burgess & Gayer, 2000; Drozdzewski, 2005; Kornpihl, 2005). The Netherlands is located in a central position in the NWECB (Fig. 4.1), in between the areas where these two subsidence mechanisms have been interpreted. However, an attempt to test if these models can adequately explain subsidence observed in the Netherlands has never been carried out. A possible explanation for this may be the relative scarcity of data; subsidence curves do not immediately reveal the dominance of one specific subsidence mechanism.

There is no consensus on how far the Variscan foreland basin extended to the north (Coward, 1993; Quirk, 1993; Süss, 1996; Maynard et al., 1997; Ricken et al., 2000; Drozdzewski, 2005). These authors present very different interpretations on the width of the Variscan foreland basin, ranging from a narrow (close to the present-day Variscan Deformation Front (VDF), Fig. 4.1) to a very wide basin (up to Cleaverbank High). Burgess & Gayer (2000) presented a modelling study in the area south of the LBM in Wales in which they reconstructed the migration of the Variscan foreland through time. However, quantitative modelling incorporating the existing ideas on the advance of the Variscan orogenic wedge (e.g. Oncken et al., 2000), with the aim to delineate the geometry of the Variscan foreland basin in western Germany/the Netherlands, has not been carried out to date. In this chapter, a simple modelling study is presented in which predictions on the geometry of the Variscan foreland basin in this area are given. A number of scenarios have been run to test the sensitivity of – amongst others – the thickness of the subducting plate (reflected in elastic thickness, Te) and the shape of the load on the resulting foreland basin geometry. Based on these modelling experiments, it is shown that the foreland basin is too narrow and too far to the south to explain a significant part of the observed subsidence in the Netherlands.

Although there is no published evidence for a Dinantian rifting event in the Netherlands and Western Germany, several authors proposed this (Coward, 1990; Bailey et al., 1993; Coward, 1993; Maynard et al., 1997; Martin et al., 2002; Hoffmann et al., 2005). Based on the results described in chapter 3, it is indeed to be expected that Dinantian rifting occurred in this area. Here, a seismic section from the central part of the Netherlands is also show in which a Lower Carboniferous carbonate buildup is interpreted. These structures are well described in the UK, where they are preferentially found on top of horst blocks developed during Dinantian rifting (Chadwick & Evans, 2005). In the second half of this chapter, the amount of Namurian-Westphalian B thermal subsidence that can be explained by a Dinantian rifting event will be investigated. A number of

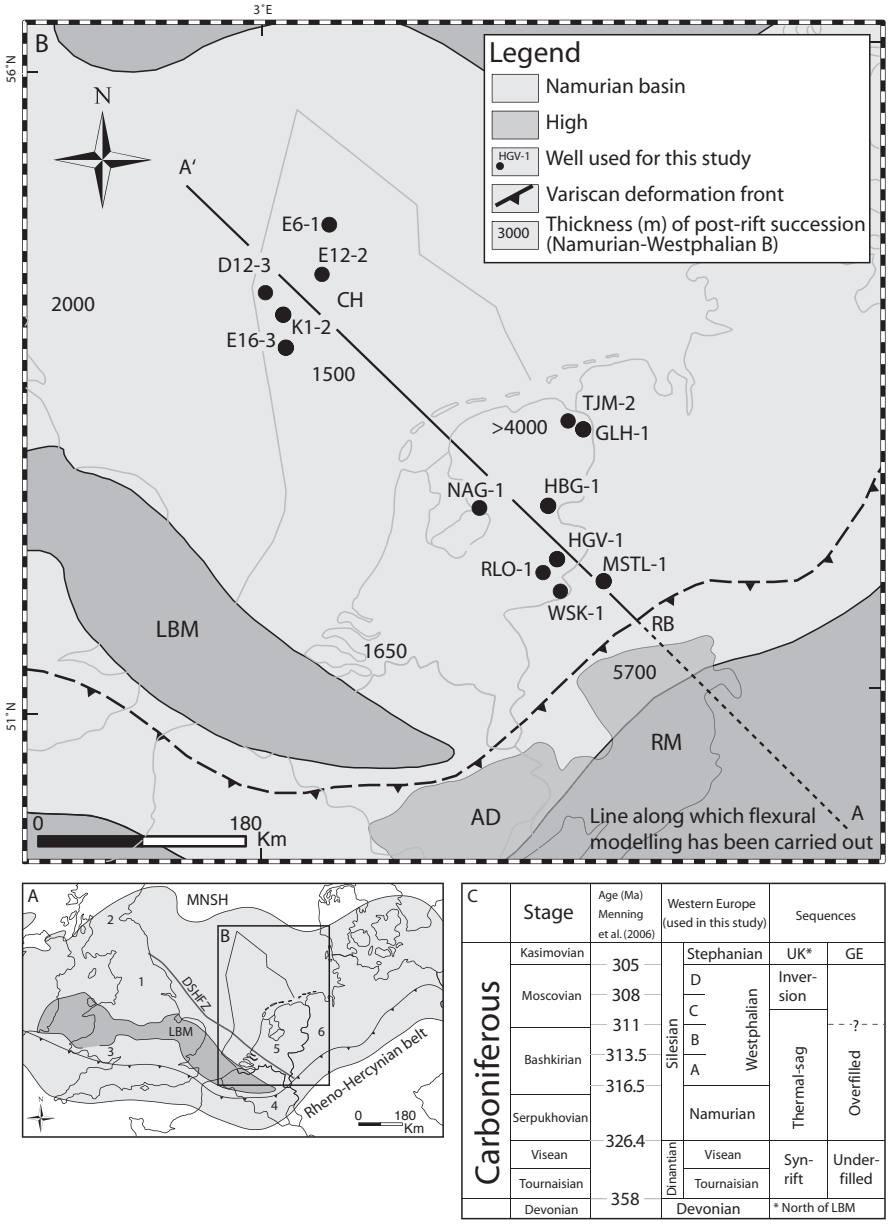

Figure 4.1 (A) Location of Northwest European Carboniferous Basin, (B) detailed map of the study area showing the location of wells used for this study and (C) stratigraphic table with global and local stages (D: Dinantian, S: Silesian, UK: United Kingdom, GE: Germany), timescale used in this study and the (tectonic) sequences recognised in the northern part of England and in the Ruhr Basin (Germany). 1: United Kingdom, 2: Midland Valley, 3: South Wales, 4: Belgium, 5: the Netherlands, 6: Germany, AD: Ardennes, CH: Cleaverbank High, DSHFZ: Dowsing-South Hewett fault zone, LBM: London Brabant Massif, MNSH: Mid North Sea High, RB: Ruhr Basin, RM: Rhenish Massif, study area of Ricken et al. (2000). Maps based on Ziegler (1990).

rifting scenarios were tested, applying uniform stretching (McKenzie, 1978). These scenarios have been run with different estimates for the palaeowater depth at the Visean-Namurian transition, as this is an important but uncertain factor. It turns out to be difficult to explain the subsidence needed to accommodate the thick Late Carboniferous sedimentary sequence assuming a Dinantian rifting event alone.

To summarise, the aims of this chapter are: (1) to quantify the geometry of the Variscan foreland basin and the amount of subsidence in the Netherlands that might be explained by crustal loading; (2) to quantify the amount of (thermal) subsidence that might be explained by a Dinantian rifting event and the comparison with subsidence data from the Netherlands and (3) to propose a number of alternative subsidence models.

4.2 Basin evolution and fill

The Dinantian is characterised by northward subduction of the Palaeo-Tethys Mid Ocean Ridge and southward subduction of the Rhenohercynian Basin beneath the Mid-European terranes, which led to the formation of the Variscan mountains (Franke, 2000; Stampfli & Borel, 2002). Basin development during the Dinantian in the area north of the LBM (onshore UK) area is characterised by extension (Fraser & Gawthorpe, 1990; Hollywood & Whorlow, 1993), which has been attributed to the effects of a phase of lithospheric stretching induced by the subduction of the Palaeo-Tethys in Brittany and Central France (Leeder, 1992). This rifting event resulted in a horst and graben topography with carbonate platforms on the horsts (e.g. Derbyshire block) and relatively deep-water settings in the neighbouring grabens (e.g. Bowland and Widmerpool Basins). The results described in chapter 3 show that a similar setting is likely for the northern part of the Netherlands onshore. Figure 4.2 shows another undrilled structure (not shown in chapter 3) that very much resembles Visean carbonate buildups as found in the UK (Fig. 4.2, compare Fig. 4.68 from Chadwick & Evans, 2005).

As a consequence of loading of the subducting plate along the southern margin of Avalonia, a series of (underfilled) foreland basins (Kulm) developed (Ricken et al., 2000). The Variscan mountains acted as the sediment source for these basins. From these underfilled basins in the south of the CNWECB, the thickness of Lower Carboniferous sediments diminishes to the north, where it can be found as a condensed sequence of black shales in the wells WSK-1 in the Netherlands and MSTL-1 in Germany (Hoffmann et al., 2005; Figs 4.1 and 4.3). Apart from these wells, Lower Carboniferous sediments have only been recovered from wells surrounding the LBM, the Mid North Sea High and onshore UK. In the remaining part of the CNWECB well control is absent (Fig. 3.1).

The Visean/Namurian transition marks the onset of collision between the Rhenohercynian northern passive margin (southern margin of Avalonia) and the terranes in the south (Oncken et al., 1999). The Late Visean subduction of oceanic domains in the Rhenohercynian Basin was accompanied by the intrusion of I-type granitoids in the northern Vosges and Odenwald. Emplacement of S-type granitoids during the Namurian suggests that by now substantial amounts of continental lithosphere subducted (Ziegler, 1990). In western Germany, the change from a narrow (underfilled) to a broad (overfilled) foreland basin is thought to occur during Visean/Namurian transition (Ricken et al., 2000; see below for more details), as a consequence of the subduction of stronger (unrifted) lithosphere. North of the LBM, in the UK, the Namurian marks the onset of regional passive subsidence, interpreted as thermally induced after the Dinantian

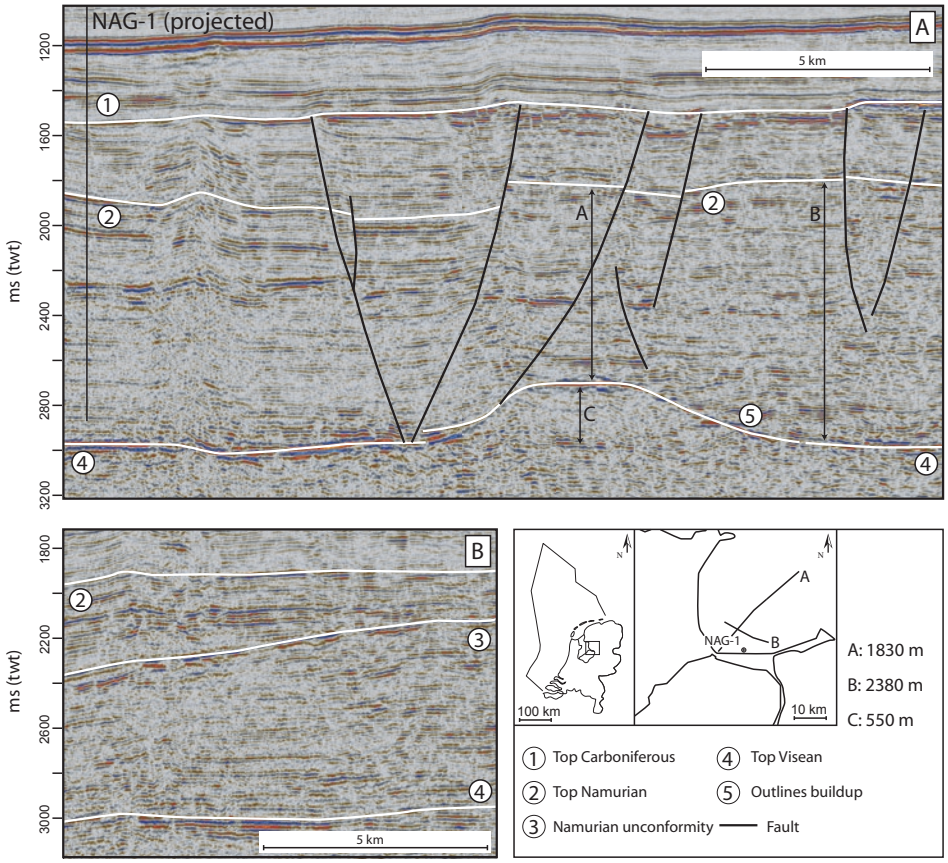

Figure 4.2 (A) Seismic section from the central part of the Netherlands where a Visean carbonate buildup has been interpreted. (B) Seismic section from the same area where an intra-Namurian angular unconformity has been mapped.

rifting event (Fraser & Gawthorpe, 1990). In the area south of the LBM (Wales, UK), backstripped subsidence curves reveal the onset of flexural subsidence during Late Namurian (Burgess & Gayer, 2000). North of the LBM, in the UK, the Namurian marks the onset of regional passive subsidence, interpreted as thermally induced after the Dinantian rifting event (**Fraser** & Gawthorpe, 1990). The Namurian in the CNWECB is also mostly seen as a period in which steady subsidence occurred (either due to thermal or to flexural foreland subsidence). However, in the central and northern parts of the Netherlands, an intra-Namurian angular unconformity has been mapped on seismics (Fig. 4.2). Although this unconformity has not been mapped regionally yet, this finding suggests a more complicated history of Namurian subsidence.

In the UK, the Namurian sedimentary sequence reflects the draping of the Dinantian carbonate platforms and the in-fill of the neighbouring (deep water) basins with mainly prodelta silty claystones and turbidites (Maynard et al., 1997). This depositional pattern resulted in significant thickness variations (Smith et al., 2005). The few wells in the Netherlands that penetrate the Namurian sequence also show a silty claystone-dominated sequence interpreted as a pro-delta

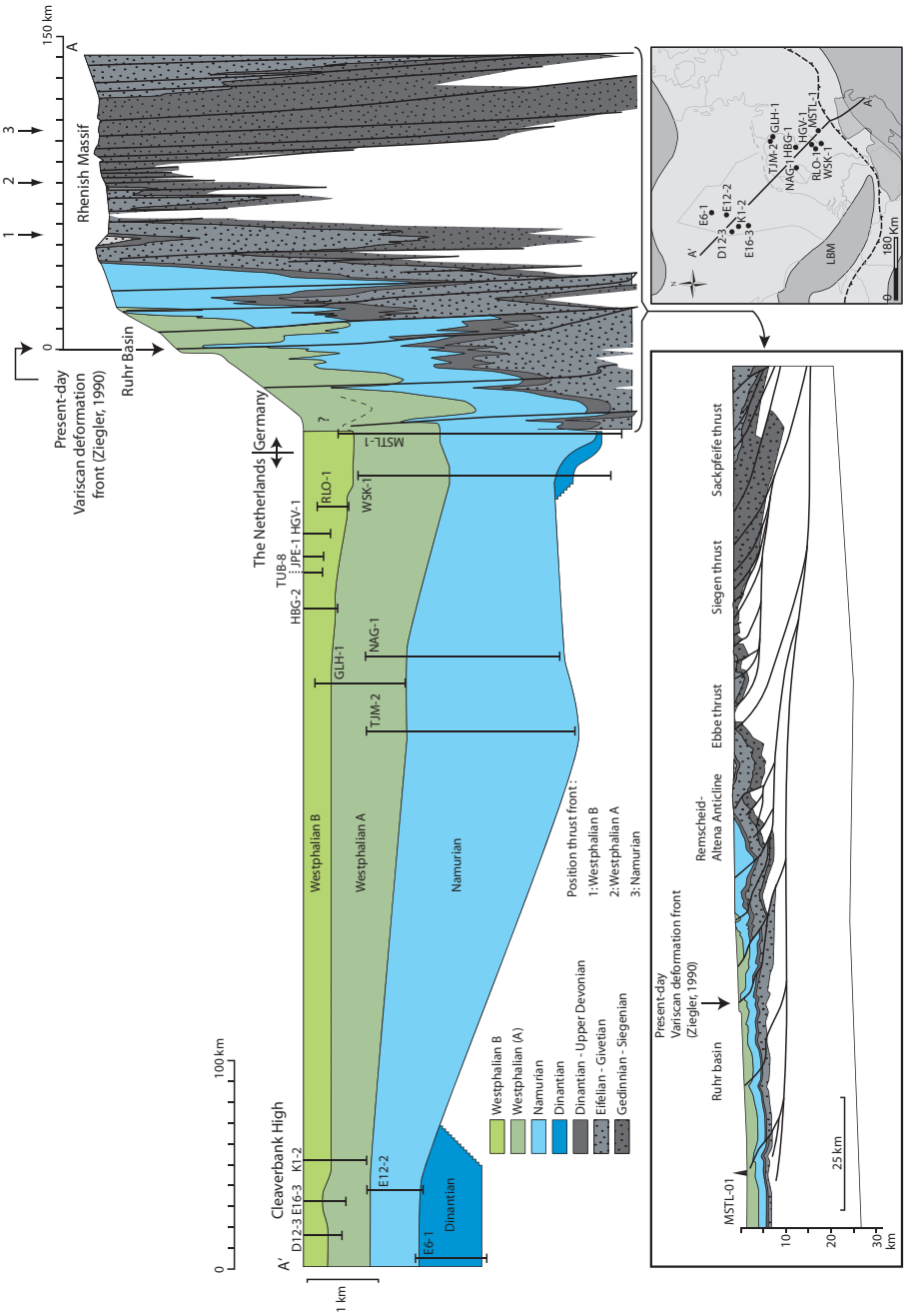

Figure 4.3 Section from the Rhenish Mountains (former passive margin of the Rhenohercynian Basin) to the Cleaverbank High area showing the thickness of the Carboniferous sediments in this area. The wells used for this study are plotted in the cross-section. Note that the Dutch part of this section is flattened and does not represent the actual depth (the depth below surface is indicated by the dashed line above the cross-section). The Rhenish Massif section is based on Oncken et al. (2000).

sediments and intercalations of (turbiditic) sandstones. Only the very northern offshore area (well E12-2) shows a northern-derived Namurian fluvio-deltaic sequence.

Collision between Laurussia and Gondwana continued during the Westphalian. Subsidence curves derived from the area south of the LBM (Wales) show a strong convex-up pattern during the Westphalian (Burgess & Gayer, 2000), indicative of increasing thrust loading of the foreland lithosphere during the northward advance of the Variscan orogenic front. From thickness data a progressive northward shift of the axis of the Variscan foreland basin has also been interpreted in the Ruhr area (Drozdzewski, 2005). Moreover, Drozdzewski (2005) interpret a forebulge *in* the Ruhr Basin. This interpretation places the Netherlands in a back-bulge position (see below for more details). North of the LBM, thermal subsidence is thought to continue (Fraser & Gawthorpe, 1990). During mid-Westphalian C, the tectonic regime turned from passive (thermal) subsidence into basin inversion as a result of the build-up of intraplate compressional stresses at crustal levels, reflecting increasing mechanical coupling of the Variscan orogenic wedge with its foreland lithosphere (Ziegler et al., 1995; Ziegler et al., 1998; Ziegler et al., 2002). Therefore, sediments younger than Westphalian B show a more dispersed distribution.

The Namurian/Westphalian transition marks the occurrence of the first thick coal seams in the CNWECB, although in proximal areas this already took place in the Namurian C (Drozdzewski, 2005). As such, the depositional environment changed during the late Namurian from broadly shallow marine to a lower delta plain with numerous coal layers during the Westphalian. The palaeowater depth can therefore be assumed to be zero from end-Namurian times onward.

4.3 Data

The Namurian and Lower Carboniferous of the Netherlands are part of the lower limit of the petroleum fairway (Cameron & Ziegler, 1997). Therefore, well control is scarce (Fig. 3.1). The wells used for this study had to fulfil two criteria: (1) they have to be located on a cross-section that more or less runs NW-SE from the Rhenish Massif because flexural modelling has to be carried out on a line perpendicular to the VDF (Figs 4.1 and 4.3) and (2) the stratigraphic penetration should be as high as possible. Fig. 4.3 shows the position and stratigraphic penetration of the most important wells used for this study. Subsidence curves have been made for 5 areas (Table 4.1, Fig. 4.4). In each area, the thickness of the Lower Carboniferous up to Westphalian B has been derived from several wells. Unfortunately, well-based thickness data for the Lower Carboniferous are lacking for the areas Netherlands-central and north because the stratigraphically deepest wells NAG-1 and TJM-2 do not penetrate the base Namurian. Moreover, the results presented in chapter 3 suggest that significant thickness changes may be expected for the Namurian. The well TJM-2 drilled a Namurian sequence of 2650 m (Fig. 3.4) but on top of the Groningen Platform the Namurian might have half the thickness. The same applies to the central part of the Netherlands. On both sides of the Nagele buildup the Namurian might have a thickness of approximately 2380 m whilst on top it is approximately 1830 m (Fig. 4.2). However, in the Lauwerszee Trough the Namurian might be even thicker than in TJM-2. For the modelling input, it was decided to use the well-based Namurian thickness data. A number of modelling scenarios with different values for the palaeowater depth at the Visean-Namurian transition and the thickness of the Lower Carboniferous succession partly take these uncertainties into account. The thickness of the Westphalian A in the Netherlands-central area is a minimum estimate, as is the thickness of the Westphalian B in the area Netherlands-north. These minimum values are caused by Early Permian

Table 4.1 Thickness data used in this study.

Well	Dinantian	Namurian	Westphalian A	Westphalian B
Germany [1]	70 m	1800 m	1100 m	900 m
Netherlands-east [2]	260 m	1525 m	1380 m	700 m
Netherlands-central [3]	200 m	2150 m	700 m	470 m
Netherlands-north [4]	200 m	2650 m	700 m	400 m
Cleaverbank High [5]	1000 m	680 m	520 m	400 m

1 Based on: Münsterland-1 (MSTL-1), Altenkamp-3 and Besenkamp-1
2 Based on: Winterswijk-1 (WSK-01), Hengevelde-1 (HGV-1), Ruurlo-1 (RLO-1) and Joppe-1 (JPE-1)
3 Based on: Nagele-1 (NAG-1) and Hardenberg-2 (HBG-2)
4 Based on: Tjuchem-2 (TJM-2) and Goldhorn-1 (GLH-1)
5 Based on: E6-1, E12-2 and K1-2

erosion or incomplete well-penetration of these stratigraphic intervals. Finally, a dip-correction was carried out for the well MSTL-1, because the strata show dips up to 80 degrees (Richwien et al., 1963).

4.4 Subsidence curves

Subsidence curves can reveal important information on the dominant subsidence mechanism. For instance, in extensional regimes typical concave-up curves occur as a consequence of decreasing subsidence related to thermal re-equilibration (McKenzie, 1978). In order to verify the modelling results as presented in the following sections, subsidence curves needed to be calculated. Basement subsidence has been calculated to verify the flexural modelling results. It is the combination of tectonic subsidence and subsidence due to sediment loading with the reference horizon being a compaction-free horizon (basement). Tectonic subsidence curves were needed to match the subsidence curves generated by simulation of a rifting event in the second modelling exercise.

The backstripping technique (Steckler & Watts, 1978) has been used to calculate the basement and tectonic subsidence curves, assuming Airy isostasy. Age constraints for backstripping were derived from the Global time scale as used in the Devonian-Carboniferous-Permian Correlation Chart 2003 (Menning et al., 2006; Fig. 4.1C). Emphasis will be put on the Dinantian, Namurian and Westphalian A/B stages. No further subdivision of stages has been made due to dating uncertainties. Standard mean porosity-depth relationships for different lithologies (cf. Sclater & Christie, 1980) were used. The complete post-Carboniferous overburden has been backstripped as well to account for Permian and Mesozoic burial.

The palaeowater depth (PWD) at the Visean-Namurian transition is a great factor of uncertainty. The Cleaverbank High is the only area where a reliable estimate of the late Visean PWD is possible. Here, Lower Carboniferous sediments reflect near-emergent conditions, which led us to decide to use only one value of 10 m. The tectonic and basement subsidence curves in the other areas have been calculated with two 'end-members' of end-Visean PWD. A number of authors propose a long term eustatic drop in sea level at the Visean – Namurian transition (Ross & Ross, 1988, their Fig. 9; Gursky, 2006). Karstification of Visean carbonate platforms is well described in the NWECB (Bless et al., 1976; Amler & Herbig, 2006). The minimum end-Visean PWD scenario in this study therefore assumes a long term drop in sea level (100 m PWD). It must be clear that this PWD estimate applies to the basinal areas and not to the top of

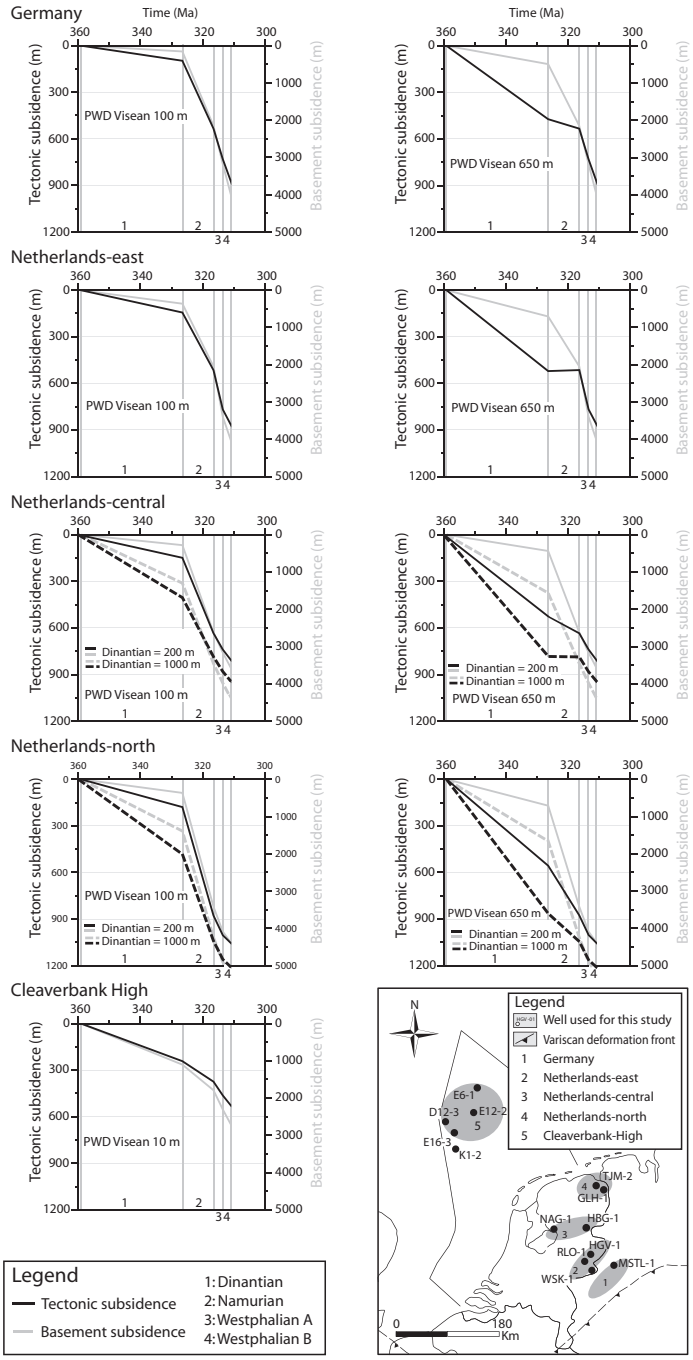

Figure 4.4 Tectonic and basement subsidence curves for selected areas for two end-members of end-Visean PWD and for two end-members of Dinantian thickness in Netherlands-central and -north. Note the difference in vertical scale between basement and tectonic subsidence.

the platforms. A maximum value of 650 m is used; if larger values of the end-Visean PWD are adopted, the amount of sediment that can be accommodated during the Namurian without any additional tectonic subsidence exceeds the observed thickness data. It can be generally assumed that the PWD at the end of the Namurian and Westphalian A/B is near zero (see above), which does not allow a significant PWD at these times. Moreover, two additional scenarios have been run for the Netherlands-central and north to account for the lack of thickness data for the Lower Carboniferous. The lower end-member is 200 m, comparable to the thicknesses as found in the southeastern part of the basin. The upper end-member is 1000 m, comparable to what has been found in E6-1 in the northern offshore.

Most tectonic subsidence curves in the low end-Visean PWD scenarios show an overall convex-up pattern, although from Westphalian A to B a slight decrease in tectonic subsidence can be seen in some areas (Fig. 4.4). However, in the high end-Visean PWD scenarios, a decrease in tectonic subsidence occurs during the Visean-Namurian transition because of the mostly passive in-fill of the deep-water basin. In this case an increase can be seen at the Namurian-Westphalian A transition. There are no large differences between the Lower Carboniferous end-member subsidence curves in the areas Netherlands-central and north. Altogether, based on the uncertainties related mostly to the end-Visean PWD, it is difficult to draw a conclusion on the dominant subsidence type, although the convex-up patterns (low end-Visean PWD) may be more likely due to the long-term drop in sea level proposed in literature.

4.5 2D forward flexural subsidence modelling

It was investigated whether subsidence in the Dutch part of the CNWECB can be (partly) explained by foreland flexure due to orogenic loading by the approaching Rheno-Hercynian belt. This was carried out by 2D flexural modelling along a NW-SE profile (Figs 4.1B and 4.3) using an elastic thin plate approach. Before presenting the modelling results, the current ideas on the kinematics of the Rheno-Hercynian belt and the geometry of the adjacent Variscan foreland basin will be shortly reviewed.

4.5.1 Constraints on kinematics of the Rheno-Hercynian belt and the geometry of the adjacent Variscan foreland basin

The kinematics of the Rheno-Hercynian belt are well constrained by the restoration of a series of sections across the Ardennes and Rhenish Massif (Oncken et al., 2000). From 335 to 325 Ma (Late Dinantian) shortening has been calculated to be 140 km, while from 325 to 305 Ma, 175 km of shortening took place (Oncken et al., 2000). The geometry of the adjacent foreland basin has been studied in particular by Drozdzewski (1993) and Ricken et al. (2000). These authors use different data to arrive at an interpretation. These will be outlined below. A cross-section displaying the Rhenish Massif in the south and the German/Dutch part of the CNWECB up to the Cleaverbank High in the north is given in Fig. 4.3.

Ricken et al. (2000), in their study area in the eastern part of the Rhenish Massif, subdivided the tectono-sedimentary evolution of the basins in front of the advancing Rheno-Hercynian Belt in two stages, the Rheno-Hercynian Turbidite Basin (RHTB) and Sub-Variscan Molasse Basin (SVMB). The RHTB developed in front of the (initially submerged) advancing belt as it was shortened from 335 to 325 Ma. It is characterised by a migrating series of narrow underfilled (Kulm) basins. The second stage of basin development, the SVMB, is characterised by a broader

basin (Ricken et al., 2000). It started in Namurian time (325 Ma) and lasted until the end of shortening in Stephanian times (305 Ma). Unfortunately, Ricken et al. (2000) do not give an estimate on the width of the SVMB. The transition between the two stages in basin evolution (from the narrow RHTB to the wide SVMB) is interpreted to correspond to the migration of the belt across the transition from weakened crust (beta from 1.7-2.4 and effective elastic thickness (Te) of 4 km) to unrifted, stronger crust (subcrustal stretching factor beta = 1.0-1.5, Ricken et al., 2000). In this chapter, the basin evolution since Namurian will be studied, i.e. corresponding to the SVMB stage.

On the basis of thickness data in the Ruhr Basin, Drozdzewski (1993) found a northward moving area of reduced subsidence (Westphalian A and B) that was interpreted to be a forebulge. In contrast to the conventional model of a foreland basin (e.g. DeCelles & Giles, 1996) in which the forebulge is an erosional feature, in this case subsidence continues but with a slightly decreased subsidence rate compared to the basinal areas. This implies the existence of another subsidence mechanism which causes the forebulge to subside. The recognition of a forebulge means that the northern limit of the Variscan foreland basin can be mapped. Combining this with the kinematic data from Oncken et al. (2000; Fig. 4.6), a rather narrow foreland basin must be interpreted.

In summary, two contrasting geometries of the Variscan foreland basin in western Germany exist. Ricken et al. (2000) interpret a broad foreland basin developed on a relatively strong plate while Drozdzewski (1993) imply a rather narrow basin when their data are combined with the kinematic data from Oncken et al. (2000; Fig. 4.6). These interpretations can be modelled by assuming a subducting plate with a high elastic thickness (Te) resulting in a broad foreland basin, and a small Te in which case a rather narrow basin will develop. In the next section, it will be investigated what part of the observed subsidence in the CNWECB can potentially be explained by flexural subsidence, using a range of parameters. This will lead to an evaluation of the existing ideas on the geometry of the Variscan foreland basin.

4.5.2 Model scenarios

Reconstruction of the tectonic history of the Dutch part of the CNWECB is hampered by deep burial of Carboniferous sediments, as described above. As a consequence of the relative scarcity of data, especially on lithosphere parameters like the elastic thickness and distribution of excess (mantle) loads, this modelling exercise presents a series of scenarios of end-member estimates. Therefore, the results must be seen as a sensitivity analysis for the geometry of the Variscan foreland basin in the CNWECB. The effects of the following parameters on the geometry of the foreland basin were studied (Fig. 4.5): (1) different values of Te (5 and 60 km) in a plate of constant rigidity. This is the simplest scenario in which only the influence of the rigidity of the subducting plate is studied. Elastic thicknesses of 5 and 60 km are naturally occurring end-members for a very weak and strong plate, respectively. (2) A strength transition sensu Ricken et al. (2000). The location of the strength transition has been derived from the reconstruction by Oncken et al. (2000). (3) An end-Visean PWD of 650 m. As mentioned above, the end-Visean PWD is an important factor in determining the amount of subsidence needed to accommodate the Namurian sedimentary sequence. For the wells MSTL-1, WSK-1, NAG-1 and TJM-2 a PWD of 650 m has been assumed, shallowing to 10 m for the Cleaverbank High area. (4) A different load geometry. When the centre of the load is moved northwards, without changing the position of the frontal thrust, the resulting foreland basin will be wider. The effects of such a change will be studied assuming a block-load.

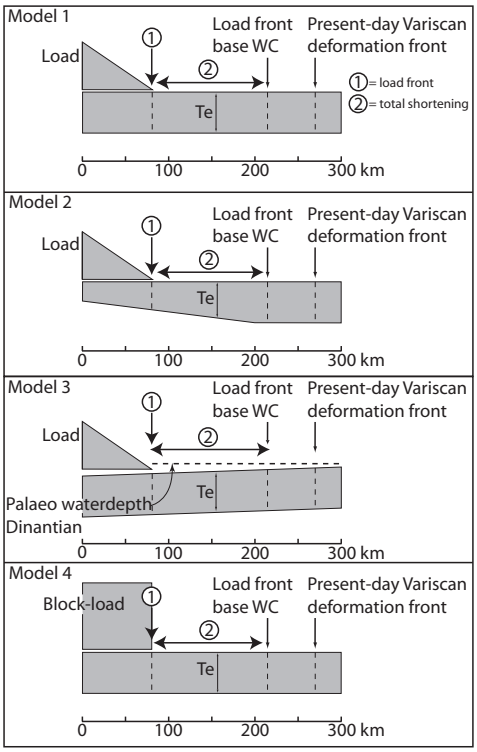

Figure 4.5 Model scenarios for flexural modelling exercise.

4.5.3 Model setup and parameters

A 2D finite difference code was used, COBRA, which calculates flexure of an elastic thin plate (for equations and their derivation, see Royden (1988) and Zoetemeijer et al. (1999). The program allows to laterally change the flexural rigidity and the application of both topographic and 'hidden' loads. It takes into account different densities for the load and basin fill and can be applied to both continuous and broken plates, the latter with or without an end load ('slab pull'). Modelling was carried out along the cross-section shown in Figs 4.1 and 4.3. In each case, the predicted basement subsidence curves will be compared with basement subsidence curves derived from well data (Fig. 4.6).

The total shortening amounts to 175 km in 20 Ma from Namurian to Stephanian (Oncken et al., 1999; Oncken et al., 2000). During this time interval, material is accreted at the thrust front according to the critically tapered wedge concept (e.g. Chapple, 1978). Therefore the width of the load increases (Tables 4.2 & 4.3) from 140 km to 180 km; the topographic slope (α) varying between 2.5 and 3°. The wedge-shaped load stays at the end of the broken plate; the pro-foreland side of the doubly vergent wedge model will be studied here (e.g. Willett, 1999). Assuming a constant shortening/displacement rate of 9 km/Ma, starting in Namurian, the model was run for three time steps (Namurian and Westphalian A and B).

The density of the basin-fill will not only affect the magnitude of the deflection but also its wavelength (Turcotte & Schubert, 2002; Fig. 2 in Leever et al., 2006). For the Namurian – Westphalian B time steps, the PWD is near zero (see above) and the basin was completely filled

Table 4.2 Parameters used for flexural modelling and input for models.

Common parameters		
Load advance rate		8.75 km/Ma
Initial load width		140 km
Final load width		180 km
Density of load, basin fill, crust, mantle		2700, 2400, 2800, 3300 kg/m^3
Model 1	Plate constant Te	Te 5 and 60 km
Model 2	Transition width	200 km
	Te south/Te north	10/40 and 10/80 km
Model 3	Maximum late-Dinantian PWD	650 – 10 m
	Plate constant Te	Te 5 and 60 km
Model 4	Block-load, constant Te	Te 5 and 60 km

with sediments. To prevent underestimation of the sediment density, a relatively high density has been used (2400 kg/m^3). For an overview of sediment densities, see Kearey et al. (2002).

4.5.4 Model results

Figure 4.6 shows the predicted basement subsidence for three load steps (Namurian – Westphalian B) for two end-members with respect to plate rigidities (Te 5 km and Te 60 km plate constant thickness). In each figure the final position of the thrust front is indicated (present-day VDF). Moreover, the forebulge positions during Westphalian A and B according to Drozdzewski, (2005) are shown. The basin is very narrow for the weakest plate (Te 5 km), having a width of some 25 km (with respect to the thrust front) and a basement subsidence of ~1000 m. It is located at such a distance from the Netherlands that none of the observed subsidence can be explained in this case. The amplitude is too small as well. A significantly wider basin, with a higher amplitude, is predicted when a Te of 60 km is assumed, having a width of >400 km and a basement subsidence of ~2 km. In this case a small part of the observed subsidence may be explained by flexural subsidence. Especially during the Westphalian B the complete succession in the southeastern part of the Netherlands might be explained by flexural foreland subsidence.

The basin-width in relation to the load migration results in an additional effect. The basins that develop on a weak plate (Te = 5 km) are so narrow that, in the subsequent time step, the load has migrated past the previous basin (compare Figs 4.6A-C). Therefore, these basins will only contain sediments that have been deposited during the previous period. In contrast, the large wavelength of the strong plates (Te > 40 km) will cause subsidence well in advance of the thrust front, far

Table 4.3 Load displacement and geometry for the different time steps (based on reconstructions by Oncken et al., 2000).

Time of base:		**Position of load center (km)**	**Position of load front (km)**	**Load width (half wedge, km)**	**Load height (km)**	**Wedge slope**
Stephanian	305	180	270	90	5	3.2
Westphalian C	311	130	215	85	4.5	3
Westphalian B	313.5	110	190	80	4	2.9
Westphalian A	316.5	90	165	75	3.5	2.7
Namurian	326.4	0	70	70	3	2.5

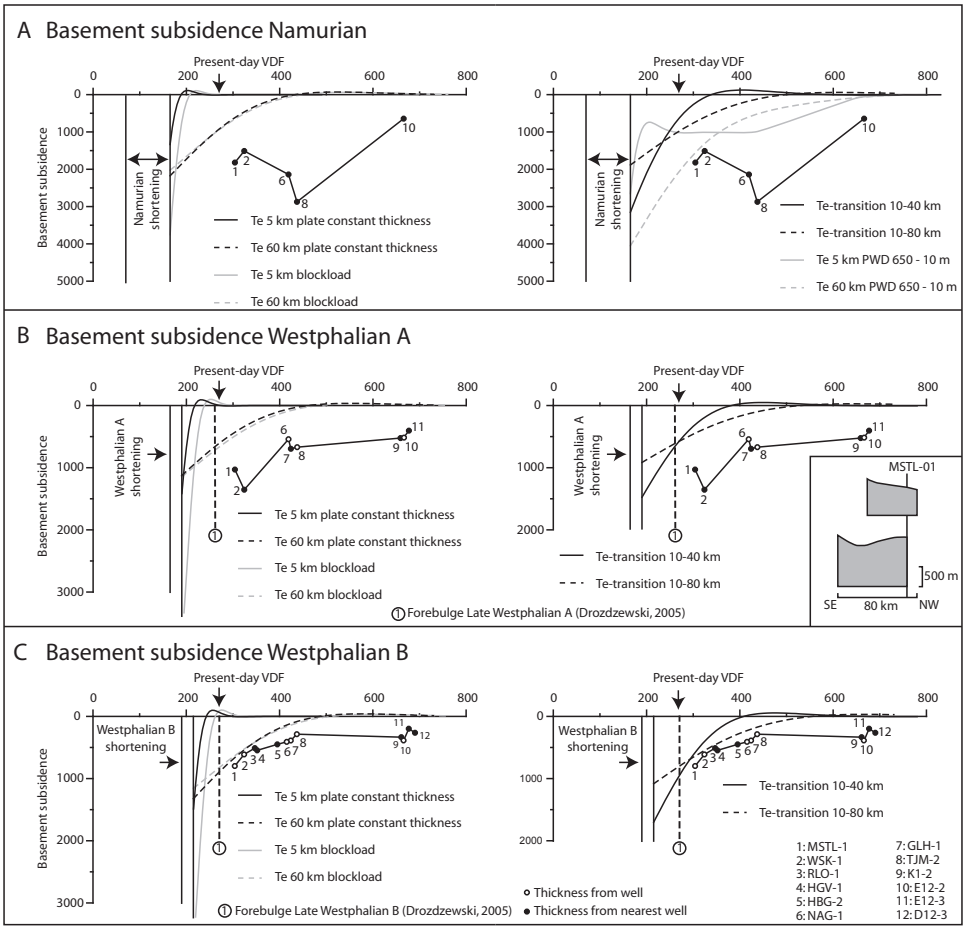

Figure 4.6 (A) Comparison between modelled (flexural) basement subsidence and the basement subsidence derived from well data for the Namurian, (B) Westphalian A and (C) Westphalian B. Location of the wells can be seen in Fig. 4.3. Four model scenarios are shown (Fig. 4.5). The inset in Fig. 4.6B shows the thickness of Westphalian A and B sediments in the Ruhr Basin, southeast of the well MSTL-1. VDF: Variscan Deformation Front.

enough to record sedimentation over a large period of time. In case of the strongest plates (Te ≥ 60 km) this even takes place since the beginning of the Namurian.

In the next scenario the same loading will be used as in the first series of experiments but a 200 km wide transition in strength in the plate is introduced (Fig. 4.5). The results (Te-transition 10-40 and 10-80 km, Fig. 4.6) are comparable to the response of the continuous plate of 60 km, as the wedge has started to advance over the transition zone from the first (Namurian) load step. Only the first load step (Namurian) shows the signature of the weaker plate. For a lateral change in lithosphere strength to cause a marked difference in Namurian – Westphalian B foreland basin geometry compared to the continuous lithosphere strength (previous scenario), the transition has to be located further to the north or the transition width has to be decreased (e.g. Leever et al., 2006).

When incorporating an initial PWD for the Late Visean, the amount of predicted basement subsidence for the Namurian increases significantly (Te 5/60 PWD 650 m, Fig. 4.6). Especially in the case of a high Te, the fit with the observed basement subsidence data is the best one so far (in amplitude as well as width). However, it is still not sufficient to explain the high subsidence in NAG-1 and TJM-2 (Netherlands-central and north respectively). As there is no reason to assume a PWD for the late-Namurian and the Westphalian A and B, the results for these stages have not been plotted, because the results are comparable with the first modelling scenario.

The application of a different load geometry (block load) results in a slight increase in basin width in both cases, while a decrease in amplitude for the high-Te and an increase in the low-Te case can be seen. However, this increase in width is far from sufficient to give better result compared to the results from the first scenarios.

4.5.5 Discussion of model results

The most important conclusion from the scenarios presented above is that the amplitude of the (observed) subsidence more or less corresponds to the modelled flexural subsidence but the width and location of the foreland basin prevent a significant part of the CNWECB to be explained by this mechanism, especially for the Namurian. Only when a high end-Visean PWD is assumed, a relatively good fit can be seen for the Namurian, although it has to be realised that the development of such a deep-water basin can not be explained by flexural subsidence. For the Westphalian A, there is a slightly better match when taking the high values of Te into account. However, in no case the complete Westphalian A sequence can be attributed to flexural subsidence. The complete basement subsidence observed in the southeastern part of the Netherlands during the Westphalian B can potentially be explained by flexural subsidence if a high Te of 60 km is assumed. A change in the geometry of the load to a block load leads to a very small and insignificant increase in basin width. A possible scenario to obtain a better match between calculated and modelled basement subsidence during the Namurian is to shift the deformation front further to the north. However, this would be in disagreement with the reconstructions from (Oncken et al., 2000; Fig. 4.3). The increase in subsidence from WSK-1 to the north during the Namurian is difficult to explain in a foreland basin setting. A possible explanation is the presence of a blind thrust. There is however no (seismic) data to support this hypothesis.

It is clear from the modelling results that the interpretation of the forebulge by Drozdzewski (1993) only fits the low-Te (5 km) model results (Fig. 4.6). This contrasts the interpretation of Ricken et al. (2000) who state that the foreland basin during the Westphalian developed on a relatively strong plate, which results in a broad basin. When the assumption is made that the forebulge interpreted by Drozdzewski (1993) is indeed at the right position, one would expect to find a very pronounced thickness difference on both sides of the forebulge area (see PWD 650 result for Te 5 km). However, thickness differences display a gradual change indeed (Fig. 4.3 and inset in Fig. 4.6B). Moreover, Fig. 4.6 shows that in case of a Te of 5 km the foreland basins are so narrow that, in the subsequent time step, the load has migrated past the previous basin. Therefore, it is not expected to find sediments of subsequent timesteps on top of each other. In the Ruhr area, sediments of Namurian – Westphalian B age have been deposited on top of each other. This observation points to a relatively high Te, in accordance with the interpretation by Ricken et al. (2000). Altogether, the thickness data for the southern part of the study area may be in favour of a relatively broad foreland basin.

4.6 Tectonic subsidence modelling applying lithospheric stretching

In the previous section it was shown that orogenic loading of a foreland plate largely fails to explain subsidence observed in the Netherlands during the Namurian. During the Westphalian A and B, the influence of flexural subsidence is limited to the southeastern part of the Netherlands. Therefore, most of the observed subsidence must be explained by a second mechanism. In this section, it will be investigate whether the observed subsidence can be explained by the simulation of a rifting event, the mechanism proposed in the UK to account for Dinantian (syn-rift) and Namurian – Westphalian B (post-rift) subsidence (Fraser & Gawthorpe, 1990). The focus will be on the areas where, according to the modelling results presented above, no or only a very small amount of flexural subsidence took place. These areas are Netherlands-central/north and Cleaverbank High (Figs 4.1 and 4.7).

4.6.1 Numerical Model

Various studies have demonstrated the possibility of inversion of subsidence curves to kinematic tectonic models (e.g. White, 1994; Van Wees et al., 1996; Bellingham & White, 2000; Van Wees & Beekman, 2000). For the modelling exercise described in this section, a (multi-) 1D probabilistic tectonic model was used. The model starts with backstrip analysis resulting in tectonic subsidence curves. Subsequently, a best fit tectonic model, matching the observed tectonic subsidence, is found using a tectonic modelling inversion procedure. The modelling approach is based on the pure-shear lithosphere thinning model of McKenzie (1978) with the possibility of different amounts of thinning in the crustal and subcrustal parts of the lithosphere (e.g. Royden & Keen, 1980). During lithospheric stretching, velocities are calculated assuming fixed strain-rates. Sedimentation or erosional velocities are assumed linear through time in accordance with backstrip analysis (e.g. Bond & Kominz, 1984).

The numerical technique to automatically find the best-fitting stretching parameters for (part of) the subsidence data was developed by Van Wees et al. (1996). In this procedure, the onset and duration of the rift phases must be specified, whereas best-fitting stretching values are found by Powell's method (Press et al., 1988). The minimum of the mean square root F of the deviation between predicted and observed subsidence is sought as a function of:

$$F = \sqrt{\frac{\sum_{i=1..n} (Sp_i - So_i)^2}{n}}$$

n is the number of subsidence data used in the fitting procedure while Sp_i and So_i represent the predicted and observed subsidence values respectively. For a given rift phase, either uniform (i.e., McKenzie, 1978), or two-layered, non-homogeneous ($\beta \neq \delta$; e.g., Royden & Keen, 1980) stretching can be implemented according to the user's choice. For uniform stretching, the solution of the equation above requires that at least one observed subsidence datapoint is given after the onset of rifting, whereas the two-layered stretching implementation requires at least two datapoints. For multiphase lithospheric stretching, the fit is accomplished in sequential order.

4.6.2 Rifting history models

In the following section the Late Carboniferous basin evolution will be simulated using 2 scenarios. As mentioned before, the end-Visean PWD can not be simply assumed as a fixed value. Therefore,

Table 4.4 Model parameters.

Model parameter	
Initial lithospheric thickness	110 km
Initial crustal thickness	32 km
Asthenospheric temperature	1330 °C
Thermal diffusivity	1×10^{-6} m^2 s^{-1}
Crustal density	2800 kg m^{-3}
Mantle density	3400 kg m^{-3}
Thermal expansion coefficient	3.2×10^{-5} °C^{-1}

it was chosen to model the tectonic subsidence using the minimum and maximum estimates of the end-Visean PWD (100 and 650 m respectively). Moreover, these scenarios were modelled with two end-members of Lower Carboniferous thicknesses as well, because for the Netherlands-central and Netherlands-north these are lacking (see above).

Estimates on the crustal thickness are given by Mooney et al. (1998, in Fischer et al., 2004) and Henk (1999), being 36.3 and 30-32 km respectively. A thickness of 32 km is assumed in the models used here. Further information on the input parameters can be found in Table 4.4. Like the flexural modelling exercise, the tectonic modelling has to be regarded as a search for the applicability of certain stretching regimes to the Late Carboniferous of the Netherlands rather than presenting a fully constrained tectonic model.

In model 1 a Dinantian rifting event with uniform stretching is assumed (McKenzie, 1978), followed by Namurian – Westphalian B thermal sag such as found in the UK (Leeder & McMahon, 1988; Fig. 4.1). On the basis of the poor fit of this model with the observed data, especially in the low end-Visean PWD case, it was decided to model a scenario incorporating a Namurian rifting event (model 2). In figure 4.7 the observed tectonic subsidence from well data (see also Fig. 4.2) is displayed next to the best-fit subsidence curves.

4.6.2.1 Model 1 – Dinantian rifting (syn-rift) with uniform lithospheric extension, followed by Namurian-Westphalian B thermal sag (post-rift).

Uniform lithospheric extension implies coupling of the crustal and subcrustal stretching factors δ and β respectively (McKenzie, 1978). This is the most common and simple model that has been applied in the UK to derive stretching factors needed to explain the amount of post-rift subsidence (Leeder & McMahon, 1988; Coward, 1993). From the modelling results (Fig. 4.7) it follows that a better match between syn- and postrift tectonic subsidence can be obtained when a high end-Visean PWD is assumed, irrespective of the thickness of the Lower Carboniferous succession. This is not surprising as in the low end-Visean PWD scenario anomalously high tectonic subsidence takes place during the post-rift phase when compared with the syn-rift phase. In most scenarios (high and low end-Visean PWD) the amount of syn-rift subsidence is overestimated by the model relative to the observed syn-rift subsidence to obtain a best fit. In other words, even in the case of the high end-Visean PWD and a Lower Carboniferous thickness of 1000 m, the amount of subsidence in the post-rift stage is too high relative to the syn-rift subsidence.

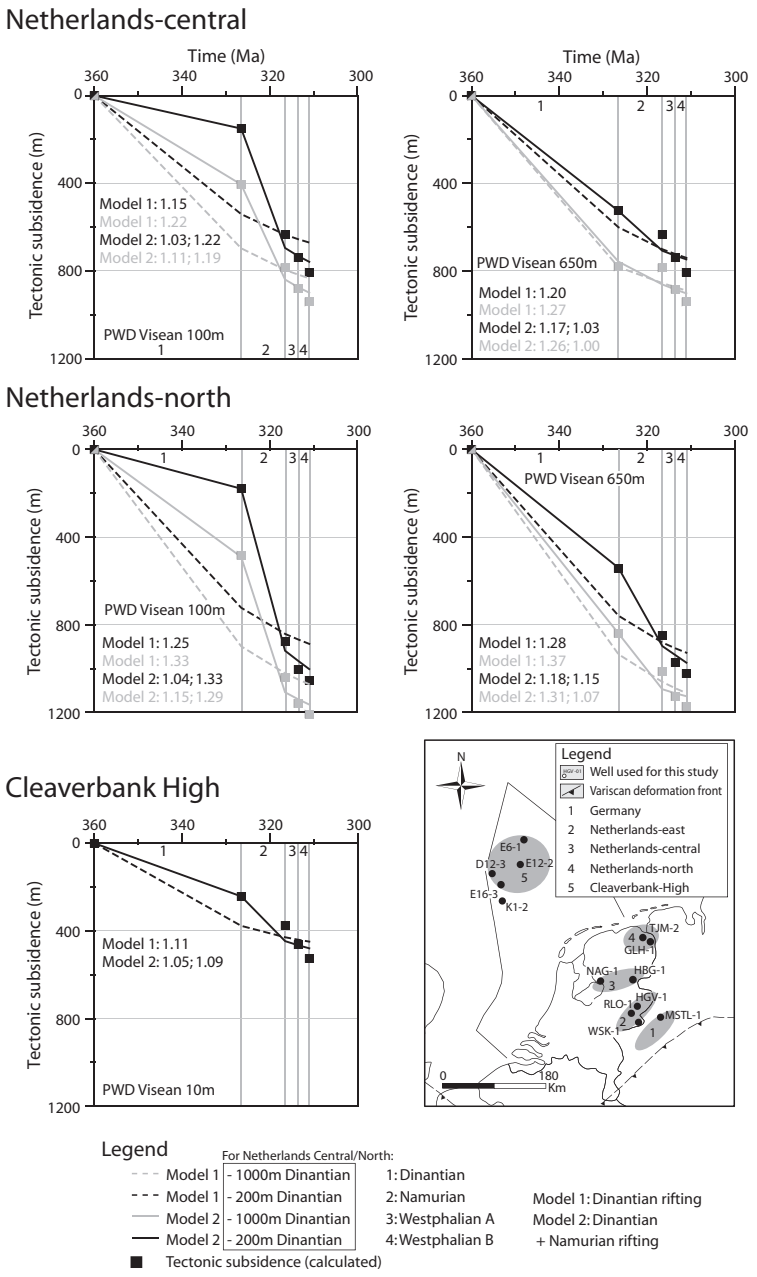

Figure 4.7 Modelled tectonic subsidence curves for models 1 and 2 for two end-members of end-Visean PWD and two end-members of Dinantian thickness in the areas Netherlands-central and north. For the Cleaverbank area only one scenario had to be calculated as the end-Visean PWD and thickness of Dinantian sediments is well known. Tectonic subsidence calculated from the well data is indicated with squares. The stretching factors are indicated for each scenario; for model 1 this value represents stretching during the Dinantian while for model 2 the second number represents the Namurian rifting event.

4.6.2.2 Model 2 – Dinantian and Namurian rifting (syn-rift), followed by Westphalian A/B thermal sag (post-rift).

In an attempt to find an alternative for the poor fit of the previous scenarios, in this model a second rifting phase during the Namurian is assumed. In this case the model is allowed to fit the Namurian tectonic subsidence with the most suitable stretching factor instead of being restricted to a predefined factor (i.e. thermal sag, no stretching). Geological evidence for a Namurian rifting event is sparse. However, Sissingh (2004) describes extrusive rocks in NAG-1 that probably have a Namurian age. This possibly indicates tectonic activity during the Namurian in this area. Moreover, an intra-Namurian angular unconformity was mapped in this area (Fig. 4.2). Although it is not a direct evidence for rifting, this mechanism may result in the formation of unconformities as a consequence of doming or the uplift of rift-shoulders (Ziegler & Cloetingh, 2004).

In this model the McKenzie (1978) concept (coupled crustal and subcrustal stretching factors) is used again. As expected, adopting a Namurian rifting event gives a better fit between the observed and modelled tectonic subsidence (Fig. 4.7). This is the case for both PWD-scenarios. In the Cleaverbank area the model – although a Namurian rifting event is assumed – can not account for the increase in (observed) tectonic subsidence from Namurian to Westphalian A.

4.6.3 Discussion of model results

The most important outcome of the results described above is that – when assuming the classical Dinantian syn-rift and Namurian-Westphalian B post-rift scenario – the amount of sediments deposited during the post-rift stage is out of proportion compared to the syn-rift stage for all areas and for all scenarios. Adopting a model in which rifting only takes place during the Dinantian (Model 1) a high end-Visean PWD is required in Netherlands-central and Netherlands-north to explain the observed Late Carboniferous subsidence. This implies the absence of a eustatic lowering of sea level, as has been observed by several authors (Ross & Ross, 1988; Gursky, 2006). Only for the Cleaverbank area, an end-Visean PWD results in a reasonable fit for Model 1 because of the better ratio of post- and syn-rift deposits.

If an additional Namurian rifting event is assumed (Model 2), a better match between calculated and observed tectonic subsidence can be obtained than in the other scenarios (Fig. 4.7). However, even with a Namurian rifting event, an increase in tectonic subsidence from Namurian to Westphalian A as observed in Netherlands-central (PWD 650 m scenario) is unlikely since this period represents the thermal sag stage, generally characterised by decreasing subsidence rates. When adopting an additional Namurian rifting event, the low end-Visean PWD scenarios are more likely, as a greater decrease in subsidence can be observed from Namurian (syn-rift) to Westphalian A (post-rift) than in case of the high end-Visean PWD scenarios. It should be realised that the stretching factors needed for the Namurian in case of the end-Visean PWD scenario are higher than in the high end-Visean PWD scenario (Fig. 4.7).

4.7 Subsidence mechanisms in the CNWECB

From the modelling results presented in this chapter, the conclusion can be drawn that most of the observed subsidence in the Netherlands during the Namurian – Westphalian B can not be explained by flexural foreland subsidence, even when a very high elastic thickness is assumed. Lithospheric stretching is a possible alternative candidate as it has been observed in northern England (Fraser & Gawthorpe, 1990). Moreover, the findings reported in chapter 3 indicate a

similar structural setting as the UK, thereby suggesting that rifting also took place in the current study area. Modelling of a Dinantian rifting event, using thickness data from the Netherlands, showed that only the assumption of a very high end-Visean PWD results in a fit between observed and modelled tectonic subsidence data. An additional Namurian rifting pulse results in a better fit. The presence of a Namurian unconformity in the central part of the Netherlands (Fig. 4.2) and the occurrence of extrusives in the same area from Namurian age show that this stage was not characterised by passive regional subsidence alone. Therefore, a subsidence model incorporating a Namurian rifting event, next to a model of a Dinantian rifting event only, is thought to be possible. A possible drop in sea level taking place at the onset of the Namurian (Ross & Ross, 1988; Gursky, 2006) supports this view since such an event would result in an increased misfit when only a Dinantian rifting event is assumed.

Lithospheric stretching by thinning and heating results in an initial weakening of the lithosphere (e.g. Ziegler & Cloetingh (2004) for an extensive review). In turn, the rigidity of the lithosphere, or its effective elastic thickness, reflects its integrated strength (Watts & Burov, 2003). Loading of an extensionally weakened plate will therefore result in a narrow foreland basin. However, thermo-mechanical modelling (Braun, 1992; Cloetingh et al., 2003) has shown that even though rifting causes an initial weakening of the lithosphere, it will finally result in stronger lithosphere due to thermal relaxation and so-called 'mantle healing'. The typical time scale for this process is some 30 Ma based on the ratio of advective- to conductive-driven heat transfer (Braun, 1992). It may vary as a function of the duration and the magnitude (crustal vs. lithosphere stretching) of extension. The Eastern and Western Black Sea regained their pre-rift strength 10 and 50 Ma after initiation of rifting respectively (Cloetingh et al., 2003). Afterwards, their strength kept increasing to double or even triple the initial value. On the other hand, in a case study of the Central Iberian Basin, Ziegler et al. (1995) point out that even though the strength of the lithosphere thermally recovers, due to reactivation of faults it never again reaches its initial value. In spite of the large differences in the predictions of the rheological models, it is likely that the lithosphere, during the Namurian, would not have fully recovered from a Dinantian rifting event. Thus, when these mechanisms have to explain the observed subsidence in the Netherlands, it is unlikely that the Te of the plate was not weakened by this rifting event.

The flexural modelling results showed that the model proposed by Ricken et al. (2000); a broad foreland basin developed on a relatively strong plate) better explains the observed thickness data because: (1) pronounced thickness differences are expected when a weak plate (Te 5 km) is assumed (Fig. 4.6). Thickness data show a gradual change indeed (inset in Fig. 4.6B). Moreover, (2) figure 4.6 shows that in case of a Te of 5 km the foreland basins are so narrow that, in the subsequent time step, the load has migrated past the previous basin. Therefore, it is not expected to find sediments of subsequent timesteps on top of each other. In the Ruhr area sediments of Namurian – Westphalian B age have been deposited on top of each other.

The apparent contradiction between a broad foreland basin on one hand and a rifted basin on the other may be explained by taking another subsidence mechanism into account; dynamic topography. This mechanism is proposed by numerous authors to explain long-wavelength (asymmetric) subsidence in a flexural foreland setting. Long wavelength subsidence such as observed in the CNWECB has been recognised in the Devono-Carboniferous Western Canada Sedimentary Basin (Pysklywec & Mitrovica, 2000), the Cretaceous Western Interior Basin, United States (Pang & Nummedal, 1995; Liu & Nummedal, 2004) and the Middle Ordovician Michigan Basin (Coakley & Gurnis, 1995). In these basins, flexural loading models could not adequately explain the observed subsidence patterns as their wavelength greatly exceeds the modelled ones

(as is the case in the study area). These authors proposed the addition of a dynamic component, following Gurnis (1992) who found that a mantle flow-induced dynamic topography could explain subsidence over such long wavelengths. This is caused by subduction of a relatively dense slab, creating a negative buoyancy anomaly (Burgess & Moresi, 1999). However, the recognition of dynamic topography is complex in ancient settings. The most reliable criterion to identify this mechanism is the observation of subsidence to occur on a greater wavelength than expected due to flexural subsidence alone (Coakley & Gurnis, 1995; Burgess & Moresi, 1999). As the flexural modelling results show that the wavelength of subduction in the CNWECB exceeds the wavelength predicted by flexural loading, such a mechanism may be proposed for the CNWECB. The observation by Gursky (2006) that the northern (passive) margin of the Rhenohercynian Basin already subsided in the Devonian might point to an early expression of dynamic topography. Another feature observed in the CNWECB can also potentially be explained by this mechanism. Burgess & Moresi (1999) indicate that the forebulge may be absent or subdued as a consequence of dynamic topography, because of the extension of the area of subsidence beyond the forebulge. Drozdzewski (1993) reported a (northward moving) area of reduced subsidence in the Ruhr Basin, which he interpreted as a forebulge. In a normal foreland basin setting, the forebulge area is an erosional feature, but incorporating a dynamic load creates the possibility for the forebulge area to subside. Unfortunately there are some drawbacks on the application of dynamic topography. First, dynamic topography is a reversible process. After a period of subsidence one can expect uplift to take place. In general, the duration of the unconformity will decrease away from the orogen (Burgess et al., 1997). However, despite the existence of an unconformity at the base of the Permian, a marked increase in duration from north to south is not evident from the CNWECB. Secondly, the direction of subduction is an issue. Most authors report dynamic topography to take place over subducting slabs (Burgess & Moresi, 1999; Pysklywec & Mitrovica, 2000). However, subduction of the Rhenohercynian oceanic plate was probably directed to the south (Franke, 2000; Oncken et al., 2000), away from the CNWECB. On the other hand, northward subduction took place somewhat further to the south where the Palaeo-Tethys oceanic lithosphere subducted below Gondwana-derived terranes (Stampfli & Borel, 2002).

A third factor which might have caused an increase in subsidence during the Namurian and Westphalian is the buildup of compressional intraplate stress, analogous to the Pliocene-Quaternary subsidence acceleration of the Cenozoic North Sea Basin (Kooi et al., 1991). Regarding the scarcity of thickness data and the proximity of the Variscan thrust front to the study area, this mechanism might also have played a role. Additional well data and seismic interpretation should reveal which of these factors is the most likely candidate.

4.8 Conclusions

Flexural foreland subsidence was modelled, likely to be the most important subsidence mechanism along the southern margin of the CNWECB, using several scenarios. The results from this study show that flexural subsidence largely fails to explain the subsidence observed from well data in the Netherlands during the Namurian, even if a very high elastic thickness (60 km) for the lithosphere is assumed along with a high end-Visean palaeowater depth. This is because the (predicted) basin-axis is located too far to the south at these times. During Westphalian A and B, when the basin-axis has been migrating further to the north, part of the subsidence observed in the

southeastern Netherlands can potentially be explained by flexural subsidence. However, this is only the case if again a Te of 60 km is assumed.

From observations in the UK, lithospheric stretching during the Dinantian and associated thermal subsidence is proposed to be the second subsidence mechanism in the CNWECB. It is suggested, based on the results described in chapter 3, that such a rifting event also took place in the Netherlands. However, a simple modelling exercise showed that uniform stretching poorly explains the Namurian-Westphalian B sedimentary sequence if only a Dinantian rifting event is assumed. Even if a high end-Visean palaeowater depth is considered, this model still does not fit the observed subsidence curves. Three factors might account for the additional tectonic subsidence in the study area. A better match between the observed and modelled tectonic subsidence can be achieved if an additional Namurian rifting event (1) is assumed, in contrast to the observations from the UK, where the Namurian is a time of tectonic quiescence (thermal sag). This might be in accordance with the finding of an intra-Namurian erosional unconformity and the presence of extrusives in the central part of the Netherlands. Although a rifting model potentially explains Namurian – Westphalian B subsidence observed in the Netherlands, it does not account for the large scale asymmetric shape of subsidence profiles. The concept of dynamic topography (2) might explain the wavelength and amplitude of the observed subsidence data as it is shown that mantle-flow induced dynamic topography causes subsidence at wavelengths in the same order as observed in the CNWECB. The third factor explaining additional tectonic subsidence is compressional intra-plate stress.

CHAPTER 5

The alluvial architecture of the Coevorden Field (Upper Carboniferous), the Netherlands

This chapter is based on: Henk Kombrink, John S. Bridge, and Esther Stouthamer (2007): The alluvial architecture of the Coevorden Field (Upper Carboniferous), the Netherlands. Netherlands Journal of Geosciences 86, 3-14.

Abstract
A detailed reconstruction of the alluvial architecture of the Coevorden Gasfield (Upper Carboniferous, Tubbergen Formation), which is located in the northeastern part of the Netherlands, is presented. The reconstruction is based on well-logs, cross-sections, and palaeogeographic maps. Sedimentological analysis of a 93 m long core allowed to refine the interpretation of the depositional environment. Accurate width determinations are necessary to correctly correlate fluvial sandbodies and reconstruct alluvial architecture. Without using sedimentological information, sand body width is likely to be overestimated. The method developed by Bridge & Tye (2000) was used to estimate the width of one sandstone body from cross-set thicknesses. From palaeogeographic reconstructions and the calculation of the width of a channel belt on the basis of cross-set thicknesses, it may be stated that on average the width of the studied channel belts in the Coevorden field does not exceed 4 km. The palaeogeographic reconstructions, which point to a northwestern direction of palaeoflow, are in accordance with earlier observations. The thickness of the Tubbergen Formation is approximately 450 m in the study area. In the adjacent German area, time-equivalent sediments show a higher thickness. This may be attributed to tectonic movements along the Gronau Fault zone and the initiation of the Ems basin, of which the Coevorden Field is the westernmost – and therefore peripheral – part.

5.1 Introduction

The Coevorden Gasfield (Westphalian C/D) is located in the northeastern part of the Netherlands and covers an area of 125 km^2 (Fig. 5.1). The Westphalian C and D sedimentary sequence in the northeastern part of the Netherlands and adjacent areas is characterised by fluvial-lacustrine deposits (Pagnier & van Tongeren, 1996). Sediments of this age have been extensively described in the Ibbenbüren and Osnabrück areas (David, 1987; David, 1990; Selter, 1990; Jankowski et al., 1993; Jones & Glover, 2005) and in the Ruhr Basin (Drozdzewski, 2005). In the eastern part of the Netherlands these sediments belong to the Tubbergen Formation (Van Adrichem Boogaert & Kouwe, 1993). Although the Tubbergen Formation has been extensively studied in the Netherlands as a consequence of the presence of hydrocarbons, most of these studies are unpublished and/or confidential. Besides a regional study (Pagnier & van Tongeren, 1996), no fieldstudies on the Tubbergen Formation have been published to date. The Coevorden Gasfield provides a unique location in which the Tubbergen Formation can be investigated in detail. About 400 m of the

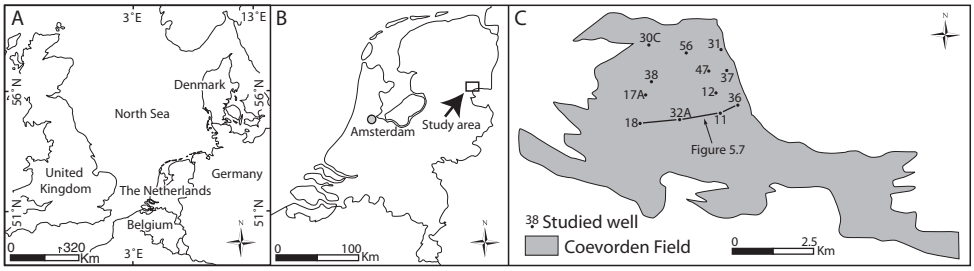

Figure 5.1 (A) Location of the Southern North Sea region, (B) the Netherlands, (C) the Coevorden Field, the studied wells, and correlation panel.

Tubbergen Formation was studied, of which the sandstone percentage is approximately 50%. It is underlain by the coaly, fine-grained Maurits Formation and disconformably overlain by the Permian (Zechstein Group; Van Adrichem Boogaert & Kouwe, 1993). Because this field is closely located to extensively studied outcrops and wells in Germany, the results can well be compared with the findings from these areas.

The objective of this chapter is to describe the alluvial architecture of the Coevorden Field, using the following methodology: (1) interpreting the origin of fluvial deposits from cores and well-logs; (2) correlating channel sandstone bodies between wells; (3) reconstructing the orientation and spatial distribution of individual channel sandstone bodies and (4) set the Coevorden Gasfield in a regional context.

5.2 Geological setting

5.2.1 The Tubbergen Formation in the northeastern part of the Netherlands

Sediments of the Tubbergen Formation are found to range in age between the Early Westphalian C and Late Westphalian D (Fig. 5.2) and occur in the (north)eastern part of the Netherlands, the Ems basin and the Lauwerszee Trough (Fig. 5.3). In the Coevorden area, the base and top of the Tubbergen Formation are thought to be of Late Westphalian C and Early Westphalian D respectively (Van Adrichem Boogaert & Kouwe, 1993).

The Tubbergen Formation is characterised by a fluvial-lacustrine depositional environment (Pagnier & van Tongeren, 1996; Quirk & Aitken, 1997). Thick and massive sandstones occur (several tens of metres in thickness) intercalated in predominantly grey coloured mudstones, which reflect poorly drained conditions. A limited number of coal seams occur in the Tubbergen Formation. The maximum thickness is approximately 500 m. Sandstone percentages range from 30 to 70% (Van Adrichem Boogaert & Kouwe, 1993). The Tubbergen Formation overlies the Maurits Formation, which is a succession of grey mudstones with numerous coal seams and only a minor amount of sandstones. The boundary between the Tubbergen and Maurits Formations is thus characterised by the appearance of thick, massive sandstones and a decrease in the number of coal seams. The De Lutte Formation overlies the Tubbergen Formation (not found in the Coevorden area), which is characterised by a succession of predominantly reddish-brown sandy mudstones, reflecting well drained conditions. Time equivalent sediments of the Tubbergen Formation have been found in the Campine Basin in the southern part of the Netherlands and

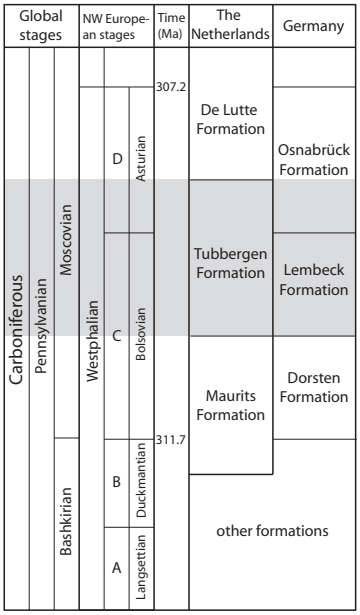

Figure 5.2 Diagram showing the global and local chronostratigraphy (Gradstein et al., 2004) used for the studied succession (grey), as well as the formation names (Van Adrichem Boogaert & Kouwe, 1993) used in the Netherlands (NL) and Germany (GE). Note that time is not to scale.

the Cleaverbank High (Van Adrichem Boogaert & Kouwe, 1993; Figs 2.4 & 5.3). A similar depositional environment has been interpreted for these formations.

5.2.2 Sediments of Westphalian C and D age in northwestern Germany

The Westphalian C and D are well studied in the Ruhr Basin (Westphalian C only) and the Ibbenbüren and Osnabrück areas (David, 1987; David, 1990; Selter, 1990; Jankowski et al., 1993; Drozdzewski, 2005; Jones & Glover, 2005). Like in the Netherlands, these sediments mainly reflect a fluvial-dominated environment. David (1990) recognised various depositional environments: braided rivers, overbank siltstones, swamps (coals) and crevasse splays. The transition from coal-bearing and sandstone-poor to sandstone-dominated as observed in the Coevorden area (Maurits Formation to Tubbergen Formation) during Late Westphalian C, took place in the Ruhr and Ibbenbüren areas during the late Early Westphalian B (Drozdzewski, 2005). The entire Westphalian C succession is thought to be approximately 850 m thick in the Ibbenbüren and Osnabrück areas (David, 1990; Jones & Glover, 2005), while the Westphalian D is approximately 750 m in thickness. The thickness of the Upper Westphalian C (Lembeck-Formation) is 465-525 m in the Ibbenbüren area (Drozdzewski, 2005). Percentages of sand in the Westphalian C vary between 60 % in the Ibbenbüren area and 40-50% in the Ruhr area (Drozdzewski, 2005). The percentage of sand in the well Bad Laer Z1 is 70% for the Westphalian C, while it is 56% for the well Osnabruck-Holte Z1 (Drozdzewski, 2005). For the Westphalian D, sand-percentages are approximately 80 % (David, 1987). In general, sandstone proportions tend to decrease westwards and northwestwards towards the Ems area (Jones & Glover, 2005). The sandstones encountered in the Osnabrück area (Early Westphalian D) show a northward-flowing channel system (David,

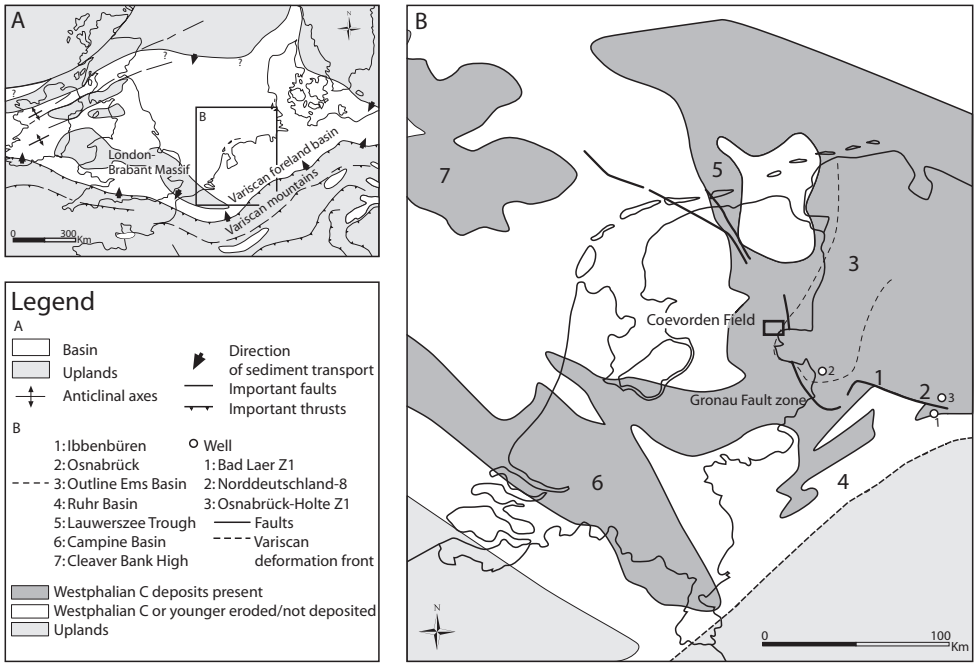

Figure 5.3 (A) Location of the Netherlands within the Northwest European Carboniferous Basin and (B) the presence of Westphalian C deposits in the Netherlands and adjacent areas in Germany. Figure 5.3A is based on Ziegler (1990).

1990). Jones & Glover (2005) found palaeocurrent directions towards west-northwest in the same area. This leads to the assumption of a northwestward direction of palaeoflow. David (1990) recognised brackish as well as freshwater environments while Jones & Glover (2005) could not find evidence for brackish-water conditions.

5.2.3 Tectonic setting

The tectonic setting of the Westphalian C and D in the Netherlands and adjacent areas must be seen in the light of the establishment of a compressional regime, resulting in reactivation of pre-existing faults, folding and basin inversion (Leeder & McMahon, 1988; Fraser & Gawthorpe, 1990; Coward, 1993; Süss, 2001; Schroot & de Haan, 2003). The transition from the sandstone-poor Maurits Formation to the sandstone-rich Tubbergen Formation is attributed to this increase in tectonic activity during the Westphalian C (Pagnier & van Tongeren, 1996). Unfortunately, seismic evidence for syndepositional deformation is scarce in the Netherlands (Süss, 2001; Geluk et al., 2002; Schroot & de Haan, 2003), although Pagnier & van Tongeren (1996) were able to identify tectonic activity of the Osning-Gronau fault zone during the Westphalian C and D. In the Ibbenbüren area, Drozdzewski (1985) identified Late Variscan tectonic activity. The area north of the Osning-Gronau fault zone has been interpreted as a Late Variscan pull-apart basin by Drozdzewski & Wrede (1994). Although there is little direct evidence of syn-sedimentary faulting during the Westphalian C and D in the Netherlands, when combined with the observations from Germany tectonic activity is likely.

5.2.4 Palaeoclimate and sea level

The Netherlands experienced an equatorial climate from Namurian to Westphalian C times, but the climate became more seasonal tropical (wet-dry extremes) by Westphalian D (Besly et al., 1993; Van der Zwan, 1993). This climate change is reflected in a decrease in coal seams and a change in palaeosol type from gley soils to redder soils with Fe- and Ca-rich concretions (e.g., Barren Red Beds of late Westphalian D age; Besly & Fielding, 1989).

The Late Carboniferous is characterised by icehouse conditions (Caputo & Crowell, 1985; Maynard & Leeder, 1992). As a consequence, it is thought that eustatic sea-level changes triggered by the waxing and waning of the Gondwanan ice-sheet occurred during this interval (Wanless & Shepard, 1936). The magnitude of the sea-level fluctuations is however difficult to constrain (45-190 m (Crowley & Baum, 1991); >42 m (Maynard & Leeder, 1992); 25-155 m, (Süss, 1996); 10-95 m (Wright & Vanstone, 2001)). The distance of the study area from the sea is equivocal (Quirk & Aitken, 1997; Hampson et al., 1999a; Hampson et al., 1999b) because direct evidence in the form of marine bands or deltaic deposits is lacking. However, hundreds-of-meter thick cycles of change in sandstone proportion (net-to-gross) in the Upper Carboniferous have been interpreted as due to cyclic change in climate and sea level (Süss, 2001; Geluk et al., 2002). The last fully marine transgression took place at the base of the Westphalian C (Aegir marine band, (Drozdzewski, 2005). A marine band represents a thin (usually <2 m) mudstone deposited under marine or brackish water conditions during transgression. In the Ruhr Basin the Aegir marine band is well developed, but it is poor in marine fauna in the Ibbenbüren area (Drozdzewski, 2005).

5.3 Data and methods

Twelve wells with a spacing of 500 to 1200 m were studied in the northwestern part of the field (Fig. 5.1). Available data comprised gamma-ray, sonic, density and neutron logs and 93 m of core (COV-17A, Fig. 5.1). Interpretation of the core led to a better grip on the depositional environment. Next, facies reconstruction based on well-logs has been carried out. Then correlation of sandbodies in the wells, based on estimates of their width, resulted in several cross-sections. Widths were estimated using width-thickness cross-plots and according to the method of Bridge & Tye (2000). Using these cross-sections, palaeogeographic maps were created.

5.4 Core description and interpretation

In the following section a description and interpretation is presented of the core from the well COV-17A. A detailed sedimentary log can be found in figure 5.4.

5.4.1 Description of the core

5.4.1.1 Sandstone body G (3066-3071 m)

The base of sand body G is developed as a clear erosional surface overlain by a breccia. Up to 3068 m planar strata in fine to medium-grained sandstone occur with small-scale cross-stratification. Layers of organic debris are common. From 3068 m to the top structureless fine to medium-grained

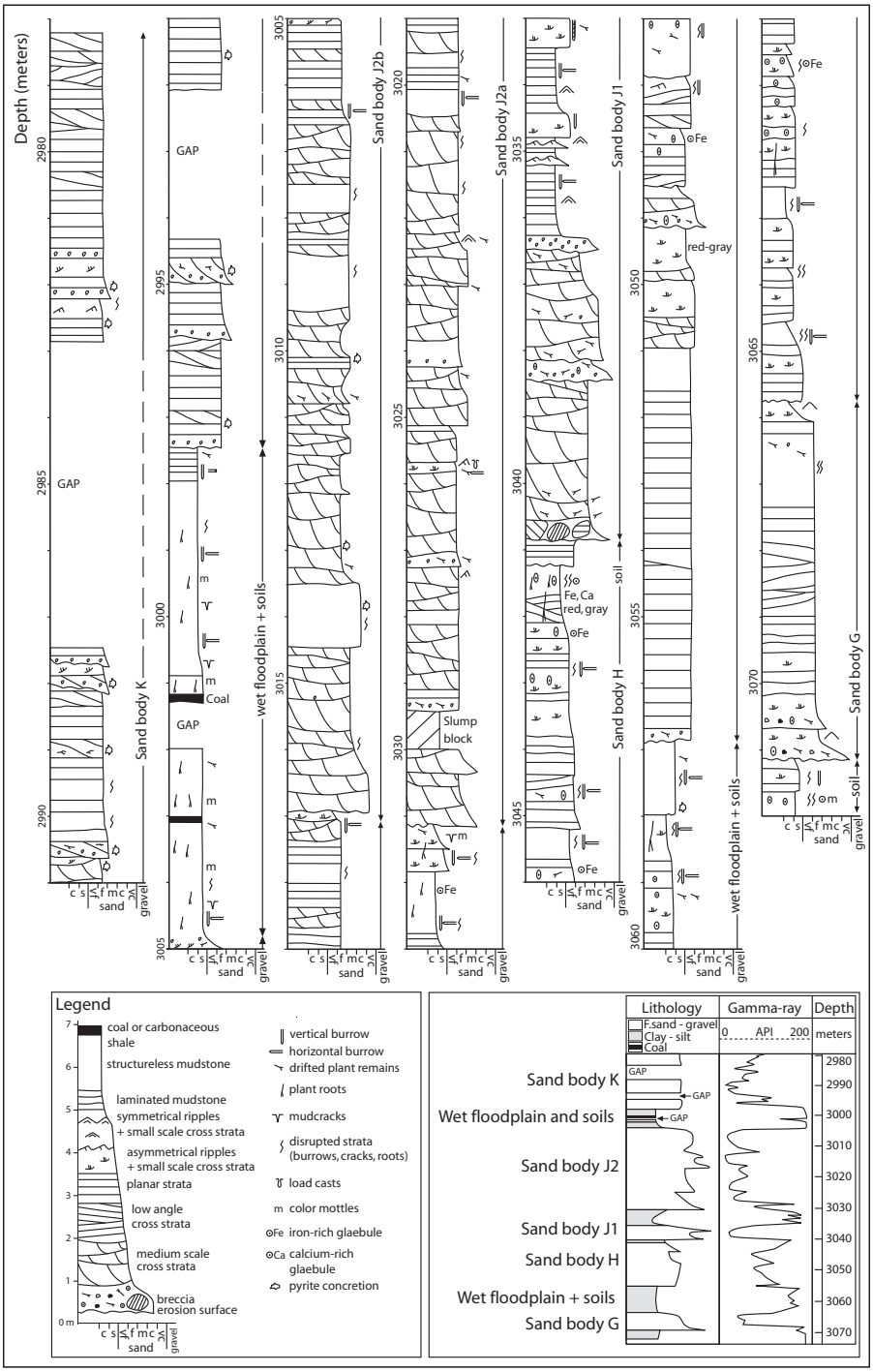

Figure 5.4 Sedimentological log of core 17A with interpretation and gamma-ray log. For location of the wells, see figure 5.1.

Figure 5.5 Photograph showing planar strata in sandstone body H. Depth corresponds to depth in figure 5.4.

sandstone predominates. The top of the sandstone shows an abrupt transition to parallel-laminated silt intercalated between mudstone.

5.4.1.2 Sandstone body H (3043-3057 m)

From the base up to 3051 m, this well-sorted fine-grained sandstone is characterised by planar strata (Fig. 5.5). The section from 3051 m to 3043.8 m shows cross-strata with intraformational breccias but intervals with structureless sandstone can be seen as well. Brown siderite concretions associated with organic debris occur near the fine-grained tops of stratasets. Locally, small-scale cross-strata associated with symmetrical ripples, mud drapes and drifted organic debris occur. From 3043.8 m a fining-upward sequence can be seen, giving way to a palaeosol at the top of the sandstone body. Red iron staining increases towards the top of the sandstone body.

5.4.1.3 Sandstone body J1 (3036-3041 m)

This sandstone body has a clear basal erosion surface, overlain by planar-bedded fine-grained sandstone. On top of an intercalated clay-plug (possibly a slump block) medium to coarse-grained cross-bedded sandstones occur that contain organic debris. A breccia containing pebbles is intercalated in this sandstone. The top consists of a pebble-layer sharply overlain by laminated mudstones.

5.4.1.4 Sandstone body J2 (3005-3031 m)

Sandstone body J2 occurs as two storeys (J2a and J2b), having a combined thickness of 26 m. Each storey (bases of these storeys are at 3017 and 3031 m) has a basal erosion surface. Sandstone

Figure 5.6 Photograph showing medium scale cross-strata in storey J2A. Depth corresponds to depth in figure 5.4.

is yellowish grey, mainly medium to fine-grained (rarely coarse), and contains organic debris. J2a has little vertical variation in grain size, while in J2b a slight fining-upward can be seen. The sedimentary structures are mainly medium-scale cross-sets ranging in thickness from 5 cm to 50 cm, although intervals of structureless sandstone also occur. Figure 5.6 shows a core- photo in which several cross-sets observed in sandstone body J2a can be seen. Planar strata are most abundant in the finer-grained stratasets at the top of a storey. The sandstone body has a sharp top overlain by mudstone.

5.4.1.5 Sandstone body K (2978-2997 m)

Unfortunately sandstone body K, which is approximately 20 meters in thickness, is not completely cored: there are two gaps and the top is missing. The interval from the base (2997 m) to approximately 2982 m is characterised by sharp, erosional surfaces overlain in places by intraformational breccia containing mudstone granules or pebbles, organic debris and siderite concretions. Planar strata are mostly observed on top of the breccias, although structureless sandstone occurs as well. The top part of this sandstone body (from 2982 m onwards) is characterised by planar strata. The thickness of these sets varies between 5 cm to several decimeters. The grain size of this sandstone body ranges from very fine- to fine-grained.

5.4.1.6 Fine-grained sediments

Overall, the fine-grained sediments are laminated with intercalations of small-scale cross-stratified siltstone to very fine-grained sandstone (Fig. 5.4, 3057-3065 m). Symmetrical and asymmetrical

ripples are associated with the small-scale cross-strata. The strata are dark grey to brownish grey in colour. Burrows (horizontal and vertical) and organic debris are common. Strata commonly occur in fining-upward stratasets (very fine-grained sandstone to mudstone) that are generally decimeters thick but rarely over 1 m. The top 20 cm of a strataset tends to be dark grey and organic rich and very disrupted with burrows, cracks, and brown stains.

5.4.2 Interpretation of the core

All sandstone bodies described above are interpreted to be deposited in a fluvial dominated environment because of: (1) the clear basal erosion surfaces, (2) one dominant transport direction and (3) the dominance of cross-bedded and planar strata. The main difference between sandstone bodies J1/J2 and G, H and K is the dominance of medium-scale cross-strata in J1/J2 and planar and low-angle cross-strata in G, H and K (Fig. 5.4). Planar strata are commonly associated with mouth-bar or crevasse splay deposits (e.g., Tye & Coleman, 1989a; Bristow et al., 1999; Pèrez-Arlucea & Smith, 1999). For instance, the succession from planar strata to (low angle) cross-strata observed in sand body H could be interpreted as a crevasse splay overlain by a fining-upward channel-bar deposit. Based on the distinct basal erosion surface, sand body G is thought to represent a channel-bar deposit although the remainder of the sandstone body is characterised by planar and low-angle cross-strata. Because of the absence of a basal erosion surface and the presence of planar strata all through sand body K, it is interpreted as a mouth-bar deposit. The combination of a fining-upward sequence of very fine sandstone to mudstone and the relatively thin sandstone body J1 leads to the interpretation of a basal channel-bar sandstone overlain by a channel fill. Sandstone body J2 clearly shows two storeys dominated by medium-scale cross-strata. These storeys are interpreted as channel-bar deposits.

The fine-grained sediments are thought to represent deposition in waterlogged floodplains or lakes. These types of deposits are common in modern marshes, swamps, lakes, and distal levees (e.g. Coleman & Gagliano, 1964; Coleman & Prior, 1982; Saucier, 1994). No strong evidence for marine or brackish depositional environments was found. Apart from some mud drapes in sandstone body H, no sedimentary structures were found that could indicate marine or tidal influence.

Palaeosols are up to meters thick, mottled grey-brown siltstones with burrows, crack fills, root traces, and concretions of calcium carbonate and siderite (e.g., Fig. 5.4, 3071.5 m and 3041.5 m). Some grey palaeosols with relatively few concretions contain cm-thick, dark-grey, plant-rich layers and cm-thick coals (Fig. 5.4, 2998-3005 m). Most palaeosols could be classified as weakly developed (inceptisols), with some moderately developed (histosols and vertisols; Bridge, 2003; Tables 6.2 and 6.3). Such palaeosols are typical of wet floodplains in tropical seasonal climates (Cojan, 1999; Kraus & Aslan, 1999). The palaeosol with calcareous concretions (Fig. 5.4, 3041.5 m) is indicative of relatively drier (better drained) depositional conditions (Wright, 1999).

5.5 Interpretation of lithology in well-logs

In the following section an interpretation is given of the lithology as encountered in the well-logs. A cross-section (Fig. 5.7) is presented in which four wells have been correlated. For location of the wells, see figure 5.1.

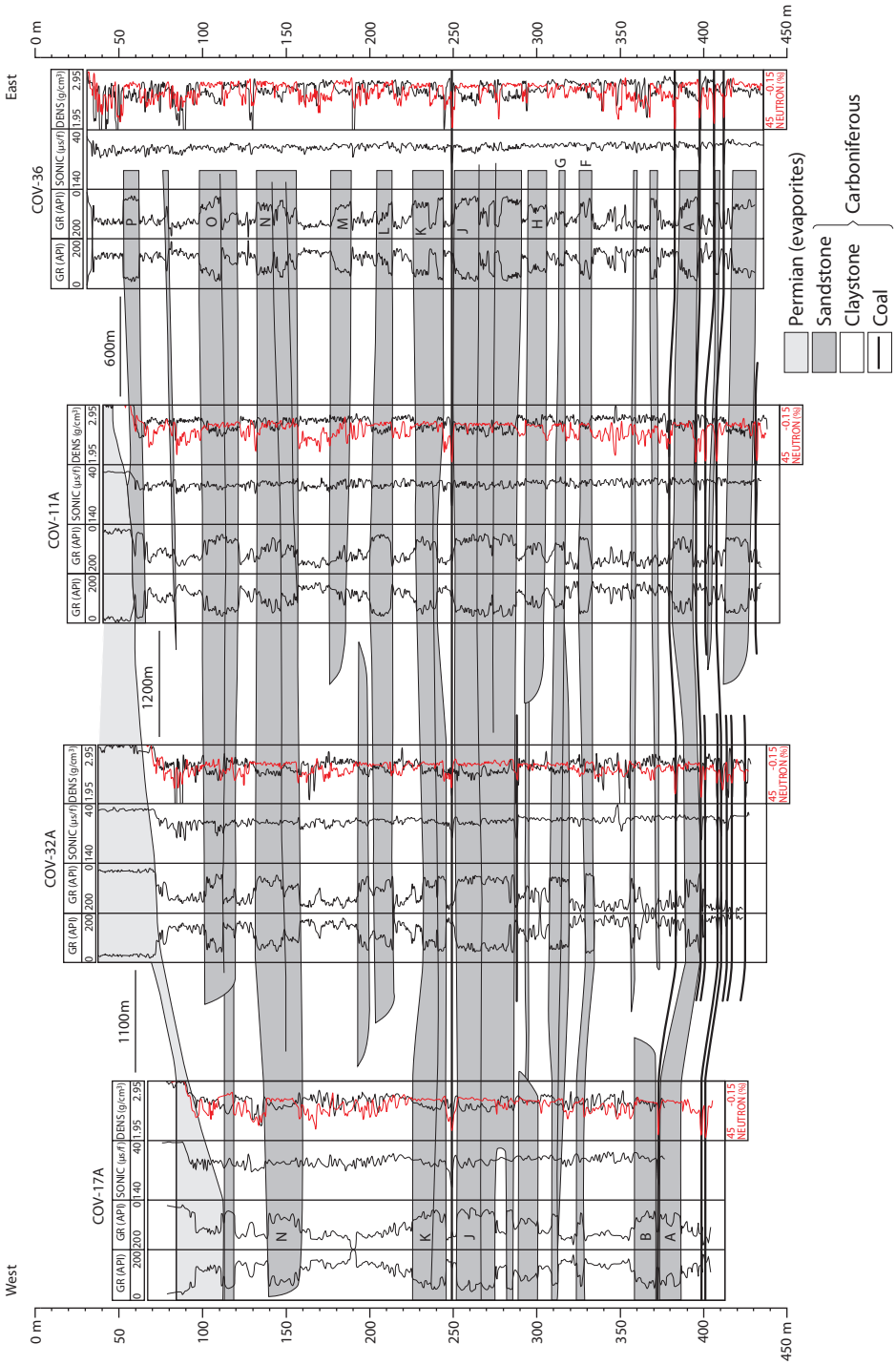

Figure 5.7 Well-log correlation panel (for location of this panel see figure 5.1).

5.5.1 Sandstone bodies in well-logs

Channel-bar deposits can be recognised based on consistent fining-upward trends within sandstones, but also sandstone bodies that do not change grain size vertically and even a few sequences that coarsen upward occur. The sandstone bodies (or storeys as is the case for J2) range in thickness from about 8 to 14 m (mainly 10 to 12 m), indicating a maximum bankfull depth of about 14 m and a mean bankfull depth of around 8 m (Bridge & Tye, 2000). Usually, systematic lateral changes in thickness and vertical sequence of grain size in these channel-bar deposits occur (Bridge, 1993; Lunt et al., 2004). For example, the bar thickness may change by a factor of two over a lateral distance of the order of a kilometre. Fining-upward sequences may change into those with little vertical variation in grain size over a similar distance.

Most of the channel sandstone bodies in figure 5.7 are interpreted to be composed of untruncated channel-bar and channel-fill deposits within isolated channel belts. It is possible that truncated channel-bars are preserved near the bases of some of these sandstone bodies, especially the relatively thick ones, as is the case in sandstone body J2 at 3017 m (Fig. 5.4). Criteria to determine this include different grain size trends within the different channel-bars, and the lower truncated bars being much thinner than the uppermost untruncated one (e.g., Fig. 5.7, sandstone bodies O and N in COV-11A).

Crevasse deposits in well-logs can be recognised by the relatively thin sandstone bodies with a thickness of 2-5 m (between sand body A and F, Fig. 5.7). Often, these thin sandstone bodies cannot be correlated in all wells, which indicates their restricted width. In some cases the crevasse deposits can be correlated to a channel belt (H, Fig. 5.7).

5.5.2 Fine-grained deposits and coals in well-logs

Floodbasin mudstones are meters in thickness and laterally continuous. Meter-scale variations in grain size (clay proportion) of floodplain deposits are clearly discernible. These are fining upward and coarsening upward, and normally include sandstone bodies interpreted as crevasse splays/levees, lacustrine deltas and mouth-bars. Four to 8 of these sequences commonly occur within the floodplain sequences between channel belt deposits. According to (Bridge, 1984), such meter-scale floodplain sequences may be related to avulsion of main channels. However, avulsions do not necessarily result in discernible changes in deposition throughout the floodplain, and crevasse splays and lacustrine deltas can develop and prograde in the absence of avulsions. A number of coal seams can be observed at the base of the studied succession (Fig. 5.7) and a prominent coal seam occurs on top of sand body J. Some coals are laterally continuous, but others are truncated by channel belt deposits. For instance, a coal seam just below sand body J in COV-32A (Fig. 5.1) is absent in the other wells which suggests erosion or non-deposition at these locations. It is possible that such isolated coal seams at the base of sandstone bodies may represent a(n) (isolated) channel fill.

5.6 Correlation

In this section, the correlation scheme (Fig. 5.7) and the palaeogeographic maps (Fig. 5.8) will be discussed. The top of the Maurits Formation (Fig. 5.2), where a characteristic group of coal seams occurs, and a prominent coal seam immediately above sandstone body J (Fig. 5.7) were used as correlation data. Another common feature of the studied wells is the cyclic nature of sandstone proportion (well developed in COV-17A). This also served as a guideline for correlation.

Table 5.1 Widths of sandbodies J2A and J2B.

	Sand body J2A	Sand body J2B
Flow depth	5.4 – 9 m	5.2 – 8.7 m
Width (min-max)	1246 – 3895 m	1164 – 3719 m

5.6.1 Width of sand bodies

When correlating fluvial sandstone bodies it is important to take the direction of palaeoflow into account. The correlation scheme in figure 5.7 is perpendicular to the expected direction of palaeoflow to the north or northwest, based on regional palaeogeography (Jones & Glover, 2005), a decrease in sediment size to the north-northwest (Den Hartog Jager et al., 1993), and palaeocurrent data from cross-strata measured in cores from nearby wells. In most subsurface studies, the width of fluvial sandstone bodies is obtained by plotting the thickness of the sandstones in a width-thickness cross-plot. This is also the case for this study. However, Bridge & Tye (2000) used the mean thickness of cross-sets to calculate the potential channel belt width. For sand body J the medium-scale cross-sets could be measured in the COV-17A core (Figs 5.4 & 5.5). For the other sandbodies present in the core (G, H and K) the amount of cross-sets did not permit to apply this method as well. Sandstone bodies J2A and J2B have average medium-scale cross-set thicknesses (s) of 27 +/- 17 cm (n = 22) and 26 +/- 18 cm (n = 23) respectively. The mean dune height (h_m) can be calculated as follows:

$h_m = 6*(s/1.8)$ (1)

The relationship between flow depth (d) and mean dune height is
(Bridge & Tye, 2000): $d/h_m = 6\text{-}10$ (2)

From the obtained flow depth, a range in channel belt width (*cbw*) can be calculated using the empirical equations given by Bridge & Mackey (1993b) and Bridge & Tye (2000):

$cbw = 59.9d_m^{1.8}$ (min) (3)

$cbw = 192d_m^{1.37}$ (max) (4)

with d_m being mean flow depth. The results are presented in table 5.1.

The calculated flow depths are in agreement with the interpretation that sand body J consists of two superimposed channel belts (J2A and J2B) because the obtained flow depths correspond to the individual storey-thickness. When sand body J2 would be interpreted as one single channel belt, the calculated flow depth would be much less than the thickness of the entire sand body. Superimposed channel belts are likely to result in wider sandstone bodies than those made of single channel belts (Bridge, 1993). As the mean width of sandstone bodies J2A and J2B is approximately 2500 m, superposition of these channel belts is likely to result in a width exceeding 2500 km. This is supported by the observation that sandstone body J is present across the entire study area which is 3 km in length and width.

5.6.2 Palaeogeographic maps

Some sandstone bodies extend across the whole study area. For sandstone body J, this is expected based on calculations of the width. The margin of channel belt sandstone bodies can be identified in some cases because it is lacking in one or more wells (Fig. 5.8; sandstone bodies B, H, M and N). In two cases (sandstone bodies A and L), both sides of the channel belt can be identified. This illustrates the benefit of making palaeogeographic reconstructions on such a scale. The sandstone bodies are oriented between NW (A, L, M and N?) and NNE (B and H). The northwestward directions agree with the palaeoflow directions from literature (David, 1990; Jones & Glover,

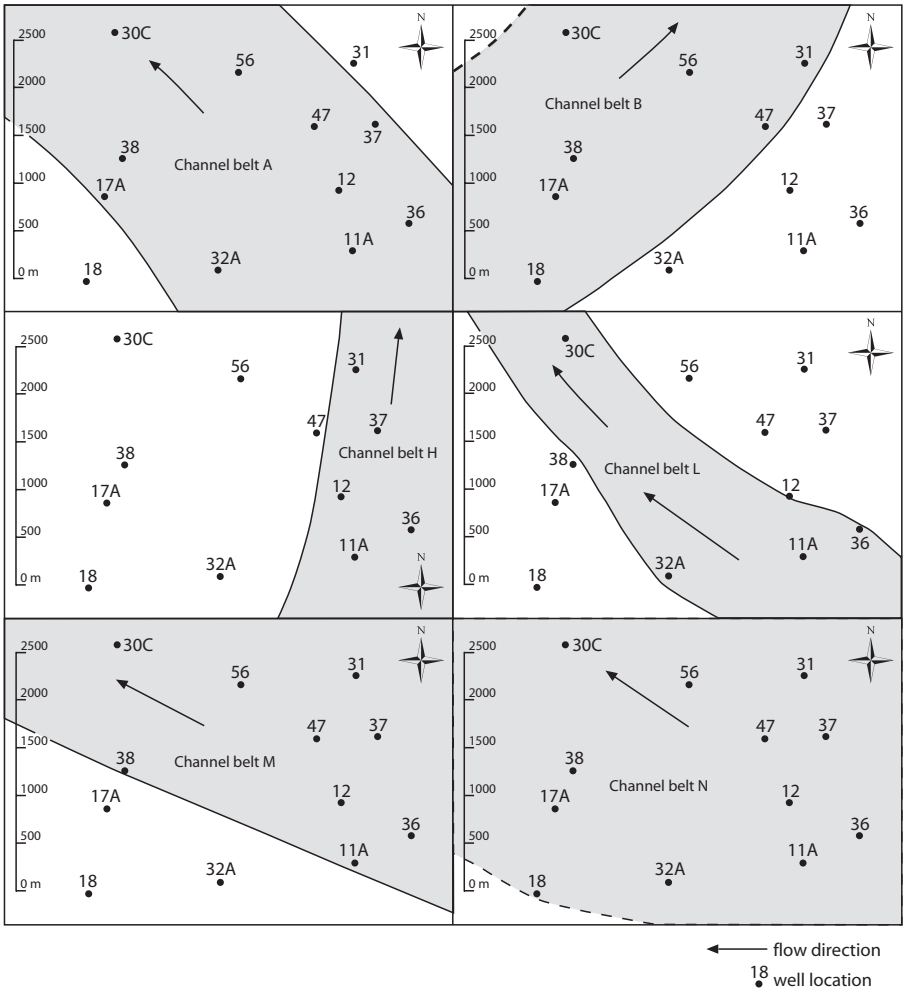

Figure 5.8 Palaeogeographic maps of some channel belts in the study area.

2005). The inferred north-northeast direction is considered not to be in direct conflict with the palaeoflow directions from literature because: (1) a small area has been studied and (2) only one margin of these sandstone bodies could be identified.

5.7 Concluding discussion

The alluvial architecture of the Coevorden Field is characterised by untruncated channel bar deposits within isolated channel belts although one sandstone body is probably composed of stacked channel belts (J2). This is in accordance with studies on time-equivalent rocks in the Osnabrück and Ibbenbüren areas (David, 1987; Jones & Glover, 2005). Based on the palaeogeographic reconstructions (Fig. 5.8) and the calculations presented in table 5.1, it may be stated that on average the width of the channel belts studied in the Coevorden field does not exceed 4 km. Jones

& Glover (2005) interpret the width of the stacked channel belts to be in the order of tens of kilometres. According to the results obtained for this study, this is an overestimation.

Interpretation of cores is a useful source of information along with well-logs because a better description can be given of the sedimentary environment. However, using only well-logs, it remains very difficult to distinguish facies associations such as fining-upward sequences associated with channel fills from a sequence of overbank sandstone overlain by muddy floodbasin deposits. Meters-thick coarsening-upward sequences (mud to sand) in well-logs could be produced by progradation of a levee, a crevasse splay, a lacustrine delta (in a floodbasin or into an abandoned channel), or a mouth-bar of a main channel. For this reason, in figure 5.7 only channel belts and crevasse splays were interpreted.

From palaeocurrent measurements in the Coevorden area and a decrease in sandstone percentage to the north-northwest (Den Hartog Jager et al., 1993) it was concluded that the direction of palaeoflow has been to the northwest. The palaeogeographic reconstructions agree with these observations. Moreover, David (1987) and David (1990) interpret the sandstone bodies in the Osnabrück and Ibbenbüren areas as northward flowing systems, while Jones & Glover (2005) found a direction to the west-northwest. These observations also match the results obtained here.

Although David (1990) interprets brackish-water deposits in the Osnabrück and Ibbenbüren areas, Jones & Glover (2005) could not find evidence for brackish-water deposits. However, Hedemann et al. (1984) interpret some marine bands in the Westphalian C and even Westphalian D in northwest Germany. In the studied core, some diagenetic pyrite in the sandstones was found but pyrite has not been recognised in the claystones or coal. Besides a small amount of mud drapes that were recognised in the sandstones, no further indications of marine (or brackish) water influence have been found. However, in the light of the findings from literature periodic marine influence can not be excluded.

Percentages of sand are thought to decrease in a northwestward direction Jones & Glover (2005). The percentage of sand of the studied succession is approximately 50 %. This is indeed less than the 60 % inferred from the Ibbenbüren area (Drozdzewski, 2005) and much less than the reported 80 % for the Early Westphalian D in the Osnabrück area (David, 1987). Moreover, the thickness of the studied succession in the Coevorden area is increasing to the area around Ibbenbüren, where the Upper Westphalian C already has a thickness of 500 m. The Lower Westphalian D has a thickness of about 400 m in the Ibbenbüren and Osnabrück areas. Since the thickness of the Tubbergen Formation is approximately 450 m in the study area, a decrease in thickness of the Westphalian C and D from the Ibbenbüren and Osnabrück areas to the northwest is likely. A trend of decreasing sand percentages *and* total thickness to the northwest therefore places the Coevorden area in a basin-margin position. This may be attributed to tectonic movements along the Gronau Fault zone (Fig. 5.3) and the initiation of the Ems basin, of which the Coevorden Field is the westernmost – and therefore peripheral – part.

CHAPTER 6

Namurian black shale deposition in Northern England: marine or lacustrine?

Abstract
Siliciclastic sedimentation rates increased during the Namurian in the Northwest European Carboniferous Basin (NWECB). The relict Dinantian topography, characterised by carbonate platforms and intervening basins, was blanketed by Namurian pro-delta mudstones. As a result, the Namurian shows significant thickness changes. Some authors proposed that Namurian basinal sedimentation in Northern England took place under a fluctuating salinity regime. The Goniatite marine bands intercalated in these pro-delta mudstones are thereby thought to record deposition under fully marine conditions while the thick barren and grey mudstones were deposited under less saline conditions (lacustrine). The Namurian section found on the Derbyshire Massif (a Dinantian carbonate platform) shows a very condensed sequence of black shales ranging in age from Pendleian to Kinderscoutian. This is caused by the distal position of the Derbyshire Massif with respect to the main fluvial discharge zone. Detailed study revealed a cyclic occurrence of fossil phases which also was attributed to salinity changes (Ramsbottom, 1962). Moreover, Amin (1979) and Spears & Amin (1981) suggested that salinity changes are also reflected in the geochemistry of these sediments. This study was initiated to further investigate the proposed salinity fluctuations. Samples were taken from all fossil phases of the condensed Namurian sequence of the Derbyshire Massif. C/S, major and trace elemental concentrations were obtained. The results show that all fossil phases show a marked enrichment in trace elements usually present in marine black shales. Therefore, it is suggested that basin waters essentially remained marine throughout the Namurian. Slight variations in salinity in the photic zone may account for the observed changes in fossil content.

6.1 Introduction

Namurian sedimentation in Northern England is characterised by the infill and draping of Dinantian basins and carbonate platforms respectively (Fraser & Gawthorpe, 1990; Collinson, 2005; Figs 6.1 & 6.2). This (shallowing-upward) succession is characterised by a thick sequence of mudstones (> 2 km) in the basinal areas (Bowland/Edale Fms, Fig. 2.3). On the carbonate platforms, this sequence is much more condensed. The greatest part of Namurian rocks in the basinal areas are barren (no fossils) but a number of relatively thin (up to several meter) Goniatite-bearing marine bands are intercalated (Collinson, 1988; Leeder et al., 1990). These marine bands are interpreted to record periods when basin waters were fully saline and when connections with the ocean were well established (Holdsworth & Collinson, 1988). In contrast, the unfossiliferous mudstones are thought to indicate periods when basin waters were lacustrine (Spears et al., 1999), or at least less saline in the photic zone (Collinson, 1988; Martinsen et al., 1995). Eustatic sea-level fluctuations and the associated influx of ocean waters are thought to be the most likely underlying

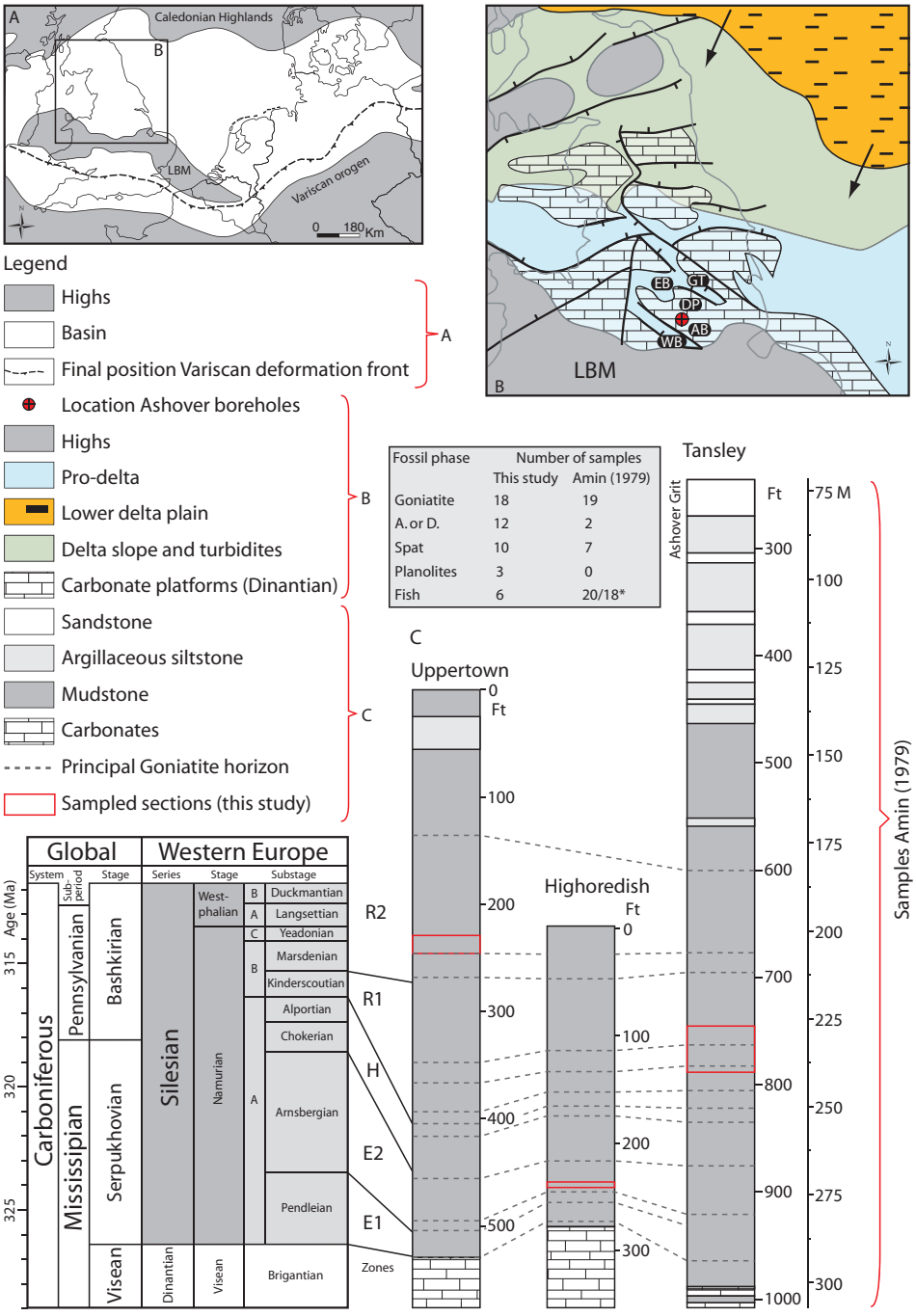
A
Caledonian Highlands
B
LBM
Variscan orogen
0 180 Km
Legend
Highs
Basin
Final position Variscan deformation front
A
Location Ashover boreholes
Highs
Pro-delta
Lower delta plain
Delta slope and turbidites
Carbonate platforms (Dinantian)
B
Sandstone
Argillaceous siltstone
Mudstone
Carbonates
Principal Goniatite horizon
Sampled sections (this study)
C
EB
GT
DP
AB
WB
LBM
B
Fossil phase
Number of samples
This study
Amin (1979)
Goniatite 18 19
A. or D. 12 2
Spat 10 7
Planolites 3 0
Fish 6 20/18*
Tansley
Ashover Grit
Ft
75 M
300
100
400
125
500
150
175
600
200
700
225
800
250
900
275
1000
300
Samples Amin (1979)
C
Uppertown
0
Ft
100
200
300
400
500
Highoredish
Ft
0
100
200
300
R2
R1
H
E2
E1
Zones
Global
Western Europe
System
Sub-period
Stage
Series
Stage
Substage
Age (Ma)
315
320
325
Carboniferous
Mississipian
Pennsylvanian
Serpukhovian
Bashkirian
Visean
Silesian
Dinantian
West-phalian
Namurian
Visean
B
A
C
B
A
Duckmantian
Langsettian
Yeadonian
Marsdenian
Kinderscoutian
Alportian
Chokerian
Arnsbergian
Pendleian
Brigantian

← *Figure 6.1* Geological and stratigraphical setting of the Ashover boreholes. (A) Contours of the Northwest European Carboniferous Basin. LBM: London Brabant Massif. (B) Detailed geological map of the study area. The location of the Early Carboniferous carbonate platforms can be seen next to the prograding Namurian deltas from the north. Note that by Namurian time the carbonate platforms in the south were covered with a thin layer of black shales. AB: Ashover boreholes; DP: Derbyshire Platform; EB: Edale Basin; GT: Gainsborough Trough; WB: Widmerpool Basin. (C) Stratigraphic subdivision of the studied boreholes Uppertown, Highoredish and Tansley. The intervals sampled for this study are indicated by red boxes. The entire Tansley borehole was sampled by Amin (1979). The table indicates the number of samples obtained for this study and the ones used from Amin (1979), ranked per faunal phase. Figure 6.1A partly redrawn after Ziegler (1990). The faunal zones and well correlation is based on the work of Ramsbottom et al. (1962).

cause of these changes in salinity (Ramsbottom et al., 1979; Holdsworth & Collinson, 1988; Martinsen et al., 1995).

Near Ashover, located on the Derbyshire Massif (a Dinantian carbonate platform), the condensed Namurian section was completely cored in three boreholes (Fig. 6.1). Besides the topmost part, the Namurian section turned out to be rich in organic matter. In contrast to the mostly barren succession in the basinal areas, a detailed palaeontological study of these boreholes (Ramsbottom et al., 1962; Figs. 6.1 & 6.2) showed the occurrence of a cyclic pattern of fossils nearly through the entire sequence (see 6.3). The main Goniatite bands, which were also found in the condensed section near Ashover, are thought to be correlatable between the condensed and the expanded sections on the platforms and basins respectively. Obviously, some of the other fossil phases must be the equivalents of the barren sequence in the adjacent basins. In analogy to the expanded Namurian sections in the adjacent basins, salinity fluctuations were proposed to explain these alternations in fossil content (Ramsbottom et al. 1962; Collinson, 1988; Martinsen et al., 1995; Collinson, 2005). Changes in salinity were also interpreted by Spears & Amin (1981) on the basis of geochemical analyses (trace element enrichments and pyrite contents). The non-marine (lacustrine) sediments are characterised by low trace element (TE) and sulphur (S) contents while the sediments deposited under marine conditions show high trace element and S contents (Spears & Amin, 1981).

Although salinity differences (marine or lacustrine) may result in different S and TE enrichment in sediments, some other critical factors play a role as well. C/S relationships in fine-grained sediments are extensively studied (Berner, 1977; Berner & Raiswell, 1984; Dean & Arthur, 1989; Aplin & Macquaker, 1993; Morse & Berner, 1995). The amount of S (pyrite) that can be fixed in sediments depends on: (1) the availability of metabolizable organic matter (OM), (2) the dissolved sulphate (SO_4^{2-}) concentration in order to produce sulphide (H_2S) via bacterial reduction and (3) the availability of reactive iron (Morse & Berner, 1995). Due to the limited availability of sulphate in freshwater (Taylor & McLennan, 1985), it is well known that lacustrine shales exhibit lower pyrite contents than marine shales (Berner & Raiswell, 1984). However, in marine shales characterised by low OM contents (0-2 wt% TOC (total organic matter)), sulphur enrichments are often also quite low (Berner & Raiswell, 1984; Lyons et al., 2003). In these cases, one has to be careful to make a palaeoenvironmental interpretation on the basis of C/S values alone.

Trace elements (TEs) commonly exhibit considerable enrichment in laminated, organic-rich facies, especially those deposited under euxinic conditions and, conversely, little if any enrichment in bioturbated, organic-poor facies (Algeo & Maynard, 2004). Therefore, carbonate-free marine and lacustrine shales deposited under oxic conditions should have broadly similar TE compositions if the lacustrine catchment area drains recycled sedimentary rocks or regions of average upper-

crustal composition (Norman & De Decker, 1990). Studies on trace element enrichment in organic rich shales have been carried out both for recent (Anderson et al., 1989; Middelburg et al., 1991; Pruysers et al., 1991; Aplin & Macquaker, 1993; Calvert & Pedersen, 1993; Crusius et al., 1996; Erickson & Helz, 2000; Sternbeck et al., 2000; Morford et al., 2001; Lyons et al., 2003; Nagler et al., 2005; Brumsack, 2006; Tribovillard et al., 2006; McKay et al., 2007) and ancient settings (Aplin & Macquaker, 1993; Arthur & Sageman, 1994; Nijenhuis et al., 1999; Fisher & Wignall, 2001; Wignall & Newton, 2001; Algeo & Maynard, 2004; Algeo et al., 2004; Cruse & Lyons, 2004; Schultz, 2004; Tribovillard et al., 2004; Lopez et al., 2005; Tribovillard et al., 2006; Van der Weijden et al., 2006). Four processes can lead to sedimentary enrichment in trace elements: (1) delivery in hydrogenous and biogenic particles, (2) scavenging in the watercolumn, (3) (partial) retention in the sediment during decomposition of host phases and (4) diffusion into the sediment across the sediment-water interface and subsequent immobilisation in response to reduction or precipitation as sulfides (Van der Weijden et al., 2006). These processes (especially 2 and 4) are often associated with organic-rich and laminated shales deposited under anoxic/euxinic conditions because: (1) the reduced form of many TEs tend to be more readily complexed with organic acids, sulfides or oxy-hydoxides and (2) many TEs are affected by processes operating more strongly under low-oxygen conditions (Mn/Fe redox cycling, high TOC contents and the presence of H_2S (Calvert & Pedersen, 1993; Algeo & Maynard, 2004). Therefore, laminated sediments (black shales) have the potential to provide high-resolution records of palaeoclimatic and palaeogeographic change (Calvert et al., 2001, Brumsack, 2006).

The *degree* of TE enrichment depends on the depth of the redox boundaries below the sediment water interface, the mass accumulation rate, bioturbation depth, and the concentration differences, together establishing the diffusional concentration gradients (Brumsack, 2006; Van der Weijden et al., 2006). Numerous authors report the positive co-variation of OM with trace elements like V, Ni, Cu, Zn, Mo, Cd and U (Brumsack, 1986; Nijenhuis et al., 1999; Werne et al., 2002; Cruse & Lyons, 2004; Van der Weijden et al., 2006). Lyons et al. (2003) observe that Mo/Al ratios do not track pyritic sulphur in euxinic sediments, but track OM. Likewise, Algeo & Maynard (2004) also found a correlation between TOC and TE enrichment in Carboniferous black shales. Lyons et al. (2003) and Arthur & Sageman (1994) observe a relationship between TOC and Mo concentrations in recent sediments. However, OM may not always have a direct coupling to trace element scavenging. Helz et al. (1996) found that the availability of dissolved sulfide is a critical control in Mo sequestration, and parallel accumulation of OM may simply drive the system capacity to generate hydrogen sulfide on both local and basin scales (Wilde et al., 2004). OM-type may also influence the degree of trace element enrichment. Humic acids, which are characteristic of terrestrial OM, have been shown to be efficient scavengers of Mo (Helz et al., 1996). Coveney et al. (1991) found that nearshore black shales (intercalated between deltaic deposits) show far higher Mo concentrations than offshore black shales. This was attributed to a higher amount of terrestrial OM. In turn, Cruse & Lyons (2004) also explain higher Mo-concentrations by a relatively high amount of terrestrial OM.

Since multiple factors are responsible for S and TE enrichment, careful analysis is needed to infer a change in basin-water salinity. There were two reasons to decide to investigate this: (1) although the fossil phases might indicate salinity differences, clear evidence of freshwater fossils is not reported. It seems to be the absence of Goniatites in some units that results in the interpretation of salinity changes; (2) the geochemical characterisation of marine and non-marine sediments is partly based on two sets of samples displaying different geochemical behaviour (Spears & Amin, 1981). Namely, a significant number of samples is derived from the top of the condensed section where the sediments tend to become coarser grained and display lower TOC

contents. In this chapter, it will be investigated whether C/S and TE-data support the cyclic change from marine to lacustrine conditions parallel to the alternation of fossil phases. To study this, the fossil phases of the condensed Namurian succession were sampled at three stratigraphic levels (Figs 6.1 & 6.3). Major and trace elemental concentrations were obtained next to C/S data. A number of thin sections were made to better investigate the sedimentary structures.

6.2 Geological setting

The Northwest European Carboniferous Basin (NWECB) developed north of the Variscan orogen and south of the Caledonian highlands (Fig. 1.1). The basin was surrounded by landmasses, with only distant connections to the open ocean in the east and west (Paproth, 1989; Ziegler, 1990; Gursky, 2006). As a result of a Dinantian rifting event, a series of (horst) blocks and basins developed in northern England (Leeder & McMahon, 1988; Fraser & Gawthorpe, 1990; see chapter 3 for a more extensive description). Carbonate platforms formed on the horst blocks, accentuating the differences in bathymetry with the neighbouring (sediment starved) basinal areas (Fraser & Gawthorpe, 1990; Leeder, 1992; Collinson, 2005; Fig. 6.1). Carbonate production ceased at the Visean-Namurian boundary probably due to a temperature change of basin waters and increasing sediment input (M. Aretz, pers. comm.). The Namurian represents a period of increasing siliciclastic sedimentation rates and infill of the Dinantian topography. In northern England, the main source of sediment supply was from the north or north-east. The London Brabant Massif shed much smaller volumes of sediment northwards (Collinson, 2005). Therefore, the area bordering the London Brabant Massif in the north experienced relatively deep water conditions during most of the Namurian while the area further northwards already experienced shallow water deposition (Collinson, 2005; Fig. 6.1). Hence, until the late Kinderscoutian the Derbyshire carbonate platform (the study area) remained uninfluenced by deltaic activity. Here, condensed sedimentation lasted from Pendleian up into Kinderscoutian (Figs 6.1 & 6.3). Sedimentation rates increase during Marsdenian, recording the prograding delta slope and the fluvial distributary channels (Kelling & Collinson, 1992). No hiatuses are found between the Namurian rocks deposited on top of the Derbyshire Massif and the underlying Visean limestones. A relatively thin transition zone is represented by an alternation of black mudstones with thin limestone bands (Ramsbottom et al., 1962).

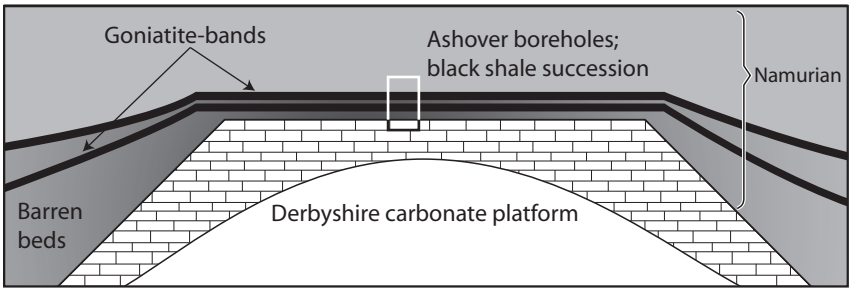

Figure 6.2 Schematic cross-section through the Derbyshire carbonate platform to show the relationship between the condensed Namurian sequence on top of the platform and the expanded succession in the basinal areas. The thick barren beds (low TOC) in the basins correspond to black shales in the Ashover cores in which several fossil phases were recognised by Ramsbottom et al. (1962).

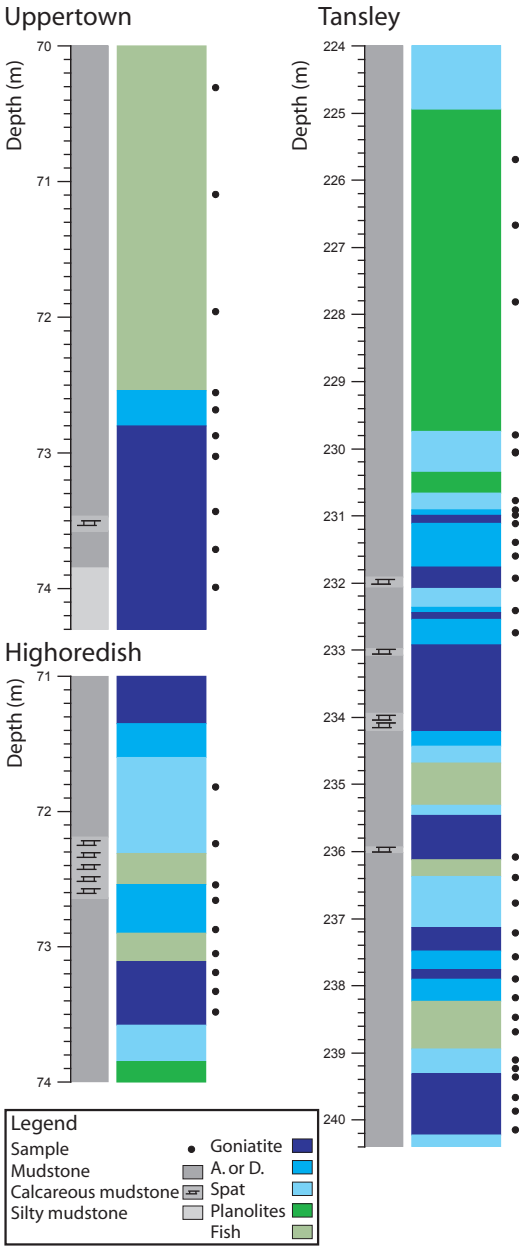

Figure 6.3 Lithology and faunal phases of the sampled sections.

6.3 Materials

The geochemical analyses were performed on samples from the Tansley, Highoredish and Uppertown cores (Figs 6.1 & 6.3). These cores were taken from boreholes drilled in 1955 by the British Geological Survey in the Ashover area of Derbyshire. Detailed faunal and lithological descriptions were published by Ramsbottom et al. (1962). The inorganic geochemistry and mineralogy from the Tansley borehole were investigated by Amin (1979) and Spears & Amin (1981). The Ashover cores cover the succession from the Upper Visean to the Upper Namurian (Fig. 6.1). Strata from three different stages were sampled: (i) the Arnsbergian (E2) from Highoredish, (ii) the Kinderscoutian (R1) from Tansley, and (iii) the Marsdenian (R2) from Uppertown (Figs 6.1 & 6.3). The sampled intervals show a predominantly uniform succession of laminated dark grey, fine-grained mudstones (Ramsbottom et al., 1962). Occasional intercalations of silty mudstones and carbonaceous mudstones occur. Forty-nine samples were taken, thirty from the Tansley borehole core, nine from Highoredish, and ten from Uppertown (Figs 6.1 & 6.3). The thickness of the samples was kept at a minimum, in order to minimise time-averaging effects. For each sample, detailed documentation on stratigraphy, fossil content and faunal phase designation is available.

Here, a short description is given on the fossil phases recognised by Ramsbottom et al. (1962). The order in which the phases are numbered is thought to reflect a gradual increase in the salinity of the environment according to Ramsbottom et al. (1962). In contrast, based on geochemical results, Amin (1979) and Spears & Amin (1981) interpret only the Fish phase to be deposited under non-marine (lacustrine) conditions.

1. Fish phase. Fish remains are the only fossils found in this phase. Marine fossils are absent. This faunal phase is usually found in dark mudstones, thought to be deposited in a non-marine (lacustrine) environment (Amin, 1979; Spears & Amin, 1981).
2. *Planolites* phase. *Planolites* (burrows) are found without any other fossils, and does not occur outside this phase. The characteristic lithology consists of mudstones, but usually not as dark as the other phases. It has been deposited in a quasi-marine environment, but not in open contact with the sea. This phase was sampled three times but only represents some 6% of the total succession.
3. Spat phase. This phase is characterised by abundant mollusc Spat (shells developed during the larval planktonic stage) unaccompanied by macrofossils. The phase is marine, but either the mollusc Spat drifted into a reduced-salinity environment or, at the close of the pelagic larval stage, bottom conditions were unsuitable for benthonic development. All shells found as Spat are of benthonic types, suggesting that free-swimming forms, such as Goniatites could move on to more suitable environments.
4. *Anthracoceras* or *Dimorphoceras* phase (*A.* or *D.* phase). This marine phase contains either *Anthracoceras* or *Dimorphoceras*. These Goniatite genera are characterised by having a very thin shell. The water in which this phase was deposited might have been slightly less saline than that supporting thicker-shelled Goniatite life.
5. Goniatite phase. This phase comprises typically thicker-shelled Goniatites, and may contain any of the fossils found in the less marine phases except those specifically mentioned as being restricted to one phase. Deposited in normal marine conditions, but bottom conditions did not favour a benthonic fauna.

6.4 Methods

6.4.1 Analytical techniques

All samples were ground to small particle size using a Tungsten-carbide mill in an automated grinding machine (Herzog HSM-HTP). Thermogravimetric analyses were performed by a LECO TGA 601 automated thermogravimetric analyser to measure the weight loss of the samples. X-ray fluorescence spectometry (XRF) was carried out on glass beads to obtain major element concentrations. The glass beads were analysed using an ARL9400 spectrometer with an Rh tube with full matrix correction for major elements. HF-based destruction of 125 mg of pulverised sample was done to measure trace elements by ICP-MS. The solutions were analyzed by an Agilent 7500 ICP-MS with a low uptake nebulizer. The precision and accuracy of the ICP-MS measurements is given in table 6.1. Total carbon (TC) and total sulphur (TS) contents were determined on bulk untreated samples with a LECO SC-144DR elemental analyser. Relative standard deviations are less then 5%. The TOC content was determined by first decalcifying the sample with 1N HCl on a hotplate.

6.4.2 Thin sections

Five thin sections were made from samples of the Tansley core (Fig. 6.5); two Goniatite phase and one Spat, Fish and *Planolites* phase. The main purpose is to study the sedimentary structures and to investigate if there are any differences to be seen between the fossil phase.

6.4.3 Grain size

The aim is to compare the geochemical characteristics of different faunal phases with incorporation of the dataset from Amin (1979). The comparison of samples consisting of more or less the same

Table 6.1 Precision and accuracy of ICP-MS analyses for elements used in this chapter. Concentrations for for ICP-MS: mg/kg (nd = not determined).

	Precision			Accuracy		
Element	**Mean**	**Precision (σ)**	**2σ (%)**	**Mean**	**Standard**	**Accuracy (%)**
Ag	0.3	0.01	3.51	nd	nd	nd
As	26.3	0.10	0.75	29.26	29.30	-0.15
Bi	0.2	0.00	0.67	1.07	1.03	3.76
Cd	2.6	0.01	0.77	2.16	2.38	-9.07
Co	35.1	0.06	0.34	nd	nd	nd
Cr	113.6	0.74	1.31	111.05	121.00	-8.22
Cu	75.2	2.71	7.20	76.79	88.60	-13.33
Mn	996.6	7.41	1.49	nd	nd	nd
Mo	15.2	0.48	6.37	0.97	1.14	-15.17
Ni	69.8	0.51	1.45	37.38	41.90	-10.78
Pb	21.5	0.07	0.65	175.80	167.00	5.27
Sb	6.8	0.02	0.48	2.36	2.45	-3.80
Tl	3.3	0.00	0.12	1.11	0.98	13.09
U	14.5	0.01	0.15	2.28	2.31	-1.29
V	297.7	2.11	1.42	80.31	90.80	-11.55
Zn	92.7	1.16	2.51	452.79	504.00	-10.16

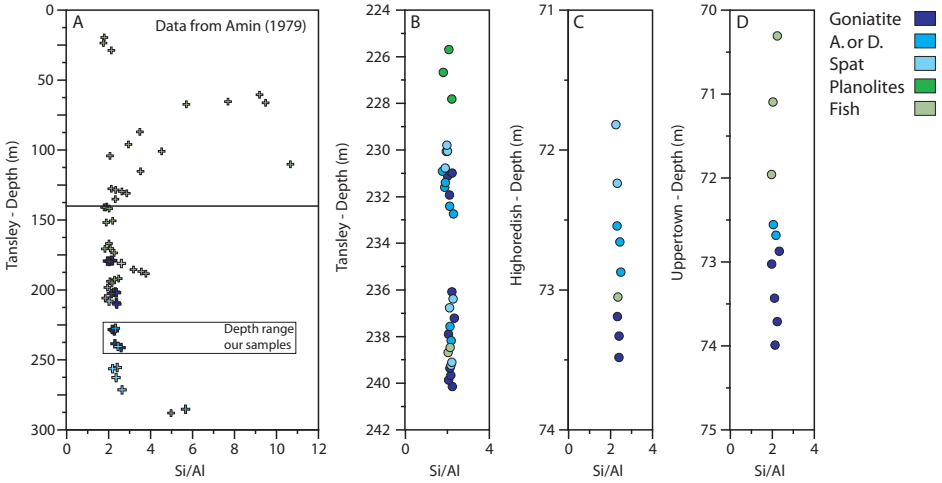

Figure 6.4 (A) Si/Al ratios for samples obtained by Amin (1979) and those sampled for this study; (B) Tansley, (C) Highoredish and (D) Uppertown.

lithology minimizes the effect of grain size variations on geochemistry. Therefore, it was decided to split up the Fish phase samples from Amin (1979) into a group with higher Si/Al ratios (higher quartz content) and a group of Fish phase samples consisting of Si/Al ratios comparable to the remaining samples. Although direct grain size measurements are lacking, Amin (1979) showed that the Si/Al ratio can be used as a proxy for grain size. Moreover, the quartz and feldspar content increase upsection next to Zr (Amin, 1979), parallel to the increase in Si/Al. The Si/Al ratios of the samples obtained for this study and the dataset from Amin (1979) are plotted in figure 6.4. From 140 m a coarsening upward sequence can be seen in the Tansley borehole, in accordance with the core description. The majority of the samples below 140 m have a Si/Al ratio around 2, as well as all samples from the Uppertown and Highoredish sections. This value represents the finest fraction (mudstone) present in the Namurian of the Ashover area.

6.4.4 The use of C/S ratios and trace elemental concentrations

In this chapter, the hypothesis will be tested that basin waters changed from marine to lacustrine, as suggested by Ramsbottom et al. (1962), Spears & Amin (1981), Collinson (1988), Holdsworth & Collinson (1988), Martinsen et al. (1995) and Collinson (2005). Interpretations on palaeosalinity are often based on C/S ratios (Berner & Raiswell, 1984; Leeder, 1988; Goldberg & Humayun, 2001; Belt et al., 2006). It is not very common to make inferences on palaeosalinity on the basis of trace elements (TEs; Shaffer, 2002). Instead, TEs are often used to infer palaeoredox conditions (Calvert & Pedersen, 1993; Morford et al., 2001). Since a black shale succession thought to be deposited under strongly varying salinities is studied here, it is inferred that it is possible to use C/S data and certain TEs to interpret the salinity of the basin waters because: (1) the C/S ratios of the sediments deposited under lacustrine conditions should be much higher than those found for the sediments reflecting marine conditions and (2) especially U and Mo have much lower concentrations in fresh water than in marine waters (Taylor & McLennan, 1985), most likely leading to significantly lower TE enrichments in at least the Fish phase sediments.

6.5 Results

6.5.1 Thin sections

TY-2 (Goniatite phase): This thin section consists of a brownish-coloured silty mudstone (Fig. 6.5) with pyrite framboids and probably has a high carbonate content. The laminae are not very clear. Ostracods and carbonate shell fragments are present and all exhibit a similar orientation. No signs of re-orientation can be seen.

TY-4 (Goniatite phase): A well-laminated, dark-coloured shale with pyrite framboids can be seen in this section. The organic matter content varies between adjacent laminae. Some gastropod remains occur.

TY-5 (Spat phase): This is a laminated, very dark-coloured shale, again characterised by pyrite framboids. Some small scale (syn-sedimentary) deformation can be seen, next to some ostracod remains.

TY-7 (Fish phase): This thin section shows the darkest-coloured laminated shale. No textural variations or fossil remains can be seen.

TY-29 (*Planolites* phase): This thin section has no similarities with the others. Here, small nodules with a dark core and a transparent rim can be observed. Possibly they represent algae.

6.5.2 Organic carbon and sulfur contents

The TOC content of the Tansley borehole reported by Amin (1979) shows a gradual increase with depth, up to values around 6 wt% on average at the base of the section. Most of the Fish phase samples occur in the upper part of the section; these show relatively low TOC contents (appr. 2 wt%). The data obtained for this study correspond well to the samples from Amin (1979). Most

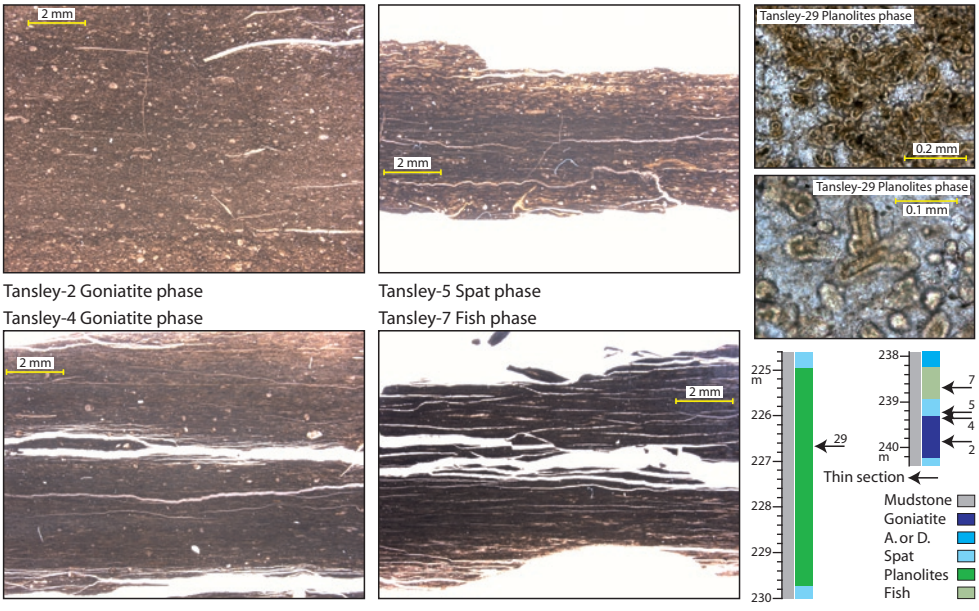

Figure 6.5 Thin sections obtained from the Tansley core.

of the samples fall between 2 and 7 wt% TOC. The Goniatite phase samples at the base show the highest TOC contents. In the Uppertown borehole, the TOC contents of the faunal phases are well comparable. A maximum of 5 wt% occurs in a *A.* or *D.* phase sample. In the Highoredish borehole, TOC contents vary around 4 wt%, with a maximum of 5 wt% in a Goniatite phase sample.

When plotting the average TOC content per faunal phase (Fig. 6.7), the Goniatite phase shows the highest value and the *Planolites* the lowest. The Fish phase samples from Amin (1979) characterised by higher Si/Al ratios display slightly lower TOC contents compared to the other Fish phase samples. When comparing the median values of the Goniatite up to the Fish phase (low Si/Al) samples (*Planolites* excluded), the TOC concentrations do not vary a lot: from 2.8 wt% in the Fish phase (Amin, 1979) to 4 wt% in the Goniatite phase (Amin, 1979). This is also expressed in the outcomes of a student's t-test in which the assumption was tested whether the TOC contents of the faunal phases are significantly different. For these t-tests, our data have been combined with the data from Amin (1979; nearly the same results were obtained when applying this to our dataset only). The *A.* or *D.* and Goniatite phases cannot be regarded as two different groups neither do the Spat and Fish phases. However, the Spat and Fish phases on one hand and the Goniatite and *A.* or *D* phase on the other can be regarded as two different groups ($P < 0.01$).

There is a marked difference between the total sulfur contents of our samples compared to the values obtained by Amin (1979; Fig. 6.7). As the accuracy of our data is good (within 5%), it is proposed to mostly rely on our data. The data of Amin (1979) show a clear difference in average sulfur content between the Fish phase samples (0.4 wt%) and the Goniatite phase samples (1.7 wt%). However, our data do not support a distinction between Goniatite and Fish phase samples on the basis of sulfur contents. Only the *Planolites* phase shows very low sulfur concentrations.

Figure 6.6 shows a graph in which S is plotted against TOC for our samples. Nearly all samples plot above the line indicating normal marine sediments, derived from (Berner & Raiswell, 1984). Only one Fish phase sample plots in the area for which a lacustrine depositional environment would be inferred. The *Planolites* phase samples occupy an isolated position near the origin due to a lack of TOC and S.

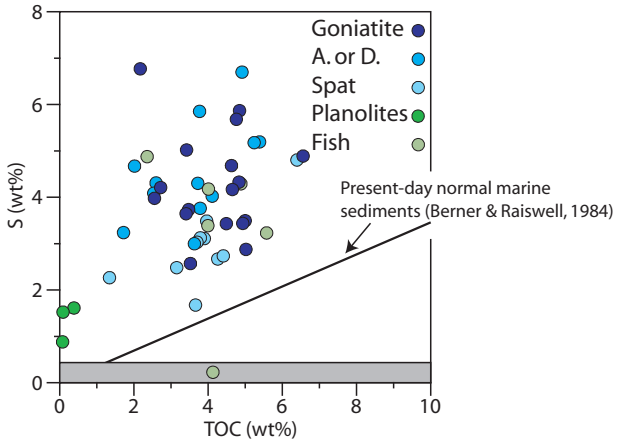

Figure 6.6 C/S data of the samples obtained for this study. Most samples plot above the normal marine line defined by Raiswell & Berner (1984). The area where lacustrine samples are expected to plot is shown in grey.

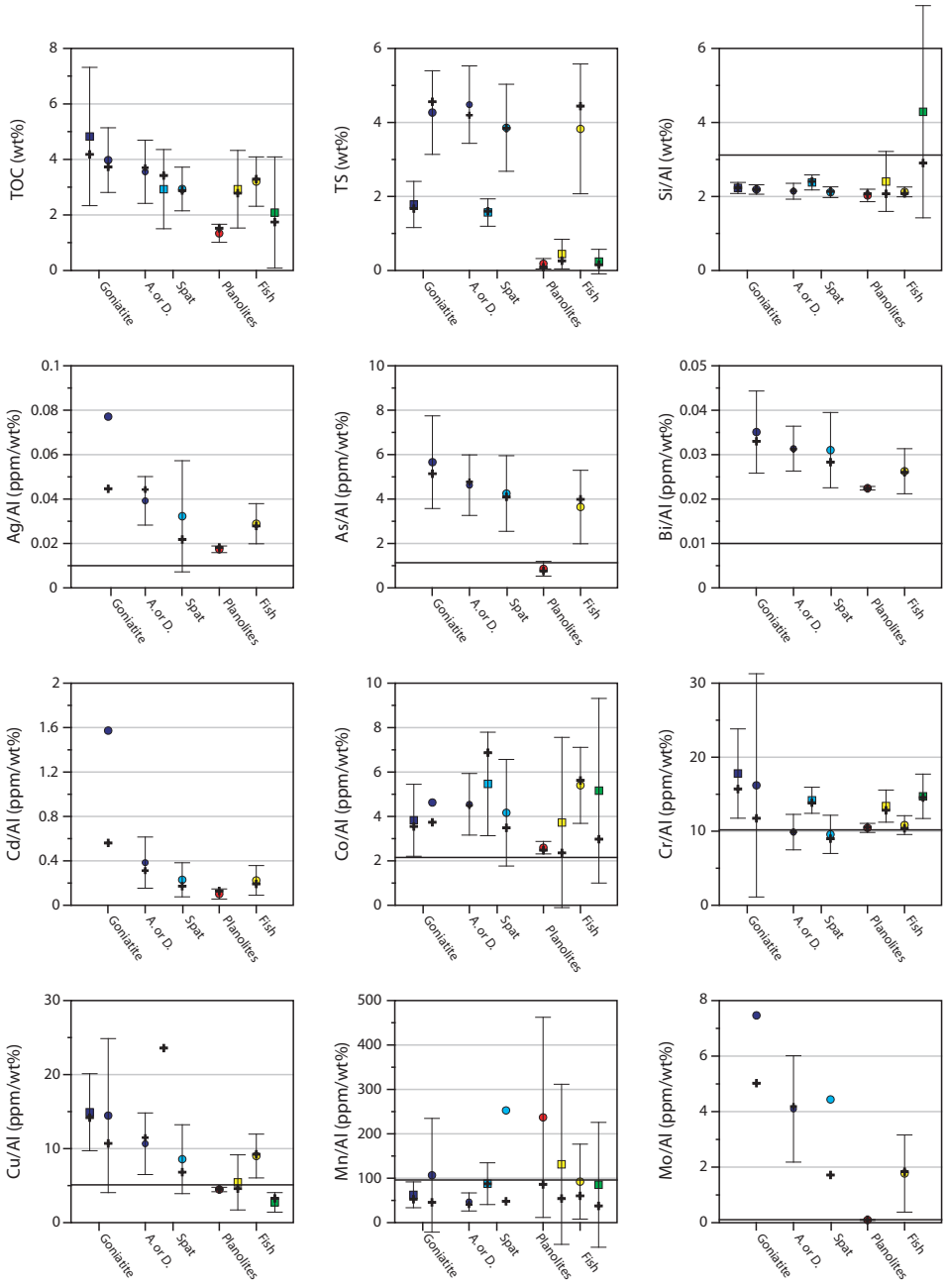

Figure 6.7 Average, median and standard deviation for TOC, TS, Si/Al and Al-normalised concentrations of the most important trace elements usually enriched in black shales. The results are shown for the samples analysed for this study next to the ones given by Amin (1979). Shown per fossil phase.

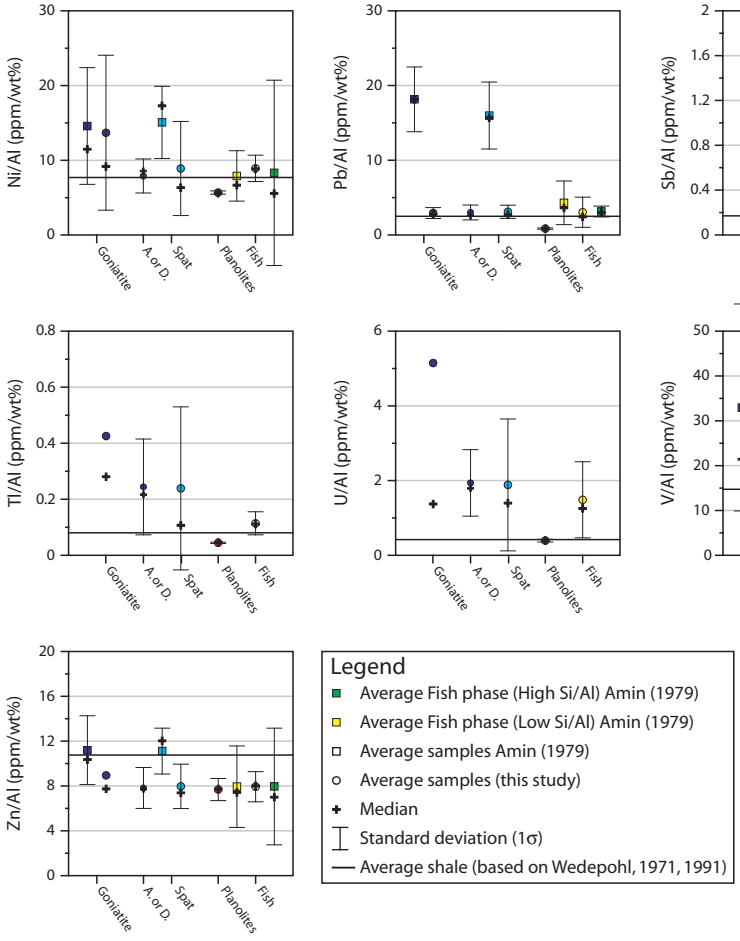

Figure 6.7 continued

6.5.3 Trace elements

Most TEs usually enriched in marine black shales show enrichment in our samples (Fig. 6.7). It is also evident that the Goniatite phase samples often show the highest EFs, followed by *A.* or *D.* Spat and Fish phase. However, besides the *Planolites* all fossil phases, including the Fish phase, do show marked enrichments. The *Planolites* phase only shows enrichment for three TEs (Ag, Bi and Cd). Mn shows depletion relative to the average shale in all faunal phases. The *Planolites* phase shows the least Mn depletion.

Correlation coefficients were calculated for the most important TEs with TOC, Al and TS (Table 6.2). Pb shows the best correlation with Al. This is in accordance with the minor enrichment of Pb in our samples. Most TEs associated with black shales are best correlated with TOC; in decreasing order of correlation these are: Cu, Ni, Se, V, Te, Ag, Mo, Zn, Sb, Tl, Cd and Cr. Only three TEs show the highest correlation coefficients with total sulfur: As, Bi and U. The R^2 for U is very low. After exclusion of one anomalous sample (330.8 ppm U) the R^2 is highest for TS.

Table 6.2 Correlation coefficients of most important trace elements (usually enriched in black shales) with Al, TOC and TS. The bold numbers indicate the highest correlation coefficients. In two cases (between brackets) the best correlation is achieved after removal of one exceptional trace element concentration.

Element	Al	TOC	TS
Ag	0.21	**0.39**	0.07
As	0.00	0.33	**0.67**
Bi	0.18	0.13	**0.52**
Cd	0.31	**0.28 (0.45)**	0.00
Co	0.00	0.02	**0.05**
Cr	0.03	**0.11**	0.00
Cu	0.11	**0.64**	0.24
Mo	0.27	**0.38**	0.19
Ni	0.22	**0.47**	0.11
Pb	**0.18**	0.00	0.14
Sb	0.14	**0.31**	0.15
Tl	0.22	**0.29**	0.05
U	0.13	0.09	**0.0015 (0.17)**
V	0.31	**0.40**	0.00
Zn	0.02	**0.35**	0.06

Most TEs usually enriched in marine black shales are obtained for the samples obtained for this study but only a small subset of TEs is available for the samples analysed by Amin (1979). Table 6.3 presents a comparison of TE enrichment factors (EFs) between the black shales investigated in this study, some recent (Brumsack, 2006) and a number of time-equivalent black shales (Algeo & Maynard, 2004; Cruse & Lyons, 2004) found in North America. In most cases, the mean EF of our sections is lower than the numbers found in recent black shales (Ag, Cd, Cu, Mo, Ni, V and Zn).

6.6 Discussion

6.6.1 Thin sections

The studied thin sections show dark and well-laminated sediments in most cases (except for the *Planolites* thin section). This is in accordance with the macroscopic observations of the core material (Ramsbottom, 1962; Amin, 1979). Based on this, it is suggested that the majority of the studied samples can be classified as black shales. Benthic life is seriously restricted in black shale environments (Wignall, 1994; Algeo et al., 2004). Therefore, most of the macrofossils described by Ramsbottom et al. (1962) in the Ashover boreholes are thought to have a pelagic origin (all Goniatite species, molusc spat, fish remains). However, the thin sections clearly revealed some shells (probably benthonic) in the Goniatite and Spat phase samples. This suggest brief episodes of opportunistic benthic colonization, a phenomenon described by Arthur & Sageman (1994). These authors noted the persistent and widespread occurrence of small, thin-shelled benthonic taxa in black shales.

Ramsbottom et al. (1962) interpreted the *Planolites* phase as a relatively light coloured shale, characterised by burrows. The light colour is in agreement with the low TOC contents, but the

Table 6.3 Element enrichment factors of recent and ancient black shales obtained from Brumsack (2006), Cruse and Lyons (2004), Algeo & Maynard (2004) and this study. The second number between brackets in our data represents the median value. This is only given when the difference between the mean and median differs significantly (35%). R: recent, A: ancient, EF: Enrichment factors. Brumsack (2006): (1) Perumargin, (2) Namibian mud lens, (3) Gulf of California, (4) Mediterranean sapropels >2% TOC, (5) Black Sea Unit 1, (6) Black Sea Unit 2, (7) C/T mean. Cruse & Lyons (2004): (1) C-TW-1, (2) IRC. Algeo & Maynard (2004): Pennsyvanian core shale.

	Brumsack (2006)							Cruse and Lyons (2004)		Algeo & Maynard (2004)	This study				
	1	2	3	4	5	6	7	1	2	1	Goniatite	A. or D. Spat		Planolites	Fish
	R	R	R	R	R	R	A	A	A	A	A	A	A	A	A
Ag	15	19	5.3	15	9.9	9.5	91				9.7 (5.6)	5.0	4.1	2.2	3.6
As	3.9	10	1.2	14	3.8	2.6	7.2				5.0	4.1	3.8	0.8	3.2
Bi	3	5.3	2	2.9	4.7	4	4.3				3.1	2.8	2.7	2.0	2.3
Cd	566	1733	36	180	17	18	418				106.9 (38.1)	26.1	15.6	6.9	15.3
Co	0.6	1.4	0.7	8.3	3	1.8	7			1.5	2.2	2.1	1.9	1.2	2.5
Cr	2.4	7.1	0.9	2.8	1.2	1.3	4.1			6.6	1.6	1.0	0.9	1.0	1.1
Cu	2.3	6.3	1.1	6.5	3.5	4.7	8.6			2.8	2.8	2.1	1.7	0.9	1.8
Mn	0.5	0.3	0.4	2.1	1.3	0.6	1.3			0.2	1.1 (0.47)	0.5	2.6 (0.49)	2.4 (0.9)	0.9
Mo	70	246.7	17	186	98	174	409	47	346	64	66.0	36.2	39.2 (15.2)	0.8	15.6
Ni	2.6	5.3	1.1	7.1	2.2	3.2	8.5	3.4	7.5	4.4	1.8	1.0	1.2	0.7	1.2
Pb	1.4	1.5	1.4	1.2	2.1	1.5	1.8	12	2.8	26	1.2	1.2	1.2	0.3	1.2
Sb	2.9		5	15	3.4	1.9	23				8.1 (4.6)	4.3	3.6 (2.0)	0.2	3.3
Tl	4.3	32	1	7.5	1.6	2.3	15				5.5	3.2	3.1 (1.4)	0.6	1.5
U	5.5	68	2.9	9.8	7.6	7.9	15	8.3	45	25	12.3 (3.2)	4.6	4.5	0.9	3.5
V	2.5	8.4	1.4	9.3	1.9	2.9	18	7	21	8.3	2.6 (1.1)	1.3	1.2	0.8	1.2
Zn	2.2	2.6	1.7	2.3	1.7	1.6	41	5.4	33		1.2	0.9	0.8	0.7	0.9

thin sections revealed an unexpected high concentration of (probably) algae. Although this fossil phase represents only 6% of the cored interval, it remains to be investigated if this facies can be found in more Planolites sections.

6.6.2 Sedimentation rate

As long as the biostratigraphic interpretations remain valid for the Ashover cores (no hiatuses are reported), there are not many places in the NWECB where Namurian sedimentation was so highly condensed and undisturbed for such a long time. Black shale deposition lasted until the Marsdenian. From the base Namurian up to the last marine band (*R. bilinque*) only 122 m of mudstones was deposited in a timespan of approximately 11 Ma. This results in a sedimentation rate of 1 cm/kyr. Corrected for about 50% shale compaction this would be 2 cm/kyr, which is still extremely low. Comparable sedimentation rates are reported for time equivalent black shales in North America. Algeo & Maynard (2004) calculated 1 cm/kyr while Algeo et al. (2004) adopted a tentative estimate of 0.5-2.0 cm/kyr for mean sedimentation rates during deposition of a 52-cm-thick black shale. However, a marked difference between the black shales described by Algeo & Maynard (2004) and Algeo et al. (2004) and the ones described here is the length of deposition: about 0.1 Ma in America against 11 Ma in Ashover. The burial efficiency of OM

is low when sedimentation rates are so low (Arthur & Sageman, 1994). This is because OM is relatively long exposed at the sediment water interface. Since the degradation rate of labile OM is independent of oxygen concentration (Canfield, 1994), the productivity or delivery (of terrestrial-derived) organic matter must have been high. It seems to be unlikely to explain the lower TOC contents of the Spat/Fish phase samples by an increase in sedimentation rate (dilution) because: (1) a doubling or more of the siliciclastic sedimentation is still too low to cause significant dilution and (2) the thin sections suggest that the Fish and Spat phase samples are well developed black shales. Due to the low sedimentation rates, an effective diffusion of TEs into the sediment might promote TE enrichment (Van der Weijden et al., 2006). Brumsack (2006) also proposes an inverse relationship between sedimentary oxyanion concentration and sedimentation rate.

During the Marsdenian, sedimentation rates increase due to the southwards advance of the delta system in the north. The disappearance of the alternation of fossil phases during the Marsdenian is an indication for this. In the top 180 m of the Tansley borehole, hardly any fossils are reported except for plant remains and some rare fish scales (Ramsbottom et al., 1962). The increase in sedimentation rate *and* grain size (Fig. 6.4) probably caused the decrease of TOC contents. This must be a clear indication of the dilution effect, which is applicable to the basinal areas during nearly the entire Namurian (Fig. 6.2).

6.6.3 Inferences on palaeosalinity

The C/S ratios obtained from our samples nearly all plot above the normal marine line defined by Berner & Raiswell (1984; Fig. 6.6). Therefore, all suggest deposition under marine and anoxic (enhanced TOC and S contents) conditions, except for one Fish phase sample and the *Planolites* samples. Thus, a change in basin water conditions from marine to lacustrine is not supported by our C/S data.

One of the factors influencing the degree of TE enrichment is the concentration difference between the watercolumn and the pore-waters, together establishing the diffusional concentration gradients (Brumsack, 2006; Van der Weijden et al., 2006). Assuming that the Fish phase samples are indeed deposited under non-marine (=lacustrine) conditions, one factor that certainly has to change between the black shales deposited in the Fish phase and the other phases is a concentration difference of the basin waters: the concentration of TEs like U, Mo and V should have been much lower. Therefore, TE enrichment factors (EFs) of the Fish phase sediments are expected to be significantly lower. This is not reflected in the data. Especially U and Mo are still significantly enriched in the Fish phase samples (Fig. 6.7). The same applies to most other TEs usually enriched in black shales. Moreover, the Spat phase samples are mostly a little less enriched than the Fish phase samples (Fig. 6.7). The Goniatite phase samples do show higher EFs than the Fish phase samples, but this is attributed to varying TOC contents. Table 6.2 shows that most redox-sensitive TEs display the highest correlation coefficient with TOC (compared to Al and TS) which indeed suggests that varying TOC contents can account for the observed concentration differences. In section 6.1, it has been shown that numerous authors also found a relationship between TEs and TOC. Although OM might not function as a direct scavenger of these trace elements (Helz et al., 1996), its capacity to generate hydrogen sulfide (Wilde et al., 2004) probably stimulates the enhanced fixation of trace elements. Altogether, based on the results it is concluded that the variation in TE enrichment between the faunal phases can be explained by (slight) variations in TOC. Combined with the observation of significant TE enrichments in the Fish phase samples (often even higher than the Spat phase samples), a salinity change is not needed to explain the geochemical variation in this dataset.

6.6.4 Limitations to a model of continuous marine sedimentation

There are some limitations to a model of permanently marine waters: (1) as the Fish phase layers are intercalated in between sediments deposited under marine conditions, S and TE enrichment can also be explained by diagenetic enrichment; (2) Spears et al. (1999) describe two Namurian tonsteins which are interpreted to have formed under freshwater conditions; (3) The alternation of fossil phases stills requires an explanation.

Ad 1) In the Kau-bay, Middelburg et al. (1991) reported higher sulfur contents in freshwater sediments than in overlying marine sediments, attributed to diffusion of sulphides. This process is also described in the Black Sea (Middelburg et al., 1991; Nagler et al., 2005) and in sediments underlying Mediterranean sapropels (Pruysers et al., 1991; Passier et al., 1996). Thus, sulfur enrichments might not be the most reliable discriminator between marine and lacustrine sedimentation as diffusion of sulfides into the relatively thin Fish phase layers cannot be ruled out. Trace elements might be less susceptible to diffusion. Nagler et al. (2005) showed that neither the downward migration of sulphate through the sapropels nor sulfide diffusion within the previously oxic sediments did result in significant Mo mobility during diagenesis. Likewise, Lyons et al. (2003) found no direct evidence for significant Mo enrichment via diffusion into sulfide rich pore waters of sediments from the Cariaco Basin even though they underwent a heavily sulfide overprint. Pruysers et al. (1991) measured TEs in a core from the Mediterranean Sea where 4 sapropels were found: Mo and V did not show enrichments in the sections just below the sapropels, while S did. Sternbeck et al. (2000) found that only Mn and As were remobilised due to downward sulphide movement. Therefore, it can be concluded that anoxic sediments bear a high potential to preserve pre-diagenetic TE signals. Based on this information, sulfur must be used with caution but the interpretation of continuous marine sedimentation seems to be still valid.

Ad 2) Spears et al. (1999) describe 9 bentonites, with thicknesses varying from 3 to 10 mm, from the Arnsbergian in the Pennine Basin (north of the study area). Seven of these are classified as K-bentonites, consisting of mainly mixed-layer smectite-illite. However, two kaolinite-dominated bentonites are found. These can be classified as tonsteins. There is agreement that tonsteins or kaolinite mostly form under freshwater conditions (Spears & Duff, 1984; Yalcin & Gumuser, 2000). In this way, Spears et al. (1999) interpret the basin to be freshwater dominated during deposition of these volcanic ashes, although the fossil content of these rocks do not clearly suggest a freshwater origin (e.g. sponge spicules, spat, nautiloids). Another limitation to this model is that alternation of volcanic ash takes place during burial and the geochemistry of pore waters during diagenesis is more important than the waters it was deposited in. However, it still remains to be explained why 2 out of 9 bentonites turn out to kaolinite-dominated. The tonsteins reported by Spears et al. (1999) are not the only findings of this category: in the Namurian of Belgium a 15 mm tonstein is reported in marine shales (Bouroz, 1963).

Ad 3) A direct indication for reduced salinity is the occurrence of relatively thin-shelled Goniatites (*Anthracoceras* or *Dimorphoceras*; *A.* or *D.* faunal phase) at the top and/or base of thicker shelled Goniatite bands (Ramsbottom et al., 1962; following Parker, 1955). In analogy, Dodd (1963) found a positive correlation between shell thickness and salinity of North American molluscs. However, using Tertiary and recent oyster populations Kirby (2001) showed that increasing marine predation is the reason for thicker shelled oysters in shallow marine conditions compared to their brackish equivalents. If variation in Goniatite shell thickness can be attributed to a change in salinity, a change of photic-zone salinity, which these fossils used to dwell in, is sufficient to explain these observations. This has already been proposed by Collinson (1988)

and Martinsen et al. (1995). These changes must probably be explained by variations in fluvial discharge from the hinterland.

6.7 Conclusions

Early Namurian distal and fine-grained sedimentation in the UK is interpreted to have varied between marine and lacustrine conditions. This has been concluded on the basis of the alternation of fossil assemblages (Ramsbottom et al., 1962) and associated geochemistry (Amin, 1979; Spears & Amin, 1981). Three cores were studied in which these transitions occur. Major and trace element, sulfur and organic matter concentrations were obtained. Based on the data from this study and the information from Amin (1979) another conclusion is drawn. Although the Goniatite phase samples (interpreted as marine) show the highest trace element enrichments, the Fish phase samples (thought to be deposited under lacustrine conditions) still show clear enrichments of most trace elements usually found in marine black shales. In accordance to the findings of many authors, the differences in trace elemental concentrations can be well explained by variations in TOC. Therefore, a fluctuating salinity basin is not needed to account for the observed changes in geochemistry. The basin in Northern England is interpreted to essentially remain marine throughout the Namurian, although surface water salinity might have changed periodically.

CHAPTER 7

Geochemistry of marine and lacustrine bands in the Upper Carboniferous of the Netherlands

This chapter is based on: Henk Kombrink, Bertil J.H. van Os, Kees J. van der Zwan & Theo E. Wong, Geochemistry of marine and lacustrine bands in the Upper Carboniferous of the Netherlands. Netherlands Journal of Geosciences (accepted).

Abstract

Geochemical studies on Upper Carboniferous marine bands showed that marked enrichment in redox-sensitive trace elements (uranium (U), vanadium (V), molybdenum (Mo)) mostly occur if they contain goniatites (Spears, 1964; Bloxham & Thomas, 1969; Fisher & Wignall, 2001). Goniatites indicate deposition in relatively distal and deep marine environments. In contrast, Westphalian marine bands found in the Netherlands predominantly show a *Lingula* facies, indicating deposition in a nearshore environment. These *Lingula* marine bands are mostly lacking significant trace element enrichments. The aim of this chapter is to explain the mechanisms causing the differences in geochemical characteristics between distal (Goniatite facies) and proximal (*Lingula* facies) marine bands. Geochemical analyses were carried out (total organic carbon (TOC), sulfur (S), major and trace elements) on a selection of these marine bands. Furthermore, a comparison was made with some lacustrine bands which broadly show the same sedimentary development as the *Lingula* marine bands. The results show that the *Lingula* marine bands, in contrast to the Goniatite and lacustrine bands, are characterised by low organic carbon contents (1-2 wt.%). A relatively high input of siliciclastics probably prevented the accumulation of organic-rich layers (dilution effect). In turn, low organic carbon contents most likely prevented the effective scavenging of trace elements. Although the lacustrine bands are characterised by high TOC contents, here the limited availability of trace elements in fresh water forms the best explanation for low trace metal enrichments. Since marine bands form stratigraphically important horizons in the Upper Carboniferous, lots of attempts have been made to recognise marine bands using well logs (gamma-ray). The results of this study show that using gamma-ray devices (detecting U-enrichments), only marine bands in a Goniatite facies are clearly recognised while *Lingula* marine bands are not detected.

7.1 Introduction

The Upper Carboniferous of the Netherlands and surrounding areas consists of a fluvio-deltaic succession with a thickness of up to 5 km. In this succession, marine bands form important stratigraphic horizons since these are thought to be correlatable basinwide (Ramsbottom et al., 1979; Leeder, 1988; Leeder et al., 1990; Dusar et al., 2000; Fig. 7.1). Marine bands are relatively thin layers (1-30m) of fine-grained sediment (clay to siltfraction; 1-50 μm) characterised by the presence of marine (micro)fossils. The origin of marine bands is commonly attributed to (glacio-

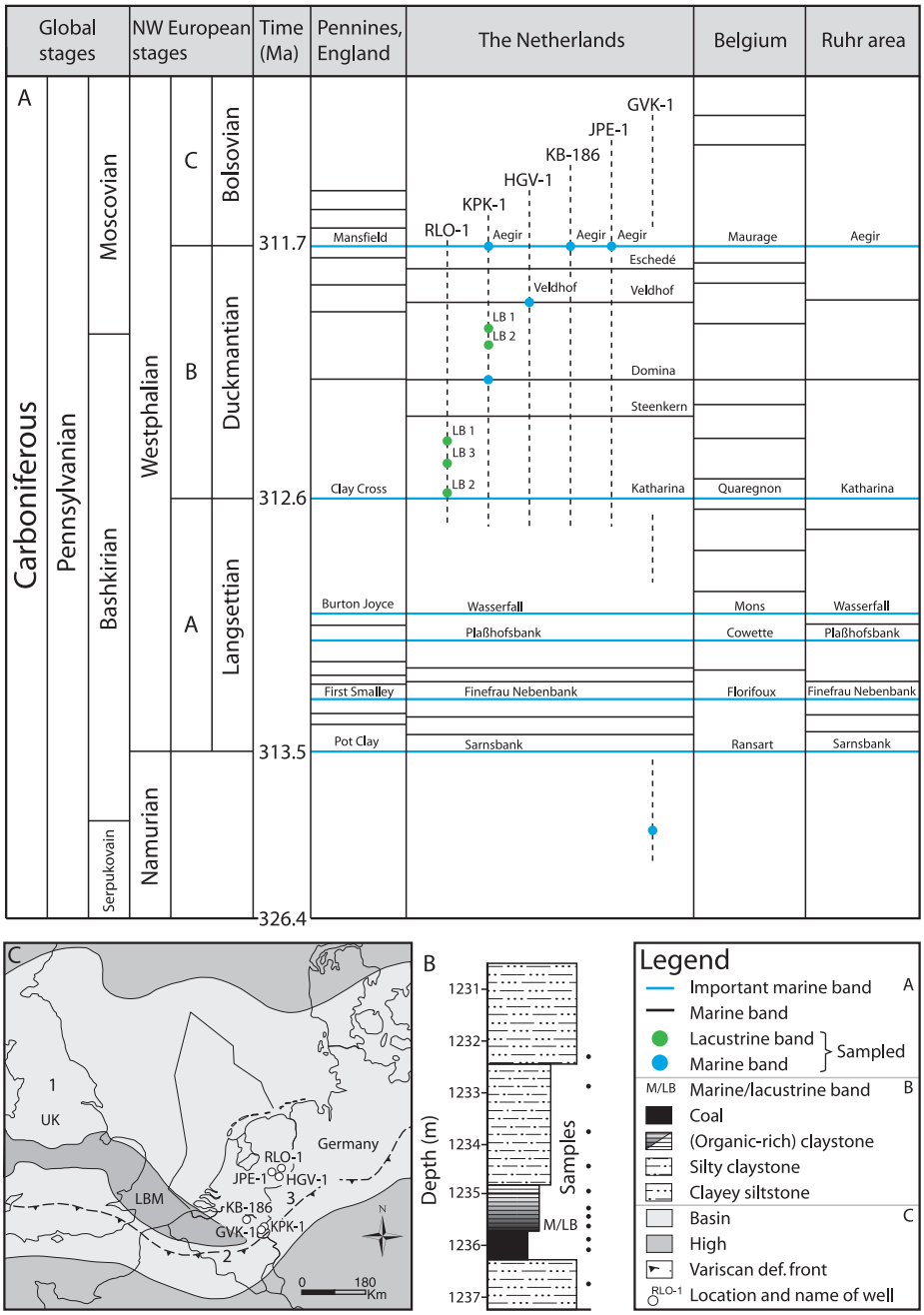
Global stages
NW European stages
Time (Ma)
Pennines, England
The Netherlands
Belgium
Ruhr area
A
Carboniferous
Pennsylvanian
Moscovian
Bashkirian
Serpukovain
Westphalian
Namurian
C
B
A
Bolsovian
Duckmantian
Langsettian
311.7
312.6
313.5
326.4
GVK-1
JPE-1
KB-186
HGV-1
KPK-1
RLO-1
Aegir
Mansfield
Eschedé
Veldhof
LB 1
LB 2
Domina
Steenkern
LB 3
Clay Cross
Katharina
Burton Joyce
Wasserfall
Plaßhofsbank
First Smalley
Finefrau Nebenbank
Pot Clay
Sarnsbank
Maurage
Quaregnon
Mons
Cowette
Florifoux
Ransart
C
B
1
UK
Germany
RLO-1
JPE-1
HGV-1
LBM
KB-186
3
GVK-1
KPK-1
2
N
0
180
Km
Depth (m)
1231
1232
1233
1234
1235
1236
1237
Samples
M/LB
Legend
Important marine band
Marine band
Lacustrine band
Marine band
Sampled
M/LB
Marine/lacustrine band
Coal
(Organic-rich) claystone
Silty claystone
Clayey siltstone
Basin
High
Variscan def. front
RLO-1
Location and name of well

Table 7.1 Fossil content of sampled sections. Fossils indicating marine conditions are: Goniatites, Conodonts, *Orbiculoidea* and marine ostracods. Brackish conditions are reflected by *Lingula* and Foraminifers. Freshwater conditions are interpreted when Carbonita and *Geisina* are found. When no fossils have been found, a freshwater depositional environment is assumed because of the findings of freshwater fossils directly above and below the sections.

Section		Fossils
Marine bands	GVK-goniatite marine band	Goniatites
	KPK-Aegir	Goniatites, Conodonts, Foraminifers, Marine ostracods, *Lingula*
	KPK-Domina	Foraminifers, *Lingula*, *Orbiculoidea*
	JPE-Aegir	Marine ostracods, Foraminifers
	KB-Aegir	*Lingula*, Trilobite, *Conularia*
	HGV-Veldhof	Foraminifers, *Lingula*
Lacustrine bands	RLO-LB 1	-
	RLO-LB 2	*Geisina arcuata*
	RLO-LB 3	-
	KPK-LB 1	*Carbonita*
	KPK-LB 2	-

eustatic) sea-level rises (Holdsworth & Collinson, 1988; Martinsen et al., 1995). Based on fossil content, Calver (1969), Rabitz (1966) and Ramsbottom (1969) distinguished several faunal phases in marine bands, reflecting the relative position to the shoreline. The fossils indicating the deepest water and most distal conditions are goniatites (ammonoids), whereas a *Lingula* (brachiopod) facies indicates deposition in nearshore or even brackish environments.

Attempts to identify the stratigraphically important marine bands in the Carboniferous succession using well logs or geochemical analyses have long been made. Hoogteijling (1948) found the strongest enrichments in U (one of the 3 elements picked up by gamma-ray devices) in the finest sediments but he doubted the possibilities to identify marine bands using gamma-ray. De Magnée (1952) turned out to be more confident in this method. More recently, several authors showed – using spectral gamma-ray (Archard & Trice, 1990; Hollywood & Whorlow, 1993; Davies & McLean, 1996) or geochemical analyses (Spears, 1964; Bloxham & Thomas, 1969; Fisher & Wignall, 2001) – that the Goniatite facies in marine bands often display enhanced U-concentrations. They concluded that an extremely slow sedimentation rate under anoxic and organic rich conditions favours enrichment in U. Indeed, the Goniatite facies in marine bands

← *Figure 7.1* (A) Stratigraphic distribution of sampled sections, next to distribution of Westphalian marine bands recognised in the UK (Calver, 1969), Belgium (Paproth et al., 1983b), the Netherlands (Thiadens, 1963 and several biostratigraphy reports) and the Ruhr Basin (Drozdzewski, 2005). Note that the number of marine bands mentioned in the text does not exactly correspond with the number of marine bands showed in this diagram because some have been grouped for clarity. The large number of Namurian marine bands is not shown in this figure. RLO-1: Ruurlo-1; KPK-1: Kemperkoul-1; HGV-1: Hengevelde-1; KB-186: Kolen boring-186; JPE-1: Joppe-1; GVK-1: Geverik-1; LB: Lacustrine band. (B) Generalised sedimentary log of a marine/lacustrine band and (C) outlines of Northwest European Carboniferous Basin. 1: Pennines, UK, 2: Belgium, 3: Ruhr area, LBM: London Brabant Massif. Figure 7.1C modified after Ziegler (1990). Timescale after Gradstein et al. (2004).

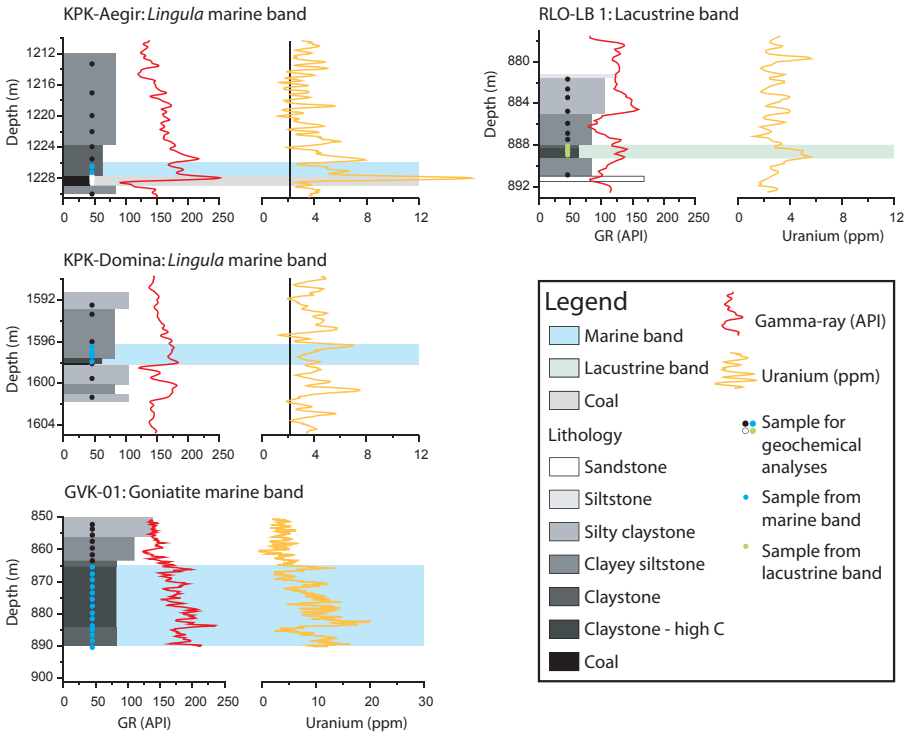

Figure 7.2 Some examples of well log response (gamma-ray and spectral gamma-ray (uranium plotted here) and sonic) for marine and lacustrine bands. Sample locations are given. Note the scale change for the uranium-log in GVK-1.

Table 7.2 Depth of sampled intervals, number of samples taken and thickness of investigated sections. The last column shows the maturity of the sections.

Section	Depth (m)	Number of samples	Interval thickness (m)	Thickness marine/ lacustrine band (m)	Vitrinite reflectance (%Rm)
GVK-MB	850-890	21	40	25	> 3
KPK-Aegir	1226	17	30	0.8	0.82
KPK-LB 1	1495	11	4	0.9	1.08
KPK-LB 2	1571	10	4	0.2	1.16
KPK-Domina	1597	11	10	1.5	1.16
JPE-Aegir	1300	18	15	7.8	0.82
KB-Aegir	1130	9	5	1.4	1.07
HGV-Veldhof	1242	12	3	0.8	0.75
RLO-LB 1	888	13	9	0.9	1.01
RLO-LB 2	1184	11	4	0.5	1.15
RLO-LB 3	1235	15	6	0.8	1.29

often shows enhanced organic matter contents (Calver, 1969; Ramsbottom, 1969). The term black shale has therefore often been used as a descriptive term for these U-enriched marine bands.

The marine bands found in the Netherlands mostly display a *Lingula* facies (Table 7.1) and (spectral) gamma-ray logs show weak or only faint peaks (Fig. 7.2). For instance, it can be seen that in the well Kemperkoul-1 (KPK-1) the marine band named Domina does not show a clear peak. Moreover, when a peak can be seen (for instance in the Aegir marine band in KPK-1), it turns out to be located in the coal underlying the marine band.

Most geochemical work has been performed on Goniatite marine bands. The availability of some continuously cored wells in the Netherlands, in which *Lingula* bands already are proven by fossil evidence, provides an excellent dataset to study the geochemical characteristics of these type of marine bands. The aims of this chapter are to (1) explain the geochemical development of (proximal marine) *Lingula* marine bands and (2) put them into perspective using data from (distal marine) Goniatite marine bands and lacustrine bands (reflecting entirely freshwater conditions). In this way, a transect from lacustrine up to (deep) marine conditions will be investigated. Published geochemical data from the UK has been used to further illustrate the results.

7.2 Geological setting

During Namurian times, sedimentation in the Northwest European Carboniferous Basin (NWECB, Fig. 7.1) mainly took place under deltaic conditions. In general, the lower part of the Namurian sequence is characterised by pro-delta basinal shale, giving way to typical coarsening and shallowing-upward cycles of pro-delta shale via fluvial silt/sandstone to a coal (see chapter 2). The marine bands are intercalated between the basinal shales or overlie the coal, reflecting the peak of transgression where most distal conditions are reached. Glacio-eustatic sea-level fluctuations probably form the driving mechanism of the observed cyclicity and deposition of marine bands in the NWECB. During the Westphalian these cycles are gradually replaced by continuous fluvial sedimentation characterised by the alternation of fluvial channel sands, floodplain mudstones and coals. The Westphalian marine bands are mostly found on top a coal.

Marine bands were extensively studied in the UK (Calver, 1969; Ramsbottom, 1969), Belgium (Paproth et al., 1983; Dusar et al., 2000) and the Ruhr area in Germany (Rabitz, 1966; Fig. 7.1). In the Namurian succession, numerous marine bands (>30) were found (not shown in figure 7.1). The UK Westphalian succession contains 19 marine bands (Calver, 1969), whereas in Germany, 15 marine bands occur (Rabitz, 1966). In the Netherlands, 14 marine bands are found in the Westphalian (Thiadens, 1963; Van Amerom & Meessen, 1985; Van Amerom et al., 1985). Most of the Namurian marine bands are developed in Goniatite facies, representing deep marine and distal conditions. However, most of the Westphalian marine bands have a *Lingula* facies while only a limited number displays (Fig. 7.1) a Goniatite facies (Calver, 1969; Drozdzewski, 2005). Extensive research on the fossil content of marine bands in the UK and Germany showed that one marine band can be developed in different faunal phases laterally and on one location. *Lingula* facies mainly occurs along basin margins and intervening highs such as the London Brabant Massif (Fig. 7.1), whereas the Goniatite marine bands are found in the basin centre (Calver, 1969; Ramsbottom, 1969). Moreover, the most complete record of marine bands is found in the basin centre as certain bands are lacking in the marginal areas (Calver, 1969). For example, marine bands change from *Lingula* to Goniatite facies across the Craven fault in the Pennines (Calver, 1969).

7.3 Materials

In the 1980s, the Netherlands Geological Survey drilled five wells with complete core coverage of the Carboniferous (Fig. 7.1): Ruurlo-1 (RLO-1), Joppe-1 (JPE-1), Hengevelde-1 (HGV-1), Kemperkoul-1 (KPK-1) and Geverik-1 (GVK-1). 148 samples from 11 intervals (Fig. 7.1 and Table 7.2) were taken from these cores stored in the core-lab of TNO-Netherlands Geological Survey. The *Lingula* marine band KB-Aegir was sampled in the core-lab of the Geological Survey of Belgium in Brussels.

Five lacustrine bands, five *Lingula* marine bands and one Goniatite marine band were sampled. The *Lingula* marine bands were selected on the basis of the fossil content derived from the cores. Sampling of the Goniatite marine band was performed on the basis of spectral gamma-ray and fossil content. The spectral gamma-ray log shows enhanced uranium contents (Fig. 7.2) whereas the findings of numerous goniatites point to a marine depositional environment (Table 7.1). The thickness of this marine band is relatively high (25 m). The lacustrine bands were selected on the basis of sedimentological criteria (parallel laminated, fine-grained and TOC-rich sediments). No fossils were found in three lacustrine sections (Table 7.1). However, a freshwater environment is assumed, based on the presence of freshwater fossils immediately below and above the sections (Van Amerom & Glerum, 1984; Meessen, 1985).

The investigated marine bands form a small subset of the total amount that has been recognised (Fig. 7.1). The stratigraphically lowest Westphalian marine band studied in this chapter is Domina, which has a Middle Westphalian B age. In the Ruhr basin, Domina has only been found in the northwestern part, indicating a continuation of paralic sedimentation in the southeast (Drozdzewski, 2005). The Veldhof marine band was discovered in the 1980's and has been tentatively correlated with German marine bands (Van Amerom & Meessen, 1985). The most important marine band sampled in this study is the Aegir. It has a rich fauna in the Ruhr Basin (Rabitz, 1966), where it can attain a thickness of 30 m. This is the last fully marine flooding in this part of the NWECB (in the UK the Top marine band is found in Middle Westphalian C sediments). In KPK-1 and JPE-1, the Aegir is characterised by some goniatite remains but these occur together with other fossils (Table 7.1).

From a sedimentological point of view, the *Lingula* bands are comparable to the lacustrine bands (Figs 7.2 & 7.3). Both are characterised by the following sedimentary succession: at the base a grey and mostly mottled clayey siltstone occurs, deposited in a floodplain where bioturbation caused mixing of the sediments. This floodplain was drowned and peat formation started, resulting in a coal of variable thickness (usually <1m). In case of the *Lingula* bands, seawater flooded the swamps and shallow marine conditions were established. A lacustrine setting developed because subsidence probably exceeded peat-growth. In both cases parallel laminated clay, (slightly) enriched in organic matter was subsequently deposited. Organic carbon contents decrease upwards and parallel lamination gives way to ripple lamination while bioturbation increases. In turn, the shallow marine and lacustrine sediments are overlain by fluvial mouthbar or channel sandstones and fine grained sediments deposited in floodplains. The Namurian Goniatite marine band of the Geverik well entirely consists of a claystone, deposited under relatively deep marine conditions. The sediments are well laminated and dark coloured because of the high organic matter content. Going upwards, the first pro-delta coarsening upward sequence marks the onset of the Namurian progradational basin fill.

7.4 Methods

All samples were ground to small particle size using a Tungsten-carbide mill in an automated grinding machine (Herzog HSM-HTP). X-ray fluorescence spectometry (XRF) was carried out on glass beads to obtain major element concentrations (see table 7.3 for precision). The glass beads were analysed using an ARL9400 spectrometer with an Rh tube with full matrix correction for major elements. However, before XRF analysis could be carried out, TGA (thermo-gravometric analysis) was performed on 3-4 g of grounded samples, using a LECO® TGA 601. The TGA results were used for the determination of the moisture (105 °C), organic matter (450-550 °C) and carbonate content (800-1100 °C).

Total carbon content (TC) and total sulphur content (TS) were obtained using a LECO® SC 144DR C/S analyzer. Determination of the total organic carbon content (TOC) was carried out

Figure 7.3 Core-photograph of a lacustrine band (RLO-LB 2). The mottled sediment (1) below the coal is well developed, as well as the organic-rich section (2) on top of the coal (lacustrine band). The white labels indicate the sample locations.

Table 7.3 Precision and accuracy of C/S (LECO), XRF (only precision) and ICP-MS analyses for elements used in this chapter. Concentrations for C/S and XRF: wt%, for ICP-MS: mg/kg (nd = not determined).

		Precision			Accuracy		
Element	**Method**	**Mean**	**Precision (σ)**	**2σ (%)**	**Mean**	**Standard**	**Accuracy (%)**
TS (wt%)	LECO	1.52	0.02	2.64	0.51	0.50	2.40
TC (wt%)	LECO	2.00	0.06	5.99	3.91	3.60	8.60
Al (wt%)	XRF	18.57	0.11	1.18	nd	nd	nd
Fe (wt%)	XRF	6.31	0.03	0.95	nd	nd	nd
K (wt%)	XRF	3.69	0.04	2.17	nd	nd	nd
Ca (wt%)	XRF	0.28	0.01	7.05	nd	nd	nd
Mo (mg/kg)	ICP-MS	2.91	0.11	7.57	1.20	1.14	5.22
U (mg/kg)	ICP-MS	3.98	0.16	8.04	2.28	2.31	-1.18
V (mg/kg)	ICP-MS	126.16	8.51	13.49	87.41	92.00	-4.99
Zn (mg/kg)	ICP-MS	105.67	6.61	12.52	622.31	528.00	17.86
Pb (mg/kg)	ICP-MS	256.03	3.04	2.38	164.39	167.00	-1.56
Ni (mg/kg)	ICP-MS	63.82	5.01	15.71	42.85	43.60	-1.72
Cu (mg/kg)	ICP-MS	46.58	2.72	11.68	90.16	95.00	-5.10
Th (mg/kg)	ICP-MS	10.29	0.76	14.77	9.28	9.74	-4.72

by subtracting the carbon content attributed to CaO (obtained by XRF) from the TC content. This corresponds well with the determination of TOC using carbonate from the TGA-results (not shown). Due to maturation, some loss of organic matter took place. However, except for GVK-1 the original TOC values have not been restored. There are two reasons for this: (1) the maturities of these sections are well comparable and not very high and (2) probably most of the organic matter is of terrestrial origin, implying only moderate loss of organic matter. Using the method published by Raiswell & Berner (1987), the original TOC for GVK-1 will fall within a range of 8-10 wt%.

It is assumed, based on Leeder et al. (1990), that the total sulphur concentrations obtained from the siliciclastic sediments are present in the form of pyrite. When plotted against Fe (Fig. 7.4), most of the samples with clear enrichment in sulphur are situated near the pyrite line, which indeed suggests the dominant residence of sulphur in pyrite. Based on studies by Diessel (1992) and Spears et al. (1999) it is also assumed that enrichments in sulphur (>1.5 wt%) in the coals analysed in this study are caused by pyrite.

HF-based destruction of 125 mg of pulverised sample was carried out to measure trace elements by ICP-MS. The solutions were analyzed by an Agilent 7500 ICP-MS with a low uptake nebulizer. The analytical quality of the XRF, C/S and ICP-MS analyses was determined by calculation of the precision of duplicate sample pairs. Accuracy was calculated with the mean values of the standard measurements and the reported mean element concentrations of these standards (Table 7.3).

Trace elements enrichment factors (EF) were calculated for a number of elements. The mean EF for a particular marine/lacustrine band or overlying sediment layer is based on the following formula:

$$EF = \frac{\sum_{i=1}^{N} (El/Al)_{sample} \; / (El/Al)_{av.shale}}{N}$$

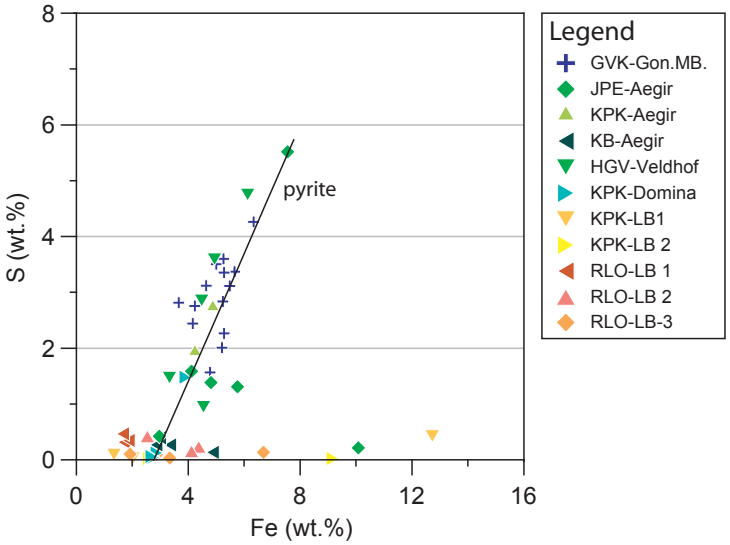

Figure 7.4 Cross-plot displaying the Fe/S ratio for the marine and lacustrine bands. The samples enriched in pyrite plot relatively well on the pyrite line.

where *El* and *Al* are the trace element and aluminium concentrations (ppm) respectively for the average shale (*av.shale*) and *sample* (Taylor & McLennan, 1985) whilst *N* refers to the number of samples taken from the marine band or overlying sediments. Normalisation on Al has been carried out to remove the effect of the changing clay-percentages per sample. The EF for coal has been calculated in a different way because Al concentrations are very low in coal (Dellwig, 1999). Moreover, some trace elements may have an association with organic matter (Goodarzi & Swaine, 1993) which causes normalisation on Al alone to overestimate the enrichment. Therefore, world mean trace elemental concentrations in coal were used (Swaine, 1990; Gayer et al., 1999) to calculate the EF. The following formula was used:

$$EF = \frac{\sum_{i=1}^{N} (El_{sample} / El_{mean})}{N}$$

The following parameters were used to characterise the geochemistry of the marine and lacustrine bands:

1. *TOC*. Marine bands are often associated with enhanced TOC contents (Bloxham & Thomas, 1969; Spears & Sezgin, 1985; Wignall, 1994; Fisher & Wignall, 2001). The analysis of the sampled sections therefore starts with a description of TOC.
2. *Pyrite*. Pyrite is often used as an indicator of marine sulphate-reducing conditions (Berner & Raiswell, 1984). However, clear enrichment of pyrite only occurs under high TOC conditions (when degradable organic matter is present) because under low TOC conditions reduction of sulphate is limited (Lyons et al., 2003).
3. *Trace elements*. It is widely recognised that marine bands often display enrichment in U (Leeder et al., 1990; Davies & McLean, 1996; Fisher & Wignall, 2001) next to other trace elements like Molybdenum (Mo), Vanadium (V), Nickel (Ni), Zinc (Zn), Lead (Pb) and Copper (Cu) (Coveney et al., 1991; Algeo & Maynard, 2004; Algeo et al., 2004; Schultz, 2004). Enrichment

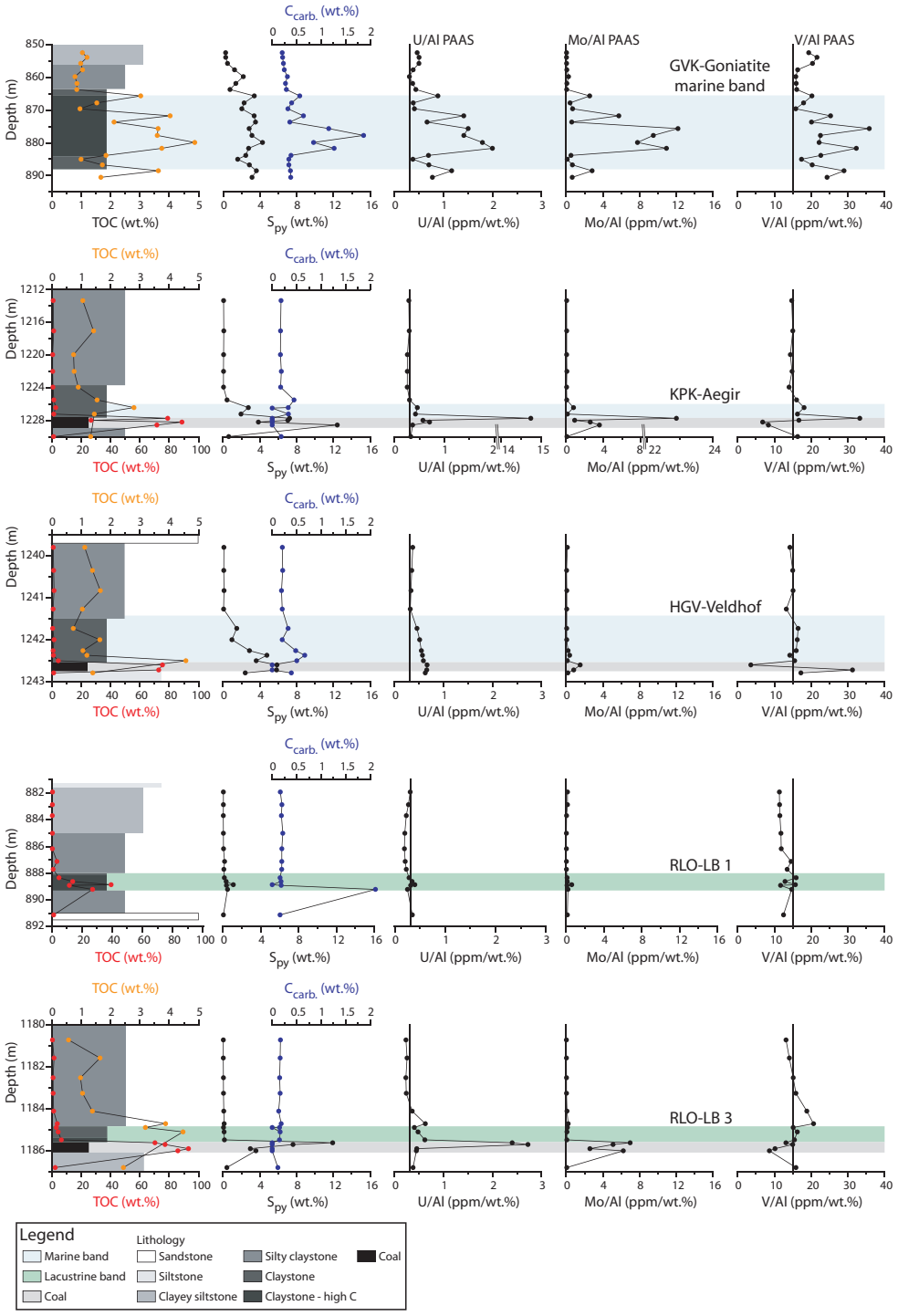
GVK-Goniatite marine band
KPK-Aegir
HGV-Veldhof
RLO-LB 1
RLO-LB 3
Depth (m)
TOC (wt.%)
$C_{carb.}$ (wt.%)
S_{py} (wt.%)
U/Al PAAS
Mo/Al PAAS
V/Al PAAS
U/Al (ppm/wt.%)
Mo/Al (ppm/wt.%)
V/Al (ppm/wt.%)
Legend
Lithology
Marine band
Lacustrine band
Coal
Sandstone
Siltstone
Clayey siltstone
Silty claystone
Claystone
Claystone - high C
Coal

of uranium and other trace elements in marine sediments will only occur if anoxic conditions prevail in the sediments and if there is a source. As the main source for trace elements like U, Mo and V is seawater (Taylor & McLennan, 1985), these elements will be investigated in particular.

7.5 Results

7.5.1 Organic matter

The TOC content of the Goniatite marine band varies from 1 to 4.9 wt%, which is an underestimation regarding the very high maturity (see above). In the grey shale on top of the marine band, a mean TOC content of 1 wt% is common. In general, the *Lingula* marine bands are characterised by lower TOC contents compared to the Goniatite marine band. A maximum of 4.6 wt% occurs in HGV-Veldhof whereas in KPK-Aegir and JPE-Aegir maxima around 2 wt% were obtained. In KPK-Domina and KB-186, the TOC content is only slightly higher than 1 wt%. The maxima mostly occur in the interval just above the coal and rapidly decrease upward (Fig. 7.5). The TOC contents in the 'normal' shale on top of the *Lingula* marine bands vary around 1 wt%, comparable to the values obtained in GVK-1.

In the lacustrine bands, higher TOC contents occur than in both types of marine bands (Fig. 7.5 & appendix B). A maximum of 40 wt% was obtained in RLO-LB-1 whereas in KPK-LB 1, RLO-LB 2 and RLO-LB-3 maxima of 17, 7 and 6.6 wt% occur respectively. Only in KPK-LB 2, TOC contents are comparable to those in the *Lingula* marine bands; the maximum percentage amounts to 2.4 wt%. The TOC maxima of the lacustrine sections also occur in the interval just on top of the coal and decrease upwards (Fig. 7.5). The TOC contents of the normal shale overlying the lacustrine bands are comparable to those found in the sections on top of the *Lingula* marine bands (appr. 1 wt%).

7.5.2 Pyrite

In the *Lingula* marine bands KPK-Aegir, JPE-Aegir, HGV-Veldhof, enhanced S contents (up to 5.52 wt% in JPE-Aegir) occur in the basal part overlying the coal. In KPK-Domina only one sample shows an enrichment of >1 wt% S, whereas in KB-186 none of the samples from the marine band is >1 wt%. An upward decrease in pyrite content can in most cases be observed *within* the marine band (Fig. 7.5 and appendix B), leading to a "background" value of ≤ 0.1wt% in the normal shale overlying the *Lingula* marine bands. The only exception is JPE-Aegir in which pyrite contents remain relatively high (S ≥ 1.5 wt%) throughout the marine band. The Goniatite marine band shows marked enrichments in pyrite (Fig. 7.5 and appendix B). The lacustrine bands are characterised by low S contents without exception. In RLO-LB 2 a maximum of 0.42 wt% (of all lacustrine bands) has been measured, which is significantly lower than the S contents in the *Lingula* marine bands.

← *Figure 7.5* Plots of two *Lingula* marine bands, two lacustrine bands and the Goniatite marine band to show the distribution of TOC, S, $C_{carbonate}$ and a selection of trace metals. Note the different scales used for TOC. In this figure the Al-normalised values for coal are shown. Note that the enrichment factors for coal displayed in figure 7.6 has been calculated in a different way. The coal-values in this figure are probably slightly over-estimated (see Methods). PAAS: Post Archean Average Shale.

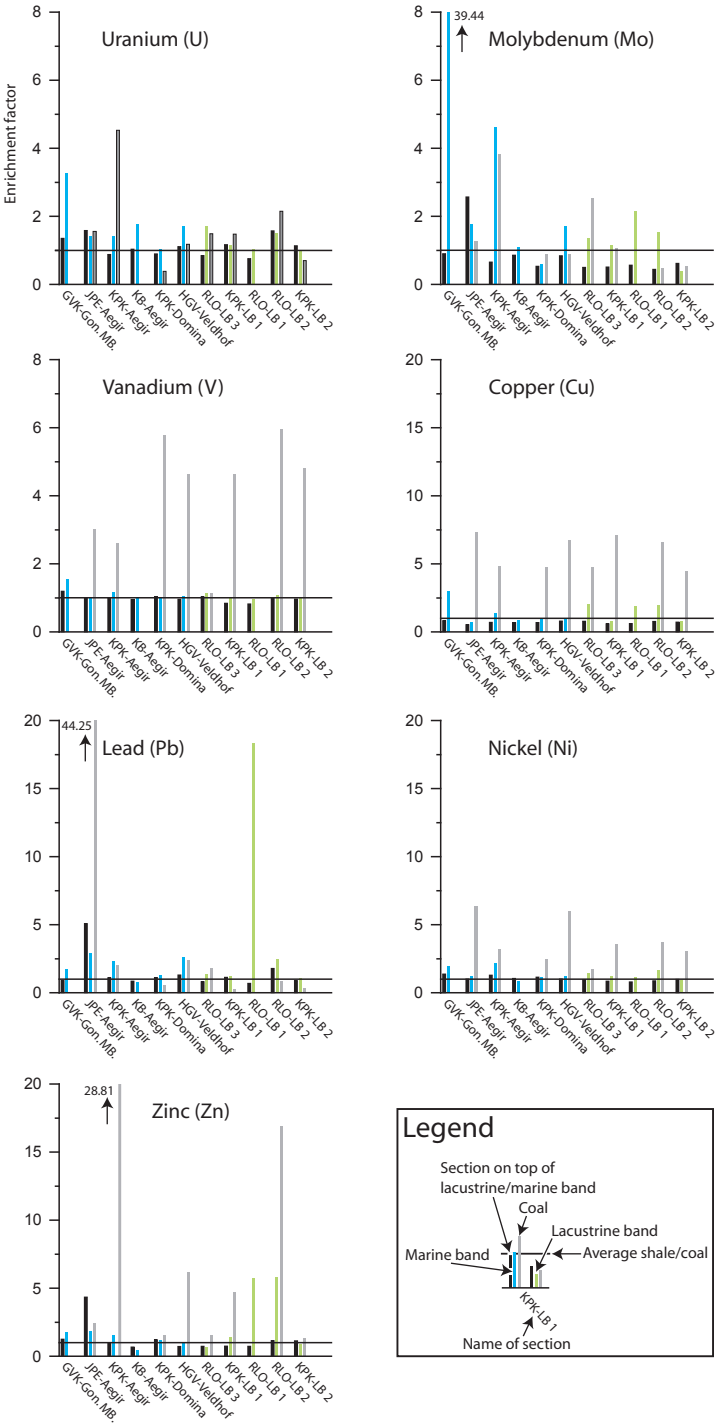
Enrichment factor
Uranium (U)
Molybdenum (Mo)
39.44
Vanadium (V)
Copper (Cu)
Lead (Pb)
44.25
Nickel (Ni)
Zinc (Zn)
28.81
GVK-Gon.MB.
JPE-Aegir
KPK-Aegir
KB-Aegir
KPK-Domina
HGV-Veldhof
RLO-LB 3
KPK-LB 1
RLO-LB 1
RLO-LB 2
KPK-LB 2
Legend
Section on top of lacustrine/marine band
Coal
Lacustrine band
Marine band
Average shale/coal
KPK-LB 1
Name of section

← *Figure 7.6* Bar charts displaying the enrichments factors for the marine/lacustrine bands, the underlying coal and the overlying sediments. It is important to realise that the enrichment factors for the coals have been calculated differently (see text). Therefore, an enrichment of a certain element in a coal (for instance vanadium) does not necessarily means that the absolute concentrations are higher in the coal than in the under and overlying sediments (see appendix B).

The coals located below the *Lingula* marine bands show even higher sulphur contents than the overlying shale (Fig. 7.5 and appendix B). At the base of the coal below KPK-Aegir, a maximum of 12.4 wt% S has been measured. These sulphur contents are probably related to percolating seawater after the marine flooding, a process well-known from literature (Chou, 1984; Spears et al., 1999). In contrast, the coals below the lacustrine bands does not have strong enrichments in sulphur. The only exception is the RLO-LB 3 coal in which S is present up to 12 wt%. This coal is probably directly influenced by seawater, regarding the lack of S enrichments in the overlying lacustrine shale.

7.5.3 Trace elements

The Goniatite marine band shows a relatively high mean EF for U and Mo, whereas V is only moderately enriched (Fig. 7.6). None of the *Lingula* marine and lacustrine bands shows a mean EF higher than 2 for U, Mo and V; KPK-Aegir and RLO-LB 1 for Mo excluded. Apart from Pb/Zn and Zn in RLO-LB 1 and RLO-LB 2 respectively, in general the EFs for Cu, Ni, Pb and Zn are very low to insignificant for both the marine and the lacustrine bands (Fig. 7.6). Some sections do not show enrichments and even depletions relative to the average shale can be seen. The highest EF of U, Mo and V do not occur in the *Lingula* marine bands but in some of the underlying coals instead. This is also applies to some coals underlying the lacustrine bands (Fig. 7.6). An example is the coal located below the Aegir marine band in KPK-1. In the topmost sample in the coal a 30 ppm concentration for U was obtained, which clearly corresponds with the peak in the spectral gamma-ray at that depth (Fig. 7.1).

Th/U ratios, which are used to distinguish marine bands from normal shale, were obtained for all marine and lacustrine bands (Fig. 7.7). Davies & McLean (1996) considered Th/U ratios lower than 3.8 diagnostic for marine bands whereas Adams & Weaver (1958), used by Hollywood & Whorlow (1993), thought a ratio lower than 2 representative for fully marine conditions. This figure again shows that the *Lingula* marine bands display the same order of U enrichments as the lacustrine bands whereas the Goniatite marine band is the only one clearly enriched.

7.6 Discussion

The data suggest that the *Lingula* marine bands have a low organic carbon content compared to the Goniatite marine band and the lacustrine bands. Pyrite contents are, however, clearly enriched in most *Lingula* bands which set them apart from the lacustrine bands. Trace element enrichment in the *Lingula* and lacustrine bands is low and often absent, in contrast to the Goniatite marine band investigated here and reported in literature (Bloxham & Thomas, 1969; Fisher & Wignall, 2001). Although it has to be realised that the enrichment factors in figure 7.6 are mean values and that individual samples sometimes have higher enrichment factors, the mean EFs for the *Lingula* marine bands are considered to be insignificant. They are comparable to the EFs obtained for the sediments overlying the marine bands. Moreover, in general EFs are far higher (3.5-200 times)

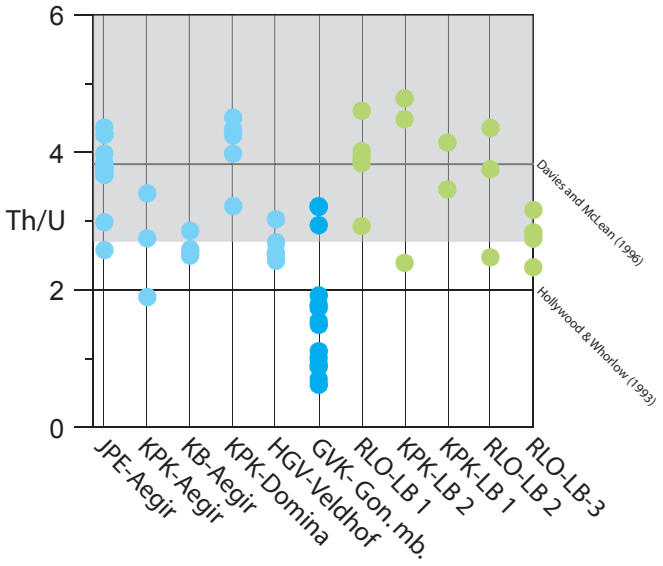

Figure 7.7 Th/U ratios for marine and lacustrine bands. The grey box indicates the area where the Th/U ratios plot derived from the sediments overlying the marine and lacustrine bands. It can be seen that only the Goniatite marine band (dark blue) clearly displays an enrichment in U. The *Lingula* marine (light blue) and lacustrine bands (green) display minor or no enrichment in U compared to the overlying sediments.

in marine bands/black shale reported in literature (Coveney et al., 1991; Fisher & Wignall, 2001, their table 1; Algeo & Maynard, 2004; Cruse & Lyons, 2004). Therefore, the *Lingula* marine bands can not be easily distinguished using the Th/U ratio alone. To effectively find marine bands on the basis of the Th/U ratios the ratio defined by Hollywood & Whorlow (1993) should be used. The ratio defined by Davies & McLean (1996) is not diagnostic because a lot of samples derived from floodplain sediments fall into the marine bands-field.

Based on the results obtained here and those reported in literature, i.e. the clear enrichment of U in Goniatite marine bands and the absence in *Lingula* marine bands, recognition of marine bands using the gamma-ray log is only promising when they are found in Goniatite facies. Since the *Lingula* marine bands mainly occur along the basin margins, in these areas recognition of marine bands using gamma-ray only would be complicated. Although our dataset is limited, it might be concluded that the southern part of the Netherlands and Belgium did not belong to the main depocentre during Westphalian B/C.

In addition, the following questions remain to be answered: (1) what determines the TOC in the *Lingula*/Goniatite marine bands and the lacustrine bands; (2) why such poor trace element EFs in the *Lingula* marine and (3) lacustrine bands; (4) why are the trace element EFs in the coals mostly higher than in the overlying marine/lacustrine bands and (5) are the EFs syn-sedimentary or diagenetic?

Ad 1) Ramsbottom (1969) observed that although the total succession (of, for instance the Westphalian A) thins towards the basin margins, the individual marine horizons are thicker when benthonic fossils are present (like the *Lingula* marine bands) than when they only contain goniatites. Therefore, the siliciclastic sedimentation rate in the goniatite bearing intervals is probably lower than in the *Lingula* marine bands. A relatively high siliciclastic sedimentation rate,

together with the absence of anoxic bottom water conditions (thus causing enhanced oxidation and dilution of organic matter) probably lead to lower TOC in the *Lingula* bands. A comparable situation was observed in Mediterranean sapropels, which tend to become thicker and therefore show "diluted" TOC towards the Nile delta (ten Haven et al., 1987). The higher TOC of the lacustrine bands probably has to be explained by a combination of a rather slow sedimentation rate plus a high influx of (non-degradable) organic matter.

Ad 2) Algeo & Maynard (2004) found that the trace elements U, Mo, V, Zn and Pb show strong enrichments under euxinic (>10 wt% TOC) circumstances, forming complexes with sulphides preferentially. During anoxic (TOC <10 wt%, non-sulphidic) conditions these TEs show a strong correlation with TOC, but the EF remain rather limited. In this light, the original TOC values of the Goniatite marine band (up to 10%) are in accordance with the higher trace element EFs. In the *Lingula* marine bands, TOC concentrations do not even exceed 5 wt%. This suggests that at the most, anoxic and no euxinic conditions prevailed during deposition of the marine bands, which forms an explanation for the small enrichment of trace elements in the sampled sections. The presence of *Lingulas* (brachiopods) already suggests that the oxygen concentration in the bottom waters is not too low to prevent these animals to live there. In addition, Bloxham & Thomas (1969) and Fisher & Wignall (2001) concluded that U is concentrated in the most organic rich parts of marine bands. Another explanation for the poor trace element enrichment may be a brief period of oxygenation which leads to the dissolution of scavenged elements Anderson et al. (1989).

Ad 3) Trace elements can also be enriched in organic-rich freshwater sediments (Elbaz-Poulichet et al., 1997; Fisher & Wignall, 2001). However, it has to be realised that the concentrations of U and Mo in fresh water are much lower than in seawater (Taylor & McLennan, 1985) which probably means that anoxic conditions have to be more prolonged than in marine anoxic environments. Although the TOC contents of the lacustrine bands are in general much higher than the *Lingula* marine bands, the strongly limited availability of these trace elements prevents a significant enrichment.

Ad 4) Mo and U show higher EFs in the coals located below two of the *Lingula* marine bands than observed in the coals below the lacustrine bands (Fig. 7.6). Although it does not apply to all coals below the *Lingula* marine bands, it is suggested here that the influence of percolating seawater may lead to enhanced enrichments of U and Mo in the underlying coal. An example of this phenomenon is the U peak in the coal located below the Aegir marine band in the well KPK-1. The same process is probably responsible for the enrichment of Mo in the RLO-LB-3 coal, which also showed marine influence through its high sulphur contents. This is in accordance with the study of Gayer et al. (1999) who also found higher U and Mo contents in marine influenced coal than in coal overlain by lacustrine deposits. However, independent of the composition of the overlying sediment, coal tends to act as traps for migrating trace elements (Laznicka, 1985). It is therefore suggested that the enrichment of Ni, Pb, Zn and Cu as observed in the coals is mainly due to diagenetic processes because there is no preferential enrichment of these metals for marine or lacustrine influenced coal (Fig. 7.6). Late diagenetic enrichment of these metals was also interpreted by Dill & Pöhlmann (2002) in their study on Carboniferous coals in the Ruhr Basin. Uranium can also be diagenetically enriched. Jedwab (1966) reported a late-diagenetic enrichment of uranium in coal intercalated in a sequence of lacustrine black shale whereas Davidson & Ponsford (1954) concluded that uranium enrichments in coal were caused by percolating meteoric waters. Nekrasova (1957) also concluded that the permeability and reducing conditions in Jurassic coal caused the diagenetic enrichment of U. The observation (in this study) that U mainly occurs in

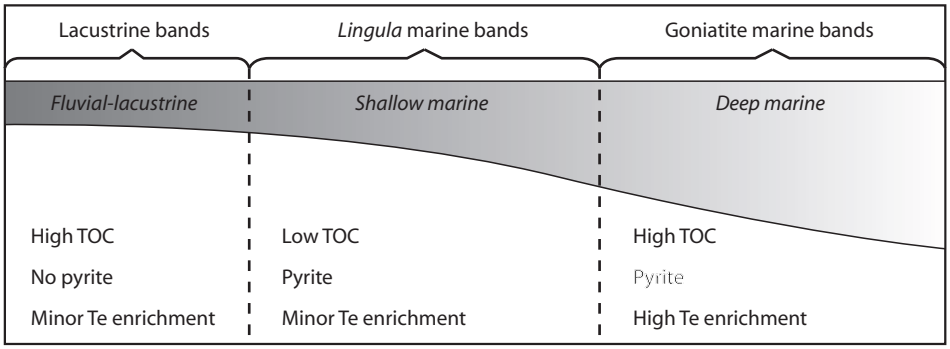

Figure 7.8 Schematic cross-section displaying the areal distribution and geochemical characteristics of the intervals studied in this chapter. TOC: total organic carbon; Te: trace elements.

coal that experienced marine influence, does not prove that this is the only way to get enrichment but rather the absence of other mechanisms or sources.

Ad 5) Most authors imply that enrichment of trace elements in marine bands/black shale took place syn-genetically by scavenging of trace elements by organic matter or Fe-sulphides (Bloxham & Thomas, 1969; Fisher & Wignall, 2001; Algeo & Maynard, 2004). However, Laznicka (1985) attributed enrichment of trace elements on top of coals (where marine bands are located) to late diagenetic processes. Realising that iron ore formation together with the associated enrichment in trace elements frequently took place above coal seams in the Carboniferous (Laznicka, 1985), this clearly leaves the possibility for a diagenetic enrichment of iron-sulfide and associated trace elements. Although the EFs in the lacustrine and *Lingula* marine bands are very low, such a process cannot be ruled out as the highest enrichments of the samples consequently takes place just on top of the coal seam.

7.7 Conclusions

Lingula and Goniatite marine bands can be distinguished in the Upper Carboniferous fluvio-lacustrine sedimentary sequence of the Netherlands and surrounding areas (Calver, 1969; Ramsbottom, 1969). *Lingula* bands formed in a nearshore environment whereas Goniatite marine bands are characterised by a deeper marine setting. The marine bands show a marked difference in enrichment of redox-sensitive trace elements such as U and Mo. The geochemical characteristics of both marine band types were analysed. Lacustrine bands were also investigated because these show the same sedimentological characteristics as the *Lingula* marine bands. These depositional environments show a typical set of geochemical characteristics (Fig. 7.8), which will be explained shortly below.

The Goniatite marine band displays high TOC (up to 10 wt%), sulphur and redox sensitive trace element contents. Therefore, Goniatite marine bands can typically be characterised as marine black shale. Condensed sedimentation under marine and anoxic bottom water conditions lead to the effective scavenging of redox-sensitive trace elements. An important difference between the Goniatite and *Lingula* marine bands is the much lower TOC contents in the latter (1-2 wt%). This is attributed to a relatively high siliciclastic sedimentation rate during marine flooding, leading to dilution. It is proposed that the absence of high TOC concentrations (and possibly the absence

of anoxic bottom water conditions) prevented the effective scavenging of trace elements during deposition of *Lingula* bands. Next to this explanation, a diagenetic process like the migration of an oxidation front or late-diagenetic enrichment cannot be ruled out. The lacustrine bands are characterised by high TOC contents but low sulphur and trace element concentrations. The high TOC contents can be explained by a combination of a slow siliciclastic sedimentation rate and a high influx of (non-degradable) organic matter. Enrichment of trace elements and sulphur in the lacustrine bands is absent or moderate. The limited availability of elements like S, U, Mo and V in fresh water is the most likely explanation.

Based on the results obtained during this study it is proposed that detection of marine bands with a gamma-ray device is only promising when they are developed in Goniatite facies. Along the margins of the basin, where marine bands occur in shallow marine *Lingula* facies, this method will probably fail.

CHAPTER 8

Synthesis

This thesis addresses several research questions related to Carboniferous geology in the Northwest European Carboniferous Basin (NWECB). Here, an attempt is made to integrate the most important conclusions.

An interesting result is the finding of Early Carboniferous carbonate platforms in the central part of the NWECB. Due to a lack of data, widely varying palaeogeographical reconstructions of this area were published so far (Bless et al., 1976; Ziegler, 1990; Bridges et al., 1995; Gerling et al., 1999; Collinson, 2005; Geluk et al., 2007; Korn, 2008; Van Hulten & Poty, 2008). For the first time, seismic data are presented which clearly show the outlines of carbonate platforms in the northern part of the Netherlands onshore and southern offshore. One of the platforms was found on the Groningen High below the northern part of the Groningen Gasfield. The other one, which is even greater, formed on the Friesland High. North of the island of Ameland the third platform was recognised in the M09 offshore block (Fig. 3.9A). Based on a comparison with the extensively studied Dinantian platforms in the UK (Gawthorpe et al., 1989; Gutteridge, 1989; Fraser & Gawthorpe, 1990; Gawthorpe & Gutteridge, 1990; Gutteridge, 1991), it is suggested that (ramp-type) carbonate sedimentation commenced in the basinal areas during the Tournaisian (e.g. the Lauwerszee Trough in between the Groningen and Friesland Highs). Ongoing subsidence led to the establishment of rimmed shelf carbonate platforms on the topographically elevated areas (horst blocks) during the Visean (Fig. 3.5). In the basinal areas, shallow carbonate sedimentation was replaced by a mixture of deep-water carbonate muds, calciturbidites and possibly some terrigenous input. In order to explain the observed basin configuration, a tilted fault block model for the study area is proposed, comparable to the model proposed for the UK (Fig. 3.5). These fault blocks probably resulted from Late Devonian/Early Carboniferous rifting (Fraser & Gawthorpe, 1990; Hollywood & Whorlow, 1993).

Due to a combination of factors (increased sediment supply, changing climate conditions or circulation patterns) carbonate production ceased at the Visean-Namurian transition (M. Aretz, pers. comm.). The presence of Early Namurian black shales over major areas (Bowland Formation in the UK, Geverik Formation in the Netherlands and Upper Alum Shales in Germany, see chapter 2), excludes an increase in sedimentation rate to account for this transition. In the Ashover area in northern England (Fig. 6.1), just north of the London Brabant Massif, black shale deposition took place from the Visean-Namurian transition up till the Marsdenian. During an 11 Myr's period, 120 m of sediment accumulated at the very low sedimentation rate of approximately 0.01 mm/yr. This succession has been extensively studied by Ramsbottom et al. (1962), who found a cyclic occurrence of fossil phases. He attributed these fossil alternations to changes in basin-water salinity. Amin (1979) and Spears & Amin (1981) arrived at the same conclusion based on geochemical investigations. Their hypothesis, which is also proposed by Collinson (1988), Holdsworth & Collinson (1988) and Martinsen et al. (1995), is that marine conditions might have periodically changed to lacustrine conditions. This model of changing salinities is questionable, based on two observations: (1) although the fossil phases might indicate salinity differences, clear evidence of freshwater fossils is lacking. It seems to be the absence of Goniatites in some units

that results in the interpretation of salinity changes; (2) the geochemical characterisation of marine and non-marine (Fish phase) sediments is partly based on two sets of samples displaying different geochemical behaviour (Spears & Amin, 1981). Namely, a significant number of Fish phase samples is derived from the top of the condensed section where the sediments tend to become coarser-grained and display lower total organic carbon (TOC) contents. It is proposed that basin-water salinity did not change dramatically throughout the Namurian. This is mainly based on the occurrence of significant trace element concentrations, normally enriched in marine black shales, in the majority of the analysed samples (Fig 6.6). Variations in trace element enrichment can be well explained by variations in total organic matter content. Whether organic matter has a direct control on trace element enrichments or not, this relationship has been described by numerous authors (Brumsack, 1986; Nijenhuis et al., 1999; Werne et al., 2002; Cruse & Lyons, 2004; Van der Weijden et al., 2006). There is no need to incorporate a change in basin-water salinities to explain the differences in geochemistry.

The very limited thickness of the Namurian section in the Ashover area probably forms an exception in the NWECB. In order to explain the very thick Namurian section (>2500 m, compacted) in, for instance, the northern part of the Netherlands, sedimentation rates must have been very high (Fig. 3.4). This led us to question which subsidence mechanisms have been responsible for the accumulation of these sediments. Based on modelling results, it is suggested that flexural subsidence, which took place along the southern margin of the NWECB, could not explain the tectonic subsidence in the northern part of the Netherlands (Fig. 4.6; Kombrink et al., 2008). As an alternative, numerous authors proposed a thermal sag phase following an Early Carboniferous rifting event (Coward, 1990; Bailey et al., 1993; Coward, 1993; Maynard et al., 1997; Martin et al., 2002; Hoffmann et al., 2005). The results described in chapter 3 indeed suggest that a Dinantian rifting event took place in the Netherlands. However, based on the modelling scenarios it is difficult to explain the expanded Namurian successions when only a thermal sagging phase for the Namurian is assumed (Fig. 4.7). Therefore, an additional extensional phase is proposed (next to Early Carboniferous stretching) during the Namurian in the central part of the NWECB. Namurian and even with a Westphalian A extrusives have been reported from the study area (Sissingh, 2004; Van Buggenum & den Hartog Jager, 2007). These observations fit a model of tectonic activity during the Namurian.

The interaction of flexural subsidence and rifting in the area further northwards creates an interesting problem. As a consequence of extensional movements, the continental crust is weakened, leading to a lowering of its elastic thickness. Since the width of foreland basins depend on the strength of the lithosphere, it may be likely that the Variscan foreland basin along the southern margin of the NWECB remained relatively narrow. Due to the northward progradation of the axis of the flexural foreland basin, it may be expected to find significant thickness changes. However, this contrasts the thickness distributions observed in the NWECB. Sperber (1993) mentions: "*The frequently quoted migration of the depocentre of the trough to the north during the Upper Carboniferous is in doubt because of the wide range of strata thickness from Namurian C to the Upper Westphalian C which do not form an identifiable trend. Extensive reconnaissance has confirmed the fact that the sedimentary environment was very uniform in time and space. It is worth considering why we find similar stratigraphic formations (referring to thickness, lithology, fauna and flora) again and again in similar forms in localities which are far apart.*" Coward (1993) states: "*There is no indication of depocentre or pinch-out migration as would be expected in an advancing foredeep.*" The incorporation of the dynamic topography-concept may account for these gradually changing thicknesses. This mechanism is proposed by numerous authors to explain long-wavelength (asymmetric) subsidence in a foreland

basin setting (Coakley & Gurnis, 1995; Pang & Nummedal, 1995; Pysklywec & Mitrovica, 2000; Liu & Nummedal, 2004). In these studies, flexural loading models could not adequately explain the observed subsidence patterns as their wavelength greatly exceeds the modelled ones (as is the case in the study area). Therefore, the addition of a dynamic component was proposed, following Gurnis (1992) who postulated that a mantle flow-induced dynamic topography could explain subsidence over such long wavelengths. Although the recognition of this mechanism is difficult in ancient settings (Burgess & Moresi, 1999), it may well explain the observed thickness differences in the NWECB (Fig. 4.3). A third factor which might have accounted for additional tectonic subsidence during the Namurian and Westphalian is compressional intra-plate stress, such as found in the North Sea during the Tertiary by Kooi et al. (1991).

During the Westphalian, near-emergent depositional conditions prevailed in the greatest part of the NWECB. Lower delta plain conditions dominated during the Early Westphalian, giving way to better drained conditions during the Late Westphalian. The Lower Westphalian fluvial sequence in particular is characterised by the occurrence of thin (up to several metres) mudstone horizons deposited under marine or brackish conditions (marine bands). These marine bands can be found in a proximal (*Lingula*, brachiopods) or a distal (Goniatite, ammonoids) facies, following Calver (1969). The majority of the marine bands known in the Netherlands are characterised by *Lingula* facies. Here, the question is to be answered whether there is a relationship between these *Lingula* marine bands and the frequently observed lack of gamma-ray peaks (no enrichment in uranium). Therefore, the total organic carbon (TOC), major- and trace elemental concentrations of a number of *Lingula* marine bands were investigated. These were compared with a Goniatite marine band and some mudstone horizons deposited under freshwater conditions (lacustrine bands, Fig. 7.1). Although the *Lingula* marine bands can mostly be distinguished from lacustrine beds by enhanced sulphur contents, the TOC and trace element enrichment is very poor compared to the investigated Goniatite marine band and the ones described in literature (Fig. 7.5; Bloxham & Thomas, 1969, Fisher & Wignall, 2001). It is suggested that the principal reason for low trace element enrichments in these *Lingula* marine bands is a relatively high siliciclastic sedimentation rate during transgressions, leading to dilution of TOC. This prohibits the effective scavenging of trace elements. Moreover, anoxic conditions were probably not as severe as during the deposition of the Goniatite marine bands regarding the fact that *Lingulas* are benthic organisms.

The question may be asked whether these *Lingula* marine bands can be correlated over great distances. Studies carried out in the mining areas have the highest potential to provide information on the lateral continuity of marine bands. In this respect, the classical report by Van Waterschoot van der Gracht (1918) provides valuable information. Here, it is described that research by particularly Belgian geologists led to the discovery a lot of Goniatite and *Lingula* marine bands and the transition between those. It became clear that these marine bands often have a *local* distribution. This means that the correlation of wells using marine bands should be performed with care.

The youngest rocks investigated in this thesis have a Westphalian C/D age. In this time interval, the most important Carboniferous reservoir sandstones were deposited in the Netherlands and surrounding areas. Chapter 5 presents a detailed study based on 12 wells drilled into the Coevorden Gasfield in the northeastern part of the Netherlands (Fig. 5.1). Next to the benefit of publishing detailed field-studies, these kinds of data also provide information of the direction of palaeoflow and the width/thickness distribution of Late Westphalian sandstones.

Due to inversion and lateral fault movements, the NWECB probably became fragmented into a number of sub basins during the Westphalian C and D (Besly, 1988, Fraser & Gawthorpe,

1990). In the northern part of the Netherlands, the Lauwerszee Trough and the Ems Graben probably acted as main discharge zones (Fig. 5.3). Based on palaeogeographical maps compiled for the Coevorden area (Fig. 5.9), a direction of palaeoflow to the north/northwest is proposed. This suggests that sandstones deposited in the Coevorden area might also occur in the Lauwerszee Trough.

References

Adams, J.A. & Weaver, C.E., 1958. Thorium-uranium ratios as indicators of sedimentary processes: example of concept of geochemical facies. *Bulletin American Association of Petroleum Geologists* **42**: 387-430.

Aitken, J.F., Quirk, D.G. & Guion, P.D., 1999. Regional correlation of Westphalian sandbodies onshore UK; implications for reservoirs in the southern North Sea. *In:* A.J. Fleet and S.A.R. Boldy (eds), Petroleum geology of Northwest Europe; proceedings of the 5th conference. The Geological Society (London) **5**: 747-756.

Algeo, T.J. & Maynard, J.B., 2004. Trace-element behaviour and redox facies in core shales of Upper Pennsylvanian Kansas-type cyclothems. *Chemical Geology* **206**: 289-318.

Algeo, T.J., Schwark, L. & Hower, J.C., 2004. High-resolution geochemistry and sequence stratigraphy of the Hushpuckney Shale (Swope Formation, eastern Kansas); implications for climato-environmental dynamics of the Late Pennsylvanian Midcontinent Seaway. *Chemical Geology* **206**: 259-288.

Amin, M.A., 1979. Geochemistry and Mineralogy of Namurian Sediments in the Pennine Basin, England. Unpublished PhD thesis, Sheffield University (Sheffield).

Amler, M.R.W. & Herbig, H.-G., 2006. Ostrand der Kohlenkalk-Plattform und Übergang in das Kulm-Becken im westlichsten Deutschland zwischen Aachen und Wuppertal. *In:* M.R.W. Amler and D. Stoppel (eds), Stratigraphie von Deutschland, VI – Unterkarbon (Mississippium). Schr.-R. Dt.Ges. Geowiss. (Hannover) **41**: 441-477.

Amler, M.R.W. & Stoppel, D., 2006. Stratigraphie von Deutschland, VI – Unterkarbon (Mississippium). Schriftenreihe der Deutschen Gesellschaft für Geowissenschaften (Hannover): **41**: 590 pp.

Anderson, R.F., LeHuray, A.P., Fleisher, M.Q. & Murray, J.W., 1989. Uranium deposition in Saanich Inlet sediments, Vancouver Island. *Geochimica et Cosmochimica Acta* **53**: 2205-2213.

Aplin, A.C. & Macquaker, J.H.S., 1993. C-S-Fe geochemistry of some modern and ancient anoxic marine muds and mudstones. *Philosophical Transactions Royal Society of London, Physical Sciences and Engineering* **344**: 89-100.

Archard, G. & Trice, R., 1990. A preliminary investigation into the spectral radiation of the Upper Carboniferous marine bands and its stratigraphic application. *Newsletters on Stratigraphy* **21**: 167-173.

Aretz, M. & Chevalier, E., 2007. After the collapse of stromatoporid-coral reefs – the Famennian and Dinantian reefs of Belgium: much more than Waulsortian mounds. *In:* J.J. Álvaro, M. Aretz, F. Boulvain, A. Munnecke, D. Vachard and E. Vennin (eds), Palaeozoic Reefs and Bioaccumulations: Climatic and Evolutionary Controls. Geological Society Special Publication (London) **275**: 163-188.

Arthur, M.A. & Sageman, B.B., 1994. Marine Black Shales: Depositional mechanisms and environments of ancient deposits. *Annual Review of Earth and Planetary Science* **22**: 499-551.

Atkinson, C.D., Verwest, B., Baker, G. & O Mara, P., 2001. Direct gas detection in the Rotliegendes sandstone; a potential new opportunity for exploration in the UK Southern gas basin. American Association of Petroleum Geologists 2001 annual meeting.

Bailey, J.B., Arbin, P., Daffinoti, O., Gibson, P. & Ritchie, J.S., 1993. Permo-Carboniferous plays of the Silver Pit Basin. *In:* J.R. Parker (ed.), Petroleum geology of Northwest Europe; Proceedings of the 4th conference. The Geological Society (London) **4**: 707-715.

Banka, D., Pharaoh, T.C., Williamson, J.P., Lee, M.K., Thybo, H. & Wybraniec, S., 2002. Potential field imaging of Palaeozoic orogenic structure in Northern and Central Europe. *Tectonophysics* **360**: 23-45.

Beijer, H. & Fermont, W.J.J., 1987. The Geological Bureau for the mining district, the Geological Foundation and the Geological Survey of the Netherlands. *In:* W.A. Visser, J.I.S. Zonneveld and A.J. van Loon (eds), Seventy-five years of geology and mining in the Netherlands. KNGMG (The Hague): 51-62.

Belka, Z., Skompski, S. & Sobon Podgorska, J., 1996. Reconstruction of a lost carbonate platform on the shelf of Fennosarmatia; evidence from Visean polymictic debrites, Holy Cross Mountains, Poland. *In:* P. Strogen, I.D. Somerville and G.L. Jones (eds), Recent advances in Lower Carboniferous geology. Geological Society Special Publications (London) **107**: 315-329.

Bellingham, P. & White, N., 2000. A general inverse method for modelling extensional sedimentary basins. *Basin Research* **12**: 219-226.

Belt, E.S., Martino, R.L., Lentz, L.J., Lyons, T.W. & Heckel, P.H., 2006. Proximal facies of the upper Freeport and associated cyclothems in the vicinity of the Allegheny Front, northern Appalachian Basin. 40th annual meeting Geological Society of America.

Bénard, F. & Bouché, P., 1991. Aspects of the petroleum geology of the Variscan foreland of Western Europe. *In:* A.M. Spencer (ed.), Generation, accumulation, and production of Europe's hydrocarbons. Special Publication of the European Association of Petroleum Geoscientists **1**: 119-137.

Berner, R.A., 1977. Sulfate reduction and the rate of deposition of marine sediments. *Earth and Planetary Science Letters* **37**: 492-498.

Berner, R.A. & Raiswell, R., 1984. C/S method for distinguishing freshwater from marine sedimentary rocks. *Geology* **12**: 365-368.

Bertelsen, F., 1972. A Lower Carboniferous microflora from the Ørslev No. 1 borehole, island of Falster, Denmark. Danm. Geol. Und. (II) **99**: 78 pp.

Besly, B.M., 1998. Carboniferous. *In:* K.W. Glennie (ed.), Petroleum Geology of the North Sea, basic concepts and recent advances. Blackwell (Oxford): 104-136.

Besly, B.M., 2005. Late Carboniferous redbeds of the UK southern North Sea, viewed in a regional context. *In:* J.D. Collinson, D.J. Evans, D.W. Holliday and N.S. Jones (eds), Carboniferous hydrocarbon geology: southern North Sea and surrounding onshore areas. Yorkshire Geological Society Occasional Publication **7**: 225-226.

Besly, B.M., 1988. Palaeogeographic implications of Late Westphalian to Early Permian red-beds, central England. *In:* B.M. Besly and G. Kelling (eds), Sedimentation in a synorogenic basin complex: the Carboniferous of northwest Europe. Blackie (Glasgow): 200-221.

Besly, B.M., Burley, S.D. & Turner, P., 1993. The Late Carboniferous "barren red bed" play of the Silver Pit area, southern North Sea. *In:* J.R. Parker (ed.), Petroleum Geology of Northwest Europe: Proceedings of the 4th conference. The Geological Society (London) **4**: 727-740.

Besly, B.M. & Fielding, C.R., 1989. Palaeosols in Westphalian coal-bearing and red-bed sequences, central and northern England. *Palaeogeography, Palaeoclimatology, Palaeoecology* **70**: 303-330.

Bless, M.J.M., Bouckaert, J., Bouzet, P., Conil, R., Cornet, P., Fairon-Demaret, M., Groessens, E., Longerstaey, P., Meesen, J.P.M.T., Paproth, E., Pirlet, H., Streel, M., Amerom, H.W.J. & Wolf, M., 1976. Dinantian rocks in the subsurface north of the Brabant and Ardenno-Rhenish massifs in Belgium, the Netherlands and the Federal Republic of Germany. *Mededelingen Rijks Geologische Dienst, nieuwe serie* **27**: 81-195.

Bless, M.J.M., Bouckaert, J., Conil, R., Groessens, E., Kasig, W., Paproth, E., Poty, E., van Steenwinkel, M., Streel, M. & Walter, R., 1980. Pre-Permian depositional environments around the Brabant Massif in Belgium, the Netherlands and Germany. *Sedimentary Geology* **27**: 1-81.

Bless, M.J.M., Bouckaert, J. & Paproth, E., 1983. Recent exploration in pre-Permian rocks around the Brabant Massif in Belgium, the Netherlands and the Federal Republic of Germany. *Geologie en Mijnbouw* **62**: 51-62.

Bloxham, T.W. & Thomas, R.L., 1969. Palaeontological and geochemical facies in the Gastrioceras subcrenatum marine-band and associated rocks from North Crop of the South Wales Coalfield. *Quaterly Journal of Geological Society, London* **124**: 239-281.

Bojkowski, K. & Dembowski, Z., 1988. Paleogeografia karbonu Lubelskiego Zagłębia Węglowego na tle paleogeografii karbonu Polski. *Pr. Inst. Geol.* **122**: 18-26.

Bond, G.C. & Kominz, M.A., 1984. Construction of tectonic subsidence curves for the early Paleozoic miogeocline, southern Canadian Rocky Mountains: implications for subsidence mechanisms, age of breakup, and crustal thinning. *Geological Society of America Bulletin* **95**: 155-173.

Bouckaert, J., 1967. Namurian transgression in Belgium. *Annales de la Societe Geologique de Pologne* **37**: 145-150.

Bouroz, A., 1963. Presence d'un niveau kaolinique dans le namurien marin de Picardie. *Annales de la Societe Geologique du Nord* **83**: 281-286.

Braun, J., 1992. Postextensional mantle healing and episodic extension in the Canning Basin. *Journal of Geophysical Research* **97**: 8927-8936.

Bridge, J.S., 1993. The interaction between channel geometry, water flow, sediment transport and deposition in braided rivers. *In:* J.L. Best and C.S. Bristow (eds), Braided Rivers. Geological Society Special Publication (London) **75**: 13-72.

Bridge, J.S., 1984. Large-scale facies sequences in alluvial overbank environments. *Journal of Sedimentary Petrology* **54**: 583-588.

Bridge, J.S., 2003. Rivers and floodplains. Blackwells (Oxford): 491 pp.

Bridge, J.S. & Mackey, S.D., 1993b. A theoretical study of fluvial sandstone body dimensions. *In:* S.S. Flint and I.D. Bryant (eds), Geological modeling of hydrocarbon reservoirs. International Association of Sedimentologists Special Publication **15**: 213-236.

Bridge, J.S. & Tye, R.S., 2000. Interpreting the dimensions of ancient fluvial channel bars, channels, and channel belts from wireline-logs and cores. *Bulletin American Association of Petroleum Geologists* **84**: 1205-1228.

Bridges, P.H., Gutteridges, P. & Pickard, N.A.H., 1995. The environmental setting of Early Carboniferous mud-mounds. *In:* C.L.V. Monty, D.W.J. Bosence, P.H. Bridges and B.R. Pratt (eds), Carbonate mud-mounds; their origin and evolution. Special Publication of the International Association of Sedimentologists **23**: 171-190.

Bristow, C.S., Skelly, R.L. & Ethridge, F.G., 1999. Crevasse splays from the rapidly aggrading, sand-bed, braided Niobrara River, Nebraska: effect of base-level rise. *Sedimentology* **46**: 1029-1047.

Bruce, D. & Stemmerik, L., 2003. Carboniferous. *In:* D. Evans, G. Colin, A. Armour and P. Bathurst (eds), The Millennium Atlas; petroleum geology of the central and northern North Sea. Geological Society (London): 83-89.

Brumsack, H.J., 1986. The inorganic geochemistry of Cretaceous black shales (DSDP Leg 41) in comparison to modern upwelling sediments from the Gulf of California. *In:* C.P. Summerhayes and N.J. Shackleton (eds), North Atlantic palaeoceanography. Geological Society Special Publication (London) **21**: 447-462.

Brumsack, H.J., 2006. The trace metal content of recent organic carbon-rich sediments; implications for Cretaceous black shale formation. *Palaeogeography, Palaeoclimatology, Palaeoecology* **232**: 344-361.

Buchholz, P., Obert, C., Trapp, E., Wachendorf, H. & Zellmer, H., 2006. Westharz. *In:* M.R.W. Amler and D. Stoppel (eds), Stratigraphie von Deutschland, VI – Unterkarbon (Mississippium). Schr. R. Dt. Ges. Geowiss. (Hannover) **41**: 387-413.

Buła, Z., Jawor, E. & Baran, U., 2004. Pozycja geotektoniczna utworów karbonu w południowej części bloku górnośląskiego i małopolskiego. *In:* M. Kotarba (ed.), Możliwości generowania węglowodorów w skałach karbonu w południowej części bloku górnośląskiego i małopolskiego. Wyd Nauk. Akapit (Kraków): 9-14.

Burgess, P.M. & Gayer, R.A., 2000. Late Carboniferous tectonic subsidence in South Wales; implications for Variscan basin evolution and tectonic history in SW Britain. *Journal of the Geological Society of London* **157**: 93-104.

Burgess, P.M., Gurnis, M. & Moresi, L.N., 1997. Formation of sequences in the cratonic interior of North America by interaction between mantle, eustatic, and stratigraphic processes. *Geological Society of America Bulletin* **109**: 1515-1535.

Burgess, P.M. & Moresi, L.N., 1999. Modelling rates and distribution of subsidence due to dynamic topography over subducting slabs; is it possible to identify dynamic topography from ancient strata? *Basin Research* **11**: 305-314.

Calver, M.A., 1969. Westphalian of Britain. *Compte Rendu Congres International de Stratigraphie et de Geologie du Carbonifere* **1**: 233-254.

Calvert, S.E. & Pedersen, T.F., 1993. Geochemistry of recent oxic and anoxic marine sediments; implications for the geological record. *Marine Geology* **113**: 67-88.

Calvert, S.E., Pedersen, T.F. & Karlin, R.E., 2001. Geochemical and isotopic evidence for post-glacial palaeoceanographic changes in Saanich Inlet, British Columbia. *Marine Geology* **174**: 287-305.

Cameron, N. & Ziegler, T., 1997. Probing the lower limits of a fairway: further pre-Permian potential in the southern North Sea. *In:* K. Ziegler, P. Turner and S.R. Daines (eds), Petroleum Geology of the Southern North Sea: Future Potential. Geological Society Special Publication (London) **123**: 123-141.

Cameron, T.D.J., 1993. Carboniferous and Devonian of the Southern North Sea. *In:* R.W.O.B. Knox and W.G. Cordey (eds), Lithostratigraphic nomenclature of the UK North Sea, part 5. British Geological Survey (Nottingham): 1-93.

Canfield, D.E., 1994. Factors influencing organic carbon preservation in marine sediments. *Chemical Geology* **114**: 315-329.

Caputo, M.V. & Crowell, J.C., 1985. Migration of glacial centers across Gondwana during Paleozoic Era. *Geological Society of America Bulletin* **96**: 1020-1036.

Cebulak, S., 1988. Zarys geologii podłoża karbonu. *In:* Z. Dembowski and J. Porzycki (eds), Karbon Lubelskiego Zagłębia Węglowego. Prace Instytutu Geologicznego **122**: 31-34.

Chadwick, R.A. & Evans, D.J., 2005. A seismic atlas of southern Brittain – images of subsurface structure. British Geological Survey Occasional Publication 7 (Keyworth): 193 pp.

Chapple, W.M., 1978. Mechanics of thin-skinned fold-and-thrust belts. *Geological Society of America Bulletin* **89**: 1189-1198.

Chou, C.L., 1984. Relationship between geochemistry of coal and the nature of strata overlying the Herin Coal in the Illinois Basin, USA. *Memoir of the Geological Society of China* **6**: 269-280.

Clayton, G., Colthurst, J.R.J., Higgs, K., Jones, G.L.L. & Keegan, J.B., 1977. Tournaisian miospores and conodonts from County Kilkenny. *Bulletin Geological Survey of Ireland* **2**: 99-106.

Cloetingh, S., Spadini, G., Van Wees, J.-D. & Beekman, F., 2003. Thermo-mechanical modelling of Black Sea Basin (de)formation. *Sedimentary Geology* **156**: 169-184.

Coakley, B. & Gurnis, M., 1995. Far-field tilting of Laurentia during the Ordovician and constraints on the evolution of a slab under an ancient continent. *Journal of Geophysical Research* **100**: 6313-6327.

Cocks, L.R.M. & Fortey, R.A., 1982. Faunal evidence for oceanic separations in the Palaeozoic of Britain. *Journal of the Geological Society of London* **139**: 465-478.

Cocks, L.R.M. & Torsvik, T.H., 2005. Baltica from the late Precambrian to mid-Palaeozoic times: The gain and loss of a terrane's identity. *Earth-Science Reviews* **72**: 39-66.

Cojan, L., 1999. Carbonate-rich palaeosols in the Late Cretaceous-Early Palaeogene series of the Provence Basin (France). *In:* M. Thiry and R. Simon-Coicon (eds), Palaeoweathering, Palaeosurfaces and related Continental Deposits. International Association of Sedimentologists Special Publication **27**: 323-335.

Coleman, J.M. & Gagliano, S.M., 1964. Sedimentary structures: Mississippi River deltaic plain. *In:* G.V. Middleton (ed.), Primary sedimentary structures and their hydrodynamic interpretation. Society for Sedimentary Geology (SEPM) Special Publication **12**: 133-148.

Coleman, J.M. & Prior, D.B., 1982. Deltaic environments. *In:* P.A. Scholle and D. Spearing (eds), Sandstone Depositional Environments. American Association of Petroleum Geologists (Tulsa): 139-178.

Collinson, J.D., 1988. Controls on Namurian sedimentation in the Central Province basins of northern England. *In:* B.M. Besly and G. Kelling (eds), Sedimentation in a synorogenic basin complex; the Upper Carboniferous of Northwest Europe. Blackie (Glasgow): 85-101.

Collinson, J.D., 2005. Dinantian and Namurian depositional systems in the southern North Sea. *In:* J.D. Collinson, D. Evans, D. Holliday and N. Jones (eds), Carboniferous hydrocarbon geology: the southern North Sea and surrounding onshore areas. Yorkshire Geological Society Occasional Publication **7**: 35-56.

Colpaert, A., Pickard, N., Mienert, J., Henriksen, L.B., Rafaelsen, B. & Andreassen, K., 2007. 3D seismic analysis of an Upper Palaeozoic carbonate succession of the Eastern Finnmark Platform area, Norwegian Barents Sea. *Sedimentary Geology* **197**: 79-98.

Conway, A.M. & Valvatne, C., 2003. The Boulton Field, Block 44/21a, UK North Sea. *In:* J. Gluyas and H.M. Hichens (eds), United Kingdom Oil and Gas Fields, Commemorative Millennium Volume. Geological Society Memoir (London) **20**: 671-680.

Cook, H.E., Zhemchuzhnikov, V.G., Zempolich, W.G., Zhaimina, V.Y., Buvtyshkin, V.M., Kotova, E.A., Golub, L.Y., Zorin, A.Y., Lehmann, P.J., Alexeiev, D.V., Giovannelli, A., Viaggi, M., Fretwell, N., LaPointe, P.A. & Corboy, J.J., 2002. Devonian and Carboniferous carbonate platform facies in the Bolshoi Karatau, southern Kazakhstan; outcrop analogs for coeval carbonate oil and gas fields in the North Caspian Basin, western Kazakhstan. *In:* W.G.

Zempolich and H.E. Cook (eds), Paleozoic carbonates of the Commonwealth of Independent States (CIS); subsurface reservoirs and outcrop analogs. Special Publication Society for Sedimentary Geology (Tulsa) **74**: 81-122.

Corfield, S.M., Gawthorpe, R.L., Gage, M., Fraser, A.J. & Besly, B.M., 1996. Inversion tectonics of the Variscan foreland of the British Isles. *Journal of the Geological Society of London* **153**: 17-32.

Coveney, R.M., Jr., Watney, W.L. & Maples, C.G., 1991. Contrasting depositional models for Pennsylvanian black shale discerned from molybdenum abundances. *Geology* **19**: 147-150.

Coward, M.P., 1993. The effect of late Caledonian and Variscan continental escape tectonics on basement structure, Paleozoic basin kinematics and subsequent Mesozoic basin development in NW Europe. *In:* J.R. Parker (ed.), Petroleum geology of Northwest Europe; Proceedings of the 4th conference. The Geological Society (London) **4**: 1095-1108.

Coward, M.P., 1990. The Precambrian, Caledonian and Variscan framework to NW Europe. *In:* R.F.P. Hardman and J. Brooks (eds), Proceedings of Tectonic events responsible for Britain's oil and gas reserves. Geological Society Special Publication (London) **55**: 1-34.

Crowley, T.J. & Baum, S.K., 1991. Estimating Carboniferous sea-level fluctuations from Gondwanan ice extent. *Geology (Boulder)* **19**: 975-977.

Cruse, A.M. & Lyons, T.W., 2004. Trace metal records of regional paleoenvironmental variability in Pennsylvanian (Upper Carboniferous) black shales. *Chemical Geology* **206**: 319-345.

Crusius, J., Calvert, S.E., Pedersen, T. & Sage, D., 1996. Rhenium and molybdenum enrichments in sediments as indicators of oxic, suboxic and sulfidic conditions of deposition. *Earth and Planetary Science Letters* **145**: 65-78.

David, F., 1987. Sandkörper in fluviatilen Sandsteinen des Unteren Westfal D (Oberkarbon) am Piesberg bei Osnabrück. *Facies* **17**: 51-58.

David, F., 1990. Sedimentologie und Beckenanalyse im Westfal C und D des nordwestdeutschen Beckens. Deutsche Wissenschaftliche Gesellschaft für Erdöl, Erdgas und Kohle (DGMK) Berichte: **384-3**.

Davidson, C.F. & Ponsford, D.R.A., 1954. On the occurrence of uranium in coals. *Mining Magazine* **91**: 265-273.

Davies, S., Hampson, G., Flint, S.S. & Elliott, T., 1999. Continental-scale sequence stratigraphy of the Namurian, Upper Carboniferous and its applications to reservoir prediction. *In:* A.J. Fleet and S.A.R. Boldy (eds), Petroleum geology of Northwest Europe; Proceedings of the 5th conference. The Geological Society (London) **5**: 757-770.

Davies, S.J. & McLean, D., 1996. Spectral gamma-ray and palynological characterization of Kinderscoutian marine bands in the Namurian of the Pennine Basin. *Proceedings of the Yorkshire Geological Society* **51**: 103-114.

De Jager, J., 2007. Geological development. *In:* T.E. Wong, D.A.J. Batjes and J. de Jager (eds), Geology of the Netherlands. Royal Netherlands Academy of Arts and Sciences (Amsterdam): 5-26.

De Vos, W., 1997. Influence of the granitic batholith of Flanders on Acadian and later deformation (Brabant Massif, Belgium). *Aardkundige Mededelingen* **8**: 49-52.

Dean, W.E. & Arthur, M.A., 1989. Iron-sulfur-carbon relationships in organic-carbon-rich sequences; I, Cretaceous Western Interior Seaway. *American Journal of Science* **289**: 708-743.

DeCelles, P.G. & Giles, K.A., 1996. Foreland basin systems. *Basin Research* **8**: 105-123.

Della Porta, G., Kenter, J.A.M. & Bahamonde, J.R., 2004. Depositional facies and stratal geometry of an Upper Carboniferous prograding and aggrading high-relief carbonate platform (Cantabrian Mountains, N. Spain). *Sedimentology* **51**: 267-295.

Dellwig, O., 1999. Geochemistry of Holocene coastal deposits (NW Germany): Palaeoenvironmental reconstruction. PhD thesis, Carl von Ossietzky Universität (Oldenburg): 297 pp.

Delmer, A., Dusar, M. & Delcambre, B., 2001. Upper Carboniferous lithostratigraphic units (Belgium). *Geologica Belgica* **4**: 95-103.

Den Hartog Jager, D.G., Boekelman, W. & Mijnlieff, H.F., 1993. Regional geology of the Carboniferous in the NE Netherlands. Nederlandse Aardolie Maatschappij (NAM) 24929.

Diessel, C.F.K., 1992. Coal-bearing depositional systems. Springer-Verlag (Berlin): 721 pp.

Dill, H.G. & Pöhlmann, H., 2002. Chemical composition and mineral matter of paralic and limnic coal types of lignite through anthracite rank (Germany). Carboniferous and Permian of the world; XIV ICCP *Memoir Canadian Society of Petroleum Geologists* **19**: 851-867.

Dodd, J.R., 1963. Paleoecological implications of shell mineralogy in two pelecypod species. *Journal of Geology* **71**: 1-11.

Donato, J.A., Martindale, W. & Tully, M.C., 1983. Granites within the Mid North Sea High. *Journal of the Geological Society of London* **140**: 825-837.

Donato, J.A. & Megson, J., 1990. A buried granite batholith beneath the East Midlands Shelf of the Southern North Sea Basin. *Journal of the Geological Society of London* **147**: 133-140.

Dreesen, R., Bouckaert, J., Dusar, M., Soille, P. & Vandenberghe, N., 1987. Subsurface structural analysis of the late-Dinantian carbonate shelf at the northern flank of the Brabant Massif (Campine Basin, N-Belgium). *Mémoires Explicatives des Cartes Géologiques et Minières de Belgique (Memoirs of the Geological Survey of Belgium)* **21**: 1-37.

Drozdzewski, G., 1993. The Ruhr coal basin (Germany); structural evolution of an autochthonous foreland basin. *International Journal of Coal Geology* **23**: 231-250.

Drozdzewski, G., 1985. Tiefentectonik der Ibbenbürener Karbon-Scholle. *In:* G. Drozdzewski, H. Engel, R. Wolf and V. Wrede (eds), Beiträge zur Tiefentektonik westdeutscher Steinkohlenlagerstätten. Geol. L.-Amt Nordrh.-Westf. (Krefeld): 189-216.

Drozdzewski, G., 2005. Zur sedimentären Entwicklung des Subvariscikums im Namurium und Westfalium Nordwestdeutschlands. *In:* V. Wrede (ed.), Stratigraphie von Deutschland V – Das Oberkarbon (Pennsylvanium) in Deutschland. Cour. Forsch.-Inst. Senckenberg (Frankfurt a. M.) **254**: 151-203.

Drozdzewski, G., Henscheid, S., Hoth, P., Juch, D., Littke, R., Vieth, A. & Wrede, V., 2008. The evolution of the Carboniferous of NW Germany – based on a new map of the pre-Permian. *Zeitschrift der Deutschen Gesellschaft für Geowissenschaften.* Submitted.

Drozdzewski, G. & Wrede, V., 1994. Faltung und Bruchtektonik – Analyse der Tektonik im Subvariscikum. *Fortschritte in der Geologie von Rheinland und Westfalen (Krefeld)* **38**: 7-187.

Dusar, M., 2006. Namurian. *Geologica Belgica* **9**: 163-175.

Dusar, M., Paproth, E., Streel, M. & Bless Martin, J.M., 2000. Palaeogeographic and palaeoenvironmental characteristics of major marine incursions in northwestern Europe during the Westphalian C (Bolsovian). *Geologica Belgica* **3**: 331-347.

Eder, F.W., Engel, W., Franke, W. & Sadler, P.M., 1983. Devonian and Carboniferous limestone-turbidites of the Rheinisches Schiefergebirge and their tectonic significance *In:* H. Martin and F.W. Eder (eds), Intracontinental Fold Belts. Springer (Berlin): 93-124.

Elbaz-Poulichet, F., Nagy, A. & Cserny, T., 1997. The Distribution of Redox Sensitive Elements (U, As, Sb, V and Mo) along a River-Wetland-Lake System (Balaton Region, Hungary). *Aquatic Geochemistry* **3**: 267-282.

Elvebakk, G., Hunt, D.W. & Stemmerik, L., 2002. From isolated buildups to buildup mosaics; 3D seismic sheds new light on upper Carboniferous-Permian fault controlled carbonate buildups, Norwegian Barents Sea. *Sedimentary Geology* **152**: 7-17.

Erickson, B.E. & Helz, G.R., 2000. Molybdenum(VI) speciation in sulfidic waters; stability and lability of thiomolybdates. *Geochimica et Cosmochimica Acta* **64**: 1149-1158.

Evans, D.J. & Kirby, G.A., 1999. The architecture of concealed Dinantian carbonate sequences over the Central Lancashire and Holme highs, northern England. *Proceedings of the Yorkshire Geological Society* **52**: 297-312.

Falcon, N.L. & Kent, P.E., 1960. Geological results of petroleum exploration in Britain 1945-57. Memoir of the Geological Society of London **2**: 56 pp.

Felder, W.M., 1981. Geschiedenis van de geologische kartering in Zuid-Limburg. *Grondboor en Hamer* **3**: 65-81.

Fischer, K.D., Jahr, T. & Jentzsch, G., 2004. Evolution of the Variscan foreland-basin; modelling the interactions between tectonics and surface processes.; 3-D motions of the Earth surface; from measurements to physical modelling. *Physics and Chemistry of the Earth* **29**: 665-671.

Fisher, Q.J. & Wignall, P.B., 2001. Palaeoenvironmental controls on the uranium distribution in an Upper Carboniferous black shale (Gastrioceras listeri Marine Band) and associated strata; England. *Chemical Geology* **175**: 605-621.

Francis, B.P., Weber, L.J., Bachtel, S., Harris, P.M., Fischer, D. & Kenter, J.A.M., 2004. Prediction and mapping of deep-water slope carbonate reservoirs using seismic data, Tengiz Field, western Kazakhstan. *Annual Meeting AAPG Expanded Abstracts* **13**: 47.

Frank, F., Zinkernagel, U. & Füchtbauer, H., 1992. Zur Liefergebietsfrage der Sandsteine des Nordwestdeutschen Oberkarbons. Deutsche Wissenschaftliche Gesellschaft für Erdöl, Erdgas und Kohle (DGMK) Berichte **384-8**: 167 pp.

Franke, W., 2000. The mid-European segment of the Variscides; tectonostratigraphic units, terrane boundaries and plate tectonic evolution. *In:* W. Franke, V. Haak, O. Oncken and D. Tanner (eds), Orogenic processes; quantification and modelling in the Variscan Belt. Geological Society Special Publication (London) **179**: 35-61.

Franke, W., 1989. Tectonostratigraphic units in the Variscan Belt of Central Europe. *In:* R.D. Dallmeyer (ed.), Terranes in the Circum-Atlantic Paleozoic orogens. Geological Society of America (Boulder) **230**: 67-90.

Fraser, A.J. & Gawthorpe, R.L., 1990. Tectono-stratigraphic development and hydrocarbon habitat of the Carboniferous in northern England. *In:* R.F.P. Hardman and J. Brooks (eds), Tectonic events responsible for Britain's oil and gas reserves. Geological Society Special Publication (London) **55**: 49-86.

Fraser, A.J., Nash, D.F., Steele, R.P. & Ebdon, C.C., 1990. A regional assessment of the intra-Carboniferous play of northern England. *In:* J. Brooks (ed.), Classic Petroleum Provinces. Geological Society Special Publication (London) **55**: 417-440.

Gawthorpe, R.L. & Gutteridge, P., 1990. Geometry and evolution of platform-margin bioclastic shoals, late Dinantian (Mississippian), Derbyshire, UK. *In:* M.E. Tucker, J.L. Wilson, P.D. Crevello, J.R. Sarg and J.F. Read (eds), Carbonate platforms; facies, sequences and evolution. Special Publication of the International Association of Sedimentologists (Oxford) **9**: 39-54.

Gawthorpe, R.L., Gutteridge, P. & Leeder, M.R., 1989. Late Devonian and Dinantian basin evolution in northern England and North Wales. *In:* R.S. Arthurton, P. Gutteridge and S.C. Nolan (eds), The role of tectonics in Devonian and Carboniferous sedimentation in the British Isles. Occasional Publication Yorkshire Geological Society **6**: 1-23.

Gayer, R.A., Cole, J.E., Greiling, R.O., Hecht, C. & Jones, J.A., 1993. Comparative evolution of coal bearing foreland basins along the Variscan Northern margin in Europe. *In:* R.A. Gayer, R.O. Greiling and A.K. Vogel (eds), Rhenohercynian and subvariscan foldbelts. International Monograph series (Wiesbaden): 47-82.

Gayer, R.A., Rose, M., Dehmer, J. & Shao, L.Y., 1999. Impact of sulphur and trace element geochemistry on the utilization of a marine-influenced coal; case study from the South Wales Variscan foreland basin. *International Journal of Coal Geology* **40**: 151-174.

Geluk, M., de Haan, H., Schroot, B., Wolters, B. & Nio, S. D., 2002. The Permo-Carboniferous gas play, Cleaver Bank high area, southern North Sea, the Netherlands.; Carboniferous and Permian of the world; XIV ICCP proceedings. *Memoir Canadian Society of Petroleum Geologists* **19**: 877-894.

Geluk, M.C., Dusar, M. & de Vos, W., 2007. Pre-Silesian. *In:* T.E. Wong, D.A.J. Batjes and J. De Jager (eds), Geology of the Netherlands. Royal Netherlands Academy of Arts and Sciences (Amsterdam): 27-42.

George, T.N., Johnson, G.A.L., Mitchell, M., Prentice, J.E., Ramsbottom, W.H.C., Sevastopulo, G.D. & Wilson, R.B., 1976. A correlation of Dinantian rocks in the British Isles. Geological Society Special Publication (London): **7**: 87 pp.

Gerling, P., Geluk, M.C., Kockel, F., Lokhorst, A., Lott, G.K. & Nicholson, R.A., 1999. NW European Gas Atlas – new inplications for the Carboniferous gas plays in the western part of the Southern Permian Basin. *In:* A.J. Fleet and S.A.R. Boldy (eds), Petroleum Geology of Northwest Europe: Proceedings of the 5th Conference. The Geological Society (London): 799-808.

Goldberg, K. & Humayun, M., 2001. Environmental controls on the deposition of organic-rich rocks; the Permian Irati oil shales. Annual meeting Geological Society of America 2001.

Goodarzi, F. & Swaine, D.J., 1993. Chalcophile elements in Western Canadian coals. *International Journal of Coal Geology* **24**: 281-292.

Gradstein, F.M., Ogg, J.G. & Smith, A.G., 2004. A Geologic Time Scale 2004. Cambridge University Press (Cambridge): 589 pp.

Grayson, R.F. & Oldham, L., 1987. A new structural framework for the Northern British Dinantian as a basis for oil, gas and mineral exploration. *In:* J. Miller, A.E. Adams and V.P. Wright (eds), European Dinantian Environments. John Wiley & Sons (Chichester): 33-59.

Gurnis, M., 1992. Rapid continental subsidence following the initiation and evolution of subduction. *Science* **255**: 1556-1558.

Gursky, H., 2006. Paläogeographie, Paloozeanographie und Fazies. *In:* M.R.W. Amler and D. Stoppel (eds), Stratigraphie von Deutschland, VI – Unterkarbon (Mississippium). Schr. R. Dt. Ges. Geowiss. (Hannover) **41**: 51-68.

Gutteridge, P., 1991. Aspects of Dinantian sedimentation in the Edale Basin, North Derbyshire. *Geological Journal* **26**: 245-269.

Gutteridge, P., 1989. Controls on carbonate sedimentation in a Brigantian intrashelf basin, Derbyshire. *In:* R.S. Arthurton, P. Gutteridge and S.C. Nolan (eds), The role of tectonics in Devonian and Carboniferous sedimentation in the British Isles. Occasional Publication Yorkshire Geological Society **6**: 171-187.

Gutteridge, P., 1995. Late Dinantian (Brigantian) carbonate mud-mounds of the Derbyshire carbonate platform. *In:* C.L.V. Monty, D.W.J. Bosence, P.H. Bridges and B.R. Pratt (eds), Carbonate Mud Mounds, their origin and evolution. Special publication of the International Association of Sedimentologists **23**: 289-307.

Hampson, G.J., Davies, S.J., Elliott, T., Flint, S.S. & Stollhofen, H., 1999a. Incised valley fill sandstone bodies in Upper Carboniferous fluvio-deltaic strata: recognition and reservoir characterization of Southern North Sea analogues. *In:* A.J. Fleet and S.A.R. Boldy (eds), Petroleum geology of Northwest Europe: Proceedings of the 5th Conference. The Geological Society (London): 771-788.

Hampson, G.J., Stollhofen, H. & Flint, S., 1999b. A sequence stratigraphic model for the Lower Coal Measures (Upper Carboniferous) of the Ruhr district, north-west Germany. *Sedimentology* **46**: 1199-1231

Hance, L., Poty, E. & Devuyst, F.X., 2001. Stratigraphie sequentielle du Dinantien type (Belgique) et correlation avec le Nord de la France (Boulonnais, Avesnois). *Bulletin de la Societe Geologique de France* **172**: 411-426.

Harland, W.B., Armstrong, R.L., Cox, A.V., Craig, L.E., Smith, A.G. & Smith, D.E., 1990. A geological timescale 1989. Cambridge University Press (Cambridge): 263 pp.

Hartkopf-Fröder, C., 2005. Palynostratigrafie des Pennsylvanium in Deutschland. *In:* V. Wrede (ed.), Stratigraphie von Deutschland V – Das Oberkarbon (Pennsylvanium) in Deutschland. Cour. Forsch.-Inst. Senckenberg (Frankfurt a. M.) **254**: 133-160.

Hayward, R.D., Martin, C.A.L., Harrison, D., van Dort, G., Guthrie, S. & Padget, N., 2003. The Flora Field, blocks 31/26a, 31/26c, UK North Sea.; United Kingdom oil and gas fields commemorative millennium volume. *Memoir Geological Society of London* **20**: 549-555.

Hedemann, H.-A., Schuster, A., Stancu-Kristoff, G. & Lösch, J., 1984. Die Verbreitung der Kohlenflöze des Oberkarbons in Nordwest-deutschland und ihre stratigraphische Einstufung. *Fortschritte in der Geologie von Rheinland und Westfalen (Krefeld)* **32**: 39-88.

Helz, G.R., Miller, C.V., Charnock, J.M., Mosselmans, J.F.W., Patrick, R.A.D., Garner, C.D. & Vaughan, D.J., 1996. Mechanisms of molybdenum removal from the sea and its concentration in black shales: EXAFS evidence. *Geochimica et Cosmochimica Acta* **60**: 3631-3642.

Henk, A., 1999. Did the Variscides collapse or were they torn apart?; a quantitative evaluation of the driving forces for postconvergent extension in central Europe. *Tectonics* **18**: 774-792.

Herbig, H.-G., 2005. Die internationale Mississippium-Pennsylvanium-Grenze – Entwicklung des Konzeptes, Definition und Anwendung in Deutschland. *In:* V. Wrede (ed.), Stratigraphie von Deutschland V Oberkarbon (Pennsylvanium). Cour. Forsch.-Inst. Senckenberg (Frankfurt a. M.) **254**: 3-12.

Hoffmann, N., Joedicke, H. & Horejschi, L., 2005. Regional distribution of the Lower Carboniferous Culm and Carboniferous limestone facies in the North German Basin; derived from magnetotelluric soundings. *Zeitschrift der Deutschen Gesellschaft für Geowissenschaften* **156**: 323-339.

Holdsworth, B.K. & Collinson, J.D., 1988. Millstone Grit cyclicity revisited. *In:* B.M. Besly and G. Kelling (eds), Sedimentation in a synorogenic basin complex; the Upper Carboniferous of Northwest Europe. Blackie (Glasgow): 132-152.

Hollywood, J.M. & Whorlow, C.V., 1993. Structural development and hydrocarbon occurrence of the Carboniferous in the UK southern North Sea Basin. *In:* J.R. Parker (ed.), Petroleum

geology of Northwest Europe; Proceedings of the 4th conference. The Geological Society (London) **4**: 689-696.

Hoogteijling, P.J., 1948. Radioactiviteit en bodemgesteldheid. PhD thesis Vrije Universiteit (Amsterdam): 93 pp.

Hoth, K.A., Lindert, W., Hoth, P. & Weyer, D., 2005. Das Oberkarbon des Nordrandes der Mitteleuropäischen Senke im Bereich Vorpommern, Rügen, Pommersche Bucht. *In:* V. Wrede (ed.), Stratigraphie von Deutschland V – Das Oberkarbon (Pennsylvanium) in Deutschland. Cour. Forsch.-Inst. Senckenberg (Frankfurt a. M.) **254**: 355-368.

Hoth, P., Lindert, W., Hoth, K.A. & Weyer, D., 2005. Das Oberkarbon des zentralen Bereiches der Mitteleuropäischen Senke in Norddeutschland (Südwest-Mecklenburg, Nordwest-Brandenburg, Altmark). *In:* V. Wrede (ed.), Stratigraphie von Deutschland V – Das Oberkarbon (Pennsylvanium) in Deutschland. Cour. Forsch.-Inst. Senckenberg (Frankfurt a. M.) **254**: 335-354.

Jankowski, B., David, F. & Selter, V., 1993. Facies complexes of the Upper Carboniferous in north-west Germany and their structural implications. *In:* R.A. Gayer, R.O. Greiling and A.K. Vogel (eds), Rhenohercynian and subvariscan foldbelts. International Monograph Series (Wiesbaden): 139-158.

Jedwab, J., 1966. Les degats radiatifs dans le charbon uranifere du Schaetzel. *Geologische Rundschau* **55**: 445-453.

Johnson, G.A.L., 1967. Basement control of Carboniferous sedimentation in northern England. *Proceedings of the Yorkshire Geological Society* **36**: 175-194.

Jones, N.S. & Glover, B.W., 2005. Fluvial sandbody architecture, cyclicity and sequence stratigraphical setting – implications for hydrocarbon reservoirs: the Westphalian C and D of the Osnabrück and Ibbenbüren area, northwest Germany. *In:* J.D. Collinson, D.J. Evans, D.W. Holliday and N.S. Jones (eds), Carboniferous hydrocarbon geology – The southern North Sea and surrounding areas. Yorkshire Geological Society Occasional Publication **7**: 57-74.

Jongmans, W.J., 1944. Geologisch onderzoekingen in Zuid- en Midden-Limburg. *In:* P. Kruizinga (ed.), Verhandelingen van het Geologisch-Mijnbouwkundig Genootschap. Mouton & Co ('s Gravenhage) **14**: 277-288.

Kearey, P., Brooks, M. & Hill, I., 2002. An Introduction to Geophysical Exploration. Blackwell Science (Oxford): 262 pp.

Kelling, G. & Collinson, J.D., 1992. Silesian. *In:* P.M.D. Duff and A.J. Smith (eds), The Geology of England and Wales. The Geological Society (London): 239-273.

Kent, P.E., 1966. The structure of the concealed Carboniferous rocks of north-eastern England. *Proceedings of the Yorkshire Geological Society* **35**: 323-352.

Kenter, J., A. M., van Hoeflaken, F., Bahamonde, J.R., Bracco Gartner, G.L., Keim, L. & Besems, R.E., 2002. Anatomy and lithofacies of an intact and seismic-scale Carboniferous carbonate platform (Asturias, NW Spain); analogues of hydrocarbon reservoirs in the Pricaspian Basin (Kazakhstan). *In:* W.G. Zempolich and H.E. Cook (eds), Paleozoic carbonates of the Commonwealth of Independent States (CIS); subsurface reservoirs and outcrop analogs. Special Publication Society for Sedimentary Geology (Tulsa) **74**: 181-203.

Kimpe, W.F.M., Bless, M.J.M., Bouckaert, J., Conil, R., Groessens, E., Meessen, J.P.M.T., Poty, E., Streel, M., Thorez, J. & Vanguestaine, M., 1978. Paleozoic deposits east of the Brabant Massif in Belgium and in the Netherlands. *Mededelingen Rijks Geologische Dienst* **30**: 37-103.

Kirby, M.X., 2001. Differences in growth rate and environment between Tertiary and Quaternary Crassostrea oysters. *Paleobiology* **27**: 84-103.

Kombrink, H., Bridge, J.S. & Stouthamer, E., 2007: The alluvial architecture of the Coevorden Field (Upper Carboniferous), the Netherlands. *Netherlands Journal of Geosciences* **86**: 3-14

Kombrink, H., Leever, K.A., Van Wees, J.D., Van Bergen, F., David, P. & Wong, T.E., 2008. Late Carboniferous foreland basin formation and Early Carboniferous stretching in Northwestern Europe – Inferences from quantitative subsidence analyses in the Netherlands. *Basin Research* **20**: 377-395.

Konon, A., 2006. Buckle folding in the Kielce Unit, Holy Cross Mountains, central Poland. *Acta Geol. Polon* **56**: 375-405.

Kooi, H., Hettema, M. & Cloetingh, S., 1991. Lithospheric dynamics and the rapid Pliocene-Quaternary subsidence phase in the southern North Sea basin. *Tectonophysics* **192**: 245-259.

Korn, D., 2008. Early Carboniferous (Mississippian) calciturbidites in the northern Rhenish Mountains (Germany). *Geological Journal* **43**: 151-173.

Kornpihl, K., 2005. Tectono-sedimentary Evolution of the NE German Variscan Foreland Basin. PhD thesis, University of Bonn (Bonn): 123 pp.

Kotas, A., 1995. Moravian-Silesian-Cracovian region. Upper Silesian Coal basin. *Pr. Państw. Inst. Geol.* **148**: 124-136.

Kraus, M.J. & Aslan, A., 1999. Palaeosol sequences in floodplain environments: a hierarchical approach. *In:* M. Thiry and R. Simon-Coicon (eds), Palaeoweathering, Palaeosurfaces and related Continental Deposits. International Association of Sedimentologists Special Publication **27**: 303-321.

Krawczyk, C.M., Eilts, F., Lassen, A. & Thybo, H., 2002. Seismic evidence of Caledonian deformed crust and uppermost mantle structures in the northern part of the Trans-European suture zone, SW Baltic Sea. *Tectonophysics* **360**: 215-244.

Krull, P., 2005. Paläogeographischer Rahmen. *In:* V. Wrede (ed.), Stratigraphie von Deutschland V – Das Oberkarbon (Pennsylvanium) in Deutschland. Cour. Forsch.-Inst. Senckenberg (Frankfurt a. M.) **254**: 3-12.

Krzywiec, P., 2007. Tectonic of the Lublin area (SE Poland) – new views based on results of seismic data interpretation. *Biuletyn Państwowego Instytutu Geologicznego* **422**: 1-18.

Lane, H.R., Brenckle, P.L., Baesemann, J.F. & Richards, B., 1999. The IUGS boundary in the middle of the Carboniferous; Arrow Canyon, Nevada, USA. *Episodes* **22**: 272-283.

Langenaeker, V., 2000. The Campine Basin. Stratigraphy, structural geology, coalification and hydrocarbon potential for the Devonian to Jurassic. *Aardkundige Mededelingen* **10**: 1-142.

Lawrence, S.R., Coster, P.W. & Ireland, R.J., 1987. Structural development and petroleum potential of the northern flanks of the Craven Basin (Carboniferous), North-West England. *In:* J. Brooks and K. Glennie (eds), Petroleum geology of North West Europe. Graham & Trotman (London): 225-233.

Laznicka, P., 1985. The geological association of coal and metallic ores – a review. *In:* K.H. Wolf (ed.), Handbook of strata-bound and stratiform ore deposits. Regional studies and specific deposits **13**: 1-71.

Leeder, M.R., 1992. Dinantian. *In:* P.M.D. Duff and A.J. Smith (eds), Geology of England and Wales. The Geological Society (London): 207-238.

Leeder, M.R., 1988. Recent developments in Carboniferous geology; a critical review with implications for the British Isles and N.W. Europe. *Proceedings of the Geologists' Association* **99**: 73-100.

Leeder, M.R. & McMahon, A.H., 1988. Upper Carboniferous (Silesian) basin subsidence in northern Britain. *In:* B.M. Besly and G. Kelling (eds), Sedimentation in a synorogenic basin complex: the Carboniferous of northwest Europe. Blackie (Glasgow): 43-52.

Leeder, M.R., Raiswell, R., Al Biatty, H., McMahon, A. & Hardman, M., 1990. Carboniferous stratigraphy, sedimentation and correlation of Well 48/3-3 in the southern North Sea basin; integrated use of palynology, natural gamma/sonic logs and carbon/sulphur geochemistry. *Journal of the Geological Society of London* **147**: 287-300.

Leever, K.A., Bertotti, G., Zoetemeijer, R., Matenco, L. & Cloetingh, S.A.P.L., 2006. The effects of a lateral variation in lithospheric strength on foredeep evolution; implications for the East Carpathian Foredeep. *Tectonophysics* **421**: 251-267.

Lisovsky, N.N., Gogonenkov, G.N. & Petzoukha, Y.A., 1992. The Tengiz oil field in the pre-Caspian Basin of Kazakhstan (former USSR); supergiant of the 1980s. *In:* M.T. Halbouty (ed.), Giant oil and gas fields of the decade 1978-1988. American Association of Petroleum Geologists (Tulsa) **54**: 101-122.

Littke, R., Bueker, C., Hertle, M., Karg, H., Stroetmann Heinen, V. & Oncken, O., 2000. Heat flow evolution, subsidence and erosion in the Rheno-Hercynian orogenic wedge of Central Europe. *In:* W. Franke, V. Haak, O. Oncken and D. Tanner (eds), Orogenic Processes: Quantification and Modelling in the Variscan Belt. Geological Society Special Publication (London) **179**: 231-255.

Liu, S. & Nummedal, D., 2004. Late Cretaceous subsidence in Wyoming; quantifying the dynamic component. *Geology (Boulder)* **32**: 397-400.

Lopez, J.M.G., Bauluz, B., Fernandez Nieto, C. & Oliete, A.Y., 2005. Factors controlling the trace-element distribution in fine-grained rocks; the Albian kaolinite-rich deposits of the Oliete Basin; NE Spain. *Chemical Geology* **214**: 1-19.

Lunt, I.A., Bridge, J.S. & Tye, R.S., 2004. A quantitative, three-dimensional model of gravelly braided rivers. *Sedimentology* **51**: 377-414.

Lyons, T.W., Werne, J.P., Hollander, D.J. & Murray, R.W., 2003. Contrasting sulfur geochemistry and Fe/Al and Mo/Al ratios across the last oxic-to-anoxic transition in the Cariaco Basin, Venezuela. *Chemical Geology* **195**: 131-157.

Martin, C.A.L., Stewart, S.A. & Doubleday, P.A., 2002. Upper Carboniferous and Lower Permian tectonostratigraphy on the southern margin of the central North Sea. *Journal of the Geological Society of London* **159**: 731-749.

Martinsen, O.J., Collinson, J.D. & Holdsworth, B.K., 1995. Millstone Grit cyclicity revisited; II, Sequence stratigraphy and sedimentary responses to changes of relative sea-level. *In:* A.G. Plint (ed.), Sedimentary facies analysis; a tribute to the research and teaching of Harold G. Reading. Special Publication of the International Association of Sedimentologists (Oxford) **22**: 305-327.

Mathes-Schmidt, M.E., 2000. Mikrofazies, Sedimentationsgeschehen und palaeogeographische Entwicklung im Verlauf des oberen Viseums im Untergrund der Niederrheinischen Bucht und des Campine-Beckens. PhD thesis RWTH (Aachen): 245 pp.

Matyja, H., 2008. Pomerania Basin (NW) Poland) and its sedimentary evolution during Mississipian times. *Geological Journal* **43**: 123-150.

Matyja, H., 2006. Stratygrafia i rozwój facjalny osadów dewonu i karbonu w basenie pomorskim i w zachodniej części basenu bałtyckiego a paleogeografia północnej części TESZ w późnym paleozoiku. *Pr. Państw. Inst. Geol.* **186**: 79-122.

Maynard, J.R. & Dunay, R.E., 1999. Reservoirs of the Dinantian (Lower Carboniferous) play of the Southern North Sea. *In:* A.J. Fleet and S.A.R. Boldy (eds), Petroleum Geology of Northwest Europe: Proceedings of the 5th Conference. The Geological Society (London): 729-745.

Maynard, J.R., Hofmann, W., Dunay, R.E., Benthan, P.N., Dean, K.P. & Watson, I., 1997. The Carboniferous of Western Europe; the development of a petroleum system. *Petroleum Geoscience* **3**: 97-115.

Maynard, J.R. & Leeder, M.R., 1992. On the periodicity and magnitude of Late Carboniferous glacio-eustatic sea-level changes. *Journal of the Geological Society of London* **149**: 303-311.

McCann, T., 1999. The tectonosedimentary evolution of the northern margin of the Carboniferous foreland basin of NE Germany. *Tectonophysics* **313**: 119-144.

McKay, J.L., Pedersen, T.F. & Mucci, A., 2007. Sedimentary redox conditions in continental margin sediments (NE Pacific); influence on the accumulation of redox-sensitive trace metals. *Chemical Geology* **238**: 180-196.

McKenzie, D., 1978. Some remarks on the development of sedimentary basins. *Earth and Planetary Science Letters* **40**: 25-32.

McLean, D., Owens, B. & Bodman, D., 2004. Palynostratigraphy of the Upper Carboniferous Langsettian-Duckmantian stage boundary in Britain. *In:* A.B. Beaudoin and M.J. Head (eds), The palynology and micropalaeontology of boundaries. The Geological Society Special Publication (London) **230**: 123-135.

Meessen, J.P.M.T., 1985. Rapport betreffende het onderzoek naar microfossielen van een drietal trajecten van boring Ruurlo 1. Internal report Rijks Geologische Dienst 2085.

Menning, M., Alekseev, A.S., Chuvashov, B.I., Davydov, V.I., Devuyst, F.X., Forke, H.C., Grunt, T.A., Hance, L., Heckel, P.H., Izokh, N.G., Jin, Y.G., Jones, P.J., Kotlyar, G.V., Kozur, H.W., Nemyrovska, T.I., Schneider, J.W., Wang, X.D., Weddige, K., Weyer, D. & Work, D.M., 2006. Global time scale and regional stratigraphic reference scales of central and west Europe, east Europe, Tethys, south China, and North America as used in the Devonian-Carboniferous-Permian Correlation Chart 2003 (DCP 2003). *Palaeogeography, Palaeoclimatology, Palaeoecology* **240**: 318-372.

Menning, M. & German-Stratigraphic-Commission, 2002. A geologic timescale 2002. *In:* G.S. Commission (ed.), Stratigraphic Table of Germany 2002.

Michelsen, O., 1971. Lower Carboniferous foraminiferal faunas of the boring Ørslev No. 1, island of Falster, Denmark. Danm. Geol. Und. (II) **98**: 86 pp.

Middelburg, J.J., Calvert, S.E. & Karlin, R., 1991. Organic-rich transitional facies in silled basins; response to sea-level change. *Geology (Boulder)* **19**: 679-682.

Mooney, W.D., Laske, G. & Masters, T.G., 1998. Crust 5.1: a global crustal model at 5° x 5°. *Journal of Geophysical Research* **103**: 727-747.

Morford, J.L., Russell, A.D. & Emerson, S., 2001. Trace metal evidence for changes in the redox environment associated with the transition from terrigenous clay to diatomaceous sediment, Saanich Inlet, BC. *Marine Geology* **174**: 355-369.

Morse, J.W. & Berner, R.A., 1995. What determines sedimentary C/S ratios? *Geochimica et Cosmochimica Acta* **59**: 1073-1077.

Morton, A.C., Hallsworth, C.R. & Moscariello, A., 2004. Interplay between northern and southern sediment sources during Westphalian deposition in the Silverpit Basin, southern North Sea. *In:* J.D. Collinson, D.J. Evans, D.W. Holliday and N.S. Jones (eds), Carboniferous

hydrocarbon geology – The southern North Sea and surrounding onshore areas. Yorkshire Geological Society Occasional Publication **7**: 135-146.

Moscariello, A., 2005. Exploration potential of the mature southern North Sea basin margins; some unconventional plays based on alluvial and fluvial fan sedimentation models. *In:* A.G. Dore and B.A. Vining (eds), Petroleum geology; north-west Europe and global perspective; proceedings of the 6th Petroleum geology conference. The Geological Society (London) **6**: 595-605.

Muchez, P., Conil, R., Viaene, W., Bouckaert, J. & Poty, E., 1987. Sedimentology and biostratigraphy of the Visean carbonates of the Heibaart (DzH1) borehole (Northern Belgium). *Annales de la geologique de Belgique* **110**: 199-208.

Muchez, P. & Langenaeker, V., 1993. Middle Devonian to Dinantian sedimentation in the Campine Basin (northern Belgium); its relation to Variscan tectonism. *In:* L.E. Frostick and R.J. Steel (eds), Tectonic controls and signatures in sedimentary successions. Special Publication of the International Association of Sedimentologists **20**: 171-181.

Muchez, P., Viaene, W., Bouckaert, J., Conil, R., Dusar, M., Poty, E., Soille, P. & Vandenberghe, N., 1991. The occurrence of a microbial buildup at Poederlee (Campine Basin, Belgium); biostratigraphy, sedimentology, early diagenesis and significance for early Warnantian paleogeography. *Annales de la Societe Geologique de Belgique* **113**: 329-339.

Mundy, D.J.C., 1994. Microbialite-sponge-bryozoan-coral framestones in Lower Carboniferous (Late Visean) buildups of Northern England (UK). *Canadian Society of Petroleum Geologists, Memoir* **17**: 713-729.

Nagler, T.F., Siebert, C., Luschen, H. & Bottcher, M.E., 2005. Sedimentary Mo isotope record across the Holocene fresh-brackish water transition of the Black Sea. *Chemical Geology* **219**: 283-295.

Narkiewicz, M., 2007. Development and inversion of Devonian and Carboniferous basins in the eastern part of the Variscan foreland (Poland). *Geological Quaterly* **51**: 231-265.

Nekrasova, Z.A., 1957. K voprosu o genezise uranovogo orudeneniya v uglyakh. *Voprosy Geol. Urana* **6**: 37-54.

Neves, R., Gueinn, K.J., Clayton, G., Ioannides, N.S., Neville, R.S.W. & Kruszewska, K., 1973. Palynological Correlations within the Lower Carboniferous of Scotland and Northern England. *Transactions Royal Society of Edinburgh* **69**: 24-53.

Nijenhuis, I.A., Bosch, H.J., Sinninghe Damste, J.S., Brumsack, H.J. & de Lange, G.J., 1999. Organic matter and trace element rich sapropels and black shales; a geochemical comparison. *Earth and Planetary Science Letters* **169**: 277-290.

Norman, M.D. & De Decker, P., 1990. Trace metals in lacustrine and marine sediments: A case study from the Gulf of Carpentaria, northern Australia. *Chemical Geology* **82**: 299-318.

O'Mara, P.T., Merryweather, M., Stockwell, M. & Bowler, M.M., 2003. The Trent gas field, block 43/24a, UK North Sea. *In:* J. Gluyas and H.M. Hichens (eds), United Kingdom Oil and Gas Fields, Commemorative Millennium Volume. Geological Society Memoir (London) **20**: 835-849.

Oncken, O., Plesch, A., Weber, J., Ricken, W. & Schrader, S., 2000. Passive margin detachment during arc-continental collision (Central European Variscides). *In:* W. Franke, V. Haak, O. Oncken and D. Tanner (eds), Orogenic Processes: Quantification and Modelling in the Variscan Belt. Geological Society Special Publication (London) **179**: 199-216.

Oncken, O., von Winterfeld, C. & Dittmar, U., 1999. Accretion of a rifted passive margin; the late Paleozoic Rhenohercynian fold and thrust belt (middle European Variscides). *Tectonics* **18**: 75-91.

Owens, B., Gueinn, K.J. & Cameron, I.B., 1977. A Tournaisian miospore assemblage from the Altagoan Formation (Upper Calciferous Sandstone), Draperstown, Northern Ireland. *Pollen et Spores* **19**: 313-324.

Pagnier, H.J.M., Belt, F.J.G.v.d., Mijnlieff, H.F., Bergen, F.v. & Verbeek, J., 2002. An overview of the Carboniferous structural and sedimentary evolution of the Southern North Sea with a discussion of hydrocarbon fields and play concepts in the Dutch sector. *Conference paper for:* Hydrocarbon resources of the Carboniferous, Southern North Sea & surrounding onshore areas, 13-15 September, Sheffield

Pagnier, H.J.M. & van Tongeren, P.C.H., 1996. Lithostratigraphy and sedimentology of the Upper Carboniferous of borehole "De Lutte-6" (East Twente, the Netherlands) and evalution of the Tubbergen Formation in the eastern and southern parts of the Netherlands. *Mededelingen Rijks Geologische Dienst* **55**: 3-30.

Pang, M. & Nummedal, D., 1995. Flexural subsidence and basement tectonics of the Cretaceous Western Interior basin, United States. *Geology (Boulder)* **23**: 173-176.

Paproth, E., 1989. Die paläogeographische Entwicklung Mittel-Europas im Karbon. *Geologisches Jahrbuch Hessen* **117**: 53-68.

Paproth, E., Conil, R., Bless, M.J.M., Boonen, P., Carpentier, N., Coen, M., Delcambre, B., Deprijck, C., Deuzon, S., Dreesen, R., Groessens, E., Hance, L., Hennebert, M., Hibo, D., Hahn, G.R., Hislaire, O., Kasig, W., Laloux, M., Lauwers, A., Lees, A., Lys, M., Op de Beeck, K., Overlau, P., Pirlet, H., Poty, E., Ramsbottom, W., Streel, M., Swennen, R., Thorez, J., Vanguestaine, M., Van Steenwinkel, M. & Vieslet, J.-L., 1983a. Bio- and lithostratigraphic subdivisions of the Dinantian in Belgium, a review. *Annales de la Société Géologique de Belgique* **106**: 185-239.

Paproth, E., Dusar, M., Bless, M.J.M., Bouckaert, J., Delmer, A., Fairon-Demaret, M., Houlleberghs, E., Laloux, M., Pierart, P., Somers, Y., Streel, M., Thorez, J. & Tricot, J., 1983b. Bio- and lithostratigraphic subdivisions of the Silesian in Belgium, a review. *Annales de la Société Géologique de Belgique* **106**: 241-283.

Paproth, E., Dusar, M., Verkaeren, P. & Bless, M.J.M., 1996. Stratigraphy and cyclic nature of Lower Westphalian deposits in the boreholes KB174 and KB206 in the Belgian Campine. *Annales de la Société Géologique de Belgique* **117**: 169-189.

Parker, R.H., 1955. Macro-invertrebrate assemblages as indicators of sedimentary environments in East Mississippi Delta Region. *Bulletin American Association of Petroleum Geologists* **40**: 295-376.

Passier, H.F., Middleburg, J.J., van Os, B.J.H. & de Lange, G.J., 1996. Diagenetic pyritisation under eastern Mediterranean sapropels caused by downward sulphide diffusion. *Geochimica et Cosmochimica Acta* **60**: 751-763.

Paszkowski, M. & Szulczewski, M., 1995. Late Paleozoic carbonate platforms in Polish part of the Moravia-Małopolska shelf. *In:* M. Szulczewski and J. Dvorak (eds), Evolution of the Polish-Moravian carbonate platform in the Late Devonian and Early Carboniferous: Holy Cross Mts. Kraków Upland, Moravian Karst, Guide to Excursion. XIII International Congress on Carboniferous-Permian Stratigraphy (Kraków).

Patijn, R.J.H., 1963b. De vorming van aardgas ten gevolge van na-inkoling in het noordoosten van Nederland. *Geologie en Mijnbouw* **42**: 349-358.

Pearce, T.J., Besly, B.M., Wray, D.S. & Wright, D.K., 1999. Chemostratigraphy; a method to improve interwell correlation in barren sequences; a case study using onshore Duckmantian/ Stephanian sequences (West Midlands, U.K.). *Sedimentary Geology* **124**: 197-220.

Pearce, T.J., Wray, D., Ratcliffe, K., Wright, D.K. & Moscariello, A., 2005. Chemostratigraphy of the Upper Carboniferous Schooner Formation, southern North Sea. *In:* J.D. Collinson, D.J. Evans, D.W. Holliday and N.S. Jones (eds), Carboniferous hydrocarbon geology: the southern North Sea and surrounding onshore areas. Yorkshire Geological Society Occasional Publication **7**: 147-164.

Peelcommissie, 1963. Rapport van de Peelcommissie. Verhandelingen Koninklijk Nederlands Geologisch Mijnbouwkundig Genootschap, Mijnbouwkundige Serie. 5: 133 pp.

Pèrez-Arlucea, M. & Smith, N.D., 1999. Depositional patterns following the 1870's avulsion of the Saskatchewan River (Cumberland Marshes, Saskatchewan). *Journal of Sedimentary Research* **69**: 62-73.

Pharaoh, T.C., 1999. Palaeozoic terranes and their lithospheric boundaries within the Trans-European suture zone (TESZ); a review. *Tectonophysics* **314**: 17-41.

Phillips, J., 1836. Illustrations of the geology of Yorkshire. Part 2, The Mountain Limestone District. John Murray (London).

Pickard, N.A.H., 1996. Evidence for microbial influence on the development of Lower Carboniferous buildups. *In:* P. Strogen, I.D. Somerville and G.L. Jones (eds), Recent advances in Lower Carboniferous geology. The Geological Society Special Publication (London) **107**: 65-82.

Poty, E., 1997. Devonian and Carboniferous tectonics in the eastern and southeastern parts of the Brabant Massif (Belgium). *Aardkundige Mededelingen* **8**: 143-144.

Poty, E., 1991. Tectonique de blocs dans le prolongement oriental de Massif de Brabant. *Annales de la geologique de Belgique* **114**: 265-275.

Poty, E., Hance, L., Lees, A. & Hennebert, M., 2001. Dinantian lithostratigraphic units (Belgium). *Geologica Belgica* **4**: 69-93.

Press, W., Flannery, B., Teukolsky, S. & Vetterling, W., 1988. Numerical Recipes in C. Cambridge University Press (New York).

Pruysers, P.A., de Lange, G.J. & Middelburg, J.J., 1991. Geochemistry of eastern Mediterranean sediments; primary sediment composition and diagenetic alterations. *Marine Geology* **100**: 137-154.

Pysklywec, R.N. & Mitrovica, J.X., 2000. Mantle dynamics and the formation of large-scale intra-cratonic basins; modeling results and geological case studies.; GeoCanada 2000; the millennium geoscience summit. *Abstract Volume (Geological Association of Canada)* **25**.

Quirk, D.G., 1993. Interpreting the Upper Carboniferous of the Dutch Cleaver Bank High. *In:* J.R. Parker (ed.), Petroleum geology of Northwest Europe; Proceedings of the 4th conference. The Geological Society (London) **4**: 697-706.

Quirk, D.G. & Aitken, J.F., 1997. The structure of the Westphalian in the northern part of the southern North Sea. *In:* K. Ziegler, P. Turner and S.R. Daines (eds), Petroleum Geology of the Southern north Sea: Future Potential. Geological Society Special Publication (London) **123**: 143-152.

Rabitz, A., 1966. Die marinen Horizonte des flözführenden Ruhrkarbons. *Fortschritte in der Geologie von Rheinland und Westfalen* **13**: 243-296.

Raiswell, R. & Berner, R.A., 1987. Organic carbon losses during burial and thermal maturation of normal marine shales. *Geology* **15**: 853-856.

Ramsbottom, W.H.C., 1969. The Namurian of Britain. *Compte Rendu Congres International de Stratigraphie et de Geologie du Carbonifère* **1**: 219-232.

Ramsbottom, W.H.C., Calver, M.A., Eagar, R.M.C., Hodson, F., Holliday, D.W., Stubblefield, C.J. & Wilson, R.B., 1978. A correlation of Silesian rocks in the British Isles. Special Report Geological Society 10: 81 pp.

Ramsbottom, W.H.C., Rhys, G.H. & Smith, E.G., 1962. Boreholes in the Carboniferous rocks of the Ashover district, Derbyshire. *Bulletin of the Geological Survey of Great Britain* **19**: 75-168.

Ramsbottom, W.H.C., Ridd, M.F. & Read, W.A., 1979. Rates of transgression and regression in the Carboniferous of NW Europe; with discussion and reply. *Journal of the Geological Society of London* **136**: 147-154.

Rayner, D.H., 1953. The lower Carboniferous rocks in the north of England; a review. *Proceedings of the Yorkshire Geological Society* **28**: 231-315.

RGD, 1986. Eindrapport project inventarisatieonderzoek Nederlandse kolenvoorkomens, eerste fase 1981-1985. Report Rijks Geologische Dienst 2107: 67 pp.

Richwien, J., Schuster, A., Teichmüller, R. & Wolburg, J., 1963. Überblick über das Profil der Bohrung Münsterland 1. *Fortschritte in der Geologie von Rheinland und Westfalen* **11**: 9-18.

Ricken, W., Schrader, S., Oncken, O. & Plesch, A., 2000. Turbidite basin and mass dynamics related to orogenic wedge growth; the Rheno-Hercynian case. *In:* W. Franke, V. Haak, O. Oncken and D. Tanner (eds), Orogenic Processes: Quantification and Modelling in the Variscan Belt. Geological Society Special Publication (London) **179**: 257-280.

Ritchie, J.S., Pilling, D. & Hayes, S., 1998. Reservoir development, sequence stratigraphy and geological modelling of Westphalian fluvial reservoirs of the Caister C Field, UK southern North Sea. *Petroleum Geoscience* **4**: 203-221.

Ritchie, J.S. & Pratsides, P., 1993. The Caister Fields, Block 44/23a, UK North Sea. *In:* J.R. Parker (ed.), Petroleum geology of Northwest Europe; Proceedings of the 4th conference. The Geological Society (London) **4**: 759-769.

Ross, C.A. & Ross, J.R.P., 1988. Late Paleozoic transgressive-regressive deposition. *Special Publication Society of Economic Paleontologists and Mineralogists* **42**: 227-247.

Rouchy, J.M., Groessens, E. & Laumondais, A., 1984. Sédimentologie de la formation anhydritique viséenne du sondage de Saint Ghislain (Hainaut, Belgique). Implications paléogéographiques et structurales. *Bulletin de la Société belge de Géologie* **93**: 105-145.

Royden, L., 1988. Flexural behavior of the continental lithosphere in Italy; constraints imposed by gravity and deflection data. *Journal of Geophysical Research* **93**: 7747-7766.

Royden, L. & Keen, C.E., 1980. Rifting process and thermal evolution of the continental margin of eastern Canada determined from subsidence curves. *Earth and Planetary Science Letters* **51**: 343-361.

Saucier, R.T., 1994. Geomorphology and Quaternary Geologic History of the Lower Mississippi Valley. Mississippi River Commission (Vicksburg): 364 pp.

Scheck, M., Thybo, H., Lassen, A., Abramovitz, T. & Laigle, M., 2002. Basement structure in the southern North Sea, offshore Denmark, based on seismic interpretation. *In:* J.A. Winchester, T.C. Pharaoh and J. Verniers (eds), Palaeozoic Amalgamation of Central Europe The Geological Society Special Publication (London) **201**: 311-326.

Schroot, B.M. & de Haan, H.B., 2003. An improved regional structural model of the Upper Carboniferous of the Cleaver Bank High based on 3D seismic interpretation. *In:* Nieuwland,

D.A. (ed.), New insights into structural interpretation and modelling. Geological Society Special Publication (London) **212**: 23-37.

Schultz, R.B., 2004. Geochemical relationships of late Paleozoic carbon-rich shales of the Midcontinent, USA; a compendium of results advocating changeable geochemical conditions. *Chemical Geology* **206**: 347-372.

Sclater, J.G. & Christie, P.A.F., 1980. Continental stretching; an explanation of the post-Mid-Cretaceous subsidence of the central North Sea basin. *Journal of Geophysical Research* **85**: 3711-3739.

Selter, V., 1990. Sedimentologie und Klimaentwicklung im Westfal C/D und Stefan des nordwestdeutschen Oberkarbon-Beckens. Deutsche Wissenschaftliche Gesellschaft für Erdöl, Erdgas und Kohle (DGMK) Berichte **384-4**: 310 pp.

Shaffer, N.R., 2002. Small-scale variations in black shale sequences of Indiana. 36th annual meeting Geological Society of America.

Sintubin, M., 1999. Arcuate fold and cleavage patterns in the southeastern part of the Anglo-Brabant fold belt (Belgium); tectonic implications.; Palaeozoic to Recent tectonics in the NW European Variscan Front zone. *Tectonophysics* **309**: 81-97.

Sissingh, W., 2004. Palaeozoic and Mesozoic igneous activity in the Netherlands; a tectonomagmatic review. *Geologie en Mijnbouw* **83**: 113-134.

Skompski, S., 1996. Stratigraphic position and facies significance of the limestone bands in the subsurface Carboniferous succession of the Lublin Upland. *Acta Geol. Polon.* **46**: 171-268.

Smith, N.J.P., Kirby, G.A. & Pharaoh, T.C., 2005. Structure and evolution of the south-west Pennine Basin and adjacent area. British Geological Survey (Nottingham).

Spears, D.A., 1964. The major element geochemistry of the Mansfield marine band in the Westphalian of Yorkshire. *Geochimica et Cosmochimica Acta* **28**: 1679-1696.

Spears, D.A. & Amin, M.A., 1981. Geochemistry and mineralogy of marine and non-marine Namurian black shales from the Tansley Borehole, Derbyshire. *Sedimentology* **28**: 407-417.

Spears, D.A. & Duff, P.M.D., 1984. Kaolinite and mixed-layer illite-smectite in Lower Cretaceous bentonites from the Peace River Coalfield, British Columbia. *Canadian Journal of Earth Sciences* **21**: 465-476.

Spears, D.A., Kanaris, S.R., Riley, N. & Krause, P., 1999. Namurian bentonites in the Pennine Basin, UK; origin and magmatic affinities. *Sedimentology* **46**: 385-401.

Spears, D.A., Rippon, J.H. & Cavender, P.F., 1999. Geological controls on the sulphur distribution in British Carboniferous coals; a review and reappraisal. *International Journal of Coal Geology* **40**: 59-81.

Spears, D.A. & Sezgin, H.I., 1985. Mineralogy and geochemistry of the Subcrenatum Marine Band and associated coal-bearing sediments, Langsett, South Yorkshire. *Journal of Sedimentary Petrology* **55**: 570-578.

Sperber, B., 1993. Bituminous coal in NW Germany. *In:* G. R.A., R.O. Greiling and A.K. Vogel (eds), Rhenohercynian and subvariscan foldbelts. International Monograph Series (Wiesbaden): 269-280.

Stampfli, G.M. & Borel, G.D., 2002. A plate tectonic model for the Paleozoic and Mesozoic constrained by dynamic plate boundaries and restored synthetic oceanic isochrons. *Earth and Planetary Science Letters* **196**: 17-33.

Steckler, M.S. & Watts, A.B., 1978. Subsidence of the Atlantic-type continental margin off New York. *Earth and Planetary Science Letters* **41**: 1-13.

Stemmerik, L., 2003. Controls on localization and morphology of Moscovian (Late Carboniferous) carbonate buildups, southern Amdrup Land, northern Greenland. *In:* W.M. Ahr, P.M. Harris, W.A. Morgan and I.D. Somerville (eds), Permo-Carboniferous carbonate platforms and reefs. Special Publication Society for Sedimentary Geology (Tulsa) **78**: 253-265.

Stemmerik, L., Elvebakk, G. & Worsley, D., 1999. Upper Palaeozoic carbonate reservoirs on the Norwegian arctic shelf; delineation of reservoir models with application to the Loppa High. *Petroleum Geoscience* **5**: 173-187.

Sternbeck, J., Sohlenius, G. & Hallberg Rolf, O., 2000. Sedimentary trace elements as proxies to depositional changes induced by a Holocene fresh-brackish water transition. *Aquatic Geochemistry* **6**: 325-345.

Stoppel, D. & Amler, M.R.W., 2006. Zur Abgrenzung und Untergliederung des Unterkarbons. *In:* M.R.W. Amler and D. Stoppel (eds), Stratigraphie von Deutschland, VI – Unterkarbon (Mississippium). Schr.-R. Dt. Ges. Geowiss (Hannover) **41**: 15-26.

Sundvoll, B., Larsen, B.T. & Wandaas, B., 1992. Early Magmatic phase in the Oslo Rift and its related stress regime. *Tectonophysics* **208**: 37-54.

Süss, M.P., 2001. The Ruhr and Aachen basins – sedimentary environments, sequence stratigraphic model, and synsedimentary tectonics of variscan foreland basins (Namurian B/C to Westphalian C, W. Germany). *Canadian Society of Petroleum Geologists* **19**: 208-227.

Süss, M.P., 1996. Sedimentologie und Tektonik des Ruhr-Beckens: Sequenzstratigraphische Interpretation und Modellierung eines Vorlandbeckens der Varisciden. PhD thesis Rheinische Friedrich-Wilhelms University (Bonn): 147 pp.

Swaine, D.J., 1990. Trace elements in coal. Butterworth (London): 278 pp.

Szulczewski, M., Belka, Z. & Skompski, S., 1996. The drowning of a carbonate platform; an example from the Devonian-Carboniferous of the southwestern Holy Cross Mountains, Poland. *Sedimentary Geology* **106**: 21-49.

Tait, J.A., Bachtadse, V., Franke, W. & Soffel, H.C., 1997. Geodynamic evolution of the European Variscan fold belt; palaeomagnetic and geological constraints. *Geologische Rundschau* **86**: 585-598.

Taylor, S.R. & McLennan, S.M., 1985. The continental crust: its composition and evolution. Blackwell (Oxford): 312 pp.

Ten Haven, H.L., Baas, M., de Leeuw, J.W., Schenck, P.A. & Brinkhuis, H., 1987. Late Quaternary Mediterranean sapropels; II, Organic geochemistry and palynology of S (sub 1) sapropels and associated sediments. *Chemical Geology* **64**: 149-167.

Thiadens, A.A., 1963. The Palaeozoic of the Netherlands. KNGMG (Delft): 28 pp.

Timmerman, M.J., 2004. Timing, geodynamic setting and character of Permo-Carboniferous magmatism in the foreland of the Variscan Orogen, NW Europe. *In:* M. Wilson, E.-R. Neumann, S.J. Davies, M.J. Timmerman, M. Heeremans and B.T. Larsen (eds), Permo-Carboniferous magmatism and rifting in Europe. The Geological Society Special Publication (London) **223**: 41-74.

Total E&P UK, 2007. A regional review of the Dinantian carbonate play: Southern North Sea & onshore UK. Total E&P UK, 64 pp.

Tribovillard, N., Algeo, T.J., Lyons, T. & Riboulleau, A., 2006. Trace metals as paleoredox and paleoproductivity proxies; an update. *Chemical Geology* **232**: 12-32.

Tribovillard, N., Riboulleau, A., Lyons, T. & Baudin, F., 2004. Enhanced trapping of molybdenum by sulfurized marine organic matter of marine origin in Mesozoic limestones and shales. *Chemical Geology* **213**: 385-401.

Turcotte, D.L. & Schubert, G., 2002. Geodynamics. Cambridge University Press pp.

Tye, R.S. & Coleman, J.M., 1989a. Depositional processes and stratigraphy of fluvially dominated lacustrine deltas: Mississippi Delta Plain. *Journal of Sedimentary Petrology* **59**: 973-996.

Unrug, R. & Dembowski, Z., 1971. Rozwój diastroficzno-sedymentacyjny basenu morawsko-śląskiego. *Towarzystwa Geologicznego* **41**: 119-168.

Van Adrichem Boogaert, H.A. & Kouwe, W.F.P., 1993. Stratigraphic nomenclature of the Netherlands, revision and update by RGD and NOGEPA. *Mededelingen Rijks Geologische Dienst* **50**: 1-40.

Van Amerom, H.W.J. & Glerum, J.J., 1984. Rapport betreffende de stratigrafische interpretatie van diepboring Kemperkoul-1 op grond van de makroflora. Internal report Rijks Geologische Dienst 2003.

Van Amerom, H.W.J. & Meessen, J.P.M.T., 1985. Rapport over mariene niveaus in diepboring Hengevelde-1. Internal report Rijks Geologische Dienst 2094: 16 pp.

Van Amerom, H.W.J., Meessen, J.P.M.T. & Glerum, J.J., 1985. Rapport over mariene niveaus in diepboring Joppe-1. Internal report Rijks Geologische Dienst 2091: 16 pp.

Van Buggenum, J.M. & den Hartog Jager, D.G., 2007. Silesian. *In:* Th.E. Wong, D.A.J. Batjes and J. de Jager (eds), Geology of the Netherlands. Royal Netherlands Academy of Arts and Sciences (Amsterdam): 43-62.

Van der Weijden, C.H., Reichart, G.-J. & van Os, B.J.H., 2006. Sedimentary trace element records over the last 200 kyr from within and below the northern Arabian Sea oxygen minimum zone. *Marine Geology* **231**: 69-88.

Van der Zwan, C.J., 1993. Palynological, ecological and climatological synthesis of the Upper Carboniferous of the well De Lutte-6 (East Netherlands). *Comptes Rendus* **12**: 167-186.

Van Hulten, F.F.N. & Poty, E., 2008. Geological factors controlling Early Carboniferous Carbonate Platform development in the Netherlands. *Geological Journal* **43**: 175-196.

Van Waterschoot van der Gracht, W.A.J.M., 1918. Eindverslag der Rijksopsporing van Delfstoffen 1903-1916. Martinus Nijhoff ('S-Gravenhage): 664 pp.

Van Wees, J.-D. & Beekman, F., 2000. Lithosphere rheology during intraplate basin extension and inversion; inferences from automated modeling of four basins in Western Europe. *Tectonophysics* **320**: 219-242.

Van Wees, J.D., Stephenson, R.A., Stovba, S.M. & Shymanovskyi, V.A., 1996. Tectonic variation in the Dniepr-Donets Basin from automated modelling of backstripped subsidence curves.; Europrobe; intraplate tectonics and basin dynamics of the eastern European Platform. *Tectonophysics* **268**: 257-280.

Van Wijhe, D.H. & Bless, M.J.M., 1974. The Westphalian of the Netherlands with special reference to miospore assemblages. *Geologie en Mijnbouw* **53**: 295-328.

Verniers, J., Pharaoh, T.C., Andre, L., Debacker, T.N., De Vos, W., Everaerts, M., Herbosch, A., Samuelsson, J., Sintubin, M. & Vecoli, M., 2002. The Cambrian to mid Devonian basin development and deformation history of eastern Avalonia, east of the Midlands Microcraton; new data and a review. *In:* J.A. Winchester, T.C. Pharaoh and J. Verniers (eds), Palaeozoic amalgamation of Central Europe. Geological Society Special Publication (London) **201**: 47-93.

Visser, W.A., 1987. The state service for the exploration of mineral resources. *In:* W.A. Visser, J.I.S. Zonneveld and A.J. van Loon (eds), Seventy-five years of geology and mining in the Netherlands. KNGMG (The Hague): 39-50.

Waksmundzka, M.I., 1998. Depositional architecture of the Carboniferous Lublin basin. *Pr. Państw. Inst. Geol.* **165**: 89-100.

Waksmundzka, M.I., 2007b. Karbon. Wyniki badań litologicznych, sedymentologicznych i stratygraficznych. *In:* M.I. Waksmundzka (ed.), Profile Głębokich Otworów Wiertniczych Państwowego. Instytutu Geologicznego (Lublin) **119**: 114-119.

Wanless, H.R. & Shepard, F.P., 1936. Sea level and climate changes related to late Palaeozoic cycles. *Geological Society of America Bulletin* **37**: 1177-1206.

Warr, L.N., 1993. Basin Inversion and foreland basin development in the Rhenohercynian zone of south-west England. *In:* R.A. Gayer, R.O. Greiling and A.K. Vogel (eds), Rhenohercynian and subvariscan foldbelts. International Monograph Series (Wiesbaden): 197-224.

Watts, A.B. & Burov, E.B., 2003. Lithospheric strength and its relationship to the elastic and seismogenic layer thickness. *Earth and Planetary Science Letters* **213**: 113-131.

Weber, L.J., Francis, B.P., Harris, P.M. & Clark, M., 2003. Stratigraphy, lithofacies, and reservoir distribution, Tengiz Field, Kazakhstan. *In:* W.M. Ahr, P.M. Harris, W.A. Morgan and I.D. Somerville (eds), Permo-Carboniferous carbonate platforms and reefs. Special Publication Society for Sedimentary Geology (Tulsa) **78**: 351-394.

Werne, J.P., Sageman, B.B., Lyons, T.W. & Hollander, D.J., 2002. An integrated assessment of a "type euxinic" deposit; evidence for multiple controls on black shale deposition in the Middle Devonian Oatka Creek Formation. *American Journal of Science* **302**: 110-143.

White, N., 1994. An inverse method for determining lithospheric strain rate variation on geological timescales. *Earth and Planetary Science Letters* **122**: 351-371.

Wignall, P.B., 1994. Black shales. Oxford University Press (Oxford): 127 pp.

Wignall, P.B. & Newton, R., 2001. Black shales on the basin margin; a model based on examples from the Upper Jurassic of the Boulonnais, northern France. *Sedimentary Geology* **144**: 335-356.

Wilde, P., Lyons, T.W. & Quinby-Hunt, M.S., 2004. Organic carbon proxies in black shales; molybdenum. *Chemical Geology* **206**: 167-176.

Willett, S.D., 1999. Orogeny and orography: The effects of erosion on the structure of mountain belts. *Journal of Geophysical Research* **104**: 28957-28981.

Wrede, V., 2005. Stratigraphie von Deutschland V – Das Oberkarbon (Pennsylvanium) in Deutschland. Cour. Forsch.-Inst. (Senckenberg): **254**: 477 pp.

Wrede, V., 2000. Struktureller Bau und Mächtigkeit des „Flözleeren" (Namur A-C) im Raum Hasslinghausen (südliches Ruhrkarbon). *Zeitschrift der Deutschen Gesellschaft für Geowissenschaften* **151**: 171-185.

Wright, V.P., 1999. Assessing flood duration gradients and fine-scale environmental change on ancient floodplains. *In:* S.B. Marriott and J. Alexander (eds), Floodplains: Interdisciplinary Approaches. Geological Society Special Publication (London) **163**: 279-287.

Wright, V.P. & Vanstone, S.D., 2001. Onset of late Palaeozoic glacio-eustasy and the evolving climates of low latitude areas: a synthesis of current understanding. *Journal of the Geological Society of London* **158**: 579-582.

Yalcin, H. & Gumuser, G., 2000. Mineralogical and geochemical characteristics of Late Cretaceous bentonite deposits of the Kelkit Valley Region, northern Turkey. *Clay Minerals* **35**: 807-825.

Żelaźniewicz, A., Marheine, D. & Oberc-Dziedzic, T., 2003. A Late Tournaisian synmetamorphic folding and thrusting event in the eastern Variscan foreland: 40Ar/39Ar evidence from the phyllites of the Wolsztyn-Leszno High, western Poland. *International Journal of Earth Sciences* **92**: 185-194.

Ziegler, P.A., 1989. Evolution of Laurussia – a study in Late Palaeozoic plate tectonics. Kluwer Academic Publishers (Dordrecht, Boston, London): 102 pp.

Ziegler, P.A., 1990. Geological Atlas of Western and Central Europe (2nd edition). Shell Internationale Petroleum Maatschappij B.V.; Geological Society Publishing House (Bath): 239 pp.

Ziegler, P.A., Bertotti, S. & Cloetingh, S., 2002. Dynamic processes controlling foreland development – the role of mechanical (de)coupling of orogenic wedges and forelands. *EGU Stephan Mueller Special Publication Series* **1**: 17-56.

Ziegler, P.A. & Cloetingh, S., 2004. Dynamic processes controlling evolution of rifted basins. *Earth Science Reviews* **64**: 1-50.

Ziegler, P.A., Cloetingh, S. & Van Wees, J.-D., 1995. Dynamics of intraplate compressional deformation: the Alpine foreland and other examples. *Tectonophysics* **252**: 7-59.

Ziegler, P.A. & Dèzes, P., 2006. Crustal evolution of Western and Central Europe. *Memoirs of the Geological Society of London* **32**: 43-56.

Ziegler, P.A., Schumacher, M.E., Dèzes, P., van Wees, J.D. & Cloetingh, S., 2006. Post-Variscan evolution of the lithosphere in the area of the European Cenozoic rift system.; European lithosphere dynamics. *Memoirs of the Geological Society of London* **32**: 97-112.

Ziegler, P.A., Schumacher, M.E., Dèzes, P., van Wees, J.D. & Cloetingh, S.A.P.L., 2004. Post-Variscan evolution of the lithosphere in the Rhine Graben area; constraints from subsidence modelling. *In:* M. Wilson, E.R. Neumann, G.R. Davies, M.J. Timmerman, M. Heeremans and B.T. Larsen (eds), Permo-Carboniferous magmatism and rifting in Europe. Geological Society Special Publication (London) **223**: 289-317.

Ziegler, P.A., Van Wees, J.-D. & Cloetingh, S.A.P.L., 1998. Mechanical controls on collision-related compressional intraplate deformation. *Tectonophysics* **300**: 103-129.

Zoetemeijer, R., Cestmir, T. & Cloetingh, S.A.P.L., 1999. Flexural expression of European continental lithosphere under the western outer Carpathians. *Tectonics* **18**: 843-861.

APPENDIX A

C/S, major and trace element data described in chapter 6

Sample name	Faunal phase	Depth (m)	C/S		Major elements (wt%)			Trace elements (ppm)			
			TS (wt%)	TOC (wt%)	Si	Al	Ca	Ag	As	Bi	Cd
Tansley											
Ty-01	Goniatite	240.14	2.2	6.8	17.5	7.8	8.5	0.6	26.2	0.3	20.0
Ty-02	Goniatite	239.86	4.8	5.9	12.3	6.0	10.4	1.9	59.6	0.3	17.0
Ty-03	Goniatite	239.66	6.6	4.9	15.8	7.3	6.1	0.6	51.8	0.3	13.6
Ty-04	Goniatite	239.36	5.0	3.5	20.7	9.8	2.3	0.3	53.6	0.3	4.4
Ty-05	Spat	239.23	4.3	2.7	19.7	9.1	2.5	0.3	42.9	0.3	3.6
Ty-06	Spat	239.10	4.4	2.7	21.4	9.7	0.4	0.3	45.0	0.3	3.7
Ty-07	Fish	238.68	5.6	3.2	21.1	10.4	0.2	0.3	51.8	0.3	3.7
Ty-08	Fish	238.47	4.0	4.2	22.9	10.7	0.2	0.3	45.9	0.3	4.5
Ty-09	*A. or D.*	238.18	3.8	3.8	18.2	8.4	5.7	0.3	48.0	0.3	2.9
Ty-10	Goniatite	237.90	5.0	2.9	20.9	10.2	2.2	0.3	48.7	0.3	3.0
Ty-11	*A. or D.*	237.57	4.3	2.6	20.3	9.5	3.6	0.3	30.5	0.3	1.8
Ty-12	Goniatite	237.21	4.9	3.4	22.2	9.5	1.2	0.3	35.4	0.3	3.2
Ty-13	Spat	236.77	4.0	3.5	21.5	10.2	2.1	0.2	25.9	0.3	1.8
Ty-14	Spat	236.39	3.9	3.1	21.2	9.3	4.0	0.2	42.2	0.3	1.5
Ty-15	Goniatite	236.08	3.5	3.7	22.8	10.3	0.3	0.3	39.0	0.3	1.7
Ty-16	*A. or D.*	232.74	6.7	4.9	20.9	9.1	2.0	0.4	46.4	0.3	3.5
Ty-17	*A. or D.*	232.41	5.2	5.4	20.2	9.6	1.4	0.6	61.4	0.3	5.9
Ty-18	Goniatite	231.93	4.5	3.4	21.5	10.2	1.9	0.4	34.9	0.3	5.5
Ty-19	*A. or D.*	231.60	4.1	2.5	21.5	11.5	1.7	0.4	35.0	0.3	3.1
Ty-20	*A. or D.*	231.39	3.2	1.7	21.9	11.5	1.6	0.2	30.4	0.3	1.4
Ty-21	Goniatite	231.11	3.5	2.6	22.9	11.4	0.9	0.3	39.9	0.3	4.2
Ty-22	Goniatite	230.99	4.8	4.3	21.6	9.7	2.5	0.4	45.4	0.3	6.8
Ty-23	*A. or D.*	230.91	4.7	2.0	21.8	12.4	0.3	0.3	37.3	0.3	1.8
Ty-24	Spat	230.77	3.7	1.7	22.9	12.1	0.2	0.2	36.8	0.3	0.8
Ty-25	Spat	230.06	3.8	3.1	22.5	11.6	0.3	0.2	31.5	0.3	1.0
Ty-26	Spat	230.05	3.2	2.5	23.2	11.6	0.3	0.2	26.0	0.3	0.8
Ty-27	Spat	229.79	3.7	3.0	22.5	11.4	0.6	0.2	42.0	0.3	1.2
Ty-28	*Planolites*	227.81	0.4	1.6	25.1	11.3	0.3	0.2	14.8	0.2	1.5
Ty-29	*Planolites*	226.67	0.1	0.9	15.6	8.7	3.0	0.1	6.6	0.2	0.3
Ty-30	*Planolites*	225.69	0.1	1.5	25.1	12.1	0.3	0.2	6.2	0.3	1.7
Highoredish											
Hh-01	Goniatite	73.48	3.4	5.0	12.1	5.1	16.1	0.4	39.6	0.2	3.8
Hh-02	Goniatite	73.33	4.7	4.2	19.7	8.2	5.8	0.5	56.0	0.3	3.5
Hh-03	Goniatite	73.19	4.6	4.7	18.3	7.9	8.0	0.5	52.1	0.3	4.6

Sample name	Faunal phase	Depth (m)	C/S		Major elements (wt%)			Trace elements (ppm)			
			TS (wt%)	TOC (wt%)	Si	Al	Ca	Ag	As	Bi	Cd
Hh-04	Fish	73.05	4.9	4.3	23.0	9.8	0.4	0.5	57.2	0.3	2.7
Hh-05	*A. or D.*	72.87	3.0	3.6	21.3	8.6	4.9	0.4	43.7	0.3	4.9
Hh-06	*A. or D.*	72.66	4.0	4.1	20.2	8.3	6.1	0.4	33.8	0.3	1.8
Hh-07	*A. or D.*	72.54	5.9	3.8	21.7	9.4	1.4	0.4	55.7	0.4	2.3
Hh-08	Spat	72.24	6.4	4.8	21.3	9.2	2.1	0.5	69.0	0.4	3.2
Hh-09	Spat	71.82	1.3	2.3	5.1	2.3	21.7	0.2	15.5	0.1	1.1
Uppertown											
UT-01	Goniatite	73.99	5.7	3.7	19.9	9.4	4.0	0.6	64.5	0.4	9.6
UT-02	Goniatite	73.71	4.2	2.3	21.3	9.5	2.4	0.4	53.5	0.3	3.9
UT-03	Goniatite	73.43	3.6	3.2	21.4	10.2	2.5	0.4	40.1	0.3	6.2
UT-04	Goniatite	73.03	4.0	2.4	22.2	11.3	1.5	0.4	47.6	0.3	5.9
UT-05	Goniatite	72.87	1.7	4.7	6.6	2.8	20.9	0.8	28.6	0.2	39.2
UT-06	*A. or D.*	72.68	3.7	3.2	20.6	9.5	3.7	0.4	42.3	0.3	8.5
UT-07	*A. or D.*	72.56	5.2	5.0	21.0	10.2	0.9	0.5	69.3	0.4	6.3
UT-08	Fish	71.96	0.2	1.9	19.1	9.8	1.1	0.2	10.6	0.2	1.0
UT-09	Fish	71.09	4.9	2.3	22.5	11.1	0.2	0.3	21.6	0.2	0.9
UT-10	Fish	70.31	3.4	3.3	21.5	9.6	0.5	0.3	35.7	0.2	1.0

Sample name	Faunal phase	Depth (m)	Trace elementens (ppm)											
			Co	Cr	Cu	Mn	Mo	Ni	Pb	Sb	Tl	U	V	Zn
Tansley														
Ty-01	Goniatite	240.14	27.4	114.5	131.8	557.7	32.9	113.6	20.6	6.0	4.0	18.6	508.5	123.4
Ty-02	Goniatite	239.86	46.7	361.0	132.3	1921.8	30.2	190.0	20.0	41.9	0.9	5.9	525.5	218.4
Ty-03	Goniatite	239.66	37.3	112.8	137.9	1056.8	84.1	136.4	20.2	9.1	3.3	10.3	310.3	90.1
Ty-04	Goniatite	239.36	35.3	107.0	90.6	499.5	31.9	86.2	23.4	6.8	1.6	14.4	158.3	97.5
Ty-05	Spat	239.23	65.9	99.7	86.6	436.6	27.3	76.3	20.8	3.5	1.2	15.5	146.6	92.4
Ty-06	Spat	239.10	40.5	110.4	88.7	589.0	22.3	82.0	22.8	4.4	1.2	13.4	155.2	99.8
Ty-07	Fish	238.68	68.4	108.5	108.0	854.1	21.6	99.9	26.1	4.5	1.1	13.9	170.8	123.2
Ty-08	Fish	238.47	61.1	115.4	145.4	413.8	17.1	129.9	22.6	4.0	1.2	21.6	230.5	135.6
Ty-09	*A. or D.*	238.18	46.8	90.4	110.4	559.8	26.4	71.6	21.6	3.9	1.0	13.9	127.6	87.7
Ty-10	Goniatite	237.90	39.2	93.7	87.5	590.8	52.5	70.6	24.1	5.5	1.4	7.8	125.7	87.1
Ty-11	*A. or D.*	237.57	28.9	79.9	58.3	503.9	39.0	70.3	22.6	7.2	1.6	11.9	99.2	59.7
Ty-12	Goniatite	237.21	32.3	76.4	76.6	301.8	25.8	63.7	23.4	6.1	1.7	12.1	114.6	72.2
Ty-13	Spat	236.77	22.9	72.1	66.6	520.1	17.2	51.3	23.8	3.6	1.2	14.4	101.4	75.3
Ty-14	Spat	236.39	39.6	70.4	66.8	447.5	14.4	64.4	25.2	3.0	0.9	13.3	121.9	73.0
Ty-15	Goniatite	236.08	27.9	67.8	64.3	287.8	27.4	54.3	22.8	3.5	0.8	14.2	88.5	64.8
Ty-16	*A. or D.*	232.74	29.4	75.5	100.1	270.8	41.6	60.7	26.6	4.7	2.0	17.5	101.8	74.3
Ty-17	*A. or D.*	232.41	43.9	86.4	130.9	307.3	44.8	82.2	23.2	7.1	2.1	20.3	165.9	80.9
Ty-18	Goniatite	231.93	27.4	86.7	85.5	405.8	59.5	63.9	23.8	8.3	1.5	11.9	154.1	77.4
Ty-19	*A. or D.*	231.60	34.6	78.2	71.9	306.9	27.0	51.7	29.6	4.8	1.1	12.0	118.0	63.2
Ty-20	*A. or D.*	231.39	36.4	76.7	43.6	333.3	11.9	42.9	27.9	3.2	0.8	8.1	91.5	61.1
Ty-21	Goniatite	231.11	27.2	77.7	65.6	191.8	15.8	58.6	30.7	8.2	3.7	10.5	189.3	72.7

Sample name	Faunal phase	Depth (m)	Trace elementens (ppm)											
			Co	Cr	Cu	Mn	Mo	Ni	Pb	Sb	Tl	U	V	Zn
Ty-22	Goniatite	230.99	39.0	80.8	112.7	337.1	65.5	77.6	40.6	7.7	2.5	18.4	162.0	103.4
Ty-23	*A. or D.*	230.91	38.6	88.5	73.8	316.5	20.2	68.3	43.1	3.8	0.9	12.6	118.8	62.2
Ty-24	Spat	230.77	20.1	85.8	48.7	528.9	5.8	52.5	32.0	2.1	0.8	6.2	103.1	62.8
Ty-25	Spat	230.06	24.6	82.7	59.0	782.9	10.3	57.7	47.6	2.3	0.8	7.7	106.6	71.6
Ty-26	Spat	230.05	32.2	91.3	48.5	514.7	10.2	45.2	43.6	1.7	0.8	7.0	99.1	66.8
Ty-27	Spat	229.79	31.6	115.3	72.2	482.1	20.0	66.1	58.1	1.9	0.8	11.3	131.2	83.8
Ty-28	*Planolites*	227.81	26.3	126.4	54.8	976.8	1.2	63.6	11.0	0.6	0.5	4.9	128.2	95.8
Ty-29	*Planolites*	226.67	25.8	83.8	35.6	4817.2	0.9	47.3	6.8	0.2	0.4	3.0	101.6	42.1
Ty-30	*Planolites*	225.69	30.1	127.5	54.5	839.2	0.9	72.3	9.6	0.4	0.6	4.8	140.5	104.0
Highoredish														
Hh-01	Goniatite	73.48	34.1	70.7	92.0	1407.2	63.5	111.1	15.0	9.5	4.2	303.8	217.2	90.5
Hh-02	Goniatite	73.33	42.5	108.8	137.1	699.5	99.7	134.1	22.3	18.9	4.6	41.8	323.8	125.1
Hh-03	Goniatite	73.19	44.0	104.0	124.1	734.3	98.6	136.1	21.9	15.8	4.7	34.2	259.5	111.3
Hh-04	Fish	73.05	40.1	133.2	108.2	357.9	24.5	93.0	22.7	16.5	1.9	33.7	320.4	101.7
Hh-05	*A. or D.*	72.87	42.4	107.7	114.1	740.3	27.8	81.7	20.1	13.3	5.9	25.8	492.5	114.1
Hh-06	*A. or D.*	72.66	36.4	99.7	110.0	634.7	63.5	94.1	20.6	11.9	2.9	28.7	197.5	95.2
Hh-07	*A. or D.*	72.54	57.0	102.5	113.2	293.8	50.4	96.5	24.8	11.9	4.1	30.3	213.6	98.1
Hh-08	Spat	72.24	43.8	102.8	129.4	385.9	115.8	150.7	24.7	18.1	7.6	33.3	300.4	96.5
Hh-09	Spat	71.82	21.8	34.7	44.4	4713.4	43.6	56.0	6.7	4.3	1.8	14.8	109.3	33.0
Uppertown														
UT-01	Goniatite	73.99	45.4	114.4	134.6	366.4	46.6	89.0	42.6	8.3	2.8	12.8	192.5	78.2
UT-02	Goniatite	73.71	29.1	107.4	79.5	342.3	30.4	67.1	36.3	7.3	1.9	9.8	131.5	70.3
UT-03	Goniatite	73.43	30.7	127.2	99.8	407.4	45.0	96.8	22.9	5.8	3.2	10.3	167.3	89.8
UT-04	Goniatite	73.03	38.8	117.5	97.8	455.4	30.1	77.5	24.7	8.4	2.3	8.9	152.3	89.0
UT-05	Goniatite	72.87	34.8	157.4	148.8	1438.0	94.3	128.8	11.5	6.1	6.3	15.0	632.4	87.5
UT-06	*A. or D.*	72.68	63.1	135.5	99.3	505.5	40.5	82.2	36.7	4.4	2.4	12.8	215.4	88.2
UT-07	*A. or D.*	72.56	69.0	118.5	192.5	505.6	72.5	101.6	60.5	5.2	2.4	25.3	185.5	177.2
UT-08	Fish	71.96	77.3	94.6	52.6	2579.5	2.0	72.7	9.3	0.5	0.5	4.4	108.8	74.3
UT-09	Fish	71.09	61.6	114.3	61.4	148.9	1.1	90.9	33.7	4.0	1.0	5.7	135.4	76.2
UT-10	Fish	70.31	24.7	98.3	77.9	1138.0	40.0	64.5	70.7	4.3	1.3	11.3	112.5	80.5

APPENDIX B

C/S, major and trace elements data described in chapter 7

	Depth (m)	C/S		Major elements (wt%)				Trace elements (ppm)						
		TS (wt%)	TOC (wt%)	Al	Fe	Ca	K	U	Mo	V	Cu	Ni	Pb	Zn
GVK-bas.mb.														
g	852.39	0.3	1.0	10.1	4.0	0.2	3.0	4.7	0.5	195.4	37.8	77.5	9.4	89.7
g	853.81	0.3	1.2	9.0	4.8	0.3	2.5	4.5	0.4	194.0	43.2	87.5	12.8	134.0
g	855.67	0.5	1.0	9.7	4.2	0.2	2.8	4.8	0.5	197.2	45.0	79.6	10.5	127.0
g	857.63	1.2	1.1	9.8	4.8	0.2	2.9	3.7	0.8	159.4	35.2	62.5	15.9	80.1
g	859.72	2.2	0.8	9.8	5.1	0.2	3.0	3.0	2.6	155.7	48.2	69.9	38.8	97.5
g	861.80	1.4	0.9	9.1	4.7	0.3	2.7	3.3	0.8	144.6	33.2	69.3	21.8	94.8
g	863.66	0.7	0.9	10.3	4.6	0.3	3.1	4.5	0.6	165.4	38.5	63.6	11.2	89.8
m	865.62	3.4	3.0	8.9	5.7	1.5	2.8	7.9	22.9	180.1	135.7	94.5	61.8	79.8
m	867.76	2.3	1.5	10.0	5.3	0.6	3.1	3.8	4.3	179.5	61.7	75.2	32.3	107.1
m	869.56	2.0	1.0	10.8	5.2	0.3	3.3	4.4	7.7	171.3	42.1	74.7	20.3	92.6
m	871.72	3.4	4.0	8.1	5.3	2.1	2.5	11.4	46.4	204.7	172.5	103.6	27.2	108.9
m	873.63	3.5	2.1	9.3	5.0	0.7	2.9	6.1	5.7	186.2	112.9	84.8	25.4	119.3
m	875.63	2.8	3.6	4.8	3.7	4.5	1.5	7.3	59.0	173.6	138.5	91.5	18.0	105.9
m	877.73	3.1	3.6	6.6	5.5	5.8	1.9	9.4	63.0	149.6	146.6	77.5	19.7	115.8
m	879.88	4.3	4.9	7.6	6.3	3.2	2.2	13.6	59.0	168.4	170.5	89.3	27.1	126.4
m	881.67	2.8	3.7	5.0	4.2	4.0	1.5	10.1	55.0	162.7	134.2	87.9	22.1	114.7
m	883.84	2.5	1.8	10.0	4.2	0.6	3.1	6.9	5.3	225.7	76.6	78.8	19.8	129.1
m	885.02	1.6	1.0	11.4	4.8	0.9	3.4	4.2	1.3	198.1	48.8	74.7	21.6	122.0
m	886.74	2.9	1.7	10.6	5.2	0.3	3.2	7.4	7.2	214.6	74.8	79.4	22.7	138.8
m	888.54	3.6	3.6	8.2	5.3	1.5	2.4	9.6	23.3	238.3	183.6	85.4	42.3	190.1
m	890.55	3.1	1.7	10.0	4.6	0.3	3.1	7.7	6.6	243.3	100.8	83.4	39.5	156.4
JPE-Aegir														
g	1118.93	1.2	0.9	5.4	3.5	0.3	1.8	2.8	1.5	82.1	22.1	34.6	70.8	178.7
g	1120.26	1.2	1.7	6.9	4.8	0.4	2.4	3.2	1.7	104.2	8.4	32.7	49.8	283.8
g	1121.59	nd	nd	nd	nd	nd	nd	3.3	1.6	117.7	21.7	54.2	61.2	159.5
m	1123.04	1.3	1.8	8.0	5.8	0.4	2.9	3.0	1.2	128.4	18.4	49.0	64.9	224.0
m	1124.32	nd	nd	nd	nd	nd	nd	4.1	1.2	127.7	22.6	42.6	79.3	221.9
m	1124.73	nd	nd	nd	nd	nd	nd	4.3	1.3	129.1	21.5	49.8	54.4	286.6
m	1125.24	nd	nd	nd	nd	nd	nd	4.3	1.5	140.2	27.5	56.1	59.4	221.1
m	1126.03	1.4	1.7	10.4	4.8	0.3	3.4	4.3	2.3	147.0	30.9	59.4	50.7	291.5
m	1126.56	nd	nd	nd	nd	nd	nd	4.0	1.1	133.9	23.7	58.3	48.5	226.4
m	1127.23	nd	nd	nd	nd	nd	nd	4.0	1.2	146.5	26.7	49.0	66.0	210.7
m	1129.10	0.2	2.4	9.6	10.1	0.5	3.1	3.1	1.3	178.8	23.2	40.1	31.2	83.0
m	1129.86	0.4	0.2	12.1	3.0	0.2	4.1	4.7	0.8	180.5	39.5	51.6	56.0	97.7
m	1130.31	1.6	1.6	10.1	4.1	0.2	3.1	6.5	3.9	132.4	34.8	69.1	53.9	159.7

	Depth (m)	C/S		Major elements (wt%)				Trace elements (ppm)						
		TS (wt%)	TOC (wt%)	Al	Fe	Ca	K	U	Mo	V	Cu	Ni	Pb	Zn
m	1130.79	5.5	1.6	9.9	7.6	0.2	3.0	4.9	1.1	128.7	54.3	131.0	86.7	50.8
c	1130.99	6.5	80.5					3.1	5.1	57.3	51.3	82.7	2611.3	47.7
g	1131.05	2.5	0.6	11.4	4.9	0.1	3.6	5.0	2.0	135.6	25.1	59.7	58.0	48.1
g	1131.50	0.9	0.6	10.9	4.0	0.9	3.8	5.6	0.8	166.7	29.0	52.6	228.6	166.9
c	1131.90	1.2	83.2	3.6	nd	nd	nd	10.2	0.9	49.6	45.1	67.5	891.7	80.8
KPK-Aegir														
g	1192.41	nd	nd	nd	nd	nd	nd	2.7	0.6	145.6	26.6	63.2	15.8	99.9
g	1203.18	nd	nd	nd	nd	nd	nd	3.0	0.5	154.2	34.4	53.7	23.2	142.9
g	1213.33	0.1	1.1	11.0	3.5	0.3	3.5	3.1	0.7	162.2	32.1	73.4	23.4	120.5
g	1217.04	0.1	1.4	9.9	4.4	0.4	3.0	2.9	0.6	147.9	29.7	64.2	17.3	87.6
g	1219.95	0.1	0.7	11.9	2.8	0.2	3.7	3.0	0.7	170.9	34.9	81.4	27.9	91.4
g	1222.00	0.0	0.8	11.9	2.8	0.2	3.9	3.0	1.0	176.4	35.8	91.7	22.3	88.7
g	1223.93	0.0	0.9	12.6	3.0	0.2	4.2	3.2	0.7	176.7	40.2	60.4	34.0	66.1
g	1225.50	0.4	1.5	11.6	3.7	1.3	3.7	3.5	0.8	185.8	72.7	115.7	29.2	83.0
m	1226.44	2.7	2.8	11.2	4.9	0.3	3.6	5.1	8.8	202.4	94.0	134.7	48.2	133.4
m	1226.5	nd	nd	nd	nd	nd	nd	6.8	4.4	225.7	86.7	128.5	44.7	159.8
m	1227.23	1.9	1.5	10.9	4.2	1.4	3.3	4.6	1.5	178.2	58.0	125.4	55.1	160.3
c	1227.75	7.2	79.0	nd	nd	nd	nd	31.1	48.3	70.1	34.0	26.0	35.2	182.2
c	1227.99	7.0	26.8	nd	nd	nd	nd	3.7	6.0	109.9	52.3	78.6	188.2	706.6
c	1228.21	3.8	88.7	nd	nd	nd	nd	1.1	3.9	10.4	18.9	18.6	31.6	120.1
c	1228.57	12.4	71.6	nd	nd	nd	nd	0.3	3.1	7.2	30.2	42.1	223.3	1295.8
g	1229.99	0.6	1.3	9.9	3.2	0.4	2.8	3.2	0.9	161.9	33.3	62.9	25.1	181.9
g	1250.28	nd	nd	nd	nd	nd	nd	2.7	0.3	145.6	29.1	43.8	17.1	83.1
KB-Aegir														
g	1296.5	0.1	1.0	9.9	4.3	0.2	3.3	2.8	1.0	156.4	40.9	68.6	15.9	91.5
g	1297.7	0.1	1.1	9.9	4.6	0.2	3.3	2.8	0.6	147.5	33.8	58.8	16.3	55.6
g	1298.7	0.0	0.8	11.2	3.8	0.2	3.8	3.1	0.8	161.5	36.5	70.1	31.9	50.9
g	1299.9	0.1	1.2	11.0	3.4	0.2	3.1	4.2	1.0	139.9	36.2	55.7	10.7	57.5
g	1300.7	0.1	0.9	11.5	3.4	0.2	3.5	4.5	1.2	153.0	35.3	55.6	17.7	52.7
m	1301.1	0.1	1.3	12.0	4.9	0.3	3.7	6.0	0.9	186.6	45.4	53.9	16.0	46.1
m	1301.8	0.3	0.8	11.9	3.4	0.3	3.6	6.6	0.9	162.3	35.5	47.4	15.3	49.1
m	1302.1	0.3	0.8	11.7	2.9	0.1	3.9	6.5	1.5	173.5	50.2	53.8	17.4	47.1
m	1302.5	0.4	0.8	11.6	3.0	0.1	4.0	6.6	1.9	180.8	61.3	60.7	23.0	45.5
HGV-Veldhof														
g	1239.80	0.1	1.1	12.6	2.5	0.3	4.3	4.6	1.7	178.8	46.7	96.3	28.8	67.1
g	1240.35	0.1	1.4	11.7	3.4	0.2	3.9	4.1	0.7	175.2	49.6	47.7	27.8	58.2
g	1240.83	0.1	1.7	11.1	3.7	0.2	3.9	3.7	0.9	168.1	48.2	72.9	29.6	79.0
g	1241.27	0.1	1.0	12.7	2.7	0.2	3.9	4.1	0.9	167.9	47.2	49.6	40.3	90.4
m	1241.73	1.5	0.7	11.5	3.3	0.1	3.5	5.3	0.7	189.7	51.4	60.6	64.3	145.9
m	1242.00	1.0	1.6	11.0	4.5	0.2	3.3	5.6	0.8	179.2	49.9	53.6	42.5	155.8
m	1242.26	2.9	1.1	11.6	4.5	0.1	3.5	6.3	2.5	184.8	47.6	80.4	45.5	51.6
m	1242.37	4.8	1.2	11.5	6.1	0.2	3.4	6.5	4.5	163.3	47.7	99.1	65.4	44.9
m	1242.50	3.6	4.6	11.0	4.9	0.2	3.2	6.4	1.5	170.3	57.9	93.0	78.0	48.5
c	1242.60	5.9	75.4	nd	nd	nd	nd	1.2	2.7	6.2	26.0	55.0	103.9	42.7

	Depth (m)	C/S		Major elements (wt%)				Trace elements (ppm)						
		TS (wt%)	TOC (wt%)	Al	Fe	Ca	K	U	Mo	V	Cu	Ni	Pb	Zn
c	1242.72	5.8	72.9	nd	nd	nd	nd	3.6	4.5	169.9	68.2	100.5	174.4	205.0
g	1242.79	2.4	1.4	11.1	4.2	0.2	3.6	6.9	2.1	190.9	52.0	87.6	44.5	93.9
KPK-Domina														
g	1592.49	0.1	2.0	9.3	7.0	0.4	2.5	2.8	0.7	144.3	31.5	62.0	16.3	97.4
g	1593.37	0.0	1.0	11.9	3.8	0.2	3.6	3.1	0.5	178.5	41.5	69.8	26.0	121.0
g	1596.00	0.0	1.1	11.8	3.9	0.2	3.6	3.2	0.5	189.0	42.0	74.0	32.6	122.0
m	1596.47	0.1	1.1	12.8	2.9	0.2	3.9	4.1	0.7	200.6	56.6	81.1	42.0	95.2
m	1596.93	0.1	1.4	12.9	2.8	0.2	3.8	4.0	0.8	180.1	49.3	93.5	35.6	130.2
m	1597.1	nd	nd	nd	nd	nd	nd	3.5	0.4	191.5	53.7	59.8	18.9	110.1
m	1597.39	0.1	1.2	12.6	2.7	0.2	3.7	3.6	0.5	190.1	83.1	56.4	18.8	128.9
m	1597.93	1.5	1.3	12.5	3.9	0.1	3.6	4.9	1.1	195.4	60.9	86.9	32.5	153.3
c	1598.12	7.5	82.8	nd	nd	nd	nd	0.8	3.6	109.6	33.4	32.4	31.7	31.3
g	1599.53	0.4	0.3	11.7	1.8	0.1	3.3	3.9	0.7	160.9	27.1	257.8	40.1	75.2
g	1601.34	0.0	1.5	9.6	4.2	0.2	2.8	2.8	0.8	137.8	32.3	58.0	16.7	98.6
KPK-LB 1														
g	1491.65	0.0	1.5	11.3	3.8	0.2	3.0	3.9	0.5	134.2	28.9	40.5	24.1	94.0
g	1492.24	0.1	1.7	10.1	3.8	0.2	2.6	4.4	0.7	130.2	31.2	46.9	21.2	73.0
g	1493.16	0.0	0.8	12.1	2.2	0.1	3.4	4.2	0.5	142.9	27.2	50.5	22.6	75.1
g	1493.98	0.0	1.7	13.0	3.7	0.2	4.1	4.2	0.7	182.2	54.4	81.6	38.6	48.5
l	1495.05	0.1	6.5	13.3	1.3	0.2	4.2	3.5	0.8	177.8	17.2	60.9	29.3	51.3
l	1495.48	0.0	0.9	10.5	2.0	0.3	3.2	2.9	0.7	137.7	28.0	35.9	15.9	64.4
l	1495.90	0.4	17.4	7.7	12.7	1.1	1.9	4.1	1.7	144.0	59.6	95.6	29.1	193.1
c	1496.10	1.1	71.1	nd	nd	nd	nd	2.9	4.7	80.7	51.8	43.2	15.5	95.2
c	1496.10	1.5	75.9	nd	nd	nd	nd	2.8	5.3	75.8	51.8	42.8	15.8	100.8
c	1496.52	0.6	40.9	nd	nd	nd	nd	3.2	2.9	106.4	44.4	54.1	17.9	87.9
g	1496.72	0.2	7.1	9.3	2.2	0.1	2.6	3.5	1.1	124.1	34.3	61.4	23.0	113.7
KPK-LB 2														
g	1569.14	0.1	1.3	8.1	3.4	0.2	1.9	3.7	0.6	113.9	32.2	44.6	17.1	95.9
g	1569.76	0.1	0.7	10.9	2.5	0.1	2.9	3.5	0.8	153.9	35.9	55.5	18.2	116.4
g	1570.48	0.1	0.6	11.9	2.3	0.1	3.4	4.2	0.7	175.6	40.8	66.1	19.8	92.5
g	1571.11	0.0	0.7	11.6	2.4	0.1	3.4	3.3	0.5	175.6	42.3	63.8	19.2	94.3
l	1571.44	0.0	1.0	12.6	2.6	0.1	3.8	4.0	0.6	204.1	60.9	69.0	25.2	68.2
l	1571.58	0.0	2.4	9.9	9.2	0.2	2.6	3.1	0.4	137.8	31.4	48.0	21.7	91.9
c	1571.70	0.8	93.2	nd	nd	nd	nd	1.0	2.5	189.3	31.5	69.5	23.5	37.5
c	1572.04	0.7	99.4	nd	nd	nd	nd	0.2	1.8	6.6	19.7	21.4	7.8	12.5
c	1572.52	0.5	75.8	nd	nd	nd	nd	3.0	2.0	77.3	42.8	27.6	28.8	28.4
g	1573.19	0.0	0.6	10.0	2.6	0.1	2.7	3.5	0.2	127.5	30.2	58.0	21.2	93.8
RLO-LB 1														
g	881.92	0.0	0.5	9.1	2.8	0.2	2.5	2.8	1.2	103.3	30.0	42.6	15.3	92.3
g	882.87	0.0	0.5	10.6	3.1	0.2	3.1	2.9	1.4	120.5	26.9	43.3	14.2	74.0
g	883.69	0.0	0.4	12.0	2.9	0.1	3.7	2.8	0.4	137.7	31.3	50.2	16.8	61.0
g	885.01	0.0	0.5	12.6	3.0	0.1	4.0	2.5	0.3	148.7	60.7	44.1	11.0	59.5
g	886.17	0.0	0.4	13.1	3.1	0.1	4.2	2.5	0.3	155.9	32.7	50.8	9.1	61.0
g	887.12	0.2	3.5	9.3	14.2	0.7	2.8	1.9	0.2	134.9	24.6	51.7	17.0	44.0

	Depth (m)	C/S		Major elements (wt%)				Trace elements (ppm)						
		TS (wt%)	TOC (wt%)	Al	Fe	Ca	K	U	Mo	V	Cu	Ni	Pb	Zn
g	887.71	0.1	1.0	12.7	4.0	0.1	4.2	2.9	0.3	171.3	41.1	62.9	23.4	92.6
l	888.34	0.1	4.8	11.8	4.8	0.2	3.9	3.4	1.2	188.1	84.3	74.6	44.8	92.9
l	888.62	0.3	13.9	9.7	1.7	0.0	2.4	3.3	1.1	124.5	41.8	50.2	84.0	311.7
l	888.86	1.1	39.3	nd	nd	nd	nd	3.2	4.6	124.2	63.6	66.6	330.7	271.9
l	888.91	0.4	11.7	9.8	1.9	0.0	2.5	3.1	0.9	114.8	40.2	49.1	59.0	124.9
l	889.21	0.5	27.0	6.3	1.7	8.3	1.5	1.6	1.2	93.0	140.6	35.5	776.0	979.3
g	891.12	0.0	1.3	8.7	4.3	0.2	2.3	3.1	1.1	108.8	22.8	43.7	13.5	69.5
RLO-LB 2														
g	1180.73	0.0	0.6	12.1	2.9	0.1	3.4	2.8	0.4	159.1	32.0	52.3	11.6	67.6
g	1181.59	0.0	1.6	10.7	6.2	0.3	3.0	2.7	0.4	151.3	35.7	70.9	20.3	122.4
g	1182.53	0.0	1.0	12.7	3.5	0.2	3.7	2.9	0.5	192.0	40.1	72.7	17.4	76.7
g	1183.27	0.0	1.1	13.2	2.7	0.2	3.9	3.1	0.6	209.4	47.6	68.0	23.0	61.0
g	1184.12	0.1	1.4	13.2	2.6	0.3	3.9	4.7	1.3	248.3	92.0	65.9	29.3	43.9
l	1184.72	0.1	3.9	12.0	1.9	0.1	3.4	7.5	2.7	248.1	163.2	98.0	47.5	59.5
l	1184.90	0.0	3.2	12.0	3.3	0.2	3.4	4.8	1.7	181.7	93.7	77.3	27.0	60.7
l	1184.9	nd	nd	nd	nd	nd	nd	4.9	1.6	210.2	118.0	68.5	23.8	54.8
l	1185.11	0.1	4.5	12.0	2.9	0.2	3.3	5.7	1.1	194.6	116.6	83.5	30.0	57.8
l	1185.49	0.1	6.6	9.7	6.7	0.4	2.3	6.0	0.8	150.2	86.4	94.2	19.8	75.6
c	1185.63	11.9	70.3	2.9	nd	nd	nd	7.1	20.5	38.7	52.4	44.8	99.8	29.9
c	1185.71	7.6	77.2	1.3	nd	nd	nd	3.4	6.4	18.9	26.2	10.6	220.2	30.1
c	1185.91	3.0	93.1	1.6	nd	nd	nd	0.7	4.1	16.2	19.0	10.4	40.5	28.6
c	1186.01	3.6	85.9	1.5	nd	nd	nd	0.7	9.4	13.1	36.1	22.7	59.2	33.0
g	1186.81	0.4	2.4	7.6	2.0	0.1	2.0	2.9	0.6	120.5	33.5	43.4	17.5	47.5
RLO-LB 3														
g	1232.39	0.1	1.0	12.2	3.6	0.2	3.7	5.2	0.6	142.6	37.8	60.9	31.2	131.6
g	1232.86	0.0	2.4	11.4	8.6	0.5	3.5	5.9	0.4	188.7	46.1	51.1	48.4	104.1
g	1233.80	0.0	2.0	11.6	6.9	0.3	3.6	5.9	0.5	190.7	46.6	57.9	46.3	120.7
g	1234.47	0.0	0.9	12.5	3.5	0.2	3.9	6.2	0.6	188.9	52.6	62.0	42.9	107.7
l	1234.99	0.2	4.2	11.7	4.4	0.2	3.5	7.3	1.9	179.5	118.1	107.0	60.0	141.0
l	1235.31	0.2	3.5	11.9	4.1	0.2	4.2	4.0	1.8	207.6	92.0	99.5	54.8	129.4
l	1235.51	0.4	7.0	11.7	2.5	0.0	3.7	5.0	1.8	183.9	137.3	111.9	60.7	1454.7
c	1235.55	0.6	66.7	nd	nd	nd	nd	4.6	1.5	236.7	38.3	77.2	51.0	899.7
c	1235.72	0.6	79.6	nd	nd	nd	nd	1.4	2.0	55.1	34.6	36.7	30.9	79.1
c	1236.15	1.0	87.2	nd	nd	nd	nd	6.9	2.4	47.9	64.6	30.3	62.6	34.6
g	1236.71	0.0	1.2	12.6	1.4	0.0	2.1	4.4	0.4	215.6	48.3	99.0	30.3	32.2

Legend	
Marine band	m
Lacustrine band	l
Coal	c
Grey shale	g
nd: not determined	

Epiloog

In het najaar van 2001 vertokken de vierdejaars Fysische Geografie uit Utrecht voor de doctoraalexcursie naar Denemarken. Toen besloten Thijs, Matthijs, Michiel en ik om dit concept voortaan ook zelf toe te gaan passen. We stelden een programma op met te bezoeken plekken en hebben inmiddels een hele lijst afgewerkt. Van de Slufter op Texel naar de Heimansgroeve in Limburg en van de kliffen van Calais naar de zandafgravingen in Drenthe en Noord Duitsland. De tweeweekse reis naar de Pyreneeën en Aliaga dit jaar vormde daarbij het koningsnummer. Een van onze excursies voerde naar het Carboon rond Ibbenbüren en Osnabrück, net over de grens in Duitsland. Aangezien ik op dat moment een stage uitvoerde bij de NAM in Assen en aan het Carboon werkte, was dit een uitgelezen kans om de gesteentes die ik met behulp van logs bestudeerde nu eens in het echt te zien. Een korte tijd later realiseerde ik me dat deze gesteentes het onderwerp van een meer dan vier jaar durig promotie-onderzoek zouden gaan worden.

Dikwijls wordt beweerd dat de bekende promotie-dip optreedt tijdens het derde jaar, in de periode dat er geschreven moet gaan worden. Nu, ik ben er maar meteen mee begonnen. Achteraf is dit allemaal heel verklaarbaar. Hoe ordening te scheppen in zo'n enorme berg gegevens? Toen dit eenmaal een beetje gelukt was, werd het steeds leuker. De laatste jaren heb ik dan ook met veel plezier aan het project gewerkt. Allereerst bedank ik daarvoor mijn promotoren Theo Wong en Kees van der Zwan. Zij hebben het project opgezet, begeleid en meegeholpen het geheel af te ronden. Then, I would like to express my thanks to the members of the dissertation committee for the critical reading and positive comments on my manuscript: Prof. Dr. P.L de Boer, Dr. J.D. Collinson, Prof. Dr. A. Schäfer, Prof. Dr. A.D. Spears and Prof. Dr. P.A. Ziegler.

Een groot aantal mensen heeft inhoudelijk bijgedragen aan dit proefschrift, waar ik hen zeer erkentelijk voor ben. Vanuit TNO zijn dit Henk Pagnier, Oscar Abbink, Frank van Bergen, Barthold Schroot, Ed Duin, Hans Doornenbal, Cees Geel, Harald de Haan (werkt nu bij EBN), Petra David, Jan-Diederik van Wees, Nora Witmans en Harmen Mijnlieff. Met Frank en Petra heb ik twee aangename en nuttige bezoeken gebracht aan Brussel en Krefeld tijdens de beginfase van mijn onderzoek. Het TNO-lab kan ik natuurlijk niet overslaan; Bertil van Os (werkt nu bij RACM), Harry Veld en Gerard Klaver hebben mij veel geleerd over geochemie, hartelijk dank voor de tijd die jullie altijd hadden. Rob van Galen, Jan Drenth en Kathrin Reimer dank ik voor de assistentie in het lab. En daar is natuurlijk Rob de Wilde van het kernenhuis. Rob, ik heb met veel plezier rondgelopen, gezaagd, gemonsterd en natuurlijk koffie gedronken in die prachtige loods. Jouw hulp en de traktaties bij de koffie werden zeer gewaardeerd. De mensen van de bibliotheek (vooral Jan Jansen); ook hartelijk dank voor de goede hulp en de prettige omgeving.

Buiten TNO zijn er tevens een hoop mensen te bedanken voor hun inhoudelijke bijdrage en de daaraan gerelateerd discussies. Bij de Nederlandse Aardolie Maatschappij zijn dit Jos Okkerman, Frank Pardoel, Kees van Oijk, en Ton Evers. Gert de Lange en Gert-Jan Reichart van de Universiteit Utrecht en Grishja van der Veer hebben nuttig commentaar geleverd op de interpretatie van geochemische data. Günter Drozdzweski from the Geological Survey of Nordrhein Westfalen in Krefeld kindly introduced me into the geology of the German Carboniferous. He provided me with interesting literature and excursion guides. Michiel Dusar van de Belgische Geologische Dienst in Brussel heeft geholpen met het nemen van kernmonsters en heeft mij de afgelopen jaren

zo nu en dan van gegevens voorzien. In the last phase of my PhD, I had a very fruitful discussion with Markus Aretz from Cologne on the sedimentary development of Dinantian carbonate platforms. He also read one of my manuscript in really a very short time. Natuurlijk kan ik Henk van Lochem, die ik ontmoette in Stettin, niet overslaan. Hij raadde me aan toch nog eens naar de seismiek te kijken onder het Groningen veld, een gouden tip! I would like to thank Mark Geluk, Rick Donselaar, Tony Watts, Peter Burgess, Martin Gibling, Cees Geel, Poppe de Boer and Noël Vandenberghe for the constructive reviews of the papers I submitted last years. Tijdens een NGS-dag ontmoette ik Karen Leever van de Vrij Universiteit. Haar modelresultaten, die ze op een poster presenteerde, leken interessant om eens toe te passen op 'mijn' gebied. Een hele nuttige en leerzame samenwerking kwam hieruit voort. Karen, dit is de manier waarop wetenschap werkt. Ik ben je dan ook dankvoor voor je hulp en tijd en wat mooi dat dit alles heeft geresulteerd in een goed paper!

Het was een genoegen om twee studenten te mogen begeleiden. Maarten heeft middels zijn werkzaamheden voor de SPBA-Atlas een nuttige bijdrage geleverd aan dit product. Gion wilde graag zijn afstudeerscriptie schrijven in het kader van mijn onderzoek. Dat is gelukt. Gion, het is bijna een proefschrift op zich geworden! Je hebt een enorme ontwikkeling doorgemaakt, wat uiteindelijk heeft geresulteerd in een mooie baan in Bideford, bij een consultant op het gebied van de geochemie. Alle goeds daar en we gaan zeker dat paper nog schrijven hè?

Tijdens mijn promotie kwam ik in aanraking met het project waarbij een petroleum geologische atlas wordt gemaakt van het Zuidelijk Permbekken (SPBA-Atlas). Langzaam ben ik erin gerold, uitmondend in het hoofdauteurschap van een hoofdstuk. Dankzij dit project heb ik veel mogen reizen, veel mensen ontmoet en bovendien heel veel geleerd. Allereerst wil ik daarvoor de coördinator Hans Doornenbal bedanken. Hans, de manier waarop jij een dergelijk project leidt is indrukwekkend. Het is erg zinvol om dit een tijd van dichtbij mee te maken. Moreover, thanks to this atlas-project I was able to meet with Kenneth Glennie, the initiator of the project. The way he spends his days in Ballater (Scotland) in his own library of geological books set a future example for me. I want to thank many other people for the pleasant meetings, discussions and excursions: John Collinson, Bernard Besly, Michiel Dusar, Lars Stemmerik, Daan den Hartog-Jager, Günter Drozdzewski, Volker Wrede, Peer Hoth, Maria Waksmundzka, Thomas Pletsch and many others.

De hele business-unit Geo Energie van TNO wil ik voor de goede sfeer en de leuke borrels en uitjes bedanken. Een speciaal woord voor de karteergroep en de geobiologen bij wie ik de laatste maanden gestationeerd was. Daarnaast heb ik bijna 4 jaar met veel plezier een pot voetbal gespeeld. Simon, Frank, Ate, Tim, Sjef, Henk, Jenny en vele anderen; ik hoop nog eens mee te doen.

Van de mensen bij Aardwetenschappen wil ik ten eerste Maurits bedanken. Het is goed dat je me vaak opbelde om koffie te drinken, vooral als je zelf geneigd bent om steeds maar door te gaan. Dat is een goede eigenschap van je. Daarnaast was de begeleiding van de twee veldwerken in Tremp samen met jou en Poppe een aangename afwisseling van het werk op de Uithof. Ondanks dat we een paar kilometer van elkaar opgroeiden, ontmoette ik Hemmo pas tijdens mijn promotie. Ach, we hebben wel wat ingehaald toch? Het was leuk om je een week te helpen boren in Spanje en ik hoop onze discussies over van alles en nog wat voort te zetten in de toekomst. Verder bedank ik alle andere mensen van Strat/Pal en Sedimentologie, mede voor de aangename tijd op Sicilië tijdens die leerzame excursie.

Veel mensen zorgden voor een aangename invulling van de tijd na vijf uur. De voetballers van Sporting en de wielrenners van VoorRob hebben hier een belangrijk aandeel in, in het bijzonder de geboren orginasitoren Bram en Edo. Aafke, als we later oud zijn en tijd hebben gaan we nog

eens een boek schrijven. Met Thijs, Matthijs en Michiel heb ik de vele hierboven beschreven excursies genoten; een prachtige herinnering en een mooi idee dat nog lang niet alles is bekeken. Ik heb goede herinneringen aan de etentjes met Gerrit-Jan, Natalia, Geert-Jan en de *geovriendjes.* De familie Reitsma heeft al voor een heel aantal leuke en leerzame momenten gezorgd en daarvan zullen er vast nog meer volgen. Joop, Jet, Chris, Anja en Lies, vijf mooie mensen op rij; ik ben benieuwd wat de toekomst allemaal voor ons in petto heeft. Het laatste bericht is voor Mariël: ik zie het helemaal zitten met jou!

Curriculum Vitae

The author of this thesis was born on December 19th 1979 in Terneuzen. After having lived there for one and half years, his parents moved to the countryside in the northern part of the Netherlands. In the hamlet of Kostvlies, on the boundary between the moraine landscape and the glacial (Hunze) valley, he spend the rest of his youth. Secondary school was attended in Stadskanaal until 1998. In the same year, Henk started his study Physical Geography at Utrecht University and moved to Zeist. During his studies he got interested in (Quaternary) geology. Therefore, he carried out his master research project in the Rhine-Meuse delta, under the supervision of Dr. H.J.A. Berendsen, after having worked there during the first year of his studies as well. An internship at NAM (Netherlands Oil Company) in Assen was carried out at the very end of his studies. At that time, he learned to know the deeper subsurface of the Netherlands: the gas-bearing Carboniferous around the Coevorden area. This internship matched the PhD position which at that time became available at TNO (*Geological Survey of the Netherlands*). Besides his interest in geology, Henk likes to spend his sparetime on history, reading, organising excursions and cycling.

De auteur van dit proefschrift werd geboren op 19 december 1979 in Terneuzen. Na daar anderhalf jaar gewoond te hebben, verruilden zijn ouders de Zeeuwse stad voor het Drentse platteland. In het buurtschap Kostvlies, op de grens van het Drents Plateau en het Hunzedal, bracht hij de rest van zijn jeugd door. De middelbare school – het Ubbo Emmius Lyceum – werd in Stadskanaal genoten. Meteen na het examen in 1998 begon Henk met de studie Fysische Geografie aan de Universiteit Utrecht en verhuisde naar de Warande in Zeist. Gedurende de studie werd zijn interesse gewekt voor de (Kwartair) geologie. Daarom voerde hij zijn doctoraal veldwerk in de Rijn-Maas delta uit onder begeleiding van Dr. H.J.A. Berendsen, na hier in de propaedeuse ook al te hebben gewerkt. Gedurende zijn stage bij de NAM in Assen kwam hij in contact met de diepere ondergrond van Nederland: het gasvoerende Carboon rond Coevorden. Dit sloot goed aan bij de promotieplek die in die tijd vrijkwam bij TNO (*Geologische Dienst van Nederland*). Naast zijn interesse voor de geologie, staan voorts geschiedenis, lezen, het organiseren van excursies en fietsen in de belangstelling van de auteur.

Samenvatting

Het Carboon van Nederland en omliggende gebieden; een bekken-analyse

Tijdens het Carboon (360-300 miljoen jaar geleden) lag het huidige Nederland net iets ten zuiden van de evenaar. In het tropische klimaat dat toen heerste werd een kilometersdik pakket sediment afgezet in een bekken dat zich uitstrekte van Ierland tot Polen. Het gebergte dat een groot deel van deze sedimenten leverde wordt het Varistisch gebergte genoemd. Het bevond zich net ten zuiden van Nederland. De Ardennen, de Vogezen, de Eifel en het Zwarte Woud vormen de overblijfselen van dit gebergte. Het Carboon is bekend om zijn kolen, die intensief werden gemijnd in de laatste helft van de negentiende en de eerste helft van de twintigste eeuw. De mijngebieden liggen allemaal op plekken waar Carbonische gesteentes dicht aan het oppervlak komen, zoals in Noord Engeland, in het gebied rond Luik, Zuid Limburg en het Ruhrgebied. Het overgrote deel van het Carboonbekken is echter diep begraven in de loop van de geologische geschiedenis en bevindt zich nu op dieptes variërend van enkele honderden meters tot 8 kilometer. Ondanks dat de kolen op deze dieptes niet bereikbaar zijn met conventionele mijntechnieken, blijft de economische waarde groot. Dit komt door het feit dat de kolen door begraving gas zijn gaan genereren en dit gas wordt tegenwoordig gewonnen uit de vele reservoirs in Nederland en omliggende gebieden. Kortom, ook na de sluiting van de mijnen is het Carboon nog steeds erg belangrijk voor de energieleverantie.

De geologie van het Carboon in de mijngebieden is zeer gedetailleerd beschreven. Dit is niet het geval voor de gebieden waar het Carboon veel dieper begraven ligt. Hier zijn twee oorzaken voor te geven. Ten eerste bevinden de beste gasreservoirs zich in de zandstenen boven het Carboon; de Rotliegend zanden uit het Perm. Wanneer een boring deze zanden bereikt heeft, wordt er meestal gestopt zodra men zeker weet dat het Carboon is aangeboord. Het overgrote deel van de boringen in Nederland die het Carboon hebben bereikt, penetreert het derhalve maar enkele tientallen meters. Daarnaast zorgt de aanzienlijke dikte van het pakket Carbonische gesteentes ervoor dat het moeilijk geheel te doorboren is: vaak meer dan 5 kilometer.

Aangezien er over het Carboon in het grootste deel van Nederland nog maar weinig bekend is, werd door TNO – *Rijks Geologische Dienst* – een promotie-onderzoek opgezet, waarvan dit proefschrift het resultaat is. Mede door de vrijgave van een grote hoeveelheid seismische data de afgelopen jaren vormde dit een geschikt tijdstip. In **hoofdstuk 1** van dit proefschrift (*Introductie*) wordt dit kort toegelicht. Daarnaast tonen enkele figuren de opbouw en de diepteligging van de top van het Carboon in Nederland en wordt een korte uiteenzetting gegeven over het onderzoek dat in Nederland naar het Carboon is uitgevoerd.

In **hoofdstuk 2** (*Tektoniek en sedimentatie in het Noordwest Europees Carboonbekken*) wordt een samenvatting gegeven van de paleogeografische en structurele ontwikkeling van het Noordwest Europees Carboonbekken. Het vormt een verkorte versie van een hoofdstuk dat zal verschijnen in de petroleum geologische atlas van het Zuidelijk Perm Bekken (Atlas of the Southern Permian Basin Area, SPBA) die in 2009 zal worden gepresenteerd. In samenwerking met geologen uit Groot-Brittannië, België, Denemarken, Duitsland en Polen is een nieuw overzicht samengesteld over de geologie van het Carboon in dit gebied. Vier paleogeografische kaarten en een aantal

profielen samengesteld uit boringen geven en goede indruk over de opbouw van het Carboon in dit gebied.

Hoofdstuk 3 (*Seismische interpretatie van carbonaatplatformen uit het Vroeg Carboon (Dinantien) in Nederland; implicaties voor de paleogeografische en structurele ontwikkeling van het Noordwest Europese Carboonbekken*) is voornamelijk gebaseerd op de interpretatie van seismische gegevens die voor de exploratie naar olie en gas zijn vergaard.

Het Onder Carboon wordt in Noordwest Europa op veel plekken gekarakteriseerd door de aanwezigheid van carbonaatplatformen, zoals die tegenwoordig nog terug te vinden zijn in bijvoorbeeld de Bahama's. Deze carbonaatplatformen blijken vaak ontwikkeld te zijn op structureel hoge gebieden (horsten). Tussen deze horsten bevinden zich dalingsgebieden of slenken met een grote waterdiepte. Dit systeem van horsten (met daarop de carbonaatplatformen) en slenken is echter vooral aan de randen van het huidige bekken gevonden; in het centrum (Noord Nederland en het aangrenzende Duitse deel) was de situatie onbekend. In dit gebied is het Onder Carboon slechts door enkele boringen bereikt en deze zijn helaas nog confidentieel op het moment dat dit proefschrift werd geschreven. Veel auteurs hebben ideeën geopperd over de paleogeografie van het Vroeg Carboon in dit centrale deel van het bekken maar tot op heden was het nauwelijks mogelijk om overtuigende data te presenteren. Deze studie toont aan dat ook in het centrum van het Carboonbekken carbonaatplatformen ontwikkeld zijn. Met behulp van seismiek van hoge resolutie kon in de provincies Groningen en Friesland een tweetal grote platformen worden gekarteerd. Er tussenin heeft een diepe slenk gelegen. Mede door de vergelijking met andere gebieden wordt een model gepresenteerd waarbij tijdens het vroege Vroeg Carboon carbonaatsedimentatie in de lager gelegen delen (slenken) plaatsvond. Door voortdurende daling van de slenken ontwikkelden de platformen zich echter langzamerhand op de hogere delen, waarbij de slenken vooral dienden als plekken waar het puin dat van de platformen afkomstig is, wordt afgezet.

Uit het bovenstaande is reeds gebleken dat tijdens het Carboon een zeer dik pakket sediment is afgezet. In **hoofdstuk 4** (*Voorlandbekkenontwikkeling tijdens het Laat Carboon en extensie tijdens het Vroeg Carboon in Noordwest Europa; gevolgtrekkingen op basis van kwantitatieve dalings-analyse in Nederland*) wordt verslag gedaan van een poging om beter te begrijpen welke mechanismen verantwoordelijk zijn voor het creëren van de ruimte om deze hoeveelheid sediment te accommoderen. De twee dalingsmechanismen die in de literatuur het meest worden genoemd zijn de zogenaamde thermische daling die plaatsvindt na een fase van het oprekken (extensie) van de aardkorst en een dalingscomponent die wordt veroorzaakt door het extra beladen (door middel van een gebergteketen bijvoorbeeld) van de aardkorst. De laatstgenoemde zou vooral aan de zuidkant van het bekken hebben gespeeld omdat daar immers de Varistische gebergteketen lag. In het noordelijke en centrale deel van het bekken speelt waarschijnlijk vooral het eerste mechanisme een belangrijke rol. In samenwerking met de Universiteit van Amsterdam is met een aantal eenvoudige modelberekeningen bepaald hoeveel van de totale daling door de twee genoemde mechanismen kan worden verklaard. Het blijkt dat belading maar voor een beperkt deel van de daling heeft kunnen zorgen, zelfs in het zuidelijke deel van het bekken. Tevens blijkt de conventionele aanname dat een oprekkingsfase tijdens het Vroeg Carboon voldoende zou zijn om alle sedimenten die vervolgens tijdens het Laat Carboon worden afgezet te kunnen accommoderen, moeilijk te handhaven. Daarom wordt een extra extensiesfase gepostuleerd. In het laatste onderdeel van het hoofdstuk wordt nog een aantal andere mechanismen genoemd die eventueel ook zouden kunnen hebben bijgedragen aan de daling in het bestudeerde bekken.

In Groot Brittannie is een aanzienlijk aantal publicaties verschenen over gasvelden in Carbonische reservoirs. Hoewel in Nederland tevens gas geproduceerd wordt uit Carbonische zandstenen, zijn er tot op heden geen publicaties verschenen waarin een beeld geschetst wordt van die reservoirzanden. **Hoofdstuk 5** (*De alluviale architectuur van het Coevorden veld (Boven Carboon), Nederland*) beschrijft de opbouw van een gasveld dat bestaat uit Carbonische zandstenen; het Coevorden gasveld in het zuidoosten van de provincie Drenthe. Voor deze studie werd gebruik gemaakt van kernmateriaal en boorlogs. De natuurlijke gamma-straling is de belangrijkste log. Hiermee kan een onderscheid tussen klei- en zandsteen worden gemaakt. De gesteentes waar het gas zich in bevindt zijn afgezet door rivieren (fluviatiele systemen). De dikte van de zanden varieert van enkele meters tot 40 meter. Omdat het belangrijk is te weten hoe breed deze fluviatiele zanden zijn, wordt in dit hoofdstuk een methode gebruikt waarmee de breedte van de zandlichamen kan worden berekend. Hierbij wordt gebruik gemaakt van de dikte van pakketjes zand die door een migrerende duin in het stromende water zijn afgezet. Hiermee kon worden berekend dat de zanden waarschijnlijk een maximale breedte van ongeveer 4 kilometer hebben. Voorts wordt een dwarprofiel gepresenteerd naast paleogeografische kaartjes van een aantal belangrijke zandlichamen.

Tijdens het Namurien vindt in grote delen van het Carboonbekken de overgang plaats van hoofdzakelijk carbonaat- naar siliciclastische (zand en klei) sedimentatie. Een aantal auteurs heeft gesuggereerd dat het water waarin het sediment tot bezinking kwam in Engeland periodiek veranderde van zout naar zoet (saliniteitsverschil). Met andere woorden, op moment A is sprake van een zee, op moment B kan men spreken van een meer. Dit is onder andere geconcludeerd op basis van de cyclische manier waarop bepaalde fossielen en fossielgroepen wordt aangetroffen. In **hoofdstuk 6** (*Depositie van zwarte schalies tijdens het Namurien in Noord Engeland; marien of lacustrien?*) wordt met behulp van geochemische onderzoeksmethoden aangetoond dat het niet waarschijnlijk is dat het bekken grote saliniteitsveranderingen heeft ondergaan. Bepaalde elementen die in zeer kleine hoeveelheden in zeewater voorkomen maar nog veel minder in zoet water (uranium en molybdeen), bleken over de gehele door de auteur bemonsterde kolom aanwezig te zijn. Een andere aanwijzing is het voorkomen van pyriet (een mineraal bestaande uit een zwavel-ijzerverbinding) in alle monsters. Dit mineraal is vooral karakteristiek voor mariene sedimenten. Dit heeft geleid tot de conclusie dat de gesuggereerde schommelingen in saliniteit waarschijnlijk niet hebben plaatsgevonden en dat het bekken continu marien moet zijn geweest.

Het Westfalien is de periode die volgt op het Namurien. In die tijd worden de meeste veenlagen gevormd die miljoenen jaren later tot koollagen zouden veranderen. Deze veenlagen zijn gevormd in een fluviatiel afzettingsmilieu: ze worden afgewisseld door klei(steen) en zand(stenen) die door de rivieren zijn afgezet in een groot delta-systeem. Af en toe werd de delta door de zee overstroomd. Hierdoor werd een laagje mariene klei afgezet. Deze mariene horizons, die met behulp van hun karakteristieke fossielinhoud makkelijk kunnen worden aangetoond, vormen een belangrijk middel om de relatieve ouderdom van het gesteente te bepalen. Omdat met de moderne boortechnieken vaak alleen maar logs zoals de gamma-ray beschikbaar zijn en dus de fossielen niet kunnen worden verzameld, is geprobeerd die mariene horizons met behulp van de gamma-ray te detecteren. Vaak lukt dat omdat deze kleien een verhoogd concentratie uranium bezitten, wat wordt gedetecteerd door de gamma-ray. In **hoofdstuk 7** (*Geochemie van mariene en lacustriene horizons in het Boven Carboon van Nederland*) worden deze mariene kleilagen geochemisch onderzocht om de vraag te beantwoorden waarom veel mariene horizons die in Nederland bekend zijn toch niet goed met de gamma-ray log waar te nemen zijn. Op basis van de fossielassociatie is al duidelijk

dat de mariene horizons in Nederland onder relatief ondiepe omstandigheden zijn afgezet. Het blijkt dat dit soort ondiep-mariene afzettingen wordt gekarakteriseerd door lage concentraties aan organisch materiaal. Daardoor heeft er waarschijnlijk geen effectieve fixatie van sporenelementen als uranium kunnen plaatsvinden. Deze mariene kleien zijn gebonden aan ondiepe en proximale omstandigheden terwijl de mariene kleien die wel een aanrijking aan sporenelementen bezitten in een distaal milieu worden afgezet. Ter vergelijking van deze mariene horizons is tevens een aantal lacustriene kleien gekarakteriseerd omdat deze vaak op vergelijkbare plekken voorkomen als de mariene horizons. Deze lacustriene horizons verschillen weer van de mariene door de afwezigheid van pyriet en tevens een zeer lage tot geen aanrijking aan sporen-elementen.